Role of Interleukin-1β and Neuroinflammation in the Persistence of Neuropathic Pain

by

Myung-chul Noh

A thesis submitted in partial fulfillment of the requirements for the degree of

Doctor of Philosophy

Department of Pharmacology
University of Alberta

Abstract

Persistent hyperexcitability in the primary sensory afferents contributes substantially to the onset and the maintenance of neuropathic pain. Inteleukin-1β (IL-1β) has been implicated to directly interact with interleukin 1 receptor type I (IL-1RI) expressed in dorsal root ganglion (DRG) neurons to not only modulate ion channel function and excitability in a cell type specific manner, but also modify gene expressions to trigger a 'phenotypic switch'. This thesis aims to illuminate the role of IL-1β in the persistent DRG neuron hyperexcitability and the maintenance of neuropathic pain.

To do so, we examined the consequences of chronic IL-1β exposure and neuroinflammation, which occur in various animal models of neuropathic pain, on DRG neuron excitability as well as mechanical allodynia. Whole-cell patch clamp analysis of the effects and reversibility of chronic 5-6 day IL-1β exposure was examined in male rat, neuron-enriched DRG cultures as well as in acutely dissociated female mice DRG neuron culture to induction of autoimmune encephalomyelitis (EAE). Furthermore, differential reversibility of mechanical allodynia (pain due to innocuous stimuli) seen in spared nerve injury (SNI) and chronic constriction injury (CCI) models of neuropathic pain was examined in the context of degree and duration of neuroinflammation in the DRG.

Through the experiments done in this thesis, I illustrated potential IL-1β mediated mechanisms that work in parallel to promote persistent DRG neuron hyperexcitability as well as mechanical allodynia in animal models of neuropathic pain and potentially in humans. I demonstrated 5-6 day 100 pM IL-1β treatment with 50 ng/ml glial cell line derived neurotrophic factor (GDNF) supplementation leads to enduring increase in the action potential duration (AP) in small IB_4^+

DRG neurons, which was largely mediated through decrease in Ca^{2+}-activated K^+ conductance ($g_{K,Ca}$), particularly large conductance BK(Ca) channels. Furthermore, by using acutely dissociated female mice DRG cultures, we showed medium-large (≥26 μm) likely myelinated DRG neurons from EAE mice exhibited increased likelihood of AP discharge, number of AP discharges, and firing frequency in comparison to DRG neurons from CFA control mice. In stark contrast, induction of EAE did not affect small (<26 μm) presumptive unmyelinated DRG neuron excitability. Remarkably, the increase in excitability in medium-large myelinated DRG neurons persisted until 7 days post-onset, when no substantial immune cells and IL-1β expression could be detected in the DRG. Finally, I showed persistent expression of cellular sources of IL-1β, such as activated satellite glial cells and macrophages, correlate with ongoing production of colony stimulating factor 1 (CSF1) as well as mechanical allodynia. Only SNI operated rats, which exhibit persistent mechanical allodynia, displayed persistent neuroinflammation and CSF1 production in the DRGs as opposed to CCI operated animals. This implied ongoing peripheral neuroinflammation mediated by IL-1β as well as other inflammatory mediators may not only promote hyperexcitability in the DRG neurons, but it may also trigger *de novo* induction of critical mediators such as CSF1.

The work from this thesis provides additional support to growing evidence that neuropathic pain, sometimes referred to as the "disease of pain," is a 'neuroimmune disorder.' The data obtained in this thesis provide potential mechanisms that neuron-immune crosstalk may facilitate persistent hyperexcitability in the primary afferents and in the DRG, which in turn can indirectly contribute to the onset and the maintenance of central sensitization and neuropathic pain.

Preface

The current research project has received research ethics approval from the University of Alberta Research Ethics Board: Project Name "Cellular electrophysiology of Neuropathic Pain", No. AUP00000338, Date: July 24th, 2018.

At the time of writing this thesis, the work done in Chapter 3 of this thesis has been submitted to Experimental Neurology for review with the title "Long-Term Actions of Interleukin 1β on K^+, Na^+, and Ca^{2+} Channel Currents in Small, IB_4-Positive Dorsal Root Ganglion Neurons and their Relevance to Neuropathic Pain". I designed aspects of the study, carried out experiments and data interpretation, statistical analysis and co-wrote the manuscript.

The data in Chapter 4 of this thesis is a part of an article that has been submitted to eNeuro with the title "Sensory neurons of the dorsal root ganglia become hyperexcitable in a T-cell mediated model of multiple sclerosis". I carried out the electrophysiology experiments.

Acknowledgements

I thank my supervisor and scientific mentor Dr. Peter Smith for incredible support and training throughout the course of my PhD. Your curiosity driven research philosophy has truly shaped my core scientific thought process. Thank you for making the journey fun and intellectually stimulating.

I would like to thank Dr. Bradley Kerr for being a part of my thesis defense committee and providing expertise and resources to make this project possible. Thank you for going out of your way to introduce me to many scientists whom I have been greatly influenced by.

I thank Dr. Peter Light for being a part my thesis committee and providing unique input and expertise on ion channel electrophysiology.

I thank Dr. Christine Webber for being in my thesis committee and providing resources and guidance on immunohistochemistry.

I would like to thank my external examiner Dr. Tuan Trang from the University of Calgary for taking the time out of your busy schedule to review my thesis.

I thank Dr. Chris Power for providing unique insight on neuroimmune interactions and immunology which greatly influenced the way I think about the nervous system.

I would also like to thank Dr. Fred Tse and Dr. William Colmers for providing guidance on electrophysiological techniques and concepts as well as Dr. Elena Posse de Chaves for providing guidance on intracellular cell signaling pathways and molecular biology.

I thank my friend and mentor Dr. Patrick Stemkowski for continued support and guidance even after leaving the Smith laboratory.

I thank my friend and mentor Dr. Yishen Lele Chen for whole-cell patch clamp training and moral support.

I thank my friends from Smith lab Dr. Sascha Alles and Dr. Paul Boakye for intellectually stimulating discussions and moral support.

I thank my friend Mr. Saad Yousef for fun scientific discussions and guidance on molecular biology and statistical analyses.

I thank our incredible laboratory technician Ms. Twinkle Joy for doing all the hard work and assistance throughout the course my PhD thesis. This project would not be possible without you.

I thank my wonderful family for the unconditional support and encouragement throughout my life.

Finally, I would like to thank the Alberta Innovates Health Solutions for granting me with graduate studentship funding and Canadian Institutes of Health Research for providing graduate scholarships to make this work possible.

Table of Contents

List of Tables

List of Figures

List of Abbreviations

AA	Antibiotic-antimycotic
AHP	Afterhyperpolarization
AM	Anti-mitotic
AMPA	α-amino-3-hydroxy-5-methyl-4-isoxazolepropionic acid receptor
ANOVA	Analysis of variance
AP	Action potential
ATF3	Activating transcription factor 3
BK	Large conductance $Ca2^{+}$-activated K^{+} channel
BSA	Bovine serum albumin
CCI	Chronic constriction Injury
cDNA	Complementary deoxyribonucleic acid
CFA	Complete Freund's adjuvant
CGRP	Calcitonin-gene related peptide
CSF1	Colony stimulating factor 1
DAPI	4′,6-diamidino-2-phenylindole
DMEM	Dulbecco's Modified Eagle Medium

DMEMHS	Dulbecco's Modified Eagle Medium with Horse Serum
DPBS	Dulbecco's phosphate buffered saline
DREADD	Designer receptor exclusively activated by a designer drug
DRG	Dorsal root ganglion
EAE	Experimental autoimmune encephalomyelitis
EDTA	Ethylenediaminetetraacetic acid
ELISA	Enzyme-Linked Immunosorbent Assay
EPSC	Excitatory postsynaptic currents
GABA	Gamma-aminobutyric acid
GAP43	Growth-associated protein 43
GDNF	Glial cell line derived neurotrophic factor
GFAP	Glial fibrillary acidic protein
GFP	Green fluorescent protein
$g_{K,Ca}$	Calcium-activated potassium conductance
g_{Na}	Voltage-gated sodium conductance
HCN	Hyperpolarization-activated cyclic nucleotide-gated channel
HIV	Human immunodeficiency virus

IB_4	Isolectin B4
Iba1	Ionized calcium binding adaptor molecule 1
IBTX	Iberiotoxin
I_{Ca}	Voltage-gated calcium current
IHC	Immunohistochemistry
I_K	Delayed rectifier voltage-gated potassium current
$I_{K,Ca}$	Calcium-activated potassium current
IL-1β	Interleukin-1 beta
IL-1RI	Interleukin 1 receptor type I
I_{Na}	Voltage-gated sodium current
IPSC	Inhibitory postsynaptic currents
MAPK	Mitogen-activated protein kinase
MOG_{35-55}	Myelin oligodendrocyte glycoprotein fragment 35-55
mRNA	Messenger ribonucleic acid
NMDA	*N*-methyl-D-aspartate receptor
OCT	Optimum cutting temperature
PBStw	Phosphate buffered saline with Tween-20

PBStx	Phosphate buffered saline with Triton X-100
PGE2	Prostaglandin E2
PPIA	Peptidylprolyl isomerase A
PSL	Partial sciatic nerve ligation
PSNL	Partial sciatic nerve ligation
RFP	Red fluorescent protein
RMP	Resting membrane potential
rt-qPCR	Real Time Quantitative Polymerase Chain Reaction
SEM	Standard error of the mean
SGCs	Satellite glial cells
SNI	Spared nerve injury
SNL	Spinal nerve ligation
TNFα	Tumor necrosis factor alpha
TrkA	Tropomyosin receptor kinase A
TrkB	Tropomyosin receptor kinase B
TRPV1	Transient receptor potential vanilloid 1
TTX	Tetrodotoxin

Chapter 1

Introduction

1.1 What is pain?

The International Association for the Study of Pain has defined pain as 'an unpleasant sensory and emotional experience associated with actual or potential tissue damage or described in terms of such damage' (Alcock 2017). Despite this, pain is critical for survival as it protects the body from actual or potential injury (Iadarola & Caudle 1997). Nociception is the physiological process of transducing external or internal noxious stimuli to electrical signals (Dubin & Patapoutian 2010, Iadarola & Caudle 1997). The process of nociception is initiated by activation of nociceptors, which are diverse specialized peripheral sensory neurons that responds to noxious mechanical, thermal, and chemical stimuli (Dubin & Patapoutian 2010). The sensory information is processed and modulated in the spinal cord, then projected to the somatosensory cortex in the brain to interpret the noxious stimuli as 'pain' (Dubin & Patapoutian 2010). Here, I will briefly describe the acute nociceptive pain pathway, which becomes maladaptive during the pathogenesis of several forms of chronic pain.

1.1.1 Primary sensory afferents

The primary sensory afferents are responsible for transducing mechanical, thermal, and chemical stimuli from the environment to the central nervous system (CNS) (Basbaum et al 2009). The dorsal root ganglion (DRG) and trigeminal ganglion (TG) contains pseudounipolar cell bodies of the primary sensory afferents, which bifurcate to innervate both the distal sensory terminals as well as the dorsal horn of the spinal cord or the brainstem (Dubin & Patapoutian 2010). The DRG neurons are neurochemically and functionally diverse, and they give rise to distinct cutaneous primary sensory afferents, which allow them to distinguish and respond to a wide variety of sensory stimuli (Abraira & Ginty 2013, Basbaum et al 2009, Chiu et al 2014, Li et al 2016, Usoskin et al 2015). Classically, primary afferents have been subdivided into two main

groups based on axon diameter, myelination, and conduction velocity (Abraira & Ginty 2013, Djouhri & Lawson 2004, Harper & Lawson 1985). General characteristics of primary afferents based on the classical definition are summarized in Figure 1-1.

First, A-fibres are myelinated sensory afferents that are involved in transduction of both innocuous and noxious stimuli (Figure 1-1). On one hand, large diameter (>40 μm) DRG neurons are generally low-threshold mechanoreceptors that give rise to heavily myelinated rapidly conducting Aβ-fibers (Harper & Lawson 1985, Lewin & Moshourab 2004). Aβ-fibres predominantly conduct innocuous mechanical stimuli, such as touch; however, they can also transduce noxious stimuli (Abraira & Ginty 2013, Djouhri & Lawson 2004). On the other hand, medium diameter (30-40 μm) DRG neurons are predominantly cell bodies of Aδ-fibres, which are thinly myelinated and have slower conduction speed than Aβ-fibres (Abraira & Ginty 2013, Harper & Lawson 1985). Aδ-fibre nociceptors conduct acute well-localized noxious mechanical, chemical, and thermal stimuli (Basbaum et al 2009, Djouhri & Lawson 2004). Aδ-fibre nociceptors can be classified further based on their thermal thresholds. Type I Aδ-fibre nociceptors are high-threshold mechanonociceptors that generally respond to temperatures above 50°C; in contrast, type II Aδ-fibre nociceptors have much lower thermal threshold, which in turn allows them to be the first responders to noxious heat or cold (Basbaum et al 2009, Lewin & Moshourab 2004).

Second, C-fibres are unmyelinated sensory afferents that have the smallest diameter and the slowest conduction velocity (Figure 1-1) (Abraira & Ginty 2013, Dubin & Patapoutian 2010, Harper & Lawson 1985). The cell bodies of C-fibre primary afferents generally have smaller diameter (<30 μm), and they are the putative nociceptors in the peripheral nervous system (PNS) that detect a wide range of noxious stimuli (Abraira & Ginty 2013, Basbaum et al 2009, Dubin &

Patapoutian 2010). That said, not all C-fibre neurons are nociceptors; the presence of C-fibre low threshold mechanoreceptors has been known since 1939, and they are implicated in transduction of tickling or pleasant stimuli (Douglas & Ritchie 1957, Liljencrantz & Olausson 2014, Zotterman 1939). Although more recent studies have revealed C-fibre nociceptors are highly heterogenous functionally and neurochemically (Chiu et al 2014, Li et al 2016, Usoskin et al 2015), they showed striking consistencies with the classically categorized peptidergic and non-peptidergic C-fibre nociceptors (Molliver et al 1995, Stucky & Lewin 1999). Peptidergic nociceptors are characterized by their expression of neurotransmitters, such as substance P and calcitonin-gene related peptide (CGRP), and tropomyosin receptor kinase A (TrkA) receptor, which is the receptor for nerve growth factor (NGF) (Molliver et al 1995, Stucky & Lewin 1999). Non-peptidergic nociceptors on the other hand specifically bind *Griffonia simplicifolia* lectin B_4 (IB_4) (Nagy & Hunt 1982, Silverman & Kruger 1990). In contrast to peptidergic nociceptors, IB_4^+ non-peptidergic nociceptors do not substantially express CGRP nor substance P, and they preferentially express glial-derived neurotrophic factor (GDNF) family receptor alpha-1,2,3 (GFRα1, GFRα2, GFRα3 and RET) complexes (Molliver et al 1995, Molliver et al 1997, Stucky & Lewin 1999). That said, more recent studies have revealed non-peptidergic nociceptors can express TrkA receptor although to a lesser extent (Chiu et al 2014, Fang et al 2006). As evident by neurochemical differences, peptidergic and non-peptidergic nociceptors are also functionally distinct (Chiu et al 2014, Stucky & Lewin 1999). For example, due to distinct receptor expressions, peptidergic IB_4^- nociceptors largely depend on NGF as opposed to non-peptidergic IB_4^+ nociceptors that depend largely on GDNF for proper function and development (Fjell et al 1999, Molliver et al 1997). Furthermore, under physiological circumstances, non-peptidergic IB_4^+ nociceptors have higher threshold, longer action potential (AP) duration, more

tetrodotoxin resistant (TTX-R) Na^+ current, and smaller capsaicin induced inward current compared to peptidergic IB_4^- nociceptors (Fang et al 2006, Stucky & Lewin 1999). Since capsaicin opens transient receptor potential vanilloid 1 (TRPV1) channel, which have been shown to transduce noxious heat, non-peptidergic nociceptors were thought to be primarily transducing noxious mechanical stimuli (Stucky & Lewin 1999). However, later analysis revealed non-peptidergic nociceptors greatly upregulate TRPV1 expression in response to inflammation in contrast to peptidergic nociceptors (Breese et al 2005). Therefore, non-peptidergic nociceptors may be involved in transducing noxious heat during inflammatory pain; whereas, peptidergic nociceptors may transduce noxious thermal stimuli during physiological conditions as well as during inflammation (Breese et al 2005). As seen here, although nociceptors can be primarily heat-sensitive or mechanosensitive, many nociceptors are polymodal and are capable of transducing combinations of noxious stimuli (Lewin & Moshourab 2004) Therefore, identification of precise nociceptor type requires identification of distinct gene expressions, such as transient receptor potential melastatin 8 (TRPM8) channel, which has been implicated for sensing cold stimuli, and Mas-related G protein-coupled receptor subtype D (MRGPRD), which has been shown to transduce noxious mechanical stimuli (Cavanaugh et al 2009, Dubin & Patapoutian 2010).

In summary, primary sensory afferent and their cell bodies make up a diverse group of mechanoreceptors, mechanonociceptors, heat/cold sensitive nociceptors, and chemically sensitive nociceptors, which can be identified based on their neurochemistry, anatomy, channel and receptor expression, as well as electrophysiological properties (Chiu et al 2014, Dubin & Patapoutian 2010, Li et al 2016, Usoskin et al 2015). As a result, they play a critical role in encoding and transducing a wide array of sensory information to the CNS.

1.1.2 Pain processing in the spinal cord and the brain

The gray matter of the spinal dorsal horn consists of I to VI Rexed laminae (Rexed 1952) and most primary sensory afferents terminate to the spinal dorsal horn (Figure 1-2A) (Todd 2013). Therefore, the spinal dorsal horn is a major site where peripheral sensory information is integrated and modulated before being projected to higher centres. Each lamina contains complex and distinct circuitry that consists of several different types of neurons, which are summarized in Figure 1-2C (Braz et al 2014, Peirs & Seal 2016, Todd 2010). There are four major group of neurons that modulate nociceptive information in the spinal cord.

First, all primary sensory afferents are glutamatergic; therefore, their synaptic transmission to spinal dorsal horn neurons will always be excitatory (Todd 2010). Aβ-low threshold mechanoreceptors, which transduce innocuous sensory information, generally project to deeper laminae (III, IV, and V). However, they can also innervate inhibitory interneurons as well as excitatory interneurons that are involved in nociceptive pain processing within lamina II and III (Peirs & Seal 2016). In contrast to Aβ-afferents, nociceptive Aδ- and C-afferents generally innervate superficial laminae (I and II), where most nociceptive information is processed and integrated (Todd 2010). Interestingly, peptidergic and non-peptidergic C-fibres form a distinct pain pathway (Braz et al 2005). IB_4^- peptidergic C-fibres generally terminate within lamina I and II to innervate both excitatory and inhibitory interneurons as well as projection neurons (Peirs & Seal 2016). In contrast, IB_4^+ non-peptidergic C-fibres predominantly innervate lamina II which contains predominantly excitatory interneurons and inhibitory neurons to lesser extent (Figure 1-2B and C) (Braz et al 2014, Braz et al 2005).

Second, interneurons are the most common neurons in the spinal dorsal horn, and laminae I to III have particularly high density of interneurons compared to rest of the laminae. Interneurons can

be either excitatory or inhibitory; that said, excitatory interneurons make up the vast majority of interneurons in the spinal dorsal horn (Peirs & Seal 2016). Excitatory interneurons form glutamatergic synapses as opposed to inhibitory interneurons that form gamma-aminobutyric acid (GABAergic) and/or glycinergic synapses (Todd 2010). Inhibitory interneurons in the spinal dorsal horn can form synapses with presynaptic terminals of primary afferent fibres and with other spinal dorsal horn neurons to inhibit their activities; however, much less is known about the excitatory interneurons and their circuitry (Todd 2010). Interneurons of the superficial dorsal horn are morphologically, neurochemically, and electrophysiologically heterogeneous and have been classified into four separate categories based on their morphology and electrophysiological characteristics: 1) islet, 2) radial, 3) central, and 4) vertical (Grudt & Perl 2002). Although it is clear that tonically firing islet cells are the putative inhibitory interneurons in the superficial dorsal horn, glutamatergic interneurons have been more difficult to identify (Todd 2010, Yasaka et al 2010). That said, radial and vertical cells, which typically display delayed firing pattern, are thought to be predominantly excitatory, and central cells can be either inhibitory or excitatory (Todd 2010).

Third, descending axons from various brain regions can also modulate spinal dorsal horn neuron activity. For example, descending serotoninergic and noradrenergic axons from raphe nuclei and locus coeruleus respectively innervate lamina I and II (Todd 2010), and both serotonin and noradrenaline have been shown to hyperpolarize membrane potentials of interneurons in the superficial dorsal horn (Lu & Perl 2007, Yasaka et al 2010). Descending axons may inhibit excitatory interneurons, or they may cause disinhibition by inhibiting the activity of inhibitory interneurons through volume transmission; however, this may enhance or suppress nociceptive stimuli depending on the specific circuitry (Todd 2010).

Fourth, projection neurons, which are concentrated in lamina I and to a lesser extent in laminae III-IV, receive sensory input that has been integrated by complex circuitry involving interneurons and primary afferents within the spinal dorsal horn (Todd 2010). Projection neurons can be further classified into two main groups. Nociceptive specific projection neurons in lamina I predominantly respond to high intensity nociceptive from C-fibres. In contrast, wide dynamic range neurons (WDR), which are located in deeper laminae, can respond to all types of sensory stimuli (West et al 2015). Furthermore, WDR neurons have been shown to go through activity-dependant plasticity upon repeated noxious input from C-fibres (West et al 2015). Once activated projection neurons transmit sensory information from the dorsal horn to brain regions through various ascending pathways such as spinothalamic and spinoreticulothalamic tracts, which terminate within the periaqueductal gray, parabrachial nucleus, and thalamus which relay information to the somatosensory cortex where perception of pain takes place (Basbaum et al 2009).

It is postulated that certain brain regions are responsible for acute nociceptive pain processing. Although many have attempted to map brain regions responsible for the perception of pain, often referred as the "Pain Matrix", by functional magnetic resonance imaging (fMRI), it is still unclear whether there is a specific region that is responsible for the sensation of pain. For instance, many have consistently reported activation in the thalamus, anterior cingulate cortex, and insula upon acute noxious stimuli (Huang et al 2013, Wager et al 2013). However, a more recent study investigating the "Pain Matrix" in individuals with loss-of function SCN9A mutation, which result in loss of $Na_v1.7$ channel function and ability to feel pain (Drenth & Waxman 2007), revealed patients with SCN9A mutation still showed the same activation pattern in the brain compared to a control group (Salomons et al 2016). Since patients with SCN9A

mutations can still feel normal tactile stimuli, previous demonstrations of the "Pain Matrix" may have been due to tactile stimuli instead of noxious painful stimuli. Consequently, it is unlikely that there is a specific brain region that is responsible for the perception of pain; thus, it is more likely that pain perception involves integration of inputs from diverse brain regions and circuits.

1.2 Neuropathic pain and its impact on society

Neuropathic pain is caused by a lesion or a disease to the somatosensory nervous system (Jensen et al 2011). It is typically chronic and may be initiated by peripheral nerve trauma, spinal cord injury, stroke, diabetes, chemotherapy, human immunodeficiency virus (HIV) and *Herpes zoster* induced neuropathies as well as multiple sclerosis (MS) (Alles & Smith 2018). Unlike acute physiological pain, which protects the body from potential or actual tissue injury, neuropathic pain is maladaptive as it persists long after an injury has healed (Iadarola & Caudle 1997). Neuropathic pain is often accompanied by debilitating symptoms and signs such as ongoing electric shock-like spontaneous pain, allodynia (painful sensation from innocuous stimuli), hyperalgesia (heightened pain sensation from noxious stimuli), and less frequently causalgia (excruciating burning sensation in a limb) (Colloca et al 2017). It is estimated 7-10 % of the global population, which accounts for 539 to 770 million people, is affected by chronic neuropathic pain (van Hecke et al 2014), and total annual economic costs in the United States alone ranges from $560 to $635 billion (Gaskin & Richard 2012). Despite the heavy socioeconomic burden, management of chronic neuropathic pain in the clinic has met with limited success (Moore et al 2013, Yezierski & Hansson 2018). Classical pain medications such as nonsteroidal anti-inflammatory drugs (NSAIDs) and strong opioids, such as morphine and oxycodone are often ineffective and unsafe for the treatment of chronic neuropathic pain (Yekkirala et al 2017). Moreover, currently available first-line therapeutic agents such as

gabapentinoids, tricyclic antidepressants (TCAs), and serotonin-norepinephrine reuptake inhibitors (SNRIs) are only modestly efficacious (Finnerup et al 2015). As a result, there is a high demand for new effective therapeutic options, and understanding the complex etiology and pathophysiology of neuropathic pain may reveal potential novel targets for the treatment of neuropathic pain (Alles & Smith 2018, Finnerup et al 2015, Moulin et al 2007, Yekkirala et al 2017).

1.3 Animal models of neuropathic pain

As neuropathic pain is a disorder caused by injury to or disease of the somatosensory nervous system, various animal models of nerve injury have been used to investigate its etiology and underlying pathophysiology. Wall et al (1979a) were the first group to utilize complete axotomy of the sciatic nerve to mimic anaesthesia dolorosa, a painful sensation from a numb area, which led to discoveries of important mechanisms underlying neuropathic pain pathogenesis (Wall et al 1979a). Since then, more animal models have been developed, which further refined our understanding of the mechanisms underlying etiology and pathophysiology of neuropathic pain. Here, I describe the most commonly used animal models of neuropathic pain and their characteristics, which are summarized in Figure 1-3.

1.3.1 Chronic constriction injury

Bennett and Xie (1988) developed chronic constriction injury (CCI), which is an alternate method of inducing neuropathic pain behavior without completely axotomizing the sciatic nerve. Instead of complete transection of sciatic nerve, the authors loosely ligated the sciatic nerve with 4 chromic gut sutures (Figure 1-3). As seen in humans, CCI leads to signs and symptoms of neuropathic pain such as mechanical allodynia/hyperalgesia, thermal hyperalgesia, cold allodynia, and spontaneous ongoing pain and mild autotomy, which is a self-mutilative behavior

(Bennett & Xie 1988, Dowdall et al 2005, Kim et al 1997). Interestingly, the CCI model leads to more pronounced spontaneous ongoing pain behavior compared to many other nerve injury models (Dowdall et al 2005, Kim et al 1997). However, CCI operated animals eventually recovers from neuropathic pain 7-12 weeks after the injury (Bennett & Xie 1988, Dowdall et al 2005, Kim et al 1997).

Since the surgical procedure of placing 'loose' chromic gut ligatures is not standardized, the CCI method developed by Bennett and Xie leads to large variability within the group (Bennett & Xie 1988, Kim et al 1997). As a result, Mosconi and Kruger (1996) developed an alternative CCI model which uses fixed diameter polyethylene tubing to constrict the sciatic nerve (Mosconi & Kruger 1996). In this model of CCI, the authors placed two polyethylene cuffs (~2 mm long) around the sciatic nerve. The Mosconi & Kruger model of CCI leads to development of mechanical allodynia and cold allodynia which peaks 2 weeks post-injury. Interestingly, in contrast to Bennett & Xie model of CCI, animals recover rapidly from neuropathic pain behaviors by 4 weeks post-injury.

1.3.3 Partial sciatic ligation

Seltzer et al (1990) developed the partial sciatic ligation (PSL) model to mimic causalgia as many partial nerve injuries to the sensory nerves lead to it in humans (Seltzer et al 1990). The injury is induced by inserting silk sutures through the sciatic nerve and ligating roughly 33-50% of the dorsal portion of the sciatic nerve (Figure 1-3) (Seltzer et al 1990). The authors have reported a rapid onset of behaviors associated with neuropathic pain, such as mechanical allodynia, thermal hyperalgesia, and spontaneous pain, which can last up to 5-7 weeks (Dowdall et al 2005, Seltzer et al 1990). Interestingly, unlike other nerve injury models, PSL leads to

bilateral development of pain behavior, which correlates with symptoms and signs of causalgia in humans.

1.3.4 Spinal nerve ligation

Kim and Chung (1992) developed the spinal nerve ligation (SNL) model, which was induced by tightly ligating the 5th and 6th lumbar segments (L5 and L6) of spinal nerves, distal to L5-L6 DRGs, with silk sutures (Figure 1-3). In contrast to complete axotomy, SNL does not lead profound motor deficits, and it is instead a sign of failed surgery (Chung et al 2004, Kim & Chung 1992). The SNL model leads to profound mechanical and cold allodynia which lasts up to 12 to 20 weeks and thermal hyperalgesia that can last up to 2 to 5 weeks (Dowdall et al 2005, Kim et al 1997). In contrast to CCI and axotomy model, SNL show no sign of autotomy and weaker signs of ongoing spontaneous pain. Furthermore, compared to CCI and PSL, the mechanical and cold allodynia behaviors in SNL rely heavily on sympathetic innervation (Kim et al 1997). SNL has been largely modified since the original description of Kim and Chung (1992). The advantage of SNL is that the degree and location of injury can be precisely controlled, and the consequences of specific injury can be observed in many ways. For instance, researchers may decide to spare L6 spinal nerve and only ligate the L5 spinal nerve to examine the consequence in L5 and L6 DRG specifically. However, authors also note the variability among different researchers can arise from unintentional modifications to the protocol due to difficulty of the surgery (Chung et al 2004).

1.3.5 Spared nerve injury

Decosterd and Woolf (2000) developed the spared nerve injury (SNI) model, which is induced by tightly ligating and subsequently transecting the common peroneal and the tibial nerves while leaving the sural nerve intact without damage (Figure 1-3) (Decosterd & Woolf 2000). Great

care must be taken not to damage the sural nerve as it can lead to complete denervation of the hind paw. In contrast to previous models, SNI leads to robust mechanical/cold allodynia and thermal hyperalgesia which can persist over 6 months. As a result, SNI allows for investigation of truly 'chronic' neuropathic pain. In addition, researchers can also manipulate injured and non-injured areas of the paw to evoke pain behaviors in SNI model to examine mechanisms underlying neuropathic pain. For example, the area innervated by non-injured sural nerve (lateral side of the plantar surface) leads to more profound and chronic pain behaviors, which demonstrates the importance of uninjured nerve for the pathogenesis of neuropathic pain (Decosterd & Woolf 2000).

1.3.6 Diabetic polyneuropathy

Diabetes is the most common cause of peripheral neuropathy (Callaghan et al 2012). In fact, up to 60% of diabetic patients develop peripheral polyneuropathy and the majority of these patients also display symptoms and signs of neuropathic pain (Callaghan et al 2012). Chemically induced diabetes in rodents is the most frequently used model to study diabetes in animals (Szkudelski 2001). This model utilizes streptozotocin (STZ), an antibiotic that is toxic to pancreatic β-cells, to cause diabetes in rodents (Courteix et al 1993, Szkudelski 2001). A single intraperitoneal administration of streptozotocin (STZ) leads to destruction of β-cells and subsequent hyperglycemia (Courteix et al 1993). As seen in diabetic patients, the STZ model leads to diabetic polyneuropathy and signs of neuropathic pain. STZ induced diabetic polyneuropathy leads to slower onset of mechanical/cold allodynia, and thermal hyperalgesia, which takes up to 2-4 weeks. Mechanical allodynia is chronic as it can persists over 12 weeks post-injection (Huang et al 2014). As a result, the STZ model has been a useful platform to examine the etiology and pathophysiology of neuropathic pain as well as diabetic polyneuropathy.

1.3.7 Experimental autoimmune encephalomyelitis

Experimental autoimmune encephalomyelitis (EAE) is an animal model most commonly used to study the pathophysiology of multiple sclerosis (Khan & Smith 2014). The most commonly used method of inducing EAE is immunizing SJL or C57BL/6 mice with proteolipid protein (PLP) or myelin oligodendrocyte glycoprotein (MOG), which are present in myelin sheath in the CNS (Khan & Smith 2014). Induction of EAE leads to T-cell mediated demyelination and inflammation in the CNS, which mimics the pathology of MS (Storch et al 1998). As seen commonly in MS (Drulovic et al 2015, Foley et al 2013), EAE also leads to symptoms and signs of neuropathic pain such as mechanical allodynia, cold allodynia, and thermal hyperalgesia depending on the model (Lu et al 2012, Olechowski et al 2009). Although sensitized T-cells infiltrate both CNS and PNS, T-cell infiltration and inflammation only persists in the CNS (Duffy et al 2016, Olechowski et al 2009). Therefore, EAE is a useful model to examine the consequence of T-cell mediated autoimmunity and neuroinflammation in the context of neuropathic pain. My work in this thesis in fact aims to identify the impact of transient peripheral neuroinflammation on DRG neuron excitability.

1.4 Mechanisms of neuropathic pain: A focus on neuroplasticity

As evident by the diverse paths to induce neuropathic pain and distinct behavioral consequences in the animal models, neuropathic pain is a truly multifaceted disease. One of the defining characteristics of neuropathic pain is numerous maladaptive changes that occur within the peripheral and central nervous system after a peripheral nerve injury (Alles & Smith 2018, Costigan et al 2009). For instance, a peripheral nerve injury often triggers adaptations in the peripheral and central nociceptive pain pathway, which include changes in sensory neuron excitability, neurochemistry, and structure. This causes the pain pathway to become

hyperexcitable, which in turn triggers aberrant pain processing and symptoms and signs of neuropathic pain such as spontaneous pain, allodynia and hyperalgesia. These changes are often collectively referred to as 'peripheral sensitization' and 'central sensitization'. Here, I go over a few important maladaptive changes of the pain pathway that underlie the pathogenesis and the maintenance of neuropathic pain.

1.4.1 Ectopic discharges in primary sensory afferents and spontaneous pain

Wall and Gutnick (1974b) were one of the first to report nerve injury mediated maladaptive changes in the primary afferents. The authors demonstrated complete axotomy of sciatic nerve, and formation of a neuroma, leads to spontaneous ongoing activity in the primary afferents (Wall & Gutnick 1974b). This was a somewhat paradoxical finding as a complete axotomy should have denervated the cutaneous primary afferent terminals. In 1979, Wall et al. used the complete sciatic nerve axotomy as a rodent model of anaesthesia dolorosa (Wall et al 1979a, Wall et al 1979b). The authors showed complete axotomy leads to autotomy, mutilation of denervated limb and a sign of anaesthesia dolorosa, which could be ameliorated by suppressing the ongoing activity in the primary afferents (Wall et al 1979b). This was a seminal discovery in the research of pain as it provided the causal link between prolonged spontaneous discharges in the primary sensory afferents with neuropathic pain behavior (Wall et al 1979a, Wall et al 1979b). The original study assumed a neuroma was the major source of spontaneous ongoing activity (Wall & Gutnick 1974b). Interestingly however, a later study revealed blocking the sensory neuron activity in neuromata with lidocaine in amputees failed to alleviate spontaneous pain, which correlated with the continued presence of spontaneous ectopic discharges (Nystrom & Hagbarth 1981). This indicated the persistent ectopic discharges are generated elsewhere, which was most likely from DRG neurons themselves. This was later confirmed as Wall and Devor and other

groups demonstrated, with both *in vitro and in vivo* recordings, hyperexcitable large diameter Aβ DRG neurons were the main source of ongoing ectopic discharges seen in various animal models of neuropathic pain (Han et al 2000, Kajander & Bennett 1992, Study & Kral 1996, Wall & Devor 1983a). In contrast, Abdulla and Smith (2001b) rarely observed spontaneous discharges in dissociated DRG neurons from axotomized rats. Instead, the authors reported large diameter DRG neurons became profoundly more excitable compared to small diameter neurons, which only showed modest increase in excitability, in animals displaying autotomy (Abdulla & Smith 2001b). The authors however did note that neurons in dissociated culture lack an axon hillock region that may contribute to spontaneous discharges *in vivo*. These results suggest hyperexcitability and/or ectopic discharges in large diameter DRG neurons underlie the spontaneous pain behavior in animal models of neuropathic pain, and potentially in humans. In contrast to previously mentioned studies, Wu et al. and Djouhri et al. utilized modified SNL to selectively injure only the L5 spinal nerve, and recorded spontaneous ectopic discharges in the uninjured L4 DRG (Djouhri & Lawson 2004, Wu et al 2002). These authors reported uninjured C-fibre nociceptors in L4 DRG produced ectopic discharges in response to the modified SNL, which correlated with spontaneous foot withdrawal and allodynia. Therefore, aberrant activity from uninjured unmyelinated C-fibre nociceptor may also contribute to spontaneous ongoing pain in nerve injured animals. Overall, due to difficulties in testing spontaneous pain behavior explicitly in animal models of neuropathic pain, the precise cause-effect relationship between ectopic discharges in the DRG and spontaneous pain is still not unequivocally clear and is still an area of active investigation (Costigan et al 2009, Devor 2009, Koplovitch & Devor 2018).

1.4.2 DRG neuron hyperexcitability and ion channels involved

Numerous studies have consistently shown strong correlation with hyperexcitable DRG neurons, indicated by increased AP discharge and frequency, and mechanical allodynia using various animal models of neuropathic pain (Han et al 2000, Liu et al 2000a, Ma et al 2003, Wu et al 2002). Indeed, blocking ectopic discharges in DRG neuron with local application of lidocaine (Sukhotinsky et al 2004), suppressing ectopic discharges (Sun et al 2005), or ablating DRG input to spinal cord by dorsal rhizotomy (Na et al 2000) ameliorated mechanical allodynia in the nerve injured animals. Furthermore, most studies have also shown more noticeable increase in medium-large DRG neuron, soma of myelinated Aδ- and Aβ-fibres, excitability compared to small diameter C-fibre neurons (Abdulla & Smith 2001b, Han et al 2000, Liu et al 2000a, Ma et al 2003, Wu et al 2002). By contrast, SNI model also leads to a large increase in small-medium diameter DRG neurons excitability (Xie et al 2018). In general, nerve injury also leads to decreased rheobase (minimum current required for AP discharge) and increased AP duration (Abdulla & Smith 2001b, Kim et al 1998, Ma et al 2006, Study & Kral 1996, Xie et al 2018). Albeit with some inconsistencies, which most likely have risen from type of injury, animal species, and experimental methods, it is undeniable DRG neurons become hyperexcitable in response to many different nerve injuries. These changes are undoubtably mediated through changes in ion channel function and expression.

First, Voltage-gated Na^+ channels play an important role during the upstroke of AP discharge and change in their function can significantly alter neuron excitability. Therefore, sodium channel function has been of substantial interest to pain researchers. Earlier studies have implicated peripheral TTX sensitive Na^+ channels were involved in nerve injury induced ectopic discharges from neurons with ‘ectopic pacemaker capabilities’ as TTX or lidocaine eliminated

spontaneous discharges in the primary afferents largely without blocking nerve conduction (Amir et al 1999, Devor et al 1992, Matzner & Devor 1994). Dissociated DRG neurons from axotomized rats displaying autotomy behavior also displayed significantly larger TTX-S I_{Na} compared to control, which further supported the involvement of TTX-S I_{Na} in pain processing (Abdulla & Smith 2002). Accordingly, blocking aberrant DRG neuron activity with local injection of lidocaine ameliorated tactical allodynia rapidly (Sukhotinsky et al 2004). Furthermore, Ranolazine, which targets neuronal $Na_v1.7$ (SCN9A) and $Na_v1.8$ (SCN10A) to inhibit late $I_{Na,}$ has also been shown to attenuate behavioral signs of neuropathic pain (Gould & Diamond 2016, Gould et al 2009). Finally, a loss of function mutation in TTX-S $Na_v1.7$ (SCN9A) led to congenial inability to feel pain without losing the ability to perceive regular tactile stimuli, which provides cause-effect relationship between pain and $Na_v1.7$ (Cox et al 2006).

Peripheral TTX-R channels, such as $Na_v1.8$, and $Na_v1.9$, have also been implicated for the pathogenesis of neuropathic pain. $Na_v1.8$, which is encoded by SCN10A gene, is more preferentially expressed in C-fibre nociceptors (Akopian et al 1996), and contributes substantially to AP upstroke in small diameter DRG neurons (Renganathan et al 2001). $Na_v1.8$ has more depolarized voltage-dependence compared to TTX-S voltage gated Na^+ channels, in other words channels require more depolarized membrane potential to open; thus, it also inactivates at a more depolarized membrane potential which can prolong AP duration (Akopian et al 1996). $Na_v1.8$ has been implicated in transducing cold stimuli as it is relatively resistant to inactivation and remains available at lower temperatures (Zimmermann et al 2007). Nerve injury induced channel phosphorylation by p38 mitogen-activated protein kinase (MAPK) can increase $Na_v1.8$ current density (Hudmon et al 2008). Moreover, selective knock-down of $Na_v1.8$ (Lai et

al 2002), a specific $Na_v1.8$ blocker (Jarvis et al 2007), and optogenetic silencing of $Na_v1.8$ expressing primary afferents (Daou et al 2016) all alleviate inflammatory and neuropathic pain behaviors in animal models. Indeed, gain of function mutation in SCN10A has been implicated to contribute to human patients with painful C-fibre neuropathy (Faber et al 2012a).

$Na_v1.9$, which is encoded by SCN11A, is referred to as persistent TTX-R I_{Na} because it has hyperpolarized voltage-dependence for activation, but slower rate of activation and ultraslow inactivation (Dib-Hajj et al 2002). Therefore, it does not directly contribute to the upstroke of AP; rather it amplifies subthreshold depolarizing pulses and contribute to the generation of AP working with other Na^+ channels (Dib-Hajj et al 2002). Furthermore, it can also prolong AP duration as the current persists long after other I_{Na} have inactivated. This is evident in small IB_4^+ DRG neurons, where $Na_v1.9$ is preferentially expressed, as small IB_4^+ DRG neurons have much longer AP duration and larger TTX-R I_{Na} amplitude compared to small IB_4^- DRG neurons (Fang et al 2006, Stucky & Lewin 1999). As a result, $Na_v1.9$ has been implicated to play an important role in pain hypersensitivity during inflammation and injury. Indeed, disruption of $Na_v1.9$ gene leads to attenuation of thermal hyperalgesia and mechanical hypersensitivity only during inflammatory conditions (Amaya et al 2006, Priest et al 2005).

Second, K^+ channels are incredibly diverse as they are encoded by up to 78 different genes in humans (Ocana et al 2004), and numerous K^+ channels are expressed in the DRG neuron (Gold et al 1996). Voltage-gated K^+ channel currents, such as delayed-rectifier (I_K) and transient-fast inactivating A-type (I_A), and calcium-activated K^+ channel currents ($I_{K,Ca}$), such as large-conductance (BK) K^+ current (I_{BK}), play an important role during AP repolarization and afterhyperpolarization (AHP); therefore, they counteract depolarization and suppress activity (Tsantoulas & McMahon 2014). Downregulation of these currents can increase AP duration and

excitability in sensory neurons, which in turn can contribute to the pathogenesis of neuropathic pain (Tsantoulas & McMahon 2014). Indeed, many studies have consistently reported downregulation of I_K (Abdulla & Smith 2001a, Zhao et al 2013), I_A (Chien et al 2007, Everill & Kocsis 1999), and $I_{K,Ca}$ (Abdulla & Smith 2001a, Rasband et al 2001, Sarantopoulos et al 2007), which correlated with neuropathic pain behaviors and increased DRG neuron excitability. Furthermore, preventing I_K downregulation (Zhao et al 2013) and promoting BK channel opening (Chen et al 2009a) have been shown to alleviate neuropathic pain behavior following peripheral nerve injury.

Third, voltage-gated Ca^{2+} channels are the primary source of calcium influx into neurons upon depolarization. Calcium influx can have numerous effects in primary sensory afferents. For example, Ca^{2+} entry into primary afferent plays a critical role in neurotransmitter release (Katz & Miledi 1967), and change in intracellular Ca^{2+} can also modulate calcium-activated K^+ channel function, which in turn can significantly alter neuron excitability. Although voltage-gated Ca^{2+} channels can be classified into several subtypes, they can be broadly divided into two groups based on their voltage-dependence of activation (Bourinet et al 2014). Two main voltage-gated Ca^{2+} channels implicated for neuropathic pain in the primary afferents are N-type ($Ca_v2.2$), high voltage-activated, and T-type ($Ca_v3.1$, $Ca_v3.2$, and $Ca_v3.3$), low voltage-activated, Ca^{2+} channels (Waxman & Zamponi 2014). N-type Ca^{2+} channels play a critical role during neurotransmitter release and they are abundantly expressed in the primary afferent presynaptic terminals (Westenbroek et al 1992); therefore, increased N-type Ca^{2+} channels function or expression can significantly increase primary afferent synaptic transmission (Bourinet et al 2014). Indeed, it has been reported CCI injury leads to enduring increase in N-type Ca^{2+} channels in the spinal dorsal horn (Cizkova et al 2002). Accordingly, a potent N-type Ca^{2+} blocker ω-conotoxins GVIA (Diaz

& Dickenson 1997) and MVIIA (Bowersox & Luther 1998) have strong analgesic effect when administered intrathecally. In fact, ziconotide, a synthetic form of ω-conotoxins, is used therapeutically to treat neuropathic pain that is refractory to other treatments (McGivern 2007). Furthermore, studies have also shown $Ca_v\alpha2\delta1$subunit, accessory subunit of high voltage-activated Ca^{2+} channels, expression is upregulated following a nerve injury (Boroujerdi et al 2008, Luo et al 2002), and gabapentinoids, a first-line pharmacotherapy for neuropathic pain, are proposed to work by binding $Ca_v\alpha2\delta1$subunit and preventing channel trafficking to the primary afferent presynaptic terminal (Alles & Smith 2018, Dolphin 2012).

T-type Ca^{2+} channels have low voltage threshold for activation and thus can be activated close to resting membrane potential of a neuron (~-60 mV) (Bourinet et al 2014). Since they are abundantly expressed in DRG neuron and primary afferent presynaptic terminals, their activation can substantially increase DRG neuron excitability and contribute to the pathogenesis of neuropathic pain (Bourinet et al 2014). This is evident in peripheral neuropathy produced by STZ administration, which increased $Ca_v3.2$ expression and DRG neuron excitability (Jagodic et al 2007). Furthermore, $Ca_v3.2$ knockdown also ameliorated hyperalgesic responses in CCI operated animals indicating their role in neuropathic pain pathophysiology (Bourinet et al 2005).

Finally, hyperpolarization activated nucleotide-gated (HCN) channels (HCN1, 2, 3, 4) have also been implicated neuropathic pain. HCN channels activate in response to hyperpolarization and depolarize the membrane potential; thus, allowing quicker recovery from AHP and more rapid AP discharges (Chaplan et al 2003, Postea & Biel 2011). Although HCN channels are primarily expressed in cardiac pacemaker cells, they are also expressed in DRG neurons (Chaplan et al 2003, Emery et al 2011, Matsuyoshi et al 2006). It has been reported that nerve injury upregulates HCN channel expression predominantly in the medium and large DRG neurons,

which correlated with increase in their excitability (Chaplan et al 2003, Sun et al 2017, Yao et al 2003). Accordingly, application of HCN channel blockers such as ZD7288 and ivabradine rapidly ameliorated aberrant neuron excitability and mechanical allodynia in various animal models of neuropathic pain (Chaplan et al 2003, Emery et al 2011, Noh et al 2014, Sun et al 2005, Young et al 2014).

Overall, these results highlight the critical importance of ongoing hyperexcitability in the DRG neurons in the pathogenesis of neuropathic pain. However, the mechanisms leading to persistent primary afferent hypersensitivity are still not completely understood. Understanding this mechanism may be of particular interest as it may underlie the transition between acute nociceptive pain to chronic neuropathic pain. Therefore, my work in this thesis aims to reveal potential mechanisms that can contribute to this persistent hyperexcitability.

1.4.3 Central Sensitization

'Central sensitization' refers to a phenomenon of injury induced maladaptive neuroplasticity occurring within the CNS that triggers aberrant and amplified processing of nociceptive and tactile sensory information (Woolf 1983b). This phenomenon was first reported by Clifford Woolf in 1983. He demonstrated repeated noxious stimuli from the primary afferents 'sensitized' flexor motor neuron in the spinal cord, which normally only activates in response to noxious stimuli (Woolf 1983b). He reported, recording from a single neuron, in an injured animal a flexor motor neuron could be activated by innocuous stimuli that were also normally outside the receptive field of the flexor motor neuron being recorded. Furthermore, he demonstrated that local anaesthetic to the site of injury did not reverse these changes once it manifested indicating plasticity within the CNS. This was a seminal discovery at the time because it was thought hyperalgesia after an injury was solely due to nociceptor sensitization. Although numerous

complex maladaptive changes underlie the phenomenon of central sensitization, it can be broadly summarized in two key defining features: 1) amplified glutamatergic transmission and 2) loss of GABAergic/glycinergic inhibition in the spinal dorsal horn (Alles & Smith 2018).

First, ongoing ectopic discharges in C-fibres and the resulting increase in glutamatergic transmission from primary afferent can lead to *N*-methyl-D-aspartate (NMDA) receptor mediated activity dependant plasticity in the spinal dorsal horn neurons (West et al 2015, Woolf & Thompson 1991). It is suggested that aberrant glutamatergic transmission by C-fibre primary afferents leads to substantial activation of α-amino-3-hydroxy-5-methyl-4-isoxazolepropionic acid (AMPA) receptors. This then triggers abnormally large excitatory postsynaptic currents (EPSCs) that depolarize the membrane potential enough to unblock NMDA receptor, which is normally blocked by Mg^{2+} at resting membrane potential and during regular low frequency synaptic transmission (Nowak et al 1984, Woolf 2011). Finally, NMDA receptors can bind glutamate and activate, which leads to increased intracellular Ca^{2+} concentration (West et al 2015). This increase in $[Ca^{2+}]_i$ is believed to trigger downstream activation of various second messenger pathways, which then modulate and modify ion channel, and receptor function and expression to promote enduring hyperexcitability in spinal dorsal horn neurons (West et al 2015).

Second, loss of inhibition or disinhibition can have profound consequences in the pain pathway. This is evident as blocking GABAergic/glycinergic inhibitory transmission in the spinal cord leads to pain hypersensitivity and allodynia (Sivilotti & Woolf 1994, Yaksh 1989). Loss of inhibition or disinhibition can not only promote aberrant presynaptic activity, but also amplified postsynaptic EPSCs (Baba et al 2003, West et al 2015). This effect has been observed in our laboratory in the past as animals subject to the Mosconi & Kruger model of CCI exhibited increased amplitude and frequency of spontaneous and miniature EPSCs in putative excitatory

delay neurons in lamina II, but decreased amplitude and frequency of spontaneous and miniature IPSCs in putative inhibitory tonic neurons (Balasubramanyan et al 2006a). These results indicated there were both presynaptic and postsynaptic plasticity that contributed to decreased inhibitory tone and amplified excitatory transmission. Of particular interest was another study indicating decreased Cl^- gradient caused by injury induced reduction in expression of potassium-chloride exporter KCC2 (Coull et al 2003a). The decrease in Cl^- gradient can lead to more depolarized anion reversal potential, which in turn attenuates GABA/glycine mediated IPSCs and hyperpolarization. Remarkably, the authors observed Mosconi & Kruger model of CCI leads to significant decrease in KCC2 expression, which in turn switched normally inhibitory GABAergic/glycinergic transmission into excitatory transmission increasing overall excitability in the lamina I spinal dorsal horn neurons (Coull et al 2003a).

Taken together with somewhat paradoxical aberrant Aβ-fibre activity mediated neuropathic pain behaviors seen in many animal models of peripheral nerve injury (Devor 2009, Han et al 2000, Kajander & Bennett 1992, Study & Kral 1996, Wall & Devor 1983a), these findings provide important links that illuminate potential mechanisms underlying ongoing spontaneous pain, allodynia, and hyperalgesia.

1.5 Neuroimmune interactions and neuropathic pain: A focus on interleukin-1β

Since the discovery of neurotransmitter receptors in peripheral lymphocytes (Hadden et al 1970), the communication between the nervous system and the immune system has been an area of substantial research interest (Dantzer 2018). Cytokines are the putative 'neurotransmitters' of the immune system that facilitate immune cell-cell communication and modulation (Bartfai & Schultzberg 1993). The line between cytokines and neurotransmitters has been becoming progressively ambiguous since the clonal identification of proinflammatory cytokine interleukin-

1β (IL-1β) (Auron et al 1984, Dinarello et al 1977). IL-1β was one of the first cytokines reported to directly influence cell activity in the nervous system through modulation of ion channels (Miller et al 1991, Plata-Salaman & Ffrench-Mullen 1992, Schettini et al 1988). It is now widely accepted that neuron-immune crosstalk mediated by cytokines, chemokines, neurotrophic factors, and neurotransmitters in the PNS and CNS are critical for maintaining physiological function as well as pathogenesis of many disease states (Carson et al 2006, Dantzer 2018, Watkins & Maier 2002).

Research on neuroimmune interactions led to substantial advances in our understanding of the etiology and the pathophysiology of chronic neuropathic pain; such that, neuropathic pain is now considered a 'neuroimmune disorder' (Grace et al 2014, Scholz & Woolf 2007a). Crosstalk between sensory neurons and resident and infiltrating immune cells filled the missing links that could not be explained before. Particularly, a proinflammatory cytokine interleukin-1β (IL-1β) has been implicated to play a critical role by mediating neuroimmune interaction during nociception and pathogenesis of neuropathic pain (Bianchi et al 1998, Binshtok et al 2008, Ferreira et al 1988, Ren & Torres 2009, Scholz & Woolf 2007a, Sommer et al 1999). In the following sections, I briefly describe a few key neuroimmune interactions that contribute to the aberrant primary afferent activity and central sensitization in the context of IL-1β (see Figure 1-4 for brief summary of important neuroimmune interactions for neuropathic pain).

1.5.1 What is IL-1β?

Before the clonal identification, fever inducing endogenous protein released by monocytes was known as leukocytic pyrogen (Dinarello et al 1977). Later, leukocytic pyrogen was sequenced and identified as IL-1α and IL-1β (Auron et al 1984). We now know IL-1β is a potent proinflammatory cytokine in the IL-1 super family, which consists of 11 distinct molecules

(Garlanda et al 2013). IL-1β is produced by innate immune cells, such as monocytes and macrophages, and glial cells, such as satellite glial cells, astrocytes, and spinal microglia upon injury or infection (Garlanda et al 2013). Although IL-1β is primarily produced by innate immune cells and glial cells, DRG neurons can also produce IL-1β in response to inflammatory stimuli and injury (Copray et al 2001). Unlike IL-1α, which is constitutively expressed (Chen et al 2007), IL-1β production and secretion are triggered by inflammatory stimuli caused by injury or infection (Garlanda et al 2013). Furthermore, IL-1β precursor is biologically inactive, and it requires further processing by proteolytic enzymes such as caspase-1, metalloprotease-2 and 9 (MMP-2, 9) to be activated (Garlanda et al 2013, Ji et al 2009). Activation of nucleotide-binding domain (NOD)-like receptor protein 3 (NLRP3) inflammasome, an intracellular signaling protein complex, and subsequent proteolytic cleavage of pro-IL-1β by caspase-1 is the most well characterized mechanism of IL-1β production (Jo et al 2016).

1.5.2 IL-1β as a modulator of primary afferent excitability and synaptic transmission

IL-1β was also the first cytokine indicated to mediate nociception as a systemic injection of it led to profound hyperalgesia in rats (Ferreira et al 1988). This was later confirmed to be a result of primary afferent sensitization by Fukuoka et al (1994) by *in vivo* recording from DRG. The authors demonstrated intraplantar injection of IL-1β led to not only augmented AP discharges in response to mechanical, heat, and cold stimuli, but it also led to decreased threshold and increased spontaneous ectopic discharges in the DRG (Fukuoka et al 1994). Furthermore, hyperalgesia by intraplantar injections of various inflammatory molecules such as lipopolysaccharides (LPS), bradykinin, IL-1β, and carrageenan was reversed by local injection of IL-1 receptor antagonist (IL-1Ra), which clearly indicated the involvement of IL-1β during nociception (Cunha et al 2000).

It was later revealed that sensory neurons abundantly express IL-1 receptor type I (IL-1RI), which can bind both IL-1α and β (Copray et al 2001, Obreja et al 2002). This was evident as brief application of IL-1β to dissociated DRG neuron cultures led to potentiation and decreased threshold of capsaicin induced inward current in small-medium DRG neurons, that give rise to heat-sensing C- and Aδ-fibres, by protein kinase C (PKC) dependant mechanisms (Obreja et al 2002). IL-1β can also bind IL-1R1 to induce cyclooxygenase-2 (COX-2) gene expression in DRG neurons and spinal cord neurons (Fehrenbacher et al 2005, Samad et al 2001a). COX-2 is not normally expressed in DRG neurons and spinal cord neurons in contrast to COX-1; therefore, IL-1β induced COX-2 gene expression greatly increases prostaglandin (Dou et al 2004, Samad et al 2001b). Since, prostaglandins have been shown to be involved in peripheral sensitization by phosphorylating voltage-gated Na^+ channels, IL-1β may be involved in the 'phenotypic switch' that is implicated to produce persistent hyperexcitability in primary afferents (Amir et al 1999, Laedermann et al 2015, Matzner & Devor 1994). Furthermore, Binshtok et al (2008) reported IL-1β can directly activate and sensitize small DRG neurons. The authors showed that 10-minute bath application of IL-1β profoundly increased nociceptor excitability, and it modulated both TTX-S and TTX-R Na^+ channel functions by p38-MAPK. p38 can phosphorylate Na^+ channels, mirroring the changes seen in response to nerve injury (Binshtok et al 2008, Hudmon et al 2008). In contrast, Liu et al (2006) reported brief incubation with IL-1β led to a reduction of total I_{Na} in capsaicin-sensitive TG neuron, but 24 hour incubation with IL-1β selectively increased TTX-S I_{Na} without affecting TTX-R I_{Na} (Liu et al 2006). These results suggest the effect of IL-1β depends on the duration of exposure. Therefore, our laboratory has utilized chronic IL-1β treatment, which mimicked the time course of IL-1β expression in the peripheral nerve following an injury (Nadeau et al 2011), to examine consequent DRG neuron excitability. We showed that

long-term IL-1β treatment leads to cell type dependent hyperexcitability in medium sized DRG neurons, and in small IB_4^+ DRG neurons to a lesser extent (Stemkowski et al 2015, Stemkowski & Smith 2012a). This was largely caused by attenuation of K^+ channel currents, which was also in line with the changes seen in the DRG neurons from nerve injured animals (Abdulla & Smith 2001a). Interestingly, the changes in medium sized DRG neuron excitability were largely reversible, which indicated chronic IL-1β treatment alone did not lead to the 'phenotypic switch' which has been implicated to trigger persistent hypersensitivity. The reversibility of IL-1β induced changes in the small IB_4^+ neuron is yet to be determined, and some of the work in my thesis intends to answer this question.

In addition, IL-1β has also been shown to modulate synaptic transmission in the spinal dorsal horn. Acute application of IL-1β led to increases in spontaneous EPSCs amplitude and frequency as well as decreases in spontaneous IPSCs amplitude and frequency in unidentified interneurons in the spinal dorsal horn (Kawasaki et al 2008b). These effects were mediated through enhanced AMPA- and NMDA-induced inward currents and diminished GABA- and glycine-induced outward currents as seen in spinal dorsal horn neurons after peripheral nerve injury (Baba et al 2003, Balasubramanyan et al 2006a, West et al 2015). It has been suggested that IL-1β amplifies glutamatergic postsynaptic transmission by phosphorylation of the NMDA receptor, which in turn leads to larger increase in intracellular calcium concentration ($[Ca^{2+}]_i$) (Viviani et al 2003). This was later confirmed as blocking IL-1RI with IL-1Ra attenuated NMDA receptor phosphorylation as well as inflammatory hyperalgesia (Zhang et al 2008). Our laboratory has also confirmed some of these findings using an organotypic cultures of rat spinal cord (Gustafson-Vickers et al 2008). Chronic IL-1β led to an overall increase in spinal dorsal horn excitability, as indicated by amplified $[Ca^{2+}]_i$ increase in response to depolarization with 35 mM

K^+, and modulation of synaptic transmission in a cell-type dependant manner. The authors observed increased amplitude of spontaneous EPSCs, indicating amplified postsynaptic glutamatergic transmission, and decreased frequency of spontaneous IPSCs, indicating presynaptic alterations of inhibitory transmission. These results suggest IL-1β mediates maladaptive changes in the pain pathway following a peripheral nerve injury.

Numerous studies have reported increased IL-1β expression in the site of injury, DRG, spinal cord, and brain following a nerve injury (del Rey et al 2011, Hashizume et al 2000, Kawasaki et al 2008a, Kiguchi et al 2010, Lim et al 2017, Nadeau et al 2011, Schuh et al 2014, Takeda et al 2008, Yang et al 2018). Of note, Yang et al. recently demonstrated IL-1β was upregulated in the uninjured nerve in modified SNL, which increased DRG neuron excitability through modulation of the N-type Ca^{2+} channel (Yang et al 2018), which provides a potential underlying mechanism of previously reported spontaneous C-fibre discharges in the uninjured nerve (Djouhri & Lawson 2004, Wu et al 2002). Neutralizing antibodies to IL-1RI attenuated mechanical allodynia and thermal hyperalgesia in nerve injured mice (Schafers et al 2001, Sommer et al 1999), and both IL-1RI knockout and IL-1Ra overexpression in mice prevented development of mechanical allodynia after SNL by attenuating spontaneous ectopic discharges in the Aδ-fibres (Wolf et al 2006). Overall, these results indicate that modulation of sensory neuron excitability and synaptic transmission by IL-1β plays an important role in neuropathic pain pathogenesis.

1.5.3 Peripheral macrophage and Satellite glial cells in neuropathic pain pathogenesis

Macrophages and satellite glial cells are major sources of IL-1β in the DRG following a nerve injury (Figure 1-4) (Garlanda et al 2013, Kawasaki et al 2008a, Kiguchi et al 2010, Takeda et al 2008). Macrophages polarize within a spectrum, which can be broadly classified by their gene expression and phenotype (Murray 2017). For instance, in one end of the spectrum, pro-

inflammatory M1 macrophages generally secrete pro-inflammatory cytokines such as IL-1β, IL-6, and tumor necrosis factor alpha (TNFα) (Murray 2017). On the other end of the spectrum, anti-inflammatory M2 macrophages generally secrete more anti-inflammatory cytokines such as IL-10 (Murray 2017). Peripheral nerve injury leads to both proliferation and infiltration of macrophage in the injury site and the DRG (Kiguchi et al 2017). This leads to subsequent release of various cytokines, such as TNFα, IL-6 and IL-1β, and chemokines, such as chemokine ligand 2 (CCL2) and CCL3 which are known to directly sensitize primary afferents and DRG neuron (Kiguchi et al 2017). Macrophage infiltration and IL-1β is also needed for Wallerian degeneration and subsequent nerve regeneration, which promote proper functional recovery following nerve injury (Nadeau et al 2011). Ablation of peripheral macrophages delayed the onset mechanical allodynia (Cobos et al 2018) and attenuated heat hyperalgesia as well as axonal degeneration (Liu et al 2000b). Furthermore, inhibition of peripheral macrophage by nicotinic acetylcholine receptor agonist 7-10 days post peripheral nerve injury attenuated IL-1β at the site of injury, mechanical allodynia, and activation of spinal microglia (Kiguchi et al 2018). These results indicate IL-1β released by peripheral macrophages may contribute to both onset and the maintenance of mechanical allodynia.

Satellite glial cells (SGCs) are the glial cells of the peripheral nervous system, and they envelop DRG and TG neurons tightly forming a functional unit (Figure 1-4) (Hanani 2013). Upon peripheral nerve injury, SGCs proliferate and activate, which in turn leads to production and secretion of proinflammatory cytokines such as IL-1β and TNFα (Ji et al 2009, Lim et al 2017, Liu et al 2012, Takeda et al 2008). Remarkably, SGCs have been implicated to receive direct input from sensory neurons (Takeda et al 2008, Takeda et al 2009, Zhang et al 2007). For example, sensory neuron depolarization can lead to exocytosis of adenosine triphosphate (ATP)

from the soma which then can bind to P2X7 receptors expressed in SGCs. This subsequently leads to activation of SGCs and increased IL-1β and TNFα release from SGCs, which in turn can modulate sensory neuron excitability (Takeda et al 2008, Takeda et al 2009, Zhang et al 2007). This is evident as blocking primary afferent activity by TTX prevents activation of SGCs following SNI and SNL in rats (Xie et al 2009). Inhibiting SGC activation and resulting decrease in IL-1β expression have been shown to alleviate mechanical allodynia and thermal hyperalgesia caused by peripheral nerve injury through reducing colony stimulating factor 1 (CSF1) production in DRG neurons (Figure 1-4) (Lim et al 2017), which has been shown to be critical for spinal microglia activation as well as onset and maintenance of neuropathic pain (Guan et al 2016, Okubo et al 2016). Interestingly, peripheral nerve injury leads to differential regulation of MMP-2 and 9 in neurons and SGCs (Kawasaki et al 2008a). Kawasaki et al. showed SGCs have delayed but persistent upregulation of MMP-2, which then can promote activation and secretion of IL-1β during the chronic phase of neuropathic pain. Since IL-1β can directly modulate DRG neuron excitability as well as induce CSF1 production, this may underlie the distinct behavioral outcome triggered by CCI (transient allodynia) and SNI (persistent allodynia). Therefore, some of the work in this thesis seeks to explain the differential reversibility of SNI compared to CCI in the context of neuroimmune crosstalk mediated by IL-1β.

1.5.4 Microglia and central sensitization

Microglia, a resident macrophage of the CNS, are one of the main producers of IL-1β in the CNS following a nerve injury (Chen et al 2018b, Garlanda et al 2013, Grace et al 2014). Of particular interest were the studies demonstrating the role of microglia activation for central sensitization. As mentioned earlier, peripheral nerve injury leads to amplified glutamatergic transmission and loss of inhibition by downregulation of KCC2 (Coull et al 2003a). It was later revealed that this

was caused by activation of microglia (Coull et al 2005). Studies have shown that peripheral nerve injury leads to profound upregulation of P2X4 receptors expressed in microglia (Tsuda et al 2003). Upon binding ATP, which may be released from primary afferents and/or spinal dorsal horn neurons, production and secretion of brain derived neurotrophic factor (BDNF) is amplified (Figure 1-4) (Ulmann et al 2008). Furthermore, the production and exocytosis of BDNF was revealed to be mediated through p38-MAPK pathway (Trang et al 2009). BDNF released by microglia then binds to TrkB receptors expressed in spinal dorsal horn neurons to cause attenuation of KCC2 and more depolarized Cl^- reversal potential (Coull et al 2005, Coull et al 2003b, Trang et al 2009). Furthermore, BDNF has also been reported to potentiate glutamatergic synaptic transmission (Biggs et al 2010, Kerr et al 1999). For instance, BDNF can activate TrkB receptor, which in turn phosphorylates GluN2B subunit of the NMDA receptor (Biggs et al 2010, Compston & Coles 2008, Hildebrand et al 2016, Kerr et al 1999). Since both IL-1β and BDNF can both promote aberrant synaptic transmission and central sensitization, activation of microglia has been suggested to play an essential role during the onset and the maintenance of neuropathic pain (Chen et al 2018b). Indeed, Grace et al. have demonstrated selective inhibition of microglia activation by a single intrathecal injection of inhibitory designer receptor exclusively activated by a designer drug (G_i DREADD) acutely ameliorated mechanical allodynia (Grace et al 2018), but this reversal of allodynia was transient as it returned by 24 hours post-injection. Furthermore, preventing production of CSF1 by *Csf1* knockout in the primary afferent (Guan et al 2016) and inhibiting CSF1 receptor (CSF1R) in the spinal cord (Okubo et al 2016) was also able to attenuate mechanical allodynia following nerve injury. These results clearly indicate the importance of microglia in the pathogenesis and maintenance of neuropathic pain. However, more recent studies have revealed microglia activation is sexually dimorphic (Sorge et al 2015,

Vacca et al 2014). Although peripheral nerve injury leads to substantial activation of spinal microglia in both male and female mice, only male mice depend on microglia activation for neuropathic pain behaviors (Sorge et al 2015). In stark contrast, T-cell infiltration to the CNS is implicated to mediate mechanical allodynia in female mice. These findings add another layer of complexity to already multifaceted etiology and pathophysiology of neuropathic pain.

1.6 Hypotheses

Although decades of rigorous research have significantly improved our understanding of etiology and pathophysiology of neuropathic pain, the transition between acute nociceptive pain to chronic neuropathic pain state is still an area of broad and current interest. It is believed that by inducing long-term changes in the excitability of sensory nerves; it indirectly drives increased excitability in the spinal dorsal horn and the development (Vaso et al., 2014) and persistence of central sensitization (Pitcher and Henry, 2008). The importance of this ongoing hyperexcitability is evident as alleviating aberrant primary afferent and DRG neuron activity readily ameliorates spontaneous pain in patients with peripheral neuropathy (Haroutounian et al 2014), phantom limb pain in amputees (Vaso et al 2014) as well as mechanical allodynia in rodents (Dou et al 2004, Noh et al 2014, Weir et al 2017, Young et al 2014) long after the establishment of neuropathic pain. However, the mechanisms responsible for maintaining the persistent primary afferent hyperexcitability are not fully understood.

The goal of my thesis is to demonstrate the role of IL-1β in the persistent DRG neuron hyperexcitability and the maintenance of neuropathic pain. The following hypotheses will be examined:

1) Long-term IL-1β treatment, with proper neurotrophic support with GDNF, will lead to persistent changes in the small IB_4^+ DRG neuron excitability.
2) EAE induction and subsequent neuroinflammation in the DRG mediated by IL-1β will trigger persistent hyperexcitability in the DRG neurons working in concert with other inflammatory mediators.
3) The degree and the duration of neuroinflammation in the DRG will underlie the differential behavior observed in CCI and SNI model of neuropathic pain.

Figure 1-1

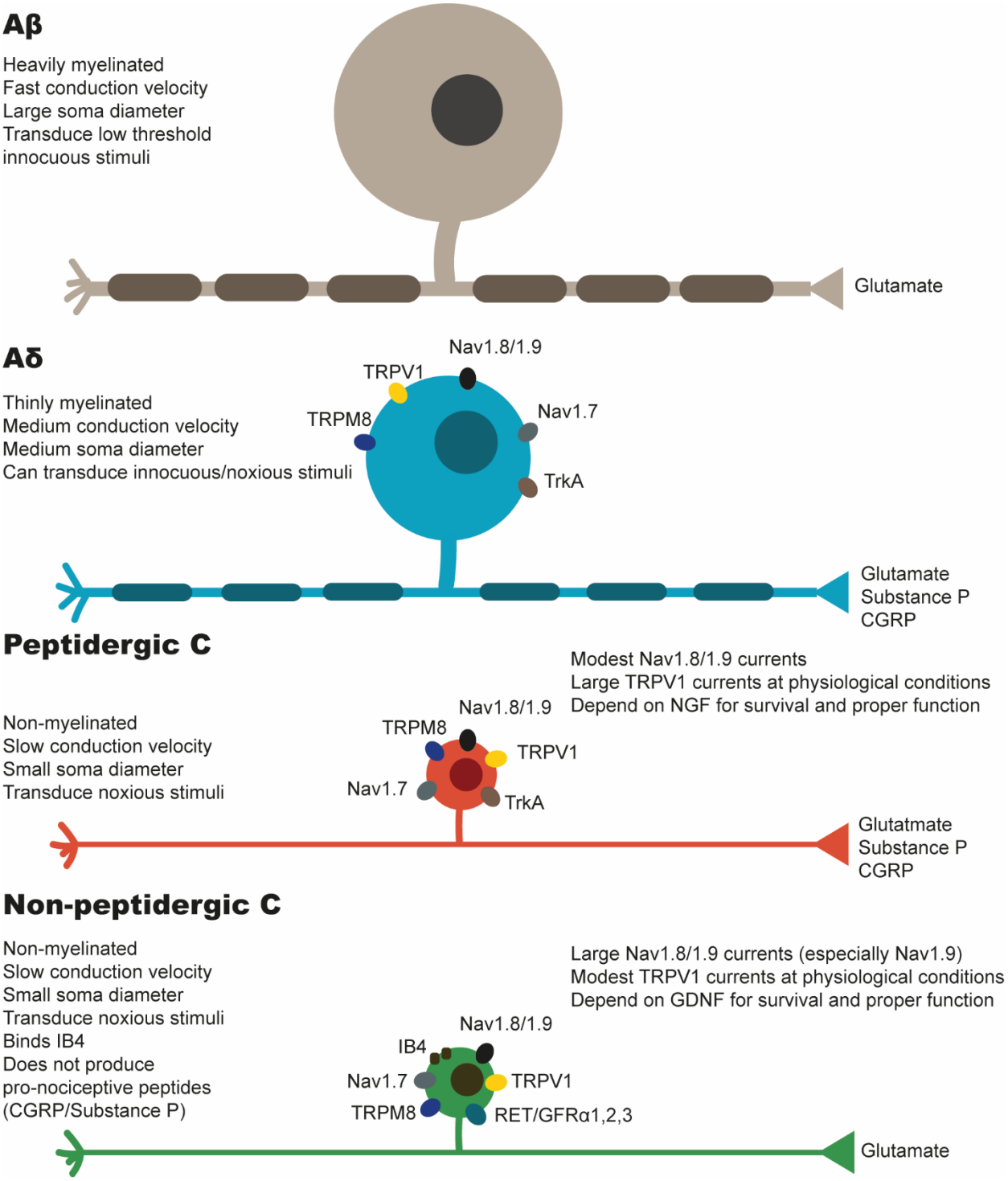
Aβ
Heavily myelinated
Fast conduction velocity
Large soma diameter
Transduce low threshold
innocuous stimuli
Glutamate
Aδ
Thinly myelinated
Medium conduction velocity
Medium soma diameter
Can transduce innocuous/noxious stimuli
Nav1.8/1.9
TRPV1
TRPM8
Nav1.7
TrkA
Glutamate
Substance P
CGRP
Peptidergic C
Non-myelinated
Slow conduction velocity
Small soma diameter
Transduce noxious stimuli
Modest Nav1.8/1.9 currents
Large TRPV1 currents at physiological conditions
Depend on NGF for survival and proper function
Nav1.8/1.9
TRPM8
TRPV1
Nav1.7
TrkA
Glutatmate
Substance P
CGRP
Non-peptidergic C
Non-myelinated
Slow conduction velocity
Small soma diameter
Transduce noxious stimuli
Binds IB4
Does not produce
pro-nociceptive peptides
(CGRP/Substance P)
Large Nav1.8/1.9 currents (especially Nav1.9)
Modest TRPV1 currents at physiological conditions
Depend on GDNF for survival and proper function
Nav1.8/1.9
IB4
Nav1.7
TRPV1
TRPM8
RET/GFRα1,2,3
Glutamate

Figure 1-1. General characteristics of primary sensory afferents. Primary afferents have been subdivided into two main groups based on axon diameter, myelination, and conduction velocity. Primary afferents exhibit diverse neurochemistry and gene expression which gives them the ability to transduce a wide spectrum of sensory information.

Figure 1-2

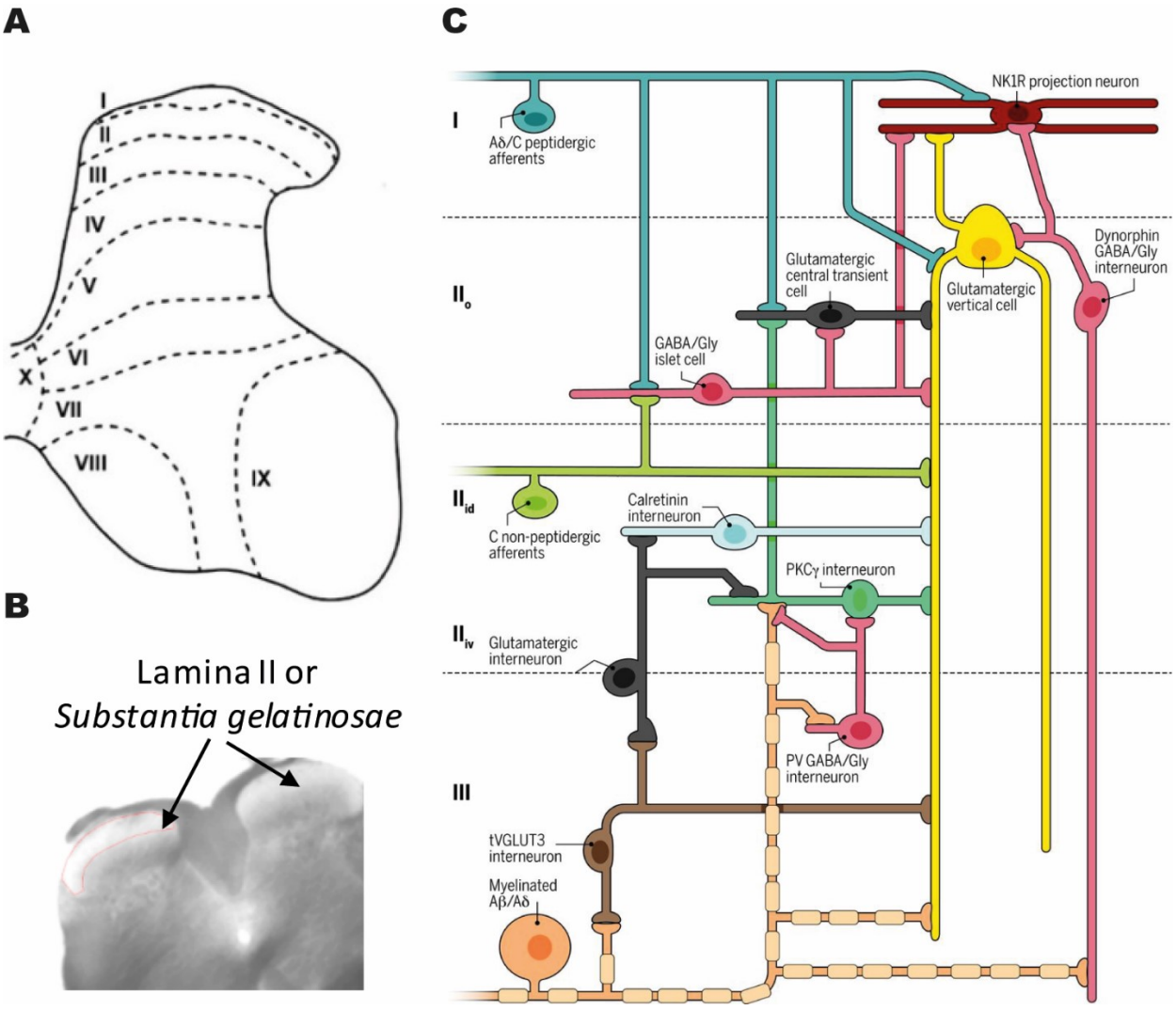

Figure 1-2. Organization of spinal dorsal horn and its neural circuitry. **A.** Rexxed laminae of the spinal dorsal horn. **B.** Representative image of the Substantia gelatinosae or Lamina II. Substantia gelatinosa predominantly process and integrate noxious stimuli. **C.** Neural circuits involved in the processing of sensory information. Reprinted from Peirs C and Seal RP (2016) Neural circuits for pain: recent advances and current views. Science 354:578?584. Reprinted with permission from American Association for the Advancement of Science.

Figure 1-3

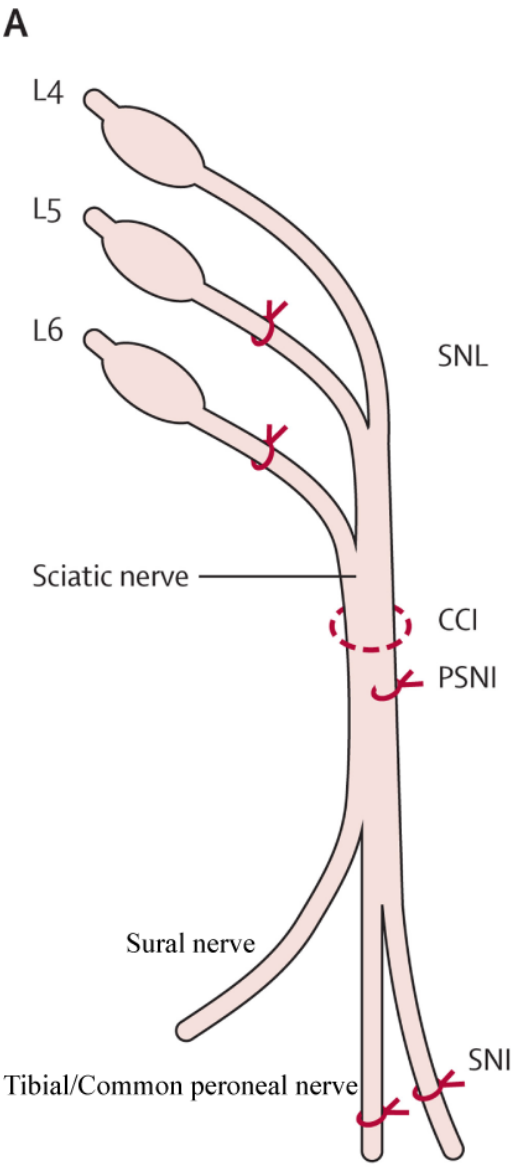

Figure 1-3. Various animal models of peripheral nerve injury. Different methods of nerve injury can lead to diverse pain phenotypes. Spinal nerve ligation (SNL), chronic constriction injury (CCI), partial sciatic nerve ligation (PSL or partial sciatic nerve injury; PSNI), and spared nerve injury (SNI) are the most commonly utilized models of peripheral nerve injury to induce neuropathic pain in rodents. Reprinted from The Lancet Neurology, Vol. 11, Calvo M, Dawes JM, Bennett DL, The role of the immune system in the generation of neuropathic pain, pages 629-42., Copyright (2012), with permission from Elsevier.

Figure 1-4

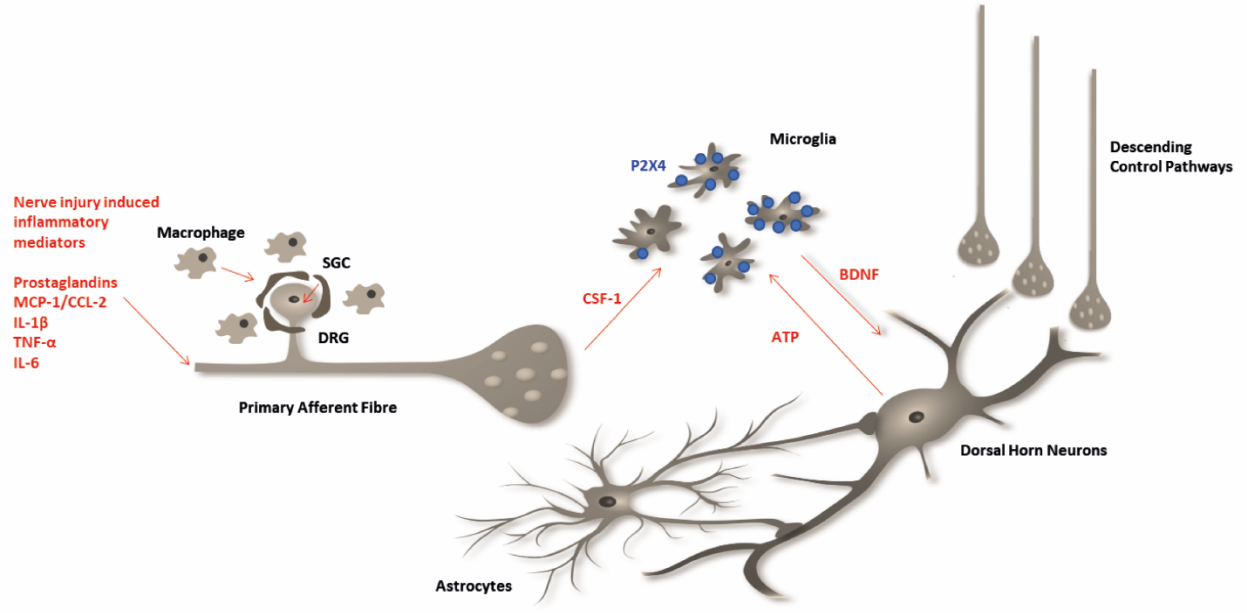

Figure 1-4. A brief summary of a few important neuroimmune interactions in the neuropathic pain pathophysiology. Macrophages and satellite glial cells are major sources of IL-1β in the peripheral nervous system. Activation of microglia by CSF-1 or ATP leads to release of BDNF, which can sensitize dorsal horn neurons to promote central sensitization.

Chapter 2

Methods

2.1 Animal Ethics

All experimental procedures complied with the guidelines of the Canadian Council for Animal Care. These procedures were reviewed and approved by the University of Alberta Health Sciences Laboratory Animal Services Welfare Committee.

2.2 Long-Term Neuron Enriched Rat Dorsal Root Ganglia (DRG) Culture

2.2.1 Culture Dish Preparation

In order to ensure cell adherence, culture dishes were pre-treated. These preparations were done a day before a dissection. Pre-plates were made with 60 mm Nunc™ Cell Culture dishes (Nalge Nunc International, Rochester, NY, USA), which were treated with 3 μg/ml polyornithine (Sigma, St. Louis, MO, USA). DRG neuron enriched culture plates were made with 35 mm Nunc™ Cell Culture dishes (Nalge Nunc). These plates were coated with 3 μg/ml polyornithine (Sigma) followed by 2 μg/ml laminin (Sigma). Furthermore, pre-plates and cell culture plates were kept inside a 150 mm culture dish (Corning, Corning, NY, USA) for additional protection.

2.2.2 Dissection and Enzymatic Digestion

Long term DRG neuron cultures were made as previously described (Stemkowski et al 2015). 16-20 days old male Sprague Dawley rats (Science Animal Support Services, Edmonton, AB, Canada) were euthanized with intraperitoneal injection of 1g/ml urethane (Sigma). Subsequently, their lumbar and thoracic DRGs, 20-28 DRGs per animal, were aseptically dissected out via laminectomy. During the dissection, spinal cord and DRGs were all immersed in a dissection solution [118mM NaCl, 2.5mM KCl, 1.3μM $MgSO_4$, 1.2mM NaH_2PO_4, 5mM $MgCl_2 \cdot 6H_2O$, 25mM D-glucose, 26mM $NaHCO_3$, and 1.5mM $CaCl_2$] with carbogen bubbling. Immediately after the dissection, DRGs were enzymatically digested through a 3-step procedure. First, DRGs were transferred to media, containing 1.25 mg/ml type IV collagenase (Worthington, Lakewood,

NJ, USA) dissolved in Dulbecco's Modified Eagle Medium with GlutaMAX™ (Gibco, Grand Island, NY, USA) (DMEM) supplemented with 10% heat inactivated horse serum (Sigma) (DMEMHS), and shaken in a water bath set at 35 degrees Celsius for 90 minutes. Following the first enzyme treatment, partly digested DRGs were carefully washed with Calcium/Magnesium-free Dulbecco's phosphate buffered saline (DPBS) (Gibco) three times. Secondly, DRGs were treated with 2.5 mg/ml trypsin (Sigma) solution made in DPBS for 30 minutes in a shaking water bath. Then, DRGs were washed 3 times with DMEMHS. Finally, 2 ml of DMEMHS containing 0.1 mg/ml deoxyribonuclease I (Sigma) and soybean trypsin inhibitor (Worthington) were added to the DRGs. Subsequently, enzymatically digested DRGs were mechanically broken up by several passages through 1 ml glass pipette.

2.2.3 Neuron Enrichment

Dissociated DRG solution (1 ml/dish) was put into pre-plates coated with 3 µg/ml polyornithine (Sigma). In order to minimize non-neuronal cell growth, 5 ml of DMEMHS containing 1% antibiotic-antimycotic (AA) solution (Gibco) and anti-mitotic (AM) mixture [10 µM cytosine β-D-arabinofuranoside (Sigma), uridine (Sigma), and 5-fluoro-2'-deoxyuridine (Sigma)], were added to each pre-plate. Then, pre-plates were kept in the incubator maintained at 36.5 °C, 95% air, and 5% carbon dioxide (CO_2) overnight. The following day, non-neuronal cells were strongly attached to the pre-plate; however, neuronal cells were loosely bound to the pre-plate. Using a defined media (1:3 Ham's F12 nutrient mix (Gibco): DMEM with 1% N-2 supplement (Gibco) and 1% AA solution), pre-plates were washed 5 times (1 ml per wash with glass pipette) to dislodge loosely adhering neuronal cells. Defined media containing neuronal cells were collected in a two separate 14 ml conical tubes (Corning) for centrifugation. Subsequently, conical tubes were centrifuged for 5 minutes at 500 rpm in a cold room (4 °C). Following the

centrifugation, supernatant containing non-neuronal cells were discarded carefully, and the pellet containing neuronal cells were resuspended in 1 ml of defined medium. Finally, 100 µl of the resulting solution was added to pre-treated 35 mm cell culture plates, and 2 ml of defined media was subsequently added per plate. Cells were maintained at 36.5 °C, 95 % air, 5% CO_2.

2.2.4 DRG Culture Treatment and Experimental Time Course

Unless otherwise specified, neurons were pretreated with 50 ng/ml glial cell line derived neurotrophic factor (GDNF) or nerve growth factor (NGF) (Alomone Labs, Jerusalem, Israel; prepared in 0.1% BSA (Sigma) dissolved in HBSS) following the initial DRG isolation, and they were continuously supplemented throughout the experiment. After 3 days in culture, dishes were divided into two groups: 100 pM IL-1β (Peprotech, Rocky Hill, NJ, USA; prepared in 0.1% BSA (Sigma)) and control (0.1% BSA). Treatments were applied for the following 5–6 days, with defined medium exchanges every 72 hours (Stemkowski et al 2015, Stemkowski & Smith 2012a). Neurons in time matched cultures treated with 0.1 % BSA alone, 50 ng/ml GDNF, or 50 ng/ml NGF also served as controls (Figure 2-1). For washout of IL-1β, medium was exchanged every 72 hours for 3-4 days, and medium was exchanged three times at each time point to ensure maximal IL-1β removal. The time course and treatment of the cultures with IL-1β with GDNF or NGF supplementation are illustrated in Figure 2-1A.

2.3 Subclassification of DRG neurons

2.3.1 Rat DRG neurons

Rat DRG neurons were classified according to soma diameter as ‘small’ (< 30 µm), ‘medium’ (30-40 µm), or ‘large’ (>40 µm) as measured with a calibrated micrometer in the eye piece of a Nikon TE300 inverted fluorescence microscope (Nikon, Tokyo, Japan). Since small diameter IB_4-positive and IB_4-negative sensory neurons display distinct phenotype with regards to pain

physiology, these cell types were distinguished by including 5 μg/ml isolectin B_4 (IB_4) Alexa Fluor® 488 conjugate in dishes of DRG neurons for 10 minutes prior to recording (Life Technologies, Eugene, OR, USA) (Fang et al 2006, Stucky & Lewin 1999). Only the most intensely stained small DRG neurons were considered IB_4^+ neurons to minimize misclassification of small IB_4^- or possibly peptidergic visceral DRG neurons as small IB_4^+ (Robinson et al 2004).

2.3.2 Mice DRG neurons

There have been reports of experimental autoimmune encephalomyelitis (EAE) leading to preferential damage to medium and large diameter sensory neurons, which give rise to thinly myelinated Aδ-fibres and heavily myelinated Aβ-fibres respectively, in the trigeminal ganglia and the DRG (Duffy et al 2016, Pender 1986, Wang et al 2017). Therefore, a more simplified classification subdividing DRG neurons into 'small' (<26 μm) neurons, which give rise unmyelinated C-fibre, and 'medium-large' (≥26 μm), which predominantly give rise to myelinated A-fibres, was used to examine the impact of EAE on the electrophysiological properties of likely-unmyelinated or likely-myelinated mice DRG neurons (Dirajlal et al 2003, Harper & Lawson 1985, Ruscheweyh et al 2007).

2.4 Electrophysiology

Whole-cell recordings were made at room temperature, (22°C) from DRG neurons using an NPI SEC-05LX amplifier (ALA Scientific Instruments Farmingdale NY, USA) in either bridge-balance current-clamp mode or discontinuous single-electrode current or voltage-clamp mode. Low resistance recording electrodes (2-5 MΩ) were used for all electrophysiology experiments. Input capacitance (C_{in}) was calculated from the membrane time constant and input resistance or by the integration of the capacitative transient generated by a 10 mV voltage step as previously

described (Abdulla & Smith 1997). The effectiveness of the voltage-clamp was determined by examining voltage recordings from neurons; if the voltage trace was slow to rise or distorted, it was discarded. Representative current records were low pass filtered to -3dB at 300Hz.

2.4.1 Current Clamp Experiments

For current-clamp experiments, external solution contained (in mM) 127 NaCl, 2.5 KCl, 1.2 NaH_2PO_4, 26 $NaHCO_3$, 2.5 $CaCl_2$, 1.3 $MgSO_4$ and 25 D-glucose saturated with 95% O2 – 5% CO2. Internal (pipette) solution contained (in mM) 130 KGluconate, 4 Mg-ATP, 0.3 Na-GTP, 10 EGTA, 2 $CaCl_2$ and 10 HEPES (adjusted to pH 7.2 with KOH; osmolarity 310-320 mOsm). Action potentials (AP) were generated with 5 ms depolarising current pulses while the resting membrane potential was held at -60 mV. Cells with resting membrane potential (RMP) more positive than -40 mV were considered not viable and were discarded. Rheobase was determined via injection of a series of 5 ms depolarizing current commands with 0.1 nA increments. The AP evoked at rheobase was used for the analysis of AP parameters. AP duration at 50% AP amplitude, spike height (amplitude), max rate of rise, max rate of decay, afterhyperpolarization (AHP) amplitude, and AHP time to peak were measured (Figure 2-1B). For the examination of calcium-activated potassium current (I_{KCa}) block on AP duration, 100 nM iberiotoxin (IBTX; Alomone Labs), which blocks the big potassium (BK) channels, was bath applied after the baseline AP recording has been made. After 5 minutes, an AP was evoked again, and its duration was recorded for comparison. For the measure of neuronal excitability, 450 ms depolarizing current ramp with 0.5 nA increments up to 2 nA were used to evoke AP discharges. Number of APs and the latency of each AP (cumulative latency) were noted in response to the 2 nA ramp.

2.4.2 Voltage Clamp Experiments

2.4.2.1 Sodium current recordings

Sodium current (I_{Na}) was recorded in an external solution containing (in mM), 75 tetraethylammonium chloride (TEA-Cl), 50 NaCl, 5 KCl, 4 $MgCl_2$, 10 HEPES and 60 D-glucose (adjusted to pH 7.4 with NaOH; osmolarity 330 mOsm). Internal solution contained (in mM), 140 CsCl, 10 NaCl, 2 MgATP, 0.3 Na_2GTP, 2 EGTA, 10 HEPES and 2 $MgCl_2$ (adjusted to pH 7.2 with NaOH; osmolarity 300-310 mOsm). Total I_{Na} was recorded in response to 40 ms depolarizing voltage commands (-80 mV to 60 mV) from a holding potential (V_h = -90 mV) and leak subtracted by means of a p/6 protocol (Stemkowski et al 2015). Then, 300 nM Tetrodotoxin (TTX) (Alomone Labs, Jerusalem, Israel) was applied to cell culture by superfusion for 5 minutes. TTX resistant (TTX-R) I_{Na} was recorded using the same protocol as total I_{Na}. Total I_{Na} was subtracted with TTX-R I_{Na} to reveal TTX sensitive (TTX-S) I_{Na}. For voltage-dependence of activation, normalized (I/I_{-20}) I-V curves were fit with a Boltzmann sigmoidal function, y = A2 + (A1-A2)/(1 + exp((x-x_0)/dx)) which yielded slope factor and voltage for half activation (V_{50}). I_{Na} steady-state fast inactivation protocol involved 300 ms pre-pulses increasing from -110 mV followed by 10ms test pulses to -10mV to determine the fraction of current available (I/I_{-110}). Current decay (fast inactivation) was fitted with a single exponent function, $f(t)=\sum_{i=1}^{n} Ai\ e^{-t/\tau i}$ + C. Fast inactivation protocol was repeated after TTX bath application, and TTX-R fast inactivation was recorded. TTX-S inactivation was then revealed by subtraction (Total I_{Na} inactivation – TTX-R I_{Na} inactivation). The I_{Na} steady-state slow inactivation protocol involved application of 5 s pre-pulses in 10 mV increments, followed by 20 ms recovery pulses to−120mV, which allows recovery from fast inactivation, followed by 10 ms test pulses to−10mV to determine the fraction of current available (I/I_{-120}).

2.4.2.2 Potassium Current Recordings

For recording K^+ channel currents, external solution contained (in mM) 145 *N*-methyl-D-glucamine (NMG)Cl, 10 KCl, 2.5 $CaCl_2$, 10 HEPES, 1.0 $MgCl_2$ and 10 D-glucose (adjusted to pH 7.4 with HCl; 320 mOsm). Internal solution contained (in mM) 100 K gluconate, 40 NMG-Cl, 2 Mg-ATP, 0.3 Na_2GTP, 11 EGTA, 10 HEPES and 0.1 $CaCl_2$ (adjusted to pH 7.2 with HCl; 300 mosm). Equilibrium potential for K^+ (E_K) was -58mV. In view of the complexity and variability of potassium currents in DRG neurons a simplified approach was used for their isolation (Abdulla & Smith 2001a, Gold et al 1996, Stemkowski et al 2015). Total I_K was recorded at voltages between -60 mV and +60 mV following a 500 ms conditioning pre-pulse to either -120 mV or -30 mV and leak subtracted by means of a p/6 protocol. Voltage commands were then repeated in the presence of 5 mM Mn^{2+} to reveal Mn^{2+} resistant I_K. Digital subtraction of Mn^{2+}-resistant I_K from the total I_K yielded Mn^{2+} sensitive I_K which corresponded to the total Ca^{2+} sensitive K^+ current and conductance ($I_{K,Ca}$ $g_{K,Ca}$) (Abdulla & Smith 2001a). A-type potassium current (I_A) was obtained via subtracting Mn^{2+} resistant I_K recorded with a -30 mV pre-pulse from that recorded with a -120 mV pre-pulse (Stemkowski et al 2015).

2.4.2.3 Calcium current recordings

Calcium current (I_{Ca}) was assessed using Ba^{2+} as a charge carrier (I_{Ba}). External solution contained (in mM) 160 TEA-Cl, 10 HEPES, 2 $BaCl_2$, 10 D-glucose and 300 nM TTX (adjusted to pH 7.4 with TEA-OH; osmolarity 330-340 mOsm). Internal solution contained (in mM) 120 CsCl, 5 Mg-ATP, 0.4 Na_2-GTP, 10 EGTA and 20 HEPES (adjusted to pH 7.2 with CsOH; osmolarity 300-310 mOsm). Cells were either held at V_h= -100 mV or V_h= -60 mV. Then, I_{Ba} was evoked via using a series of 150 ms depolarizing voltage commands (-70 mV to 30 mV) and leak subtracted by means of a p/6 protocol. For the voltage dependence of I_{Ba} inactivation, the

fraction of current available at command voltage (V_{cmd}) = -10 mV was determined in response to a series of 3.5 s incremental pre-pulses from V_h = -100 mV. Normalized (I/I_{-110}) inactivation curves were fit with a Boltzmann sigmoidal function $y = A2 + (A1-A2)/(1 + \exp((x-x_0)/dx))$ to obtain slope factor and V_{50}.

2.5 Experimental Autoimmune Encephalomyelitis (EAE) Experiments

2.5.1 EAE Induction and Assessment

EAE mice were produced in Dr. Bradley Kerr's lab using the method previously described in Olechowski et al (2009). For EAE induction, 8-10-week-old female C57/BL mice were subcutaneously injected with 50 µg of myelin oligodendrocyte glycoprotein fragment 35-55 (MOG_{35-55}) (Peptide Synthesis Facility, Stanford University, CA, USA) emulsified in complete Freund's adjuvant (CFA). In contrast, control mice only received subcutaneous injection of CFA. Furthermore, mice received intraperitoneal injection of 300 ng pertussis toxin from *Bordatella pertussis* (List Biological Labs, Campbell, CA, USA) on the day of and 48 hours after the EAE induction. Following the EAE induction, mice were examined daily for clinical signs of EAE based on a 5-point scale described in Kalyvas and David (2004): Grade 0, no clinical signs; Grade 1, limp tail; Grade 2, mild hindlimb weakness; Grade 3, severe hindlimb weakness and slow righting reflex; Grade 4, complete hindlimb paralysis; Grade 5, complete hindlimb paralysis with forelimb weakness.

2.5.2 DRG Extraction and Generation of Acute Mice DRG neuron Culture

L4-L6 DRGs were extracted from both EAE and CFA control mice at two separate time points (Figure 2-2). First, DRGs were taken out during the onset of the disease, when EAE induced mice started to show grade 1 (limp tail) clinical signs. Secondly, DRGs were extracted 7 days after the initial disease onset. DRGs from Time controlled CFA control mice were also extracted

on the same day. Mice were euthanized via intraperitoneal injection of 0.34 g/ml EUTHASOL® (Merck Animal Health, Madison, NJ, USA). Subsequently, mice were intracardially perfused with ice-cold 0.9% saline and L4-L6 DRGs were harvested. Immediately following the dissection, DRGs were transferred to ice-cold dissection solution. Subsequently, DRGs were enzymatically digested for short-term culture as before (Alier et al 2008, Noh et al 2014). DRGs were digested in a DMEM with GlutaMAX™ (Gibco) containing 1 mg/ml collagenase type IV collagenase (Worthington), 0.5 mg/ml trypsin (Sigma), and 0.1 mg/ml deoxyribonuclease I (Sigma) for 40 minutes in a shaking water bath set at 35 °C. Cells were also manually shaken by hand every 10 minutes to promote dissociation. After 40 minutes, cells were transferred into corning tubes and centrifuged at 500 rpm for 5 minutes. Supernatant was removed with care and 2 mL DMEM with 14 mg/ml soybean trypsin inhibitor (Worthington) was added. Cells were further triturated via several passages through 1 ml glass pipette. Dissociated cells were plated onto 35 mm Nunc™ Cell Culture dishes (Nalge Nunc) pre-coated with 3 μg/ml polyornithine (Sigma) and 2 μg/ml laminin (Sigma). 2 ml of DMEMHS containing 1% antibiotic-antimycotic (AA) solution (Gibco) and anti-mitotic (AM) mixture [10 μM cytosine β-D-arabinofuranoside (Sigma), uridine (Sigma), and 5-fluoro-2'-deoxyuridine (Sigma)], were added to each dish. Cells were kept in the incubator maintained at 36.5 °C, 95% air, and 5% carbon dioxide (CO_2) for at least 2 hours to allow proper cell adherence, and they were then used for electrophysiology.

2.6 Neuropathic Pain Animal Models

2.6.1 Chronic Constriction Injury (CCI)

The Mosconi-Kruger model of CCI was used for my studies (Mosconi & Kruger 1996). 200-250 g male Sprague Dawley rats (Science Animal Support Services and Charles Rivers, Wilmington, MA, USA) were used for CCI. First, rats were anesthetised with isoflurane (up to 5% during

induction and 2-3% during maintenance), and left thigh of rat was shaved with electric clipper to expose the skin. Eye lubricant (Aventix Animal Care, Burlington, ON, Canada) was applied, and Betadine (Betadine, Stamford, CT, USA) was applied to the exposed skin. Small incision was made in the skin with sterile surgical blade, and the left sciatic nerve was exposed via blunt dissection. Subsequently, two polyethylene cuffs made with PE90 tubing (Intramedic, Sparks, MD, USA), which was 2 mm long, inside diameter 0.86mm, and outside diameter 1.27mm, were carefully slid onto the exposed sciatic nerve. Then, muscle tissue was sealed with 5-0 silk suture (Henry Schein, Melville, NY, USA), and skin was closed with 4-0 silk suture (Ethicon, Somerville, NJ, USA). Finally, Betadine was applied again, and the animals were kept inside a recovery chamber until they were able to freely move around.

2.6.2 Spared Nerve Injury (SNI)

SNI was performed as described previously (Decosterd & Woolf 2000, Pertin et al 2012). 200-250 g male Sprague Dawley rats (Science Animal Support Services and Charles Rivers) were used for SNI. Animals were anesthetised, and left thigh skin was exposed; this was followed by application of eye lubricant and Betadine as previously described in CCI protocol. 1 cm incision was made mid thigh to expose the *biceps femoris* and artery *genus descendes*. Then, sciatic nerve and three terminal branches, which consisted of common peroneal, tibial, and sural nerve, were exposed via careful blunt dissection. Extreme care was taken not to stretch or damage any of the nerves. Then, common peroneal and tibial nerve was individually ligated tightly with 5-0 silk suture (Henry Schein). Subsequently, at roughly 5 mm distal to the ligation site, 2-4 mm of the common peroneal and tibial nerve was cut and removed. Sural nerve was spared, and extreme care was taken not to stretch or damage the sural nerve. As previously in CCI, muscle tissue and skin were closed with 5-0 silk suture (Henry Schein) and 4-0 silk suture (Ethicon) respectively.

Betadine was applied to the incision site, and animals were placed inside a recovery chamber until full recovery.

2.6.3 Sham Surgery

Sham surgery was performed as control. Sham surgery consisted of the same surgical procedure as aforementioned CCI and SNI; however, the sciatic nerve was exposed then muscle and skin were quickly closed back up without making any contact with the nerve.

2.6.4 Animal Housing and Experimental Time Course

Two male Sprague-Dawley rats were housed per cage with *ad libitum* access to food and water in our animal housing facility throughout the experiment. All animals were acclimatized for a day before any behavioral analysis. On the day of the surgery, animals were weighed, and baseline mechanical thresholds were examined via von Frey test. Animals were then randomly selected for sham, CCI, SNI surgery. Following the surgical procedures, they were von Frey tested every 7 days following the surgical procedures over 42 days (Figure 2-3).

2.6.5 von Frey Test

Rats were individually placed in a chamber with wire-grid bottom, and they were acclimatized for at least one hour before the test. 1.4 g, 2 g, 4 g, 6 g, 10g, and 15 g von Frey hairs were used for testing. Starting from the lightest von Frey hair, pressure was applied, until the filament buckled, to the mid-plantar area of the left hind paw for CCI and sham animals. For SNI animals, lateral surface of the hind paw, which is innervated by the spared sural nerve, was pressured instead. This was done to maximize the pain response and minimize the false negative result from pressuring the areas innervated by common peroneal and tibial nerve, which have been axotomized. Paw withdrawal, jumping, and licking of the hind paw, were considered a pain

response. For every von Frey filament, animals were tested 5 times, and if pain responses are displayed 3 or more times, weight of the von Frey filament was recorded as the paw withdrawal threshold. If a von Frey filament failed to produce enough pain responses, heavier filaments were used (up to 15 g) after a few minutes of recovery period. This was repeated until paw withdrawal threshold could be recorded. If no pain response could be obtained, paw withdrawal threshold was recorded as 15 g due to absence of heavier von Frey filament. An animal with paw withdrawal threshold below 6 g was considered mechanically hypersensitive.

2.6.6 Tissue Extraction

Following behavioral analysis, tissue samples were collected at different time points for further analysis (Figure 2-3). L4-L5 lumbar DRGs were collected for real time quantitative polymerase chain reaction (rt-qPCR) or immunohistochemistry (IHC). Rats were anesthetized with isoflurane and subsequently euthanized with lethal dose of urethane (Sigma) via intraperitoneal injection. Then, they were transcardially perfused with 0.9% saline. Animals that were used for IHC were further perfused with 4% paraformaldehyde (Acros Organics, Geel, Belgium) in 0.9% saline. Both ipsilateral and contralateral L4-L5 DRGs were dissected out. After the dissection, some DRGs were snap frozen with liquid nitrogen and stored in -80°C for ELISA, some were stored in RNAlater (Invitrogen, Carlsbad, CA, USA) for rt-qPCR, and some were fixed with 4% PFA in the fridge overnight for IHC.

2.7 Quantification of Messenger Ribonucleic Acid (mRNA)

2.7.1 Tissue Homogenization and Total RNA Extraction

Colony stimulating factor 1 (CSF1) and IL-1β mRNA levels were measured in ipsilateral DRGs of sham, CCI and SNI animals via rt-qPCR. Furthermore, mRNA level of CSF1 was measured in neuron enriched culture in order to examine the effect of long-term IL-1β exposure on DRG

neurons. All experiments described in this section have been carried out in RNase free environment. Tools, bench space, and gloves were wiped with RNase Away (Ambion) before starting the experiment; furthermore, all reagents and containers used in these experiments were RNase free. To begin with, total RNA was extracted from ipsilateral DRG tissue samples and neuron enriched DRG culture. For DRG tissue samples, tissue was washed with ice-cold PBS twice, and DRGs were mechanically homogenized with Potter-Elvehjem Tissue Grinders (Wheaton) with 700µl QIAsol lysis reagent (Qiagen, Venlo, Netherlands). For neuron enriched culture, 35mm cell culture plate (Nalge Nunc) were washed twice with ice-cold PBS, and 1 ml QIAsol lysis reagent (Qiagen) was added to both control and IL-1β treated DRG neuron enriched culture for 5 minutes. Subsequently, DRG cells were scrapped with 3cm blade BD Falcon cell scraper (Corning). Cell lysate from both DRG tissue sample and DRG cell culture were pipetted onto QIAshredder (Qiagen) and centrifuged at full speed for 2 minutes to get a fully homogenized cell lysate. In order to purify and isolate total RNA from the cell lysate, RNeasy Lipid Tissue Mini Kit (Qiagen) was used. RNase free chloroform (140 µl per 700 µl lysate) was added to the lysate, and the lysate was centrifuged for 15 minutes at 12000g at 4°C to isolate the RNA layer. Top layer, which only contained RNA, was removed and equal volume of 70% ethanol was added. Subsequently, the RNA solution was then further purified through RNeasy spin columns following the manufacturer's instructions. Purified RNA was reconstituted in 30 µl RNase free water, and the total RNA concentration of each samples were quantified via NanoPhotometer NP80 (Implen, München, Germany), which was generously provided by Dr. Basil Hubbard. Finally, the RNA samples were stored in -80°C freezer for future use.

2.7.2 Complementary DNA (cDNA) Synthesis

Complementary DNA (cDNA) was synthesized via reverse transcription. First, each RNA samples (200ng/8µl) were treated with DNase I (Invitrogen) for 15 minutes at room temperature in order to degrade any DNA contaminants in the sample. 1µl of 25mM Ethylenediaminetetraacetic acid (EDTA) was added after the incubation to block any DNase I activity before moving on to the next step. Then the samples were placed in BioRad C1000 Thermal Cycler (Bio-Rad Laboratories, Hercules, CA, USA), which was generously provided to us by Dr. Bradley Kerr, for 10 minutes at 65°C; then it was held at 4°C. Oligo(dT)12-18 Primer (Invitrogen) and dNTP (Invitrogen) were added to the sample and, they were placed back in the thermal cycler for 5 minutes at 65°C, then held at 4°C. Superscript III reverse transcriptase (Invitrogen), and RNase OUT (Invitrogen) were added to the sample following the manufacturer's instructions. In addition, negative controls were generated by not adding reverse transcriptase to the samples. Finally, reverse transcription was carried out in the thermal cycler using the following temperatures: 25°C for 5 minutes; 50°C for 1 hour; 70°C for 15 minutes; and held at 4°C. Synthesized cDNA samples and negative controls were stored in -20°C freezer for future use.

2.7.3 Real Time Quantitative Polymerase Chain Reaction (rt-qPCR)

QuantiTect primer assays were carried out by using Fast SYBR Green MasterMix (Applied Biosystems, Foster City, CA, USA) following the manufacturer's instructions. All the primers used in rt-qPCR experiments are summarized in Table 2-1. For the cDNA samples from L4-L5 DRG tissue, *Csf1*, *Il1b*, or *Ppia* (Peptidyl-Prolyl cis-trans Isomerase A) primers were mixed with SYBR Green MasterMix. For the cDNA samples from DRG neuron enriched culture, only *Csf1* or *Ppia* primers were mixed with the SYBR Green MasterMix. The primer solution was loaded

onto 96 well plate (Bio-Rad Laboratories). Subsequently, cDNA samples were loaded into each well as triplicates. 96 well plate was then covered and centrifuged for 1 minute at 500 rpm at 4°C. Finally, PCR reactions were performed on BioRad CFX96 thermocycler (Bio-Rad Laboratories), which was generously provided by Dr. Basil Hubbard. Data were obtained in Bio-Rad CFX Manager software using *Ppia* as a reference gene. Melt curves were analyzed to minimize false positive signals from primer dimerization. Data obtained in CFX manager was expressed in log2, and this was transformed on a linear scale as fold-change in gene expression relative to appropriate time-controlled sham group.

2.8 Immunohistochemistry (IHC)

2.8.1 Tissue Preparation and Sectioning

This IHC protocol was adapted and modified from Benson et al (2015). Ipsilateral L4-L5 DRGs were fixed overnight in 4% PFA made with 0.9% saline at 4°C. On the next day, the DRGs were cryoprotected via sucrose gradient method. Firstly, the DRGs was washed 3 times with PBS (Fisher Scientific), and then transferred into 20% sucrose made in PBS at 4°C until the DRGs sank to the bottom. Subsequently, DRGs were transferred to 30% sucrose made in PBS for 2 days at 4°C. Secondly, sucrose treated DRGs were embedded with optimum cutting temperature (OTC) compound (Fisher Scientific) inside an embedding mold made with aluminium foil. Both L4-L5 DRGs were embedded side by side per animal. Then, embedded tissues were frozen slowly by placing the embedding mold on a weigh boat (Fisher Scientific) inside a liquid nitrogen bath. Once the OCT compound was completely frozen, tissue was stored inside a -80°C freezer. Finally, embedded DRG samples were cryosectioned into 12-micron slices onto a Superfrost™ Plus Microscope Slides (Fisher Scientific) at -20°C via Leica CM1950 cryostat (Leica, Wetzlar, Germany), which was generously provided to us by Dr. Bradley Kerr. On a

single microscope slide, each DRG slice was separated by at least 4 sections to minimize analyzing the same cell multiple times. Prepared slides were labeled and stored in -80°C.

2.8.2 Co-Immunostaining CSF1 and GFAP

In order to examine the protein expression levels of CSF1 and GFAP between the nerve injury models; CSF1 and GFAP were double immunostained in DRG slices of sham, CCI, SNI animals. First, slides were thawed at room temperature for 15 minutes, and they were washed in PBS for 5 minutes three times on a shaker. Subsequently, small circles were drawn around the DRG slices with liquid blocker Super PAP pen (Daido Sangyo, Tokyo, Japan). Immediately after, tissues were blocked with 10% donkey serum (Sigma) block solution, made in PBS with 0.2% Triton X-100 (PBStx 0.2%) (Fisher Scientific), for 1 hour at room temperature inside an IHC incubation chamber filled with water. Care was taken to never let tissues dry out. After one hour, the block solution was discarded, and the DRG sections were incubated overnight at room temperature inside a humid IHC chamber with the primary antibody solution [1:500 goat anti CSF1 (R&D Systems, Minneapolis, MN, USA) and 1:1000 rabbit anti GFAP (Dako, Santa Clara, CA, USA) primaries in PBStx (0.02%) with 2% donkey serum (Sigma) and 2% bovine serum albumin (BSA) (Sigma)]. Next day, slides were washed 3 times in PBS (Fisher Scientific) with 0.5% Tween-20 (Sigma) (PBStw) for 10 minutes on a shaker. Then, in a dark room secondary antibody solution [1:200 Donkey Anti-Goat IgG Alexa Fluor 488 (Invitrogen) and 1:200 Donkey Anti-Rabbit IgG Alexa Fluor 594 secondaries in PBStx 0.2%] was added to each slide. Slide chamber was covered with aluminium foil, and it was incubated at room temperature for 1 hour. Following the secondary antibody incubation, slides were washed 3 times with PBS (Fisher Scientific). Finally, in a dark room, DRG slices were counterstained with VECTASHIELD® Antifade Mounting Medium with 4′,6-diamidino-2-phenylindole (DAPI) (Vector Laboratories,

Burlingame, CA, USA) and cover slipped with Fisherbrand™ Superslip Cover Slips (Fisher Scientific). Slides were sealed with nail polish, then dried for an hour under aluminium foil cover at room temperature before storing at 4°C fridge. The primary and secondary antibodies are summarized in Table 2-2.

2.8.3 Co-Immunostaining Ionized calcium binding adaptor molecule 1 (Iba1) with CSF1 and activating transcription factor 3 (ATF3) with CSF1

In order to study the expression of Iba1, CSF1, and ATF3 and their relationships in response to different nerve injuries Iba1 and CSF1 as well as ATF3 and CSF1 were co-immunostained in DRG slices from sham, CCI, and SNI animals. A different IHC protocol was used AffiniPure Anti-Goat IgG Alexa Fluor 594 (Jackson Immunoresearch, West Grove, PA, USA), was not compatible with bovine serum albumin (BSA). With AffiniPure Anti-Goat IgG Alexa Fluor 594, DRGs stained with the antibody solution containing BSA produced substantially greater background and unspecific binding. Therefore, an IHC protocol modified from Braz and Basbaum (2008), which used 10% serum block solution as an antibody solution, was utilized instead. First, tissues were thawed and washed with PBS 3 times for 5 minutes on a shaker as before. Then, small circles were drawn with Super PAP pen (Daido Sangyo), and DRG slices were incubated for 1 hour at room temperature with 10% donkey serum (Sigma) block solution, made in PBStx (0.5%) instead of PBStx (0.2%), in a humid IHC slide chamber. After blocking, serum block solution was discarded, and slices were incubated overnight at room temperature in the primary antibody solutions [1:500 goat anti CSF1 (R&D Systems) and 1:1000 rabbit anti Iba1 (Wako, Osaka, Japan) primary antibodies in PBStx (0.5%)] or [1:500 goat anti CSF1 (R&D Systems) and 1:500 rabbit anti ATF3 (Santa Cruz Biotechnology, Dallas, TX, USA) in PBStx (0.5%)]. Then, slides were washed 3 times for 10 minutes with PBStw on a shaker. Subsequently

slides were incubated with secondary antibody solution [1:200 AffiniPure Donkey Anti-Goat IgG Alexa Fluor 594 (Jackson Immunoresearch) and 1:200 Donkey Anti-Rabbit IgG Alexa Fluor 488 (Invitrogen) in PBStx (0.5%)] for an hour at room temperature. Rest of the protocol was the same as described in Chapter 2.8.2.

2.8.4 Image Acquisition and Analysis

2.8.4.1 ATF3-CSF1 and Iba1-CSF1 Double Labelled DRG Slices

Iba1-CSF1 and ATF3-CSF1 co-immunostained slides were imaged with an Olympus IX-81 microscope (Olympus Corporation, Tokyo, Japan) equipped with CSU X1 spinning disk confocal scan-head (Yokogawa Electric, Tokyo, Japan). Entire DRG slice was imaged using 20X oil immersion lens using appropriate filters (DAPI, GFP, and RFP). Images were automatically stitched in Volocity Acquisition software (Quorum Technologies Inc., Guelph, ON, Canada), and they were imported to Fiji software for analysis. For all IHC analysis, at least 2 DRG sections were analyzed per animal, and minimum of 300 DRG neurons were analyzed per animal. CSF1 expression was analyzed by counting CSF1 positive cells, which were determined by thresholding the signal intensity in Fiji software. Then, every DRG neurons in each DRG section were counted, and the number of CSF1 expressing DRG neurons were divided by the total number of cells to get the percentage of CSF1 positive DRG neuron. ATF3 positive cells were manually counted after thresholding, and it was divided by the total number of DRG neurons in a slice to calculate the percentage of ATF3 positive neurons. DRG neurons expressing both CSF1 and ATF3 were also counted, and it was divided by the total ATF3 positive DRG neurons to determine the percentage of injured DRG neurons that also express CSF1. Total Iba1-immunoreactive cells were counted via thresholding and particle analysis in Fiji. Furthermore, to study the potential spatial association between macrophage and CSF1 production, the number of

'Iba1-ring' around the DRG neuron were quantified (Vega-Avelaira et al 2009). Then the proportion of cells co-expressing CSF1 immunoreactivity and the 'Iba1-ring' were quantified.

2.8.4.2 GFAP-CSF1 Double Labeled DRG Slices

GFAP and CSF1 co-immunostained DRG slides were imaged with Zeiss Axiocam MRm camera and Zeiss Observer Z1 inverted fluorescence microscope (Zeiss, Oberkochen, Germany). The entire DRG was imaged by taking multiple images with 20X lens using appropriate filters (DAPI, green fluorescent protein (GFP), and red fluorescent protein (RFP)). For analysis, individual images were stitched in Fiji software via the built in stitching plugin (Preibisch et al 2009). Then, the composite image was split into individual channels for analysis. CSF1 was quantified as described in section 2.8.4.i. GFAP signal was confirmed by thresholding signal intensity and area fraction of GFAP signal in a section was quantified. Furthermore, in order to examine the potential spatial association between activated satellite glial cells and CSF1 immunoreactivity, the 'GFAP-ring' around DRG neurons were quantified as described previously by Berta et al (2012). Then, DRG neurons co-expressing CSF1 and 'GFAP-ring' were quantified.

2.9 Statistical Analysis and Graphing

All electrophysiology data were obtained and analyzed by pCLAMP 10 (Molecular Devices). Statistical analyses were carried out in GraphPad Prism 7 software (GraphPad Software, San Diego, CA, USA). For comparison of two groups, unpaired two-tailed Student's t-test with Holm-Sidak post hoc analysis were performed. One-way analysis of variance (ANOVA) with Bonferroni's multiple comparisons test was utilized for 3 or more groups. Two-way ANOVA with Bonferroni's multiple comparisons test was used for comparing cumulative latencies between 3 groups. For non-parametric analyses, Mann-Whitney test was used for comparison

between 2 groups, and Kruskal-Wallis test with Dunn's multiple comparisons test was used for 3 groups or more. Correlation between variables were determined by calculating the Pearson correlation coefficient, r, and obtaining the r squared value. Two-tailed Fisher's exact test was used to compare action potential firing frequencies between control and diseased groups. For all statistical analysis, significance was assigned to $p<0.05$ with 95% confidence interval. All data were expressed as mean ± standard error of the mean (SEM). All graphs were constructed using both GraphPad 7 and Origin 2015 (Origin Lab Corp., Northampton, MA, USA).

Figure 2-1

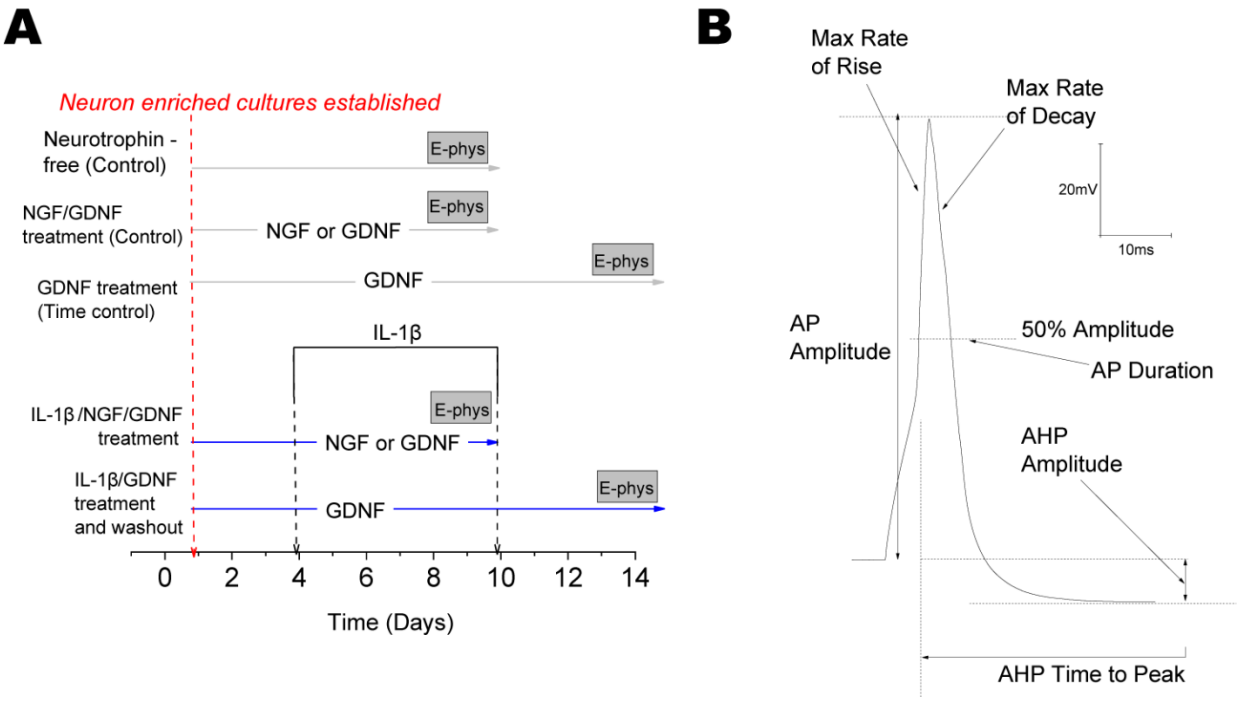

Figure 2-1. Experimental time course and AP parameters for IB_4^+ small DRG neuron experiments. **(A)** Scheme to show time course of exposure to IL-1β, NGF or GDNF from time of establishment of neuron enriched cultures. Grey bars indicate during periods in which electrophysiological recordings were made. **(B)** Representative AP describing AP parameters measured in IB_4^+ small DRG neuron.

Figure 2-2

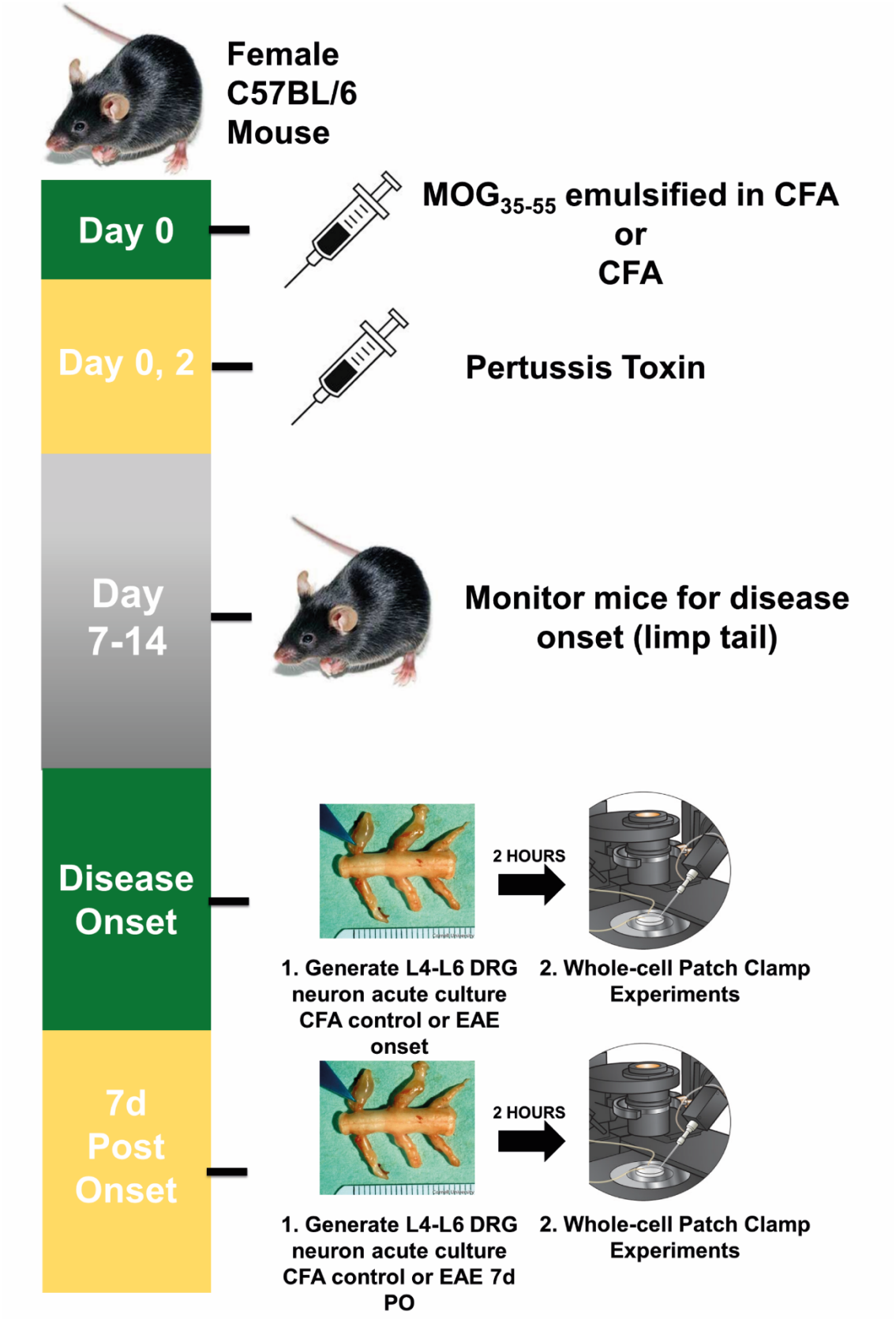
Female
C57BL/6
Mouse
Day 0
MOG35-55 emulsified in CFA
or
CFA
Day 0, 2
Pertussis Toxin
Day
7-14
Monitor mice for disease
onset (limp tail)
Disease
Onset
2 HOURS
1. Generate L4-L6 DRG
neuron acute culture
CFA control or EAE
onset
2. Whole-cell Patch Clamp
Experiments
7d
Post
Onset
2 HOURS
1. Generate L4-L6 DRG
neuron acute culture
CFA control or EAE 7d
PO
2. Whole-cell Patch Clamp
Experiments

Figure 2-2. Experimental Time Course of EAE DRG electrophysiology. EAE animals were induced and monitored for clinical signs. Mice showed Grade 1 clinical sign (limp tail) typically between 7 to 14 days post induction. L4-L6 DRGs were taken out at onset, and they were acutely cultured for whole-cell patch clamp experiments. L4-L6 DRGs were also taken 7 days post-onset (chronic), they and were acutely cultured (2 hours) for whole-cell patch clamp experiments.

Figure 2-3

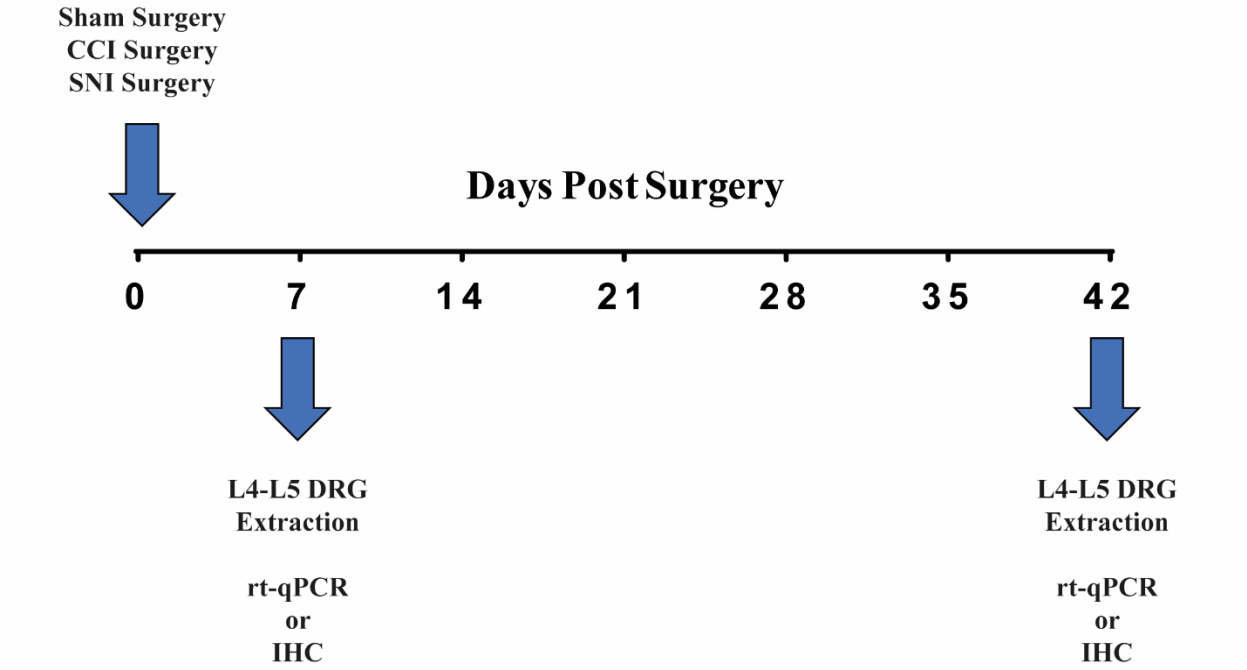

Figure 2-3. Experimental time course for the examination of behavioral differences between SNI and CCI. Following the initial nerve injury, animals were von Frey tested every 7 days, and mechanical thresholds were recorded over a 42-day period. L4-L5 DRGs were harvested on 7- and 42-days post-surgery for rt-qPCR or IHC.

Table 2-1. rt-qPCR Primers Used

Gene ID	Manufacturer, Catalogue Number
**Ppia*	Qiagen, QT00247709
Csf1	Qiagen, QT00195370
Il1b	Qiagen, QT00181657

* Primer was generously provided by Dr. Bradley Kerr (University of Alberta)

Table 2-2. IHC Antibodies

Antibody	Host	Manufacturer, Catalogue Number	Dilution
CSF1	Goat	R&D Systems, AF416	1:500
GFAP	Rabbit	Dako, 2023-05	1:1000
*Iba1	Rabbit	Wako, 019-19741	1:1000
**ATF3	Rabbit	Santa Cruz Biotechnology, SC-188	1:500
AffiniPure Anti-Goat IgG Alexa Fluor 594	Donkey	Jackson ImmunoResearch, 705-585-147	1:200
Anti-Goat IgG Alexa Fluor 488	Donkey	Invitrogen, A-11055	1:200
Anti-Rabbit IgG Alexa Fluor 488	Donkey	Invitrogen, A-21206	1:200
*Anti-Rabbit IgG Alexa Fluor 594	Donkey	Invitrogen, A-21207	1:200

*Antibodies were generously provided by Dr. Bradley Kerr (University of Alberta)

**Antibody was generously provided by Dr. Christine Webber (University of Alberta)

Chapter 3

Long-Term Actions of Interleukin-1β on K^+, Na^+ and Ca^{2+} Channel Currents in Small, IB_4-Positive Dorsal Root Ganglion Neurons and their Relevance to Neuropathic Pain

3.1 Introduction

Damage to the somatosensory nervous system often provokes peripheral and central sensitization, which in turn contributes to the pathogenesis of neuropathic pain (Alles & Smith 2018). Neuroimmune interactions, via cytokines and chemokines released by innate and adaptive immune cells, following a neve injury have been implicated to underlie these maladaptive alterations in the somatosensory nervous system (Basbaum et al 2009, Grace et al 2014, Scholz & Woolf 2007b, Watkins & Maier 2002). For instance, nerve injury induced neuroinflammation not only triggers increased neuronal excitability and ectopic discharges (Koplovitch & Devor 2018, Stemkowski & Smith 2012b, Vaso et al 2014, Wall & Devor 1983a), but it also initiates the production of numerous cytokines (e.g., tumor necrosis factor alpha; TNFα and colony stimulating factor 1; CSF1), chemokines (e.g., chemokine ligand 2, CCL2), and neurotrophic factors (e.g., brain derived neurotrophic factor; BDNF) in the dorsal root ganglia (DRG) neurons (Guan et al 2016, Obata & Noguchi 2006, Shubayev & Myers 2001, Sikandar et al 2018, White et al 2005). The peripheral sensitization and the increased release of cytokines, chemokines, neurotransmitters, and neurotrophic factors from the central primary afferent terminals then trigger enduring maladaptive neuroplasticities in the spinal superficial laminae, which amplify dorsal horn excitability, leading to central sensitization (Balasubramanyan et al 2006b, Basbaum et al 2009, Chen et al 2016, Coull et al 2003b, Grace et al 2014, Takeda et al 2008, Woolf 1983a).

IL-1β has was one of the first cytokines to be implicated to interact directly with sensory neurons in the context of pain (Ferreira et al 1988). Since then, the extensive role of IL-1β in the pathogenesis of neuropathic pain has been demonstrated (Bianchi et al 1998, Grace et al 2016, Kiguchi et al 2010, Liu et al 2013, Ren & Torres 2009, Wolf et al 2006, Zelenka et al 2005). A

peripheral nerve injury leads to significant increase in IL-1β expression at the injury site and the DRG (Echeverry et al 2017, Kiguchi et al 2010, Lim et al 2017, Nadeau et al 2011). Notably, IL-1β exposure and the activation of interleukin 1 receptor (IL-1R) in DRG sensory neurons have been implicated in both increased neuronal excitability, and alterations in gene expression such as CSF1, and transient receptor potential vanilloid 1 (TRPV-1) channels (Binshtok et al 2008, Ebbinghaus et al 2012, Lim et al 2017, Stemkowski et al 2015, Stemkowski & Smith 2012a). As a result, long-term changes in the excitability of sensory neurons by IL-1β may significantly contribute to both the onset and the maintenance of neuropathic pain by indirectly producing enduring maladaptive neuroplasticities in the spinal dorsal horn (Pinho-Ribeiro et al 2017, Pitcher & Henry 2008, Vaso et al 2014).

Previously, we have demonstrated the cell type specific effect of 5-6 days of 100 pM IL-1β treatment (Stemkowski et al 2015, Stemkowski & Smith 2012a), which mimicked the time course of IL-1β expression in the peripheral nerves following an injury (Nadeau et al 2011). We observed increased excitability and attenuation of action potential (AP) afterhyperpolarization (AHP) mediated through profound suppression of the voltage-sensitive and Ca^{2+}-sensitive K^+ currents in the medium-sized DRG neurons, which give rise to thinly-myelinated Aδ fibers (Stemkowski et al 2015). Furthermore, we discovered that the changes in electrophysiological properties mediated by long-term IL-1β treatment were in fact reversible as removal of IL-1β from the culture for 3-4 days ameliorated the increased excitability. Therefore, we concluded that IL-1β alone is not able produce persistent changes in the electrophysiological properties of the medium-sized DRG neurons.

Long-term IL-1β treatment of small isolectin B4 (IB_4) negative nociceptors and large DRG neurons, which give rise to unmyelinated C-fibres and heavily myelinated Aβ fibres respectively,

produced negligible changes in excitability. On the other hand, although 5-6 day IL-1β treatment had a small effect on the excitability of small IB_4-positive DRG neuron, which bind *Griffonia simplicifolia* isolectin B_4, we observed a profound increase in the AP duration (Stemkowski & Smith 2012a). Small IB_4^+ DRG neurons preferentially express receptors for glial cell line-derived neurotrophic factor (GDNF) and have been implicated for the pathogenesis of chronic neuropathic and inflammatory pain (Alvarez et al 2012, Bogen et al 2009, Chiu et al 2014, Joseph & Levine 2010, La et al 2016, Lippoldt et al 2016). For instance, small IB_4^+ DRG neurons were essential for the generation of persistent inflammatory pain induced by hyperalgesic priming, which is characterized by prolonged sensitization of nociceptor mediated by initial inflammatory insult and the secondary inflammatory exposure to prostaglandin E2 (PGE2) to the nociceptor nerve endings (Ferrari et al 2010, Joseph & Levine 2010, Reichling & Levine 2009). Therefore, in this study, we further examine the changes in the ion channel properties that may mediate the IL-1β-induced increase in the AP duration in the small IB_4^+ DRG neurons.

3.2 Methods

Methods used in this chapter are described in detail in Chapter 2. Briefly, long-term neuron enriched DRG culture was generated and they were supplemented with either 50 ng/ml nerve growth factor (NGF), 50 ng/ml GDNF, or nothing; then treated with 100 pM IL-1β (Figure 2-1; Chapter 2.2). Cells were classified according to Chapter 2.3. Whole-cell patch clamp experiments examining action potential parameters and properties of Na^+, K^+, and Ca^{2+} channel currents were conducted as described in Chapter 2.4. All statistics were done as described in Chapter 2.9.

3.3 Results

3.3.1 Long-term IL-1β treatment with GDNF supplementation leads to persistent increase in AP duration

The long-term exposure of small IB_4^+ DRG neurons to IL-1β had little effect on number of action potentials fired on a current ramp; however, it had profound effect on AP duration, which was increased by 35 % in response to IL-1β (Stemkowski & Smith 2012a). Since these experiments were done without neurotrophic support, which is critical for the maintenance of tetrodotoxin resistant (TTX-R) sodium channels and survival of small IB_4^+ neurons, we repeated the experiment with glial cell line derived neurotrophic factor (GDNF) supplementation (Cummins et al 2000, Fjell et al 1999, Golden et al 2010, Zwick et al 2002). First, since small IB_4^+ DRG neurons preferentially express receptors for GDNF, we examined whether addition of GDNF alone would affect the AP duration. As shown in Figure 3-1a, sole supplementation with 50 ng/ml GDNF for 5-6 days significantly increased the AP duration from 2.13 ± 0.14 ms (n=25) to 2.67 ± 0.15 ms (n=35; $p<0.02$). Then, since GDNF and IL-1β can both work through the mitogen activated protein kinase/extracellular signal-regulated kinases (MAPK/ERK) pathway we speculated IL-1β mediated increase in AP duration may be masked by the prior addition of GDNF to the culture (Binshtok et al 2008, Bogen et al 2008, Lu et al 2005, MacGillivray et al 2000). That said, as shown in Figures 3-1b and c, 5-6 day 100 pM IL-1β treatment with GDNF supplementation produced an additional increase in the AP duration to 3.39 ± 0.17ms (n=34, $p<0.0025$). As a result, unless otherwise stated, the remaining experiments were carried out with 50 ng/ml supplementation of GDNF in the culture. Since the IL-1β mediated changes in the medium DRG neuron excitability were reversible after 3-4 day washout, we examined the reversibility of increased AP duration in small IB_4^+ DRG neurons (Stemkowski et al 2015).

Surprisingly, a washout did not lead to reversal of IL-1β mediated increase in AP duration as IL-1β treated cells maintained significantly longer AP duration (4.36 ± 0.23 ms; n=32) compared to time-matched controls (3.56±0.17ms; n=35; *p<0.007;* Figures 3-1d and e).

3.3.2 NGF supplementation leads to prolonged AP duration and long-term IL-1β treatment further exacerbates the effect

Although small IB_4^+ DRG neuron preferentially express GDNF family receptor alpha-1,2,3 (GFRα1, GFRα2, GFRα3 and RET), both early and recent studies have revealed that ~35% of small IB_4^+ DRG neurons also express tropomyosin receptor kinase A (TrkA), which binds nerve growth factor (NGF) (Chiu et al 2014, Fang et al 2006, Molliver et al 1995, Molliver et al 1997). Since activation of TrkA by NGF can activate the MAPK/ERK pathway, we also examined the effect of 50 ng/ml NGF supplementation on the AP duration. Indeed, supplementation with NGF alone significantly increased the AP duration from 2.13 ± 0.14 ms (n=21) to 2.81 ± 0.26ms (n =24; Figure 3-1f; *p<0.05*). Additionally, long-term IL-1β treatment on top of NGF supplementation was also able to increase the AP duration further to 4.47 ± 0.59 ms (n=24; *p<0.015;* Figure 3-1g).

3.3.3 Long term IL-1β produces significant but predominantly reversible changes in other AP parameters

Long term IL-1β exposure also lead to significant changes in several other AP parameters. AP amplitude was significantly increased (Figure 3-2a), rheobase was significantly decreased (Figure 3-2b), maximum rate of rise (depolarization) was boosted (Figure 3-2c), maximum rate of decay (repolarization) was attenuated (Figure 3-2d), and time to reach peak AHP amplitude was prolonged (Figure 3-2e), although AHP amplitude was unaffected (Figure 3-2f). These changes are summarized in Table 3-1 and Figure 3-1.

In contrast to AP duration, many of the IL-1β mediated changes in these other AP parameters were transient. For instance, AP amplitude (Figure 3-3a), rheobase (Figure 3-3b), and time to reach AHP peak (Figure 3-3e) in IL-1β treated group were no longer significantly different from time-matched control group after the washout. However, IL-1β induced increase in maximum rate of depolarization (Figure 3-3c) and decrease in maximum rate of repolarization (Figure 3-3d) persisted as these parameters remained significantly shifted compared to time-matched controls after the washout. These data, summarized in Table 3-1 and 2, suggest that there may be both transient and enduring changes in the ion channel properties in the small IB_4^+ DRG neurons.

3.3.4 Long-term IL-1β treatment selectively alters tetrodotoxin sensitive (TTX-S) Na^+ current properties in small IB_4^+ DRG neurons

Acute IL-1β exposure has been shown to significantly enhance total, tetrodotoxin resistant (TTX-R), and tetrodotoxin sensitive (TTX-S) Na^+ currents in small nociceptive DRG neurons (Binshtok et al 2008). That said, no studies have examined the direct effect of long-term IL-1β treatment on these Na^+ channel currents in small IB4+ DRG neurons. Therefore, we further examined the effects of long-term IL-1β treatment on total, TTX-R, and TTX-S Na^+ currents in small IB4+ DRG neurons with GDNF supplementation as it is required for the maintenance of TTX-R Na_v 1.8 (SCN10A) and Na_v 1.9 (SCN11A) expressions (Fjell et al 1999).

In order to examine the effects of long-term IL-1β treatment on Na^+ channel currents in small IB_4^+ DRG neurons, total Na^+ current (I_{Na}) density was recorded by applying a series of depolarizing voltage commands from holding potential (V_h= -90 mV) up to 60 mV (Figure 3-4a). Subsequently, cells were treated with 300 nM TTX to reveal TTX-R I_{Na} (Figure 3-4b). Finally, total I_{Na} was subtracted by TTX-R I_{Na} digitally to reveal TTX-S I_{Na} (Figure 3-4c).

As described in Figure 3-4d, 5-6 day 100 pM IL-1β treatment with GDNF supplementation lead to significant increase in total I_{Na} current density compared to control group receiving only GDNF supplementation ($p<0.001$ at -40, -30 and -20mV; n = 19). However, long-term IL-1β treatment with GDNF supplementation did not significantly alter TTX-R I_{Na} (control, n=19; IL-1β, n=18; Figure 3-4e). This suggested that the increase in total I_{Na} density was most likely mediated by changes in TTX-S I_{Na}. Indeed, TTX-S I_{Na} density was profoundly increased by long-term IL-1β treatment (n=18; $p<0.001$ between -40 and 0mV; Figure 3-4f).

Furthermore, we examined the voltage-dependent gating properties of Na^+ channels in response to long-term IL-1β treatment by measuring voltage-dependence of activation and steady-state fast inactivation for total, TTX-R, and TTX-S I_{Na}. Following 5-6 day IL-1β treatment, the voltage-dependence of activation for total Na^+ conductance (g_{Na}) was shifted towards more hyperpolarized potentials (Figure 3-4g). This is indicated by significantly more negative voltage for half activation (V_{50}), which is the membrane potential where 50% of Na^+ channels are activated ($p<0.0001$; Table 3-3). That said, slope factor was not affected by IL-1β ($p>0.6$; Table 3-3). Furthermore, this leftward shift in V_{50} also clearly affects the IV plots in Figure 3-4d, as IL-1β treated small IB_4^+ DRG neurons achieved peak Na^+ conductance at -30 mV as opposed to control, which reached peak I_{Na} amplitude at -20 mV. As indicated by the activation curves in Figure 3-4h, the voltage dependence of TTX-R g_{Na} was unaffected by the IL-1β treatment as both V_{50} ($p>0.2$) and slope factor ($p>0.8$) were not changed (Table 3-3). As for the TTX-S g_{Na}, although slope factor was not affected ($p>0.75$; Table 3-3), activation curve was significantly shifted towards more negative potential in response to long-term IL-1β treatment as V_{50} was significantly more hyperpolarized compared to control ($p<0.0001$; Table 3-3) (Figure 3-4i). Thus, changes in total I_{Na} reflect changes in TTX-S I_{Na}.

Long-term IL-1β treatment also lead to significant changes in steady-state fast inactivation (Table 3-3). For total g_{Na}, IL-1β treatment lead to hyperpolarizing shift in the inactivation curve, which was accompanied by significant reduction in V_{50} (*$p<0.005$*) and slope factor (*$p<0.03$*; Figure 3-4g and Table 3-3). The inactivation curve of TTX-R g_{Na} was slightly shifted towards more depolarized potential as the inactivation V_{50} was increased from -28.29 ± 0.416 mV to -26.77 ± 0.3668 mV (*$p<0.05$*), but slope factor was unchanged (*$p>0.13$;* Figure 3-4h and Table 3-3). Furthermore, changes in the TTX-S g_{Na} inactivation generally mirrored those seen with total g_{Na} inactivation as slope factor was significantly attenuated with IL-1β treatment (*$p<0.006$*), but inactivation V_{50} was unaffected (Figure 3-4i and Table 3-3).

Furthermore, shifts in the voltage-dependence of steady-state slow inactivation, which is characterized by a decrease in the number of available channels for Na^+ conductance in response to prolonged depolarizing pulse, has been implicated in the pathogenesis of neuropathic pain (Binshtok et al 2008, Cummins et al 2000). Therefore, IL-1β treatment induced change in slow inactivation was further examined by applying 5 seconds of depolarizing pre-pulses in 10 mV increments, followed by 20 ms recovery pulses to -120 mV, which allows for recovery from fast inactivation, then 1ms test pulses to -10mV to determine the percentage of available channels for Na^+ conductance. As shown in Figures 3-4j and k, steady-state slow inactivation in both total g_{Na} and TTX-R g_{Na} were not affected by long-term IL-1β treatment with GDNF supplementation.

Finally, since the increase in AP duration may be the result of slower rate of I_{Na} decay, we also examined the fast inactivation time constants for total and TTX-R g_{Na}. However, long-term IL-1β treatment had no effect on inactivation time constants. Overall, these results indicated long-term IL-1β treatment with GDNF supplementation selectively augmented TTX-S I_{Na} amplitude and activation.

3.3.5 Long-term IL-1β treatment selectively attenuates Ca^{2+}-activated K^+ currents in small IB_4^+ DRG neurons

Since K^+ currents play an important role during repolarization phase of an AP, we also examined the effect of long-term IL-1β treatment on K^+ channel properties. Sensory neurons express a very diverse group of K^+ channels; therefore, we designed a voltage-clamp protocol that allowed us to isolate non-inactivating voltage-gated K^+ currents (I_K), Ca^{2+}-activated K^+ currents ($I_{K,Ca}$), and rapidly inactivating A-type K^+ currents (I_{KA}) (Gold et al 1996, Stemkowski et al 2015). First, we recorded total I_K by series of depolarizing voltage commands from -120 mV and subsequently bath applied external solution containing 5 mM Mn^{2+} which revealed Mn^{2+} resistant I_K (Figures 3-6A i, ii). Then Mn^{2+}-resistant I_K was digitally subtracted from total I_K to reveal Mn^{2+}-sensitive I_K, which represented $I_{K,Ca}$ (Figure 3-5a iii). Furthermore, in order to isolate I_{KA}, we recorded total Mn^{2+}-resistant I_K from -120 mV (Figure 3-5b i). Subsequently, the non-inactivating portion of Mn^{2+}-resistant I_K was revealed by applying voltage commands from -30 mV (Figure 3-5b ii). Finally, non-inactivating Mn^{2+}-resistant I_K were digitally subtracted from total Mn^{2+}-resistant I_K to reveal rapidly inactivating I_K (Figure 3-5b iii). The rapidly inactivating I_K seen in our experiments most likely were mediated by multiple channel types such as $K_v4.1$ and $K_v4.3$, which have distinct rates of inactivation (Gold 1999, Yunoki et al 2014). As a result, we found considerable variation in the rate of inactivation among the cells we recorded, thus we defined "I_A" as I_K with clear inactivation within the first 100 ms of a voltage command (Figure 3-5b iii). According to this definition, 5/19 control neurons expressed I_A and 7/18 neurons in IL-1β treated neurons expressed I_A, which were not significantly different (Fisher's exact test; *p=4951*). In contrast to our previous findings on medium sized DRG neurons, which demonstrated IL-1β treatment leads to profound decrease in I_K, long-term IL-1β treatment led to modest changes in

I_K in the small IB_4^+ DRG neurons (Stemkowski et al 2015). 5-6 day IL-1β treatment with GDNF supplementation did not significantly affect total I_K (Figure 3-5c), Mn^{2+}-resistant I_K (Figure 3-5d), nor I_{KA} (Figure 3-5e). However, IL-1β treatment lead to significant reduction in $I_{K,\,Ca}$ density at -30 to -60 mV (n=16, $p<0.02$; Figure 3-5f).

3.3.6 Ca^{2+} currents (I_{Ca}) are not directly affected by long-term IL-1β treatment with GDNF supplementation in small IB_4^+ DRG neurons

Since $I_{K,\,Ca}$ was significantly attenuated in response to long-term IL-1β treatment, we postulated this effect could be a consequence of changes in Ca^{2+} channel properties (Abdulla & Smith 2001a). Therefore, we examined the changes in I_{Ca} by using Ba^{2+} as a charge carrier. I_{Ba} was recorded by applying a series of 150 ms depolarizing voltage commands in 10 mV increments up to 30 mV as shown in Figure 3-6a. 5-6 day IL-1β treatment with GDNF supplementation had no statistically significant effect on a total I_{Ba} evoked from V_H= -100 mV (control, n=13; IL-1β, n=14; $p>0.11$; Figure 3-6b). I_{Ba} evoked from V_H= -100 mV also included T-type I_{Ca} that can activate at a more hyperpolarized potential (-40 mV), but these currents were also not significantly changed by long-term IL-1β treatment. Furthermore, since peripheral nerve injury has been reported to increase inactivation of I_{Ba} (Abdulla & Smith 2001a), we also examined the potential for long-term IL-1β treatment to affect I_{Ba} inactivation, which may be reflected by decreased I_{Ba} recorded from a more physiologically relevant holding potential of V_H= -60 mV. However, this did not seem to be the case as IL-1β treatment did not significantly alter I_{Ba} recorded from V_H= -60 mV.

3.3.7 Increased AP amplitude and duration by long-term IL-1β treatment indirectly alters I_{Ca} in small IB_4^+ DRG neurons

Since long-term IL-1β treatment with GDNF supplementation significantly increased AP amplitude and duration compared to GDNF only control (Table 3-1), we hypothesized the altered voltage trajectory encountered by Ca^{2+} channels in the IL-1β treated small IB_4^+ DRG neurons may lead to changes in the I_{Ca}. In order to examine this, we used AP parameters in Table 3-1 as a guideline to create voltage command protocols that mimic the distinct AP shape in GDNF only and that in IL-1β/GDNF treated small IB_4^+ DRG neuron (see Figure 3-1C) (Figure 3-6d). First, we generated I_{Ba} in a control neuron using the voltage protocol representing a control AP. I_{Ba} was then subsequently evoked in the same control neuron with the voltage commands representing an AP of IL-1β treated small IB_4^+ DRG neuron. As seen in Figure 3-6e, I_{Ba} evoked by AP shaped waveforms flowed mainly during the repolarization phase of the AP. Voltage protocol representing the AP of small IB_4^+ DRG neurons treated with IL-1β/GDNF produced a larger I_{Ba} compared to the AP command representative of control small IB_4^+ DRG neurons. These results indicated that long-term IL-1β treatment with GDNF supplementation may indirectly alter Ca^{2+} influx via the changes in AP parameters.

3.3.8 Decrease in functional large conductance Ca^{2+}-activated K^+ (BK) channel availability underlie IL-1β mediated increase in AP duration in the small IB_4^+ DRG neurons

Finally, since the inactivation and the current decay (tau) of g_{Na} was not significantly affected, we hypothesized that the significant attenuation in I_{KCa} by long-term IL-1β treatment may underlie the increased AP duration in small IB_4^+ DRG neurons. To test this, we utilized iberiotoxin (IBTX), a specific blocker of BK channel which is a component of $I_{K,Ca,}$ to examine

the effect of reducing $I_{K,Ca}$ on the AP duration from control and IL-1β treated neurons. First, 5-minute application of 100 nM IBTX after the baseline AP recording lead to increase in AP durations of both control and IL-1β treated neurons (Figures 3-6f and g). This indicated that reduction in I_{KCa} can indeed affect the AP duration in small IB_4^+ DRG neurons. Furthermore, the degree of IBTX mediated increase in AP duration was significantly greater in control neurons (n=7; 225.1 ± 23.5%) compared to IL-1β treated neurons (n=8; 154.3 ± 17.6%; $p<0.05$; Figures 3-6h). The weaker effect of IBTX in the IL-1β treated neurons indicated significantly less functional BK channel availability in the IL-1β/GDNF treated neurons compared to GDNF controls at resting membrane potential (V_H= -60 mV). Therefore, this attenuation of functional BK channel availability may underlie the increase in AP duration by long-term IL-1β treatment in small IB_4^+ DRG neurons.

3.4 Discussion

3.4.1 Summary of Results

In this study, we have demonstrated that long-term IL-1β treatment with GDNF supplementation leads to significant changes in the AP parameters and ion channel properties in small IB_4^+ DRG neurons. Importantly, chronic IL-1β treatment lead to enduring increase in the AP duration, which was accompanied by a persistent increase in the rate of depolarization and a decrease in the rate of repolarization (Table 3-1). Furthermore, long-term IL-1β treatment selectively enhanced TTX-S I_{Na} by increased amplitude and activation (Figure 3-4 and Table 3-3). Although majority of I_K were unaffected, IL-1β treatment lead to a profound decrease in $I_{K,Ca}$ (Figure 3-5). This change in $I_{K,Ca}$ was not the result of changes in I_{Ca} as IL-1β treatment did not significantly alter I_{Ba} (Figure 3-6). The chronic IL-1β treatment mediated increase in AP duration and

amplitude indirectly increased Ca^{2+} influx, and the decrease in functional BK channel availability contributed to the increased AP duration in small IB_4^+ DRG neurons (Figure 3-6).

3.4.2 Implication of GDNF supplementation

In our previous studies without any neurotrophic support, 3-5 day 100 pM IL-1β treatment was able to produce a significant increase in AP duration in small IB_4^+ DRG neurons (Stemkowski & Smith 2012a). Since small IB_4^+ DRG neurons require GDNF for not only survival, but also proper function and expression of TTX-R SCN10A ($Na_v1.8$) and SCN11A ($Na_v1.9$), we supplemented our long-term DRG culture with 50 ng/ml GDNF to examine the IL-1β effect on a more viable and physiologically relevant small IB_4^+ DRG neurons (Cummins et al 2000, Fjell et al 1999, Golden et al 2010, Zwick et al 2002). The addition of GDNF or NGF alone was able to prolong the AP duration significantly compared to no neurotrophic factor control. Since NGF masked IL-1β induced increase in excitability in medium sized DRG neurons, we wondered whether addition of GDNF would mask the IL-1β mediated increase in AP duration (Stemkowski et al 2015). However, supplementation with neither GDNF nor NGF masked the IL-1β mediated increase in AP duration as the addition of IL-1β produced a further increase in AP duration. This additional effect suggested a potential synergistic effect, which may lead to more profound changes in the ion channel functions in small IB_4^+ DRG neurons. Indeed, although long-term IL-1β treatment alone produced significant increase in AP duration, which was accompanied by decrease in maximum rate of repolarization, chronic IL-1β treatment with GDNF supplementation produced more profound changes in the AP parameters (Table 3-1) (Stemkowski & Smith 2012a). For instance, on top of the increased AP duration and decrease in rate of repolarization, chronic IL-1β/GDNF treatment lead to further increase in AP amplitude,

decrease in rheobase, increase in maximum rate of depolarization, and increase in time to reach AHP peak, which can all contribute to increased excitability (Table 3-1).

3.4.3 Implications of IL-1β mediated changes in ion channel conductances

Chronic IL-1β treatment leads to cell type specific effects on DRG neuron excitability and ion channel functions (Stemkowski & Smith 2012a). We have shown chronic IL-1β treatment leads to significant attenuation of K^+ channel currents (Mn^{2+}-resistant I_K, I_A, and $I_{K,Ca}$), but has little effect on Na^+ channel current in the medium sized DRG neurons (Stemkowski et al 2015). In stark contrast, 5-6 day treatment of IL-1β with GDNF supplementation lead to profound increase in the TTX-S I_{Na}, but only suppressed $I_{K,Ca}$ significantly in the small IB_4^+ DRG neurons.

The significant increase in total and TTX-S $I_{Na,}$ accompanied by a shift in the activation curve to more negative potentials, most likely contribute to the increased AP amplitude, decreased rheobase, and increased rate of depolarization. However, since we did not observe increase in inactivation V_{50} nor current decay time constant (fast inactivation tau), the changes in TTX-S I_{Na} likely does not contribute significantly to the increased AP duration in response to IL-1β treatment in small IB_4^+ DRG neurons. The lack of effect of long-term IL-1β exposure on TTX-R I_{Na} was unexpected since Na_v 1.8 is acutely affected by IL-1β in DRG nociceptors and plays an important role in the pathogenesis of neuropathic and inflammatory pain (Daou et al 2016, Faber et al 2012b, Gold 1999, Jarvis et al 2007, Lai et al 2002). This discrepancy may be attributed to the different concentration and duration of IL-1β exposure. For instance, 10 ng/ml or 571 pM IL-1β application lead to overall increase in I_{Na} in small DRG nociceptors (Binshtok et al 2008). In contrast, Liu et al (2006) demonstrated 5 minute application of high dose (20 ng/ml or 1143 pM) IL-1β leads to significant decrease in total I_{Na} in capsaicin sensitive neurons of trigeminal

ganglia. Furthermore, the authors also demonstrated longer application of IL-1β (24 h) increases TTX-S I_{Na} but does not affect TTX-R I_{Na} (Liu et al 2006). Taken together with our findings, IL-1β mediated changes in ion channel function most likely depends on the dose and the duration of application.

Interestingly, although total I_K, Mn^{2+}-resistant I_K, and I_A were not significantly altered, $I_{K,Ca}$ was significantly attenuated by chronic IL-1β treatment. The lack of statistical significance in total I_K may be explained by relatively small change in current density of $I_{K,Ca}$ (Δ=-26 $pA.pF^{-1}$), which only constitute small portion of total I_K density (~200 $pA.pf^{-1}$; Figure 3-5c). Of note, our data suggest that suppression of BK (K_{Ca} 1.1) channel function underlies the IL-1β mediated increase in AP duration in small IB_4^+ DRG neurons as 100 nM IBTX lead to significantly more profound increase in AP duration in GDNF control neurons compared to IL-1β treated neurons. Since I_{Ba} was unaffected by long-term IL-1β treatment, the changes in BK channel function is most likely a direct consequence of IL-1R activation. Interestingly, BK channels are preferentially expressed in small IB_4^+ DRG neurons, and persistent inflammation induced by subcutaneous injection of complete Freund's adjuvant (CFA) caused suppression of BK channel currents without affecting voltage-gated K^+ currents (Zhang et al 2012). This decrease in BK channel function also leads to significant increase in AP duration and excitability in small IB_4^+ DRG neuron. Taken together, these results indicate IL-1β plays a critical role in modulating AP duration in small IB_4^+ DRG neurons, and these actions are largely mediated through alteration of BK channel function. That said, since our culture was supplemented with GDNF, which increased AP duration significantly by itself, the potential for GDNF mediated alteration in BK channel function must also be considered. Indeed, bath application of 200 ng/ml GDNF for 15 to 30 minutes produced significant suppression of BK currents in small IB_4^+ DRG neurons, and this was also

accompanied by prolonged AP duration (Hendrich et al 2012). As a result, increase in AP duration mediated by GDNF treatment alone may also be mediated through suppression of BK current as well. That said, we were able to show further increase in AP duration accompanied by decrease in $I_{K,Ca}$, with or without the GDNF supplementation; therefore, the changes we observed in this study is most likely attributed to chronic IL-1β treatment (Stemkowski 2011, Stemkowski & Smith 2012a). Since IL-1β and GDNF can both work through MAPK/ERK pathway, it may underlie the molecular mechanism for the suppression of BK channel function in small IB_4^+ DRG neurons; however, the exact mechanism is still unclear, and it is an avenue for future investigation.

Finally, our data demonstrated chronic IL-1β treatment with GDNF supplementation did not significantly alter I_{Ca}. Of note, T-type Ca^{+2} channels, which have much more hyperpolarized activation curve, was not altered by IL-1β treatment. This lack of significant effect can be seen in Figure 3-6b at -40 mV. This was surprising because a recent study has shown IL-1β upregulate the function of $Ca_v3.2$ (T-type Ca^{2+} channel) in the spinal cord and DRG (Stemkowski et al 2017). This may be explained by experiments, which demonstrated acute 100 ng/ml GDNF application can potentiate I_{Ca} in dopaminergic neurons, and also increase intracellular calcium concentration in motor neurons through Ca^{2+} channel independent mechanism (Perez-Garcia et al 2004, Wang et al 2003). Although it is unclear whether these effects would also persist in small IB_4^+ DRG neurons, overall increase in I_{Ca} or intracellular Ca^+ concentration by GDNF may diminish the observable differences between GDNF control group and IL-1β/GDNF treated group.

3.4.4 Implications of reversible and persistent IL-1β effects

As discussed earlier, actions of IL-1β depend on the concentration and the duration of exposure. Thus, acute actions of IL-1β on nociceptor excitability and sodium currents are in fact reversible within 45 minutes (Binshtok et al 2008). Moreover, the actions of IL-1β also is cell type specific as increased excitability of medium sized DRG neurons by long-term IL-1β treatment is able to recover within 3-4 days (Stemkowski et al 2015). Here, we demonstrated IL-1β mediated increase in AP amplitude and rheobase, which most likely depend on the changes in TTX-S I_{Na}, are reversible (Table 3-1 and 2). This suggests IL-1β mediated modulation of TTX-S Na^+ channel most likely involves reversible mechanisms such as phosphorylation instead of long-term change in gene expression. Indeed, IL-1β has been shown to modulate Na^+ channel functions by channel phosphorylation, thus washout may reverse phosphorylation (Laedermann et al 2015). Furthermore, since surface expression of ion channels often last 8 to 24 hours, without the continuous presence of IL-1β TTX-S Na^+ will no longer be phosphorylated in the cell membrane, and no longer be able to increase AP amplitude and decrease rheobase (Chen et al 2015, Colley et al 2007).

In contrast, IL-1β mediated increase in AP duration and decrease in rate of repolarization, which are likely the result of decreased BK channel function, were persistent (Table 3-1 and 2). IL-1β has been shown to induce enduring changes in gene expression of nitric oxide synthase 2 (NOS-2) and cyclooxygenase 2 (COX-2) in DRG neurons and spinal cord (Fehrenbacher et al 2005, Igwe et al 2001, Samad et al 2001a). Therefore, the persistent increase in the AP duration and decrease in the rate of repolarization by IL-1β may be mediated through modification in gene expression of BK channels themselves or proteins that regulate their function. Indeed, BK channel mRNA and protein levels were significantly attenuated in the ipsilateral small DRG

neurons following spinal nerve ligation injury (Chen et al 2009a). However, another study has shown that persistent peripheral inflammation mediated by subcutaneous CFA injection failed to change overall BK channel protein expression in the DRG (Zhang et al 2012). The authors however postulated that neurons that are affected by subcutaneous CFA injection only constitute small portion of the whole DRG, thus the subpopulation specific effect may have been diluted. In fact, single cell PCR revealed significant changes in BK channel α subunit splice variant in the DRG neuron exposed to inflammation. A future study examining BK channel expression and modulation in response to chronic IL-1β treatment in small IB_4^+ DRG neurons may provide potential molecular mechanisms underlying the persistent increase in AP duration.

Although IL-1β treatment on top of GDNF supplementation produced an additional increase in AP duration, which persisted after the washout, the enduring changes may still be enhanced by GDNF supplementation. As discussed earlier, GDNF supplementation appears to have additive effect with IL-1β treatment as more AP parameters were changed with GDNF supplementation. Furthermore, GDNF can also directly modulate BK channel function in small IB_4^+ DRG neurons (Hendrich et al 2012). Therefore, the persistent change in AP duration may be the result of GDNF supplementation. However, GDNF mediated modulation of BK channel does not likely involve changes in gene expression as it did not significantly affect the mRNA expression of Ca^+-activated K^+ channel expressions in sensory neurons (Boettger et al 2002). Taken together, the mechanism of IL-1β/GDNF treatment mediated long-term changes in AP duration in the small IB_4^+ DRG neurons is still not fully understood, and it is another potential topic of future investigation.

3.4.5 IL-1β mediated changes in small IB_4^+ DRG neurons and its relevance to pain mechanisms

To date, there has not been a peer-reviewed publication investigating the effect of nerve injury on AP shape and ion channels function in small IB_4^+ DRG neurons. That said, peripheral nerve injury lead to increase in AP duration and amplitude in small DRG neurons that were not subdivided into IB_4^- and IB_4^+, which is consistent with findings in this study in small IB_4^+ DRG neurons (Abdulla & Smith 2001b). A peripheral nerve injury triggers significant increase in TTX-S I_{Na} and decrease in BK channel currents and expression (Abdulla & Smith 2002, Chen et al 2009a, Cummins & Waxman 1997, Hendrich et al 2012). Moreover, BK channels are not only preferentially expressed in small IB_4^+ DRG neurons, but nerve injury also leads to significant attenuation of BK channel expression and function predominantly in small nociceptive DRG neurons. Taken together with our findings, IL-1β interaction with small IB_4^+ DRG neurons is likely to contribute substantially to these changes triggered by peripheral nerve injury.

However, IL-1β modulation of ion channel functions clearly cannot explain all the changes produced by nerve injury. For instance, nerve injury reduced delayed rectifier I_K and I_{Ca} in all types of DRG neurons, yet these currents were not significantly affected by chronic IL-1β treatment in the small IB_4^+ DRG neurons (Abdulla & Smith 2001a). A more complex interactions involving several key mediators associated with the pathogenesis of neuropathic pain following nerve injury, such as TNF-α, IL-6, IL-10, and NGF, may underlie these discrepancies as these mediators can all modulate ion channel function to sensitize DRG neurons (Czeschik et al 2008, Leo et al 2015, Pinho-Ribeiro et al 2017, Shen et al 2013, Tamura et al 2014, Watkins & Maier 2002).

A change in excitability and ion channel function in small IB_4^+ has been implicated in the pathogenesis of inflammatory and neuropathic pain (Alvarez et al 2012, Bogen et al 2009, Hendrich et al 2012, Li & Zhou 2001, Taylor et al 2012, Zhang et al 2012). Our results suggest the change in AP shape induced by chronic IL-1β treatment in small IB_4^+ DRG neurons can increase AP induced Ca^{2+} influx; therefore, this may in turn increase release of not only neurotransmitters, but also chemokines and cytokines involved in sensitization of spinal dorsal horn neurons (Llinas et al 1982). In support of this, long term IL-1β exposure has also been reported to increase the frequency of spontaneous EPSC's in excitatory dorsal horn neurons (Gustafson-Vickers et al., 2008). $Na_v1.8$ expressing IB_4^+ DRG neurons have distinct pathway working in parallel with the classical peptidergic nociceptors to process and relay nociceptive information to the CNS (Braz et al 2005). Specifically, non-peptidergic IB_4^+ neurons project to both glutamatergic vertical cells, which are excitatory interneurons, and gamma-aminobutyric acid (GABA)/glycinergic islet cells, which are inhibitory interneurons, in lamina II (Peirs & Seal 2016). Therefore, increased transmission in IB_4^+ neurons can both increase in nociceptive transmission by increased glutamate release onto vertical cells and decrease transmission by excitation of inhibitory interneurons. Interestingly, it has been shown that nerve injury leads to loss of non-peptidergic terminals onto inhibitory islet cells (Bailey & Ribeiro-da-Silva 2006). In support of this, nerve injury significantly decreased synaptic drive to putative inhibitory neurons in lamina II and selective block of BK channel, which are preferentially expressed in small IB_4^+ DRG neurons, by IBTX alone lead to mechanical hyperalgesia (Balasubramanyan et al 2006b, Chen et al 2009a, Chen et al 2009b, Zhang et al 2012). Taken together with our results, IL-1β mediated chronic increase in AP duration and the decrease in BK channel function and

expression in IB_4^+ neurons may contribute significantly to both the onset and maintenance of tactile allodynia following a nerve injury.

3.4.6 Limitations of the study

Neuron enriched primary sensory neuron culture provides distinct advantage as it allows for examination of functional outcome in response to a specific external stimulus. However, it is extremely difficult to mimic a physiological condition *in vitro*. We have attempted to make our culture more physiologically relevant by addition of neurotrophic factors such as NGF and GDNF. However, this does not completely simulate the intact system, thus the changes we observed may not be mirrored *in vivo*. This is evident as ion channel modulation by IL-1β with GDNF supplementation cannot explain all the changes observed in a nerve injured animal.

Furthermore, we do our best to eliminate non-neuronal cells, such as Schwann cells and satellite glial cells, in our culture by addition of anti-mitotic mixture; however, non-neuronal cells eventually overpopulate the culture. Although the non-neuronal cells may have contributed our results, since our experiments have time-matched controls, the observable differences are likely due to the IL-1β treatment. Finally, we have only tested one concentration of IL-1β and GDNF. Since the dose and the duration of IL-1β treatment produces significantly distinct outcomes, future study with varying IL-1β and GDNF concentrations may reveal mechanisms involved in these discrepancies.

3.5 Conclusions

In this study, we demonstrated for the first time that long-term IL-1β treatment with GDNF supplementation leads to enduring increase in the AP duration in small IB_4^+ DRG neurons. This

change was predominantly mediated through suppression of BK channel function by IL-1β. The IL-1β mediated changes in voltage trajectory of AP amplified Ca^{2+} influx in small IB_4^+ DRG neurons. If the same changes occur in the presynaptic terminals, the persistent increase in AP duration can contribute indirectly to enhanced excitatory synaptic transmission and sensitization of spinal dorsal horn neurons.

Table 3-1. Effects of IL-1β on AP parameters in small IB_4^+ DRG neurons

AP Parameters	Control	IL-1β	Time Control	IL-1β Washout
AP Duration (ms)	2.67±0.15	3.39±0.17****	3.56±0.17	4.36±0.23**
AP Amplitude (mV)	120.3±1.207	124.3±1.273*	121.9±1.276	123.5±1.092
Rheobase (nA)	0.47±0.0094	0.4±0.01****	0.46±0.014	0.45±0.027
Maximum Rate of Rise (mV/ms)	151.4±6.972	204.1±9.65****	190.5±11.41	223.6±11.7*
Maximum Rate of Decay (mV/ms)	-55.09±3.187	-40.1±1.444****	-41.52±2.289	-34.41±1.202**
AHP Time to Peak (ms)	34.71±1.762	48.85±2.311****	49.01±3.698	54.67±3.331
AHP Amplitude (mV)	-10.38±0.4677	-9.80±0.536	-7.912±0.5973	-7.305±0.4446

Mann-Whitney test was used for rheobase, unpaired Student's t-test was used for the rest; Control, n=35; IL-1β, n=34; Time Control, n=35; IL-1β Washout, n=32; * $p<0.05$, ** $p<0.01$, *** $p<0.001$, **** $p<0.0001$ compared to appropriate controls. Data are represented in mean ± SEM.

Table 3-2. Summary of effects and reversibility of IL-1β on AP parameters

	Effect of IL-1β	Reversible	Conductance or current affected
AP Duration	↑	No	$g_{K,Ca}$
AP Amplitude	↑	Yes	TTX-S I_{Na}
Rheobase	↓	Yes	TTX-S I_{Na}
Rate of Rise	↑	No	TTX-S I_{Na}
Rate of Decay	↓	No	$g_{K,Ca}$
AHP Time to peak	↑	Yes	?
AHP Amplitude	↔	N/A	N/A

Table 3-3. Effects of IL-1β on Na^+ channel currents

	Control (GDNF)	IL-1β (GDNF)
Total I_{Na} Activation V_{50}	-35.26 ± 0.7021 (20)	-40.21 ± 0.4599 (19) p<0.0001****
TTX-R I_{Na} Activation V_{50}	-19.74 ± 0.6089 (18)	-18.35 ± 1.005 (17) p=0.2393
TTX-S Activation V_{50}	-35.76 ± 0.7912 (18)	-40.11 ± 0.5841 (16) p=0.0001****
Total I_{Na} Activation Slope Factor	3.299 ± 0.4205 (20)	1.932 ± 2.626 (19) p=0.6013
TTX-R I_{Na} Activation Slope Factor	2.59 ± 1.448 (18)	2.238 ± 1.167 (17) p=0.8521
TTX-S Activation Slope Factor	2.992 ± 0.4558 (18)	2.442 ± 1.777 (16) p=0.7541
Total I_{Na} Inactivation V_{50}	-36.70 ± 0.98 (21)	-41.97±1.13 (18) p=0.0011**
TTX-R I_{Na} Inactivation V_{50}	-28.29 ± 0.416 (18)	-26.77 ± 0.3668 (17) p=0.0101*
TTX-S Inactivation V_{50}	-67.08 ± 1.832 (14)	-68.37 ± 0.9757 (16) p=0.5249
Total I_{Na} Inactivation Slope Factor	-12.25 ± 0.8957 (21)	-15.49 ± 1.075 (18) p=0.0251*
TTX-R I_{Na} Inactivation Slope Factor	-4.21 ± 0.3894 (18)	-3.473 ± 0.2795 (17) p=0.1375
TTX-S Inactivation Slope Factor	-12.02 ± 1.541 (14)	-6.962 ± 0.8444 (16) p=0.0059**

Unpaired Student's t-test; * *p<0.05*, ** *p<0.01*, **** *p<0.001* compared to control. Data are represented in mean ± SEM (n).

Figure 3-1

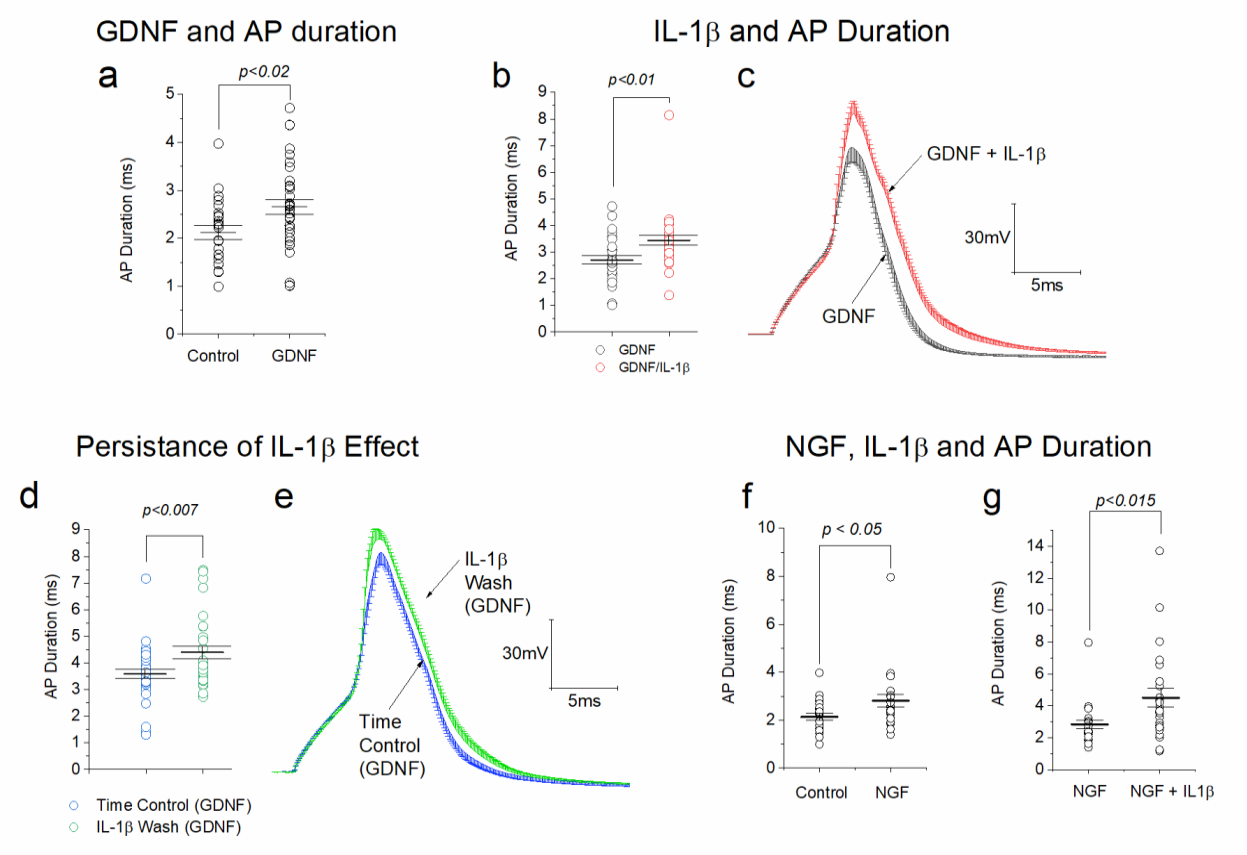

Figure 3-1. Effects of GDNF or NGF with or without IL-1β on AP duration. **a.** Graph to show effect of GDNF on AP duration. On this and all similar graphs, bold lines show mean value error bars show SEM. **b.** Graph to show increase in AP duration produced by exposure of GDNF treated neurons to IL1β for 5-6 days. **c.** Averaged recordings from 35 GDNF treated neurons and 34 GDNF neurons exposed to IL-1β for 5-6 days. Error bars shown in upward direction only show SEM. **d.** Graph to show persistance of IL-1β effect. IL-1β wash data is from neurons that were exposed to IL-1β for 5-6 days but not studied until 3-4 days after IL-1β washout. **e.** Averaged recordings obtained from 35 GDNF treated neurons 3-4 days after 5-6 days exposure to IL-1β. These are compared to time control neurons that were exposed to GDNF for 12-14 days (see Fig 1a). **f.** Graph to show effect of NGF on AP duration. **g.** Graph to show increase in AP duration produced by exposure of NGF treated neurons to IL1β for 5-6 days.

Figure 3-2

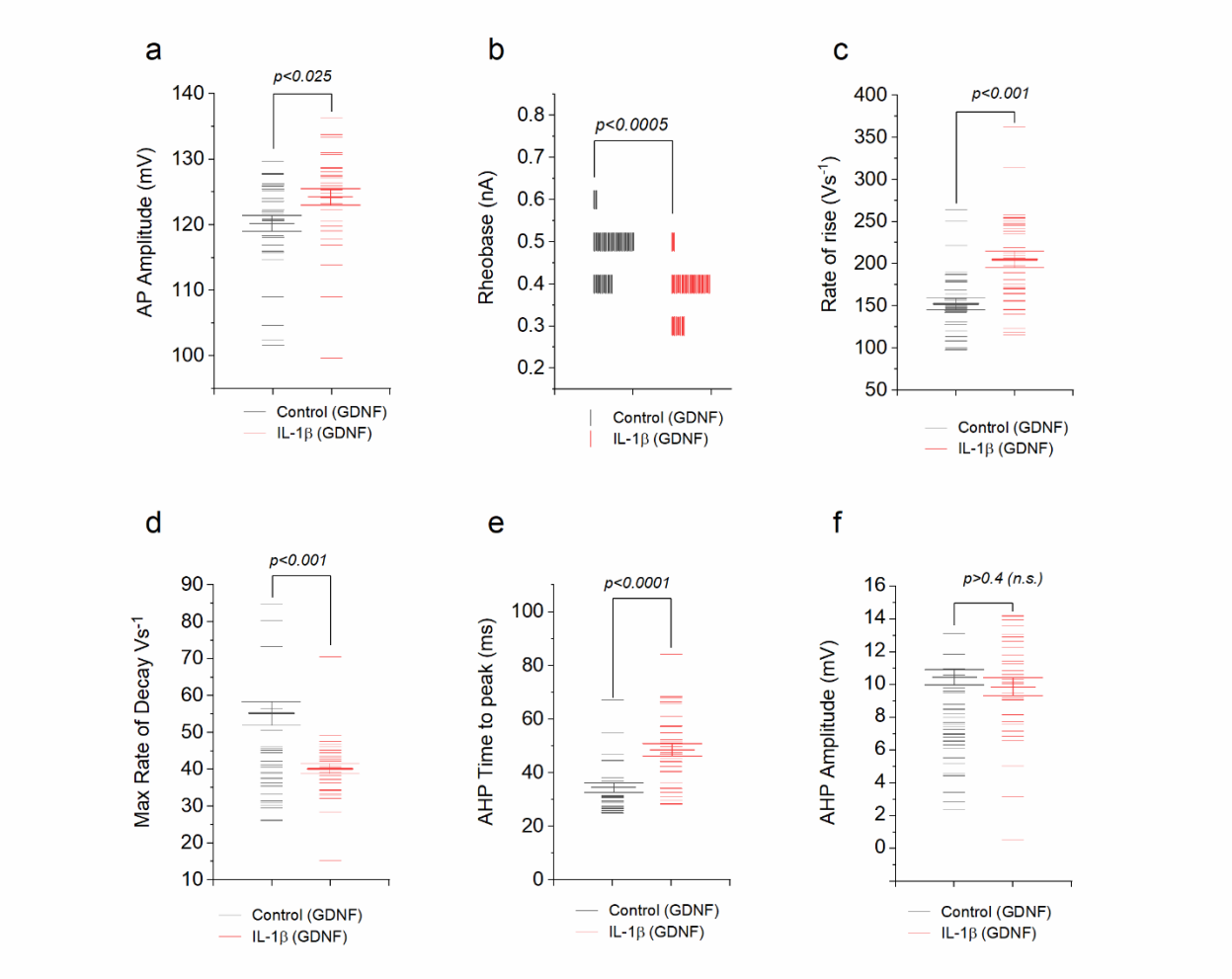

Figure 3-2. Graphs to show effect of exposure of GDNF-treated neurons to IL-1β for 5-6d. AP amplitude is increased (**a**), rheobase is reduced (**b**), rate of rise of AP is increased (**c**), Maximum rate of AP decay is decreased (**d**), AHP time to peak is increased (**e**) but AHP amplitude is unchanged (**f**).

Figure 3-3

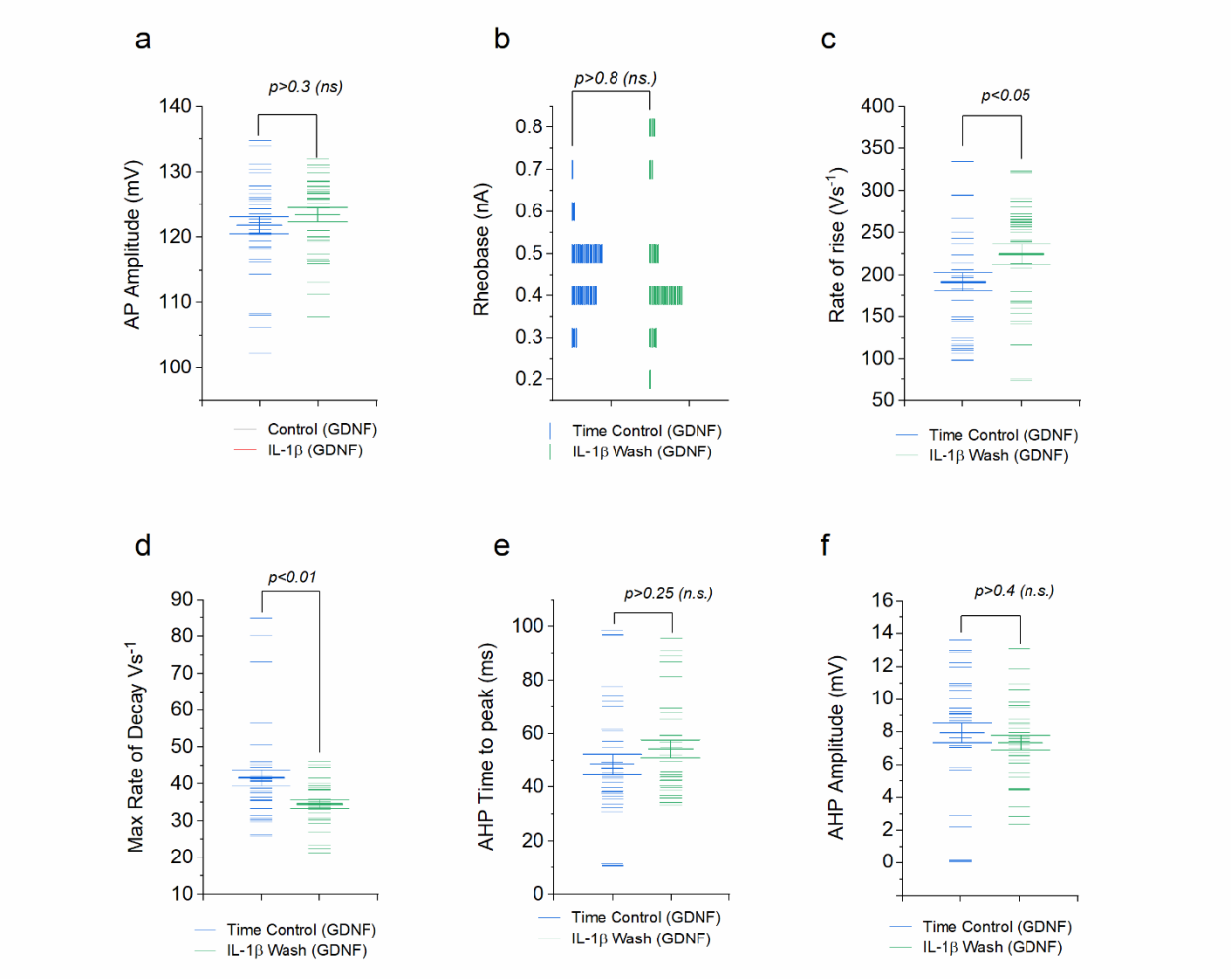

Figure 3-3. Graphs to show data from GDNF neurons 3-4 days after 5-6 days exposure compared to time control (12-14 days exposure to GDNF alone). AP Amplitude and rheobase are not different from time controls, indicating effects of IL1β is reveresed (**a** and **b**). Rate of rise and maximum rate of decay of AP are significantly different from time controls, indicating lasting effect of IL-1β (**c** and **d**). Time to peak of AHP is not different from time controls indicating another reversible action of IL-1β (**e**), AHP amplitude remains unchanged (**f**).

Figure 3-4

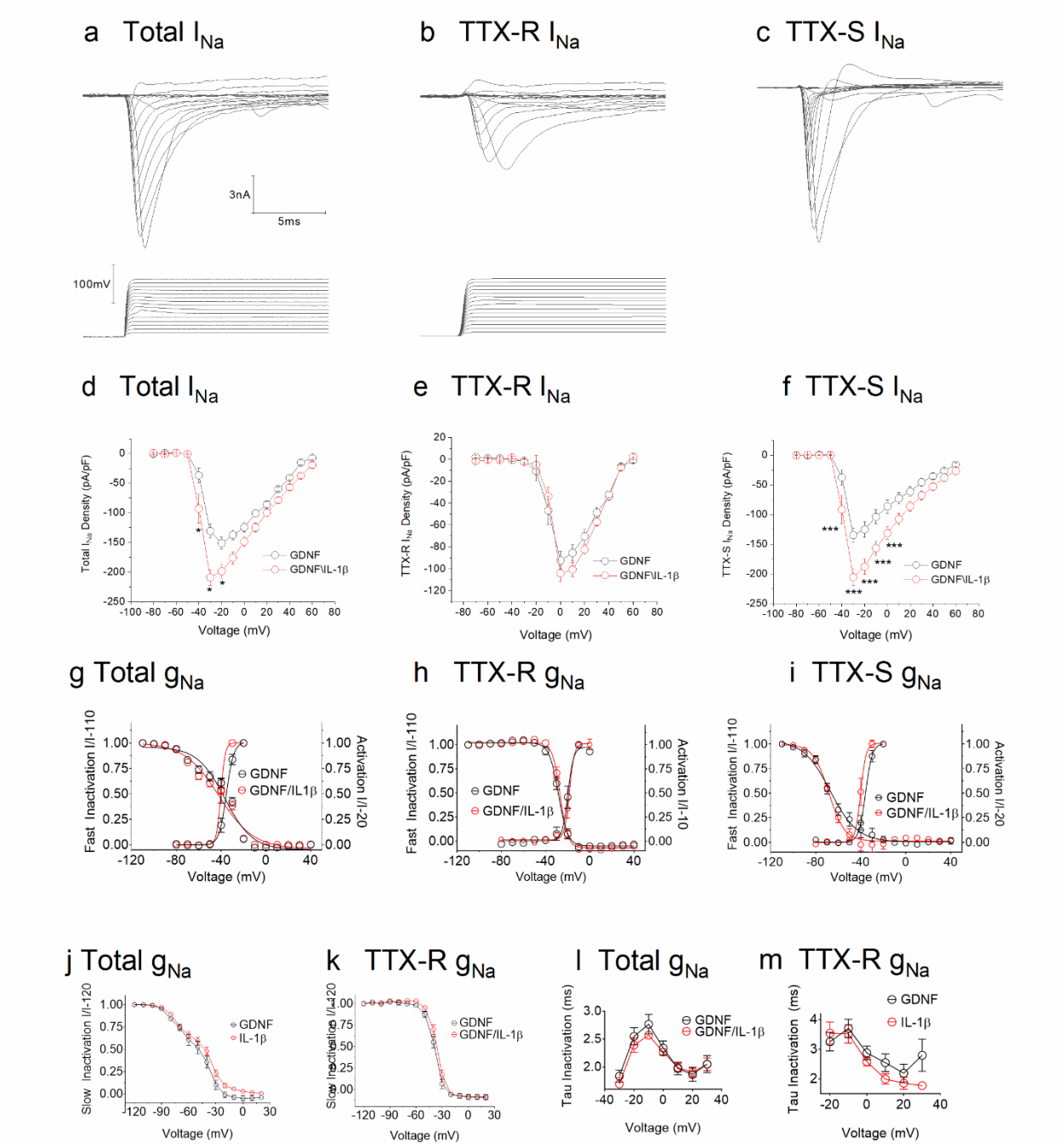
a Total I_{Na}
b TTX-R I_{Na}
c TTX-S I_{Na}
3nA
5ms
100mV
d Total I_{Na}
e TTX-R I_{Na}
f TTX-S I_{Na}
Total I_{Na} Density (pA/pF)
TTX-R I_{Na} Density (pA/pF)
TTX-S I_{Na} Density (pA/pF)
Voltage (mV)
GDNF
GDNF\IL-1β
g Total g_{Na}
h TTX-R g_{Na}
i TTX-S g_{Na}
Fast Inactivation I/I-110
Activation I/I-20
Activation I/I-10
GDNF/IL1β
GDNF/IL-1β
j Total g_{Na}
k TTX-R g_{Na}
l Total g_{Na}
m TTX-R g_{Na}
Slow Inactivation I/I-120
Tau Inactivation (ms)
IL-1β

Figure 3-4. Effects of IL-1β on I_{Na}. **a.** Typical recordings of total I_{Na} from a GDNF treated small IB_4^+ neuron. **b.** TTX-R I_{Na} in the same neuron recorded in the presence of 300nM TTX. **c.** TTX-S I_{Na} obtained by subtraction of recordings in **b** from those in **a. d,e** and **f.** Current-voltage plots for total, TTX-R and TTX-S I_{Na} obtained from 19 GDNF treated neurons and 18 GDNF neurons following 5-6d exposure to IL-1β. Total and TTX-S I_{Na} are increased by IL-1β but TTX-R I_{Na} is unaffected. **g,h** and **i.** Activation and inactivation plots for total, TTX-R and TTX-S g_{Na} obtained from GDNF treated neurons and GDNF neurons following 5-6d exposure to IL-1β. (n's range from 14 for inactivation of TTX-S g_{Na} in GDNF treated cells (**i**) to 21 for inactivation of total g_{Na} in GDNF treated neurons (**g**). **j** and **k** Slow inactivation plots for total g_{Na} and TTX-R g_{Na} in in the presence and absence of IL-1β. Total g_{Na} inactivation, n = 20 in GDNF, n = 18 in GDNF + IL-1β. TTX-R g_{Na} inactivation, n = 15 in GDNF, n = 16 in GDNF + IL-1β. **l** and **m.** Voltage dependence of time constant of inactivation (τ) for total g_{Na} and TTX-R g_{Na} in GDNF treated neurons in presence or absence of IL-1β. τ for total g_{Na} inactivation, n = 20 in GDNF, n = 18 in GDNF + IL-1β. τ for TTX-R g_{Na} inactivation, n = 15 in GDNF, n = 16 in GDNF + IL-1β. Error bars indicate SEM. *** = *$p<0.001$.*

Figure 3-5

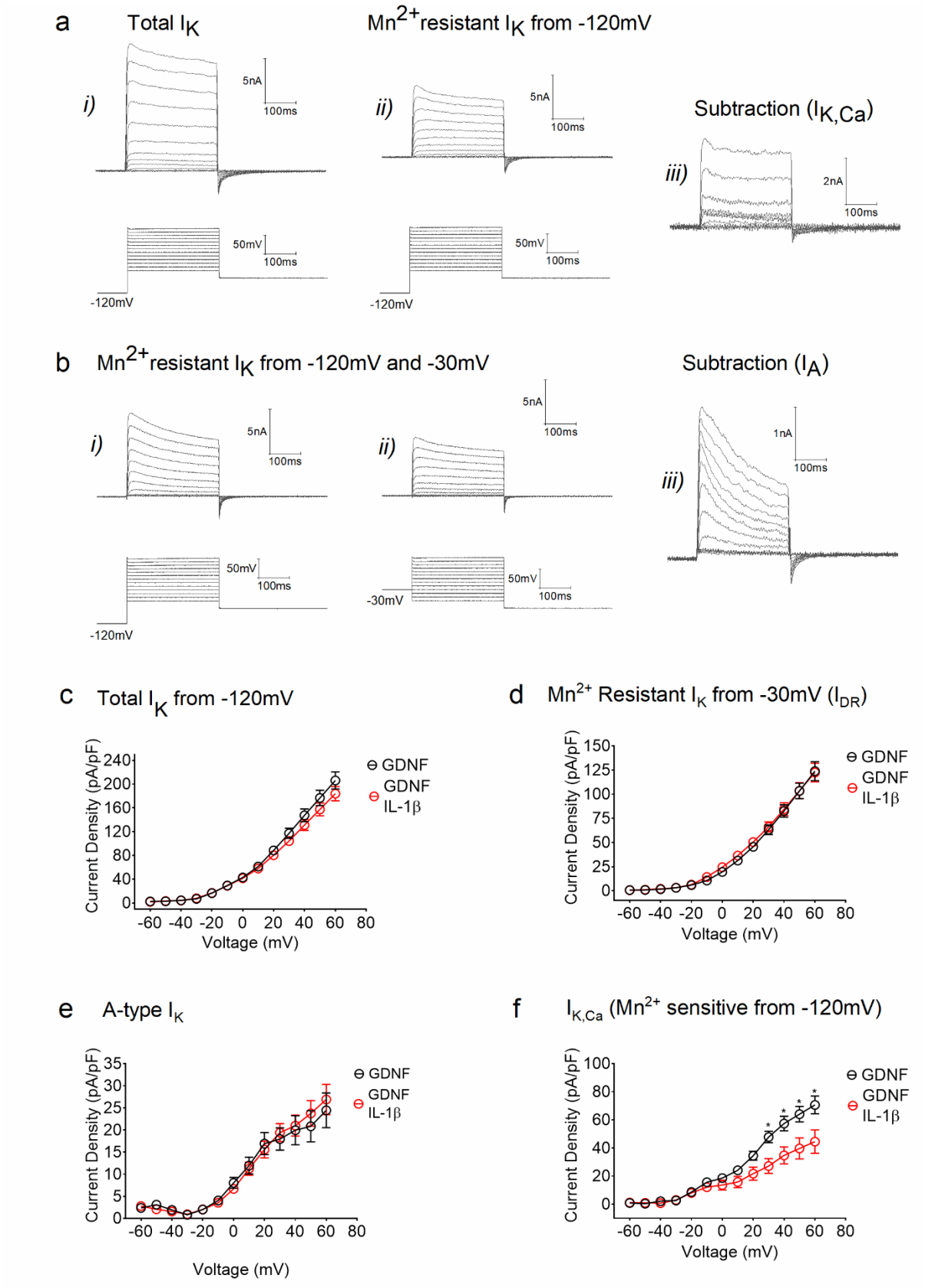
a
Total I_K
Mn^{2+}resistant I_K from -120mV
i)
ii)
iii)
Subtraction ($I_{K,Ca}$)
5nA
100ms
50mV
-120mV
2nA
b
Mn^{2+}resistant I_K from -120mV and -30mV
Subtraction (I_A)
-30mV
1nA
c
Total I_K from -120mV
d
Mn^{2+} Resistant I_K from -30mV (I_{DR})
e
A-type I_K
f
$I_{K,Ca}$ (Mn^{2+} sensitive from -120mV)
Current Density (pA/pF)
Voltage (mV)
GDNF
GDNF IL-1β

Figure 3-5. Effects of IL-1β on K^+ currents in GDNF treated neurons. **a.** *i)* Typical recordings of voltage gated K^+ currents from a holding potential of -120mV *ii)* K^+ currents from same cell recorded in the presence of 5mM Mn^{2+} and thought to reflect delayed rectifier current (I_{DR}) *iii)* Subtraction of records in *ii)* from those in *i)* to reveal $I_{K,Ca}$. **b.** *i)* and *ii)*. Mn^{2+} resistant K^+ currents from another cell (recorded in presence of 5mM Mn^{2+}) from V_h = -120 or -30mV. *iii)* Difference in records *i)* and *ii)* reveals an inactivating current we have termed I_A. Current recorded from -30mV is thought to represent I_{DR}. **c.**Total **c**urrent voltage plots for 18 GDNF treatred neurons and 16 GDNF treated neurons exposed to IL-1β (V_h = -120mV). **d.** Current voltage plots for 18 GDNF treatred neurons and 18 GDNF treated neurons exposed to IL-1β and aquired in the presence of 5mM Mn^{2+} (I_{DR} refer to panel **b** *ii)*). **e.** Current voltage plots for 18 GDNF treatred neurons and 18 GDNF treated neurons exposed to IL-1β and aquired in the presence of 5mM Mn^{2+} and obtained by subtraction (I_A refer to panel **b** *iii)*). **f.** Current voltage plots for 17 GDNF treatred neurons and 16 GDNF treated neurons exposed to IL-1β and aquired by subtraction of Mn^{2+} sensitive currents form total currents ($I_{K,Ca}$ refer to panel **a** *iii)*).

Figure 3-6

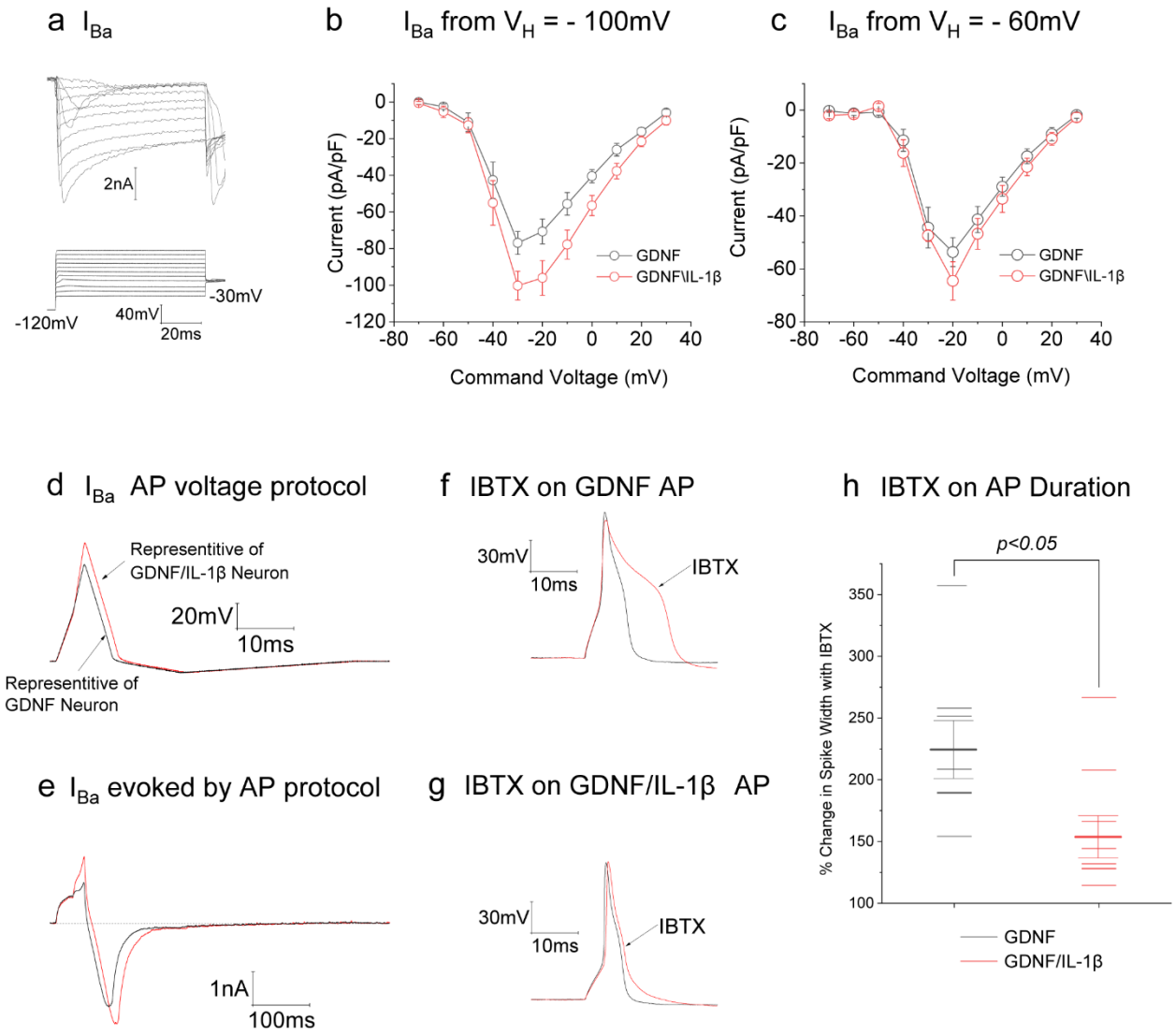

Figure 3-6. Il-1β and Ca^{2+} channel currents. **a.** Typical recordings of I_{Ba} from V_h of -100mV. **b.** Current voltage plots of I_{Ba} from V_h = -60mV, data from 13 neurons in GDNF alone, 14 neurons in GDNF + IL-1β. Differences in currents at -30, -20 and -10mV are not significant. **c.** Current voltage plots of I_{Ba} from V_h = -100mV, data from 9 neurons in GDNF alone, 12 neurons in GDNF + IL-1β. Differences in currents at -30, -20 and -10mV are not significant. **d.** Voltage protocols used to activate AP generated g_{Ba}. AP representitive of a typical GDNF neuron shown in black and that typical of an IL-1b treated neuron shown in red. Protocols written in pclamp using numbers from Table 2. **e.** I_{Ba} responses evoked in a control GDNF treated neuron in response to the two voltage protocols illustrated in **d. f.** Effect of iberotoxin (IBTX) on action potential from a control GDNF treated neuron. **g.** Effect of IBTX on IL-1β treated neuron. Note attenuation of ability of IBTX to increase AP duration. **h.** Comparison of the ability of IBTX to increase AP duration in GDNF treated cells compared to similar cells that had received IL-1β.

Chapter 4

Experimental Autoimmune Encephalomyelitis Leads to Cell Type Specific Increase in Medium-Large Dorsal Root Ganglia Neuron Excitability

N.B. EAE mice were generated and monitored in Dr. Bradley Kerr lab, and tissue extraction was performed by Mr. Muhammad Saad Yousuf.

4.1 Introduction

Multiple sclerosis (MS) is a demyelinating autoimmune disease of the central nervous system which leads to motor and sensory dysfunctions (Mandolesi et al 2015, Thompson et al 2018). Along with motor and sensory deficits, MS is frequently accompanied by debilitating chronic pain (Iannitti et al 2014). Over 60% of MS patients experience pain throughout the course of the disease; trigeminal neuralgia as well as extremities neuropathic pain are common among these patients (Drulovic et al 2015, Foley et al 2013). Experimental autoimmune encephalomyelitis (EAE) is an animal model most commonly used to study the pathophysiology of MS (Khan & Smith 2014). As seen in MS, various models of EAE lead to symptoms and signs of neuropathic pain, which include mechanical allodynia, thermal hyperalgesia, and cold allodynia (Lu et al 2012, Olechowski et al 2009). A common approach to induce EAE in mice involves the use of myelin oligodendrocyte glycoprotein (MOG), which is a component of myelin layer in the central nervous system (Constantinescu et al 2011, Iannitti et al 2014, Khan & Smith 2014). The induction of EAE simulates the MS as MOG sensitization leads to not only infiltration of sensitized T-cells and progressive demyelination, but also widespread microgliosis and astrogliosis in the central nervous system (CNS) (Mandolesi et al 2015, Olechowski et al 2009, Storch et al 1998). Therefore, the motor and sensory dysfunctions, including neuropathic pain, in clinical MS and EAE have been predominantly attributed to T-cell mediated demyelinating lesions and neuroinflammation in the spinal cord and the brain (Khan & Smith 2014, Mandolesi et al 2015, Nurmikko et al 2010, O'Connor et al 2008). Consequently, the contributions of the peripheral sensory afferents to the pathogenesis of EAE/MS induced neuropathic pain has been largely unexplored until recently.

While the demyelination and the neuroinflammation in the CNS are the primary source of clinical deficits observed in EAE and MS, increased sensory neuron excitability and ectopic discharges due to aberrant inflammation in the periphery can also contribute to the pathogenesis of neuropathic pain in EAE and MS (Basbaum et al 2009, Scholz & Woolf 2007b, Stemkowski & Smith 2012b, Wall & Devor 1983a). Indeed, more recent studies have implicated the involvement of pathological neuroimmune interactions in the primary sensory neuron for the generation of neuropathic pain in EAE (Duffy et al 2016, Frezel et al 2016, Melanson et al 2009, Thorburn et al 2016, Wang et al 2017, Zhu et al 2012). For instance, EAE leads to increased $CD4^+$ T-cell infiltration to the dorsal root ganglia (DRG) and trigeminal ganglia (TG) (Duffy et al 2016, Frezel et al 2016, Thorburn et al 2016, Wang et al 2017). Moreover, EAE leads to not only activation of satellite glial cells (SGC), but also increased activated macrophage expression in the DRG and TG (Thorburn et al 2016, Warwick et al 2014, Yousuf et al 2018). These inflammatory events coincided with the increased expression of inflammatory cytokines such as tumor necrosis factor alpha (TNFα) and interleukin 1 beta (IL-1β) in the DRG, which was also accompanied by increased expression of neuronal injury marker, activating transcription factor 3 (ATF3), in the DRG neurons (Begum et al 2013, Frezel et al 2016, Melanson et al 2009, Rodrigues et al 2016, Yousuf et al 2018).

Of particular interest is the study implicating the role of IL-1β upregulation in dorsal root ganglia for the generation of neuropathic pain in EAE animals. Rodrigues et al (2016) demonstrated induction of EAE with MOG_{35-55} leads to significant increase in IL-1β in the DRG, which peaked 10 days post-induction similar to nerve injury induced increase in IL-1β (Nadeau et al 2011), and a treatment with interleukin 1 receptor antagonist (IL-1Ra) on 8 days post-induction ameliorated mechanical hypersensitivity induced by EAE. Since pathological neuroinflammation in the DRG

can contribute to aberrant sensory neuron excitability (Basbaum et al 2009, Pinho-Ribeiro et al 2017, Scholz & Woolf 2007b, Stemkowski & Smith 2012b), the anti-allodynic effect of IL-1Ra in EAE may be mediated through diminishing the aberrant sensory neuron excitability in the DRG.

Interestingly, in contrast to chronic microgliosis and astrogliosis seen in the CNS, EAE mediated neuroinflammation in the periphery is short-lived as the levels of $CD4^+$ T-cells and macrophages decline back to baseline by 21 to 32 days post-induction, which coincided with substantial decrease in the *Il1b* mRNA transcript (Duffy et al 2016, Yousuf et al 2018). Our previous study (Stemkowski et al 2015) and the experiments in Chapter 3 have shown that long-term IL-1β treatment leads to largely reversible changes in the excitability of medium sized DRG neurons, but enduring changes in the AP duration in small IB_4^+ DRG neuron. Since we primarily tested the impact of IL-1β alone *in vitro*, we have always wondered the potential consequence of IL-1β on electrophysiological properties in DRG neurons *in vivo*. Therefore, the transient neuroinflammation seen in DRGs of EAE mice in fact provides a unique opportunity to study the potential long-term impacts of IL-1β, working in concert with other inflammatory mediators, on the electrophysiological properties of DRG neurons. Therefore, in this study, we examine the short-and long-term impact of EAE induced neuroinflammation and the increase in IL-1β on the electrophysiological properties of DRG neurons in the context of pathogenesis of neuropathic pain in EAE and MS.

4.2 Methods

4.2.1 General Methods

The detailed methods for this chapter can be seen in Chapter 2. Briefly, experimental autoimmune encephalomyelitis (EAE) was induced with MOG_{35-55} sensitization as described in Chapter 2.5. Acute female mice DRG cultures were generated as described in Chapter 2.5, and electrophysiology experiments were done as soon as cells could adhere to the dish as described in Chapter 2.4.

4.2.2 Experiment time course

Since EAE induced by MOG_{35-55} leads to transient inflammation in the DRGs, which peaks during the onset of the disease and subsided by 21-32 days post induction, we extracted L4-L6 DRGs at two separate time points to study the potential long-term consequences of EAE on DRG neuron excitability (Duffy et al 2016, Yousuf et al 2018). First, we extracted lumbar DRGs at disease onset, indicated by limp tail, at which expression of immune cells and *Il1b* mRNA transcript were prominent (Figure 2-2) (Rodrigues et al 2016, Yousuf et al 2018). Secondly, we extracted lumbar DRGs at 'chronic' time point (7 days post-onset or 21 days post-induction), at which lumbar DRGs no longer displayed significant immune cell and *Il1b* mRNA expression (Figure 2-2) (Duffy et al 2016, Yousuf et al 2018). A group of mice only receiving complete Freund's adjuvant (CFA) injection was used as a control throughout the study. From here on out these groups will be referred to as CFA control, EAE onset, and EAE chronic.

4.2.3 Mice DRG neuron subclassification

There have been reports of EAE leading to preferential damage to the medium and large diameter sensory neurons, which give rise to thinly myelinated Aδ-fibres and heavily myelinated Aβ-fibres respectively, in the TG and the DRG (Duffy et al 2016, Pender 1986, Wang et al

2017). In light of these findings, a more simplified classification, subdividing DRG neurons into 'small' (<26 μm) DRG neurons which presumably give rise unmyelinated C-fibre and 'medium-large' (≥26 μm) DRG neurons which generally give rise to myelinated A-fibres, was used to examine the impact of EAE on the electrophysiological properties in likely-unmyelinated or likely-myelinated mice DRG neurons (Dirajlal et al 2003, Harper & Lawson 1985, Ruscheweyh et al 2007). From here on out these subpopulations of DRG neurons will be referred to as 'small unmyelinated' and 'medium-large myelinated' DRG neurons.

4.3 Results

4.3.1 EAE produces cell type specific chronic increase in DRG neuron excitability

To assess the excitability of acutely cultured DRG neurons from CFA, EAE onset, and EAE chronic mice, action potentials (AP) were evoked by 450ms 2nA current ramp (Figures 4-1A, E). Then, using the evoked AP discharges, the average number of APs, proportion of AP discharge, and cumulative latencies up to 8 APs were quantified. Induction of EAE produced no observable changes in small presumptive unmyelinated DRG neurons as the number of AP discharges (Figure 4-1B), proportion of AP discharges (Figure 4-1C), and cumulative latencies (Figure 4-1D) were not affected. In stark contrast, medium-large likely-myelinated DRG neurons were severely affected by the induction of EAE (Figure 4-1E). First, the number of AP discharges were significantly increased in medium-large myelinated DRG neurons during EAE onset (n=49; 6.78 ± 1.40 APs) compared to CFA control (n=74; 3.72 ± 0.91 APs; Kruskal-Wallis test; $p<0.02$; Figure 4-1F). Furthermore, the increase in excitability persisted at the chronic timepoint as the number of AP discharges remained elevated in medium-large myelinated DRG neurons at the chronic time point (n=90; 7.13 ± 1.24 APs) compared to CFA control (Kruskal-Wallis test; $p<0.03$; Figure 4-1F). Secondly, medium-large myelinated DRGs neurons from EAE onset mice

were significantly more likely the discharge APs in response to the 450 ms 2 nA current command as 55.1% of the EAE onset DRG neurons fired APs compared to 28.4% in CFA control (Fisher's exact test; $p<0.005$; Figure 5-1G). Consistent with the excitability assessed by the number of APs, medium-large myelinated DRGs from EAE chronic group maintained the higher proportion of AP discharge compared to CFA control (48.89% vs 28.4%; Fisher's exact test; $p<0.011$). Finally, medium-large myelinated DRG neurons fired repetitive APs more rapidly indicated by the significantly reduced cumulative latencies at third to eighth AP evoked by the 2 nA current ramp (Figure 4-1H). Furthermore, the decrease in cumulative latencies persisted even at chronic timepoint from fifth to seventh AP compared to the CFA control (Figure 4-1H). The changes in cumulative latencies can be visualized in the representative AP discharges in Figure 5-1E. The dashed lines represent the cumulative latencies of medium-large myelinated DRG neuron from the CFA control. When it is superimposed onto representative AP discharges of DRG neurons from EAE onset and EAE chronic mice, the lines go beyond the assigned AP number indicating more rapid AP discharges.

4.3.2 EAE induction leads to cell type specific changes in AP parameters

Previous experiments from our laboratory and experiments in Chapter 3 demonstrated IL-1β affected AP parameters in a cell type specific manner (Stemkowski & Smith 2012a). Therefore, the impact of EAE on AP parameters and its reversibility was assessed. As seen in the excitability measures, the majority of AP parameters in small unmyelinated were not significantly affected by the induction of EAE (data summarized in Table 4-1). Only the maximum rate of depolarization was significantly reduced during the onset of EAE compared to CFA control; however, this was reversible within 7 days as small unmyelinated DRG neurons from the EAE chronic group were no longer different from CFA group (Figure 4-2E). AP

duration (Figure 4-2B), spike height (Figure 4-2C), rheobase (Figure 4-2D), maximum rate of repolarization (Figure 4-2F), and afterhyperpolarization (AHP) amplitude (Figure 4-2G) were not affected by the induction of EAE. In contrast, more AP parameters were significantly affected by the induction of EAE in medium-large myelinated DRG neurons (data summarized in Table 4-1). First, rheobase, the minimum current required for AP discharge, was significantly attenuated at EAE onset compared to CFA control (Figure 4-2D), and maximum rate of depolarization and maximum rate of repolarization were both significantly reduced during EAE onset compared to CFA (Figures 4-2E, F). However, these changes were transient as these AP parameters were no longer significantly different from the CFA control at chronic time point (Figures 4C-F). As seen in small unmyelinated DRG neurons, AP duration (Figure 4-2B), AP amplitude (Figure 4-2C), and AHP amplitude (Figure 4-2G) were not affected by the EAE induction.

4.4 Discussion

4.4.1 Summary of results

In this study, we demonstrated the induction of EAE with MOG_{35-55} sensitization leads to selective modulation of DRG neuron excitability. Predominantly likely-myelinated medium-large (≥26 μm) DRG neurons became significantly more excitable in response to the EAE induction. In contrast, the excitability in likely-unmyelinated small (<26 μm) DRG neurons were unaffected by the induction of EAE. Remarkably, the increased excitability in medium-large myelinated DRG neurons persisted at the chronic time point, at which EAE induced inflammation in the DRG has essentially resolved. EAE induced change in the AP parameters predominantly mirrored the changes in excitability as only maximum rate of depolarization was

affected in small unmyelinated DRG neurons as opposed to significant, but transient, decrease in rheobase, maximum rate of depolarization and repolarization in the medium-large DRG neurons.

4.4.2 Implications of EAE induced cell type specific increase in myelinated DRG neuron excitability on EAE induced sensory neuron injury

The EAE model mimics the pathophysiology of MS by inducing profound demyelination and neuroinflammation in the CNS, which leads to motor and sensory dysfunctions (Khan & Smith 2014, Storch et al 1998). Although T-cell mediated demyelination and axonal damage in the CNS is unequivocally clear, the damage to the peripheral sensory afferents is still not fully explored. An older study using myelin basic protein (MBP) as a myelin antigen reported demyelination of primary afferent Aδ-fibre in the sacral and coccygeal DRG (Pender 1986). Although MBP is not required for myelin formation in the periphery (Kirschner & Ganser 1980), it is commonly expressed in the peripheral nervous system (PNS) (Patzig et al 2011). Therefore, sensitization with MBP may damage myelinated fibres in the PNS. A more recent study has postulated peripheral neuropathy contributes to the pathogenesis of neuropathic pain in MOG_{35-55} sensitization induced EAE model (Wang et al 2017). Since the authors did not use pertussis toxin to permeabilize the blood brain barrier (EAE no pertussis; EAEnp), they argued the MOG sensitized T-cells are trapped in the peripheral nervous system as this coincided with the lack of severe motor deficits. The authors reported the presence of MOG mRNA transcripts in sciatic nerve and DRG, and the induction of EAEnp with MOG_{35-55} lead to myelin decompaction and myelin-fibre dissociation, which they argued as a sign of peripheral neuropathy. Since EAEnp mice displayed mechanical allodynia, the authors concluded the peripheral neuropathy by myelin damage contribute to neuropathic pain behavior in EAE animals. This was however unexpected as previous proteomic and mass spectrometry analysis did not detect MOG protein expression in

peripheral nervous system (Patzig et al 2011). In support of their hypothesis, the same group as well as the others have reported preferential upregulation of ATF3 in medium-large DRG and TG neurons that give rise to myelinated A-fibres (Duffy et al 2016, Wang et al 2017). Although these data support damage to the primary sensory neurons, significant demyelination by MOG_{35-55} sensitized T-cells is still uncertain. Contrary to Wang et al., Frezel et al (2016) have reported expression of ATF3 in peripheral sensory neurons as early as 5 days after MOG_{35-55} injection, which preceded the $CD4^+$ T-cell infiltration and motor deficits. Furthermore, although to a much lesser extent, the authors also demonstrated CFA or pertussis toxin injection alone was able to cause ATF3 expression. These results indicate sensory neuron damage is not likely due to the demyelination of sensory afferents. Despite the conflicting reports, these studies consistently demonstrated EAE induced damage to the peripheral sensory neurons, which can influence DRG neuron excitability and lead to neuropathic pain (Liu et al 2000a, Wall & Devor 1983b).

In light of these findings, we used a very basic DRG subclassification which we simply grouped DRG neurons into small (<26 μm) likely-unmyelinated DRG neurons and medium-large (≥26 μm) likely-myelinated DRG neurons according to the previous analysis of cell diameter dependant myelination in mice DRG neurons (Dirajlal et al 2003). Using this classification, our results are in line with the previous reports indicating cell type specific damage (Duffy et al 2016, Wang et al 2017). Here, we show while EAE induction with MOG_{35-55} showed no observable effect in the unmyelinated small DRG neuron excitability; it significantly increased excitability in the medium-large myelinated DRG neurons, as indicated by increased number of APs, increased proportion of AP discharge, and decreased cumulative latencies of AP discharges, during both onset and surprisingly chronic timepoints. Furthermore, AP parameters in small unmyelinated DRG neurons were largely unaffected by EAE induction as opposed to

medium-large myelinated DRG neurons which displayed significantly lower rheobase, and decreased rate of repolarization at onset after EAE induction, which can contribute to the increased neuron excitability. This cell type specific increase in DRG neuron excitability is consistent with a previous result that demonstrated larger $[Ca^{2+}]_i$ increase in response to depolarization with 30 mM KCl in medium-large DRG neurons (Mifflin et al 2018). These results are also in line with previous studies that reported increased primary afferent Aβ-fibre firing frequency induced by EAE with proteolipid protein (PLP) sensitization in SJL mice (Lu et al 2012) and increased medium-large DRG neuron excitability by spinal nerve ligation (SNL) injury (Ma et al 2003). Taken together, our data add support to cell type specific damage induced by EAE which predominantly affect medium-large diameter DRG neurons. However, precise molecular mechanism underlying this selective injury is uncertain and needs to be further investigated.

4.4.3 Role of IL-1β in the EAE mediated increase in DRG neuron excitability

The changes in DRG neuron excitability coincided with increased $CD4^+$ T-cells and macrophages expression in the DRG (Duffy et al 2016, Rodrigues et al 2016, Yousuf et al 2018). MOG sensitized $CD4^+$ T-cells and activated macrophages are the primary sources of key inflammatory cytokines, such as IL-1β, IL-17, and TNF-α, implicated in the EAE induced neuropathic pain (Begum et al 2013, Hu et al 2018, Komiyama et al 2006, Li et al 2004, Schuh et al 2014). These cytokines have been shown to directly modulate DRG neuron excitability (Chen et al 2011, Czeschik et al 2008, Ebbinghaus et al 2017, Richter et al 2012, Stemkowski et al 2015, Stemkowski & Smith 2012a); therefore, the change in medium-large myelinated neuron excitability may be attributed to neuroimmune interaction facilitated through release of inflammatory cytokines. Previous publications from our laboratory have shown 5-6 day IL-1β

treatment leads to significant increase in number of APs discharge in response to 2 nA current ramp in medium sized (30-40 μm) rat DRG neurons, but did not affect small (<30 μm) rat DRG neuron excitability (Stemkowski et al 2015, Stemkowski & Smith 2012a). Although, we used short-term dissociated mice DRG neuron culture and a more simplified subclassification with small (<26 μm) unmyelinated and large (≥26 μm) myelinated DRG neurons, the results we find mirror the previous studies with long-term rat DRG neuron culture indicating EAE mediated modulation of DRG neuron excitability is likely facilitated through the actions of IL-1β. On top of this, subcutaneous injections of IL-1Ra days before the onset of EAE lead to significant attenuation of mechanical hypersensitivity in EAE animals (Rodrigues et al 2016). At this time point, mechanical hypersensitivity was present which coincided with the elevated IL-1β levels in the DRG, but motor dysfunction was absent which coincided with lack of detectable upregulation of IL-1β or TNFα in the spinal cord (Begum et al 2013). As EAE developed normally after the IL-1Ra administration, the anti-allodynic effects of IL-1Ra was likely facilitated through antagonizing IL-1R in the DRG neurons and normalizing the aberrant excitability in the DRG neuron as our laboratory and the others have shown previously (Stemkowski & Smith 2012a, Takeda et al 2008).

Furthermore, although TNFα has been shown to be upregulated in the DRG after EAE induction with Mycobacterium Tuberculosis in female Lewis rats (Melanson et al 2009), a later analysis from the same group revealed that main cellular source of TNFα was the DRG neurons themselves (Begum et al 2013). The time course for substantial TNFα upregulation in the DRG neuron coincided with the level of TNFα in the spinal cord as well as the onset of motor deficits (Begum et al 2013). Since pain behavior appears before the onset of the disease (Olechowski et al 2009), lack of sufficient TNFα expression before disease onset indicates TNFα may not be

critically involved for the onset of mechanical hypersensitivity in EAE. In support of this, injection of infliximab, a monoclonal antibody against TNFα, days before the onset (pain is present but the motor deficits are absent at this timepoint) failed to alleviate mechanical hypersensitivity in EAE model with MOG sensitization (Rodrigues et al 2016). That said, anti-TNFα has been shown to alleviate EAE induced hyperexcitability in female medium-large DRG neurons (Mifflin et al 2018). Therefore, TNFα is likely to play a role during the maintenance of mechanical hypersensitivity in EAE animals. Taken together, these results suggest the EAE induced changes in medium-large myelinated DRG neuron excitability are likely mediated through IL-1β, and the increase in DRG neuron excitability by IL-1β contributes to the onset of mechanical hypersensitivity in EAE animals.

4.4.4 Inconsistencies with IL-1β mediated changes in DRG neuron excitability and AP parameter at EAE onset

Although IL-1β appears to be a significant contributor of EAE induced changes in medium-large myelinated DRG neuron and mechanical hypersensitivity, IL-1β is unquestionably not the only cytokine involved in the EAE induced changes in DRG neuron excitability. This is evident as there are inconsistencies that cannot be explained by mechanisms of IL-1β alone. First, although our results are consistent with the studies indicating cell type specific damage to sensory neuron by EAE (Duffy et al 2016, Wang et al 2017) and modulation of DRG neuron excitability by IL-1β (Stemkowski et al 2015, Stemkowski & Smith 2012a), the complete lack of effect on excitability in small unmyelinated DRG neurons was somewhat surprising. The receptors for the key inflammatory cytokines involved in the generation of pain in EAE animals, such as IL-1β, IL-17 and TNFα (IL-1R, IL-17R and TNFR), are abundantly expressed in small unmyelinated DRG neurons, and their activation has been shown to increase small DRG neuron excitability

(Binshtok et al 2008, Ebbinghaus et al 2017, Li et al 2004, Ozaktay et al 2002, Richter et al 2012, Schafers et al 2003). Furthermore, since our previous studies have shown consistent increase in AP duration in response to IL-1β in small IB_4^+ DRG neurons, the lack of significant change in the AP duration and the rate of repolarization in small myelinated DRG neurons in the EAE model was also unexpected (Stemkowski & Smith 2012a) (Chapter 3). One possible explanation for these inconsistencies may be that we did not distinguish between small IB_4^+ and IB_4^- DRG neurons. Since the actions of cytokines are often cell type dependant (Li et al 2004, Richter et al 2012, Stemkowski & Smith 2012a), this may have diluted the significance of EAE induced changes in the excitability and AP parameter in small unmyelinated DRG neurons. That said, the lack of thermal hyperalgesia in EAE model with MOG_{35-55} sensitization (Lu et al 2012, Olechowski et al 2009), is in line with our observations. Thus, small unmyelinated DRG neurons may indeed be unaffected by EAE. Second, since key cytokines, such as IL-1β, TNFα, and IL-17, shown to be involved in the pathogenesis of neuropathic pain and EAE has been shown to enhance both TTX-S and TTX-R Na^+ channels, lack of significant effect on AP amplitude and decrease in maximum rate of depolarization is puzzling (Binshtok et al 2008, Chen et al 2011, Czeschik et al 2008, Ebbinghaus et al 2017, Huang et al 2014, Jin & Gereau 2006, Liu et al 2006). A potential mechanism for this may involve bradykinin, which has been implicated to play an important role in both EAE and pain (Dray & Perkins 1993, Uzawa et al 2014), as bradykinin treatment leads to delayed rate of depolarization, but increase in DRG neuron excitability (Davidson et al 2014).

Taken together, complex neuroimmune interactions facilitated by several inflammatory mediators in the DRG far beyond the scope of the current study most likely have contributed to

the discrepancies. Furthermore, these inconsistencies undoubtedly have also risen from the use of different species, models of injury, culture method, and sex.

4.4.5 EAE induced chronic increase in medium-large DRG neuron excitability and relevance to chronic pain

The most interesting observation in this study was the persistence of EAE mediated increase in excitability in the medium-large myelinated DRG neuron without the continued presence of inflammatory stimuli, at the chronic timepoint. This is in stark contrast to the effect of IL-1β on cultured medium sized DRG neuron, which recovered from aberrant increase in excitability in the absence of continued inflammatory stimulus from IL-1β (Stemkowski et al 2015). The changes in gene expression is most likely involved as key inflammatory mediators involved in EAE are capable of modulating channel function and expression in the DRG neuron (Binshtok et al 2008, Fehrenbacher et al 2005, Huang et al 2014, Segond von Banchet et al 2013). However, $Na_v1.8$ and transient receptor potential cation channel (TRPV1) mRNA expressions were not changed by the induction of EAE (Rodrigues et al 2016). This is consistent with the lack of thermal hyperalgesia in MOG induced EAE model (Olechowski et al 2009) as well as our electrophysiological data since these channels are primarily expressed in small unmyelinated DRG neurons that are involved in thermal hypersensitivity (Binshtok et al 2008, Segond von Banchet et al 2013, Vilceanu et al 2010, Yu et al 2008). Since we have not explicitly examined the ion channel expression and function in the EAE model, the processes underlying the persistent increase in medium-large DRG neuron excitability is unclear. This is a great avenue for future investigation which may reveal important mechanisms responsible for transition from acute to chronic pain state. In addition, there is also a possibility of continued or induced presence of unknown stimuli in the DRG that may maintain the increased excitability. This may

be mediated through chronic activation of satellite glial cells and subsequent IL-1β and TNFα secretion, which has been implicated in the pathogenesis and maintenance of neuropathic pain (Kawasaki et al 2008a, Lim et al 2017, Liu et al 2012, Takeda et al 2008).

Interestingly, our findings of EAE induced increase in medium-large DRG neuron excitability can be also seen in peripheral nerve injury model of neuropathic pain. For instance, chronic constriction injury (CCI) (Bennett & Xie 1988) and spinal nerve ligation (SNL) (Chung et al 2004) lead to not only preferential damage to medium-large diameter DRG neurons, but they also increased excitability of these neurons selectively without affecting smaller unmyelinated DRG neurons (Kajander & Bennett 1992, Liu et al 2000a, Ma et al 2003, Obata et al 2003). Aberrant Aβ-fibre activity is required for both onset and maintenance of neuropathic pain (Suter et al 2009, Xu et al 2015). This is evident as ameliorating aberrant medium-large DRG neuron excitability by HCN channel blockers or targeted silencing of Aβ-fibre readily reversed mechanical allodynia induced by peripheral nerve injury (Noh et al 2014, Xu et al 2015, Young et al 2014). Moreover, nociceptor sensitization alone was not enough for spinal microglia activation, which is critical for central sensitization (Suter et al 2009). Therefore, our results demonstrating persistent increase in medium-large myelinated DRG neuron excitability by EAE induction provides a potential mechanism underlying chronic pain behavior seen in EAE animals (Lu et al 2012, Olechowski et al 2009, Thorburn et al 2016). Furthermore, since microgliosis by colony stimulating factor 1 (CSF1) produced by activated astrocytes has been implicated to play a critical role in the maintenance of chronic neuroinflammation and demyelination in the CNS in EAE animals (Gushchina et al 2018), persistence of aberrant Aβ-fibre DRG neuron excitability may also contribute indirectly to astrogliosis and microgliosis by increased chemokine, cytokine,

and neurotransmitter release onto spinal dorsal horn (Grace et al 2014, Pinho-Ribeiro et al 2017, Scholz & Woolf 2007a).

4.4.6 Limitations

As evident by large variations in sample sizes (Table 4.1), medium-large myelinated DRG neurons were much more frequently recorded in this experiment. This was partially due to their abundance in our cell culture. The vast majority of viable cells in our culture were medium-large DRG neurons. Furthermore, the current study used a very basic subclassification of DRG neurons, which could have underestimated significance in a specific subpopulation of DRG neurons. Since we directly adapted an acute dissociated rat DRG neuron culture, optimization for mice DRG culture may improve small DRG neuron viability and population.

4.5 Conclusion

In this study, we demonstrate, for the first time, the induction of EAE leads to increase in medium-large likely-myelinated DRG neuron excitability. Remarkably, this effect persisted without the presence of substantial inflammatory mediators in the DRG at chronic time point. Since the aberrant medium-large DRG neuron excitability is required for the pathogenesis of neuropathic pain, our data provides a potential mechanism that may underlie the chronic neuropathic pain observed in EAE and MS. The precise mechanism underlying the transition between acute to chronic pain state is still unclear. The results from this study suggest complex neuroimmune interactions, likely involving IL-1β, in the DRG may contribute to the transition. Therefore, understanding the mechanism underlying the EAE induced chronic increase in DRG neuron excitability may reveal important insight for the treatment of chronic neuropathic pain.

Table 4.1. Effects of EAE on AP parameters

AP Parameters	Unmyelinated (<26 µm)			Myelinated (≥26 µm)		
	CFA	EAE Onset	EAE Chronic	CFA	EAE Onset	EAE Chronic
AP Duration (ms)	3.868±0.4037 (26)	4.411±0.794 (17)	3.919±0.3425 (31)	1.12±0.0962 (73)	1.434±0.1371 (48)	1.186±0.0789 (90)
AP Amplitude (mV)	116.1±2.011 (26)	108.6±3.083 (17)	115.9±2.15 (31)	105.5±1.674 (73)	102.7±2.141 (48)	108.6±1.411 (90)
Rheobase (nA)	0.2654±0.01659 (26)	0.2824±0.02141 (17)	0.3 ± 0.02 (31)	0.474±0.02847 (73)	0.35±0.030 (48)*	0.4211±0.02282 (90)
Max Rate of Rise (mV/ms)	171.3±21.16 (26)	84.8 ± 4.95(17)**	150.2±9.997 (31)#	243.8±14.69 (73)	110.1±4.551 (48)****	219.7±13.02 (90)####
Max Rate of Decay (mV/ms)	-63.92±6.35 (26)	-52.64±7.632 (17)	-63.24±7.398 (31)	-136.9±5.839 (73)	-98.17±5.822 (48)****	-120.5±4.887 (90)#
AHP Amplitude (mV)	-14.25±0.8962 (26)	-11.11±1.216 (17)	-13.35±0.6395 (31)	-13.87±0.6163 (73)	-12.03±0.6672 (48)	-12.43±0.4831 (90)

Kruskal-Wallis test with Dunn's multiple comparisons test was used for the rheobase. One-way ANOVA with Bonferroni's multiple comparisons test for the rest of the parameters. * $p<0.05$, ** $p<0.01$, **** $p<0.0001$ compared to CFA control; # $p<0.05$, #### $p<0.0001$ compared to EAE onset. All data are represented in mean ± SEM (n)

Figure 4-1

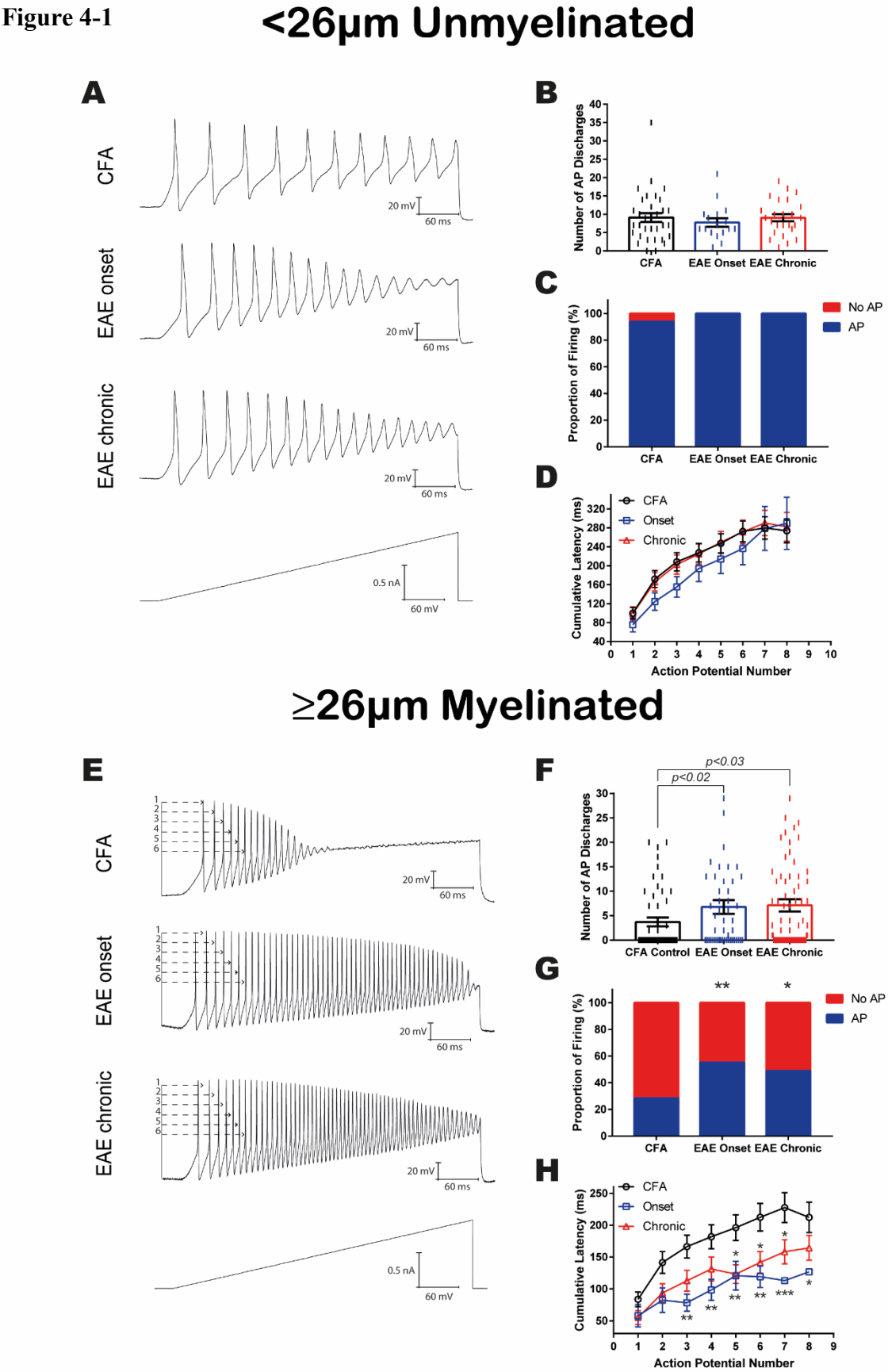
<26µm Unmyelinated
A
CFA
EAE onset
EAE chronic
20 mV
60 ms
0.5 nA
60 mV
B
Number of AP Discharges
CFA
EAE Onset
EAE Chronic
C
Proportion of Firing (%)
No AP
AP
D
Cumulative Latency (ms)
CFA
Onset
Chronic
Action Potential Number
≥26µm Myelinated
E
F
p<0.03
p<0.02
CFA Control
G
**
*
H
***

Figure 4-1. EAE leads to persistent cell type specific increase in excitability in DRG neurons. **(A-D)** Current ramp experiments with small (<26μm) unmyelinated DRG neurons from CFA (n=33), EAE onset (17), and EAE chronic mice (n=25). **(E-H)** Current ramp experiments with large (≥26 μm) myelinated DRG neurons from CFA (n=74), EAE onset (n=49), and EAE chronic mice (n=90). **(A, E)** Representative recordings of APs evoked by 2 nA current ramp. Each number represents AP number and dashed lines represent cumulative latencies of a large (≥26 μm) myelinated DRG neuron from CFA mice. The same cumulative latency lines are superimposed on large (≥26 μm) myelinated DRG neuron recordings from EAE onset and EAE chronic mice. (**B, F)** Average number of AP discharges at 2 nA current ramp (Kruskal-Wallis test with Dunn's multiple comparisons test) (**C, G)** Proportion of AP discharge at 2 nA current ramp (Fisher's exact test; * $p<0.05$, ** $p<0.01$ compared to CFA control) **(D, H)** Cumulative latency of AP discharges at 2 nA current ramp (Two-way ANOVA with Bonferroni's multiple comparisons test, * $p<0.05$, ** $p<0.01$, *** $p<0.001$ compared to CFA control). All data are represented as mean ± SEM.

Figure 4-2

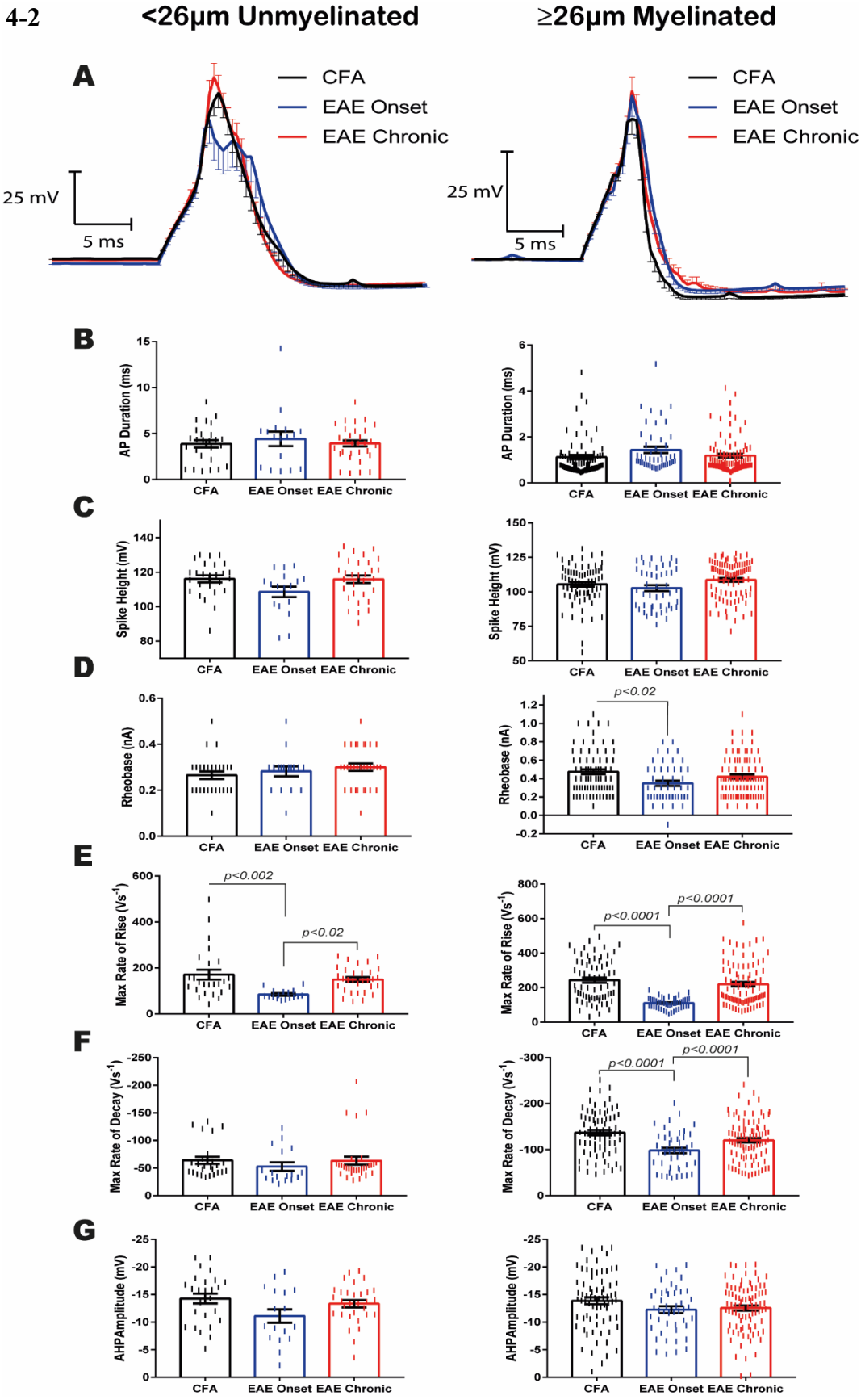
<26µm Unmyelinated
≥26µm Myelinated
A
CFA
EAE Onset
EAE Chronic
25 mV
5 ms
B
AP Duration (ms)
C
Spike Height (mV)
D
Rheobase (nA)
p<0.02
E
Max Rate of Rise (Vs-1)
p<0.002
p<0.02
p<0.0001
F
Max Rate of Decay (Vs-1)
G
AHPAmplitude (mV)
CFA
EAE Onset
EAE Chronic

Figure 4-2. Effects of EAE on action potential parameters of small (<26μm) unmyelinated and large (≥26 μm) myelinated DRG neurons. **(A)** Left panel represents averaged AP recordings of small (<26μm) unmyelinated DRG neurons from CFA (n=26), EAE onset (n=17), and EAE chronic (n=31) mice. Right panel represents averaged AP recordings of large (≥26 μm) myelinated DRG neurons from CFA (n=93), EAE onset (n=48), and EAE chronic (n=90) mice. (**B-G)** Average AP duration **(B)**, spike height **(C)**, rheobase **(D)**, max rate of depolarization **(E)**, max rate of repolarization **(F)**, and afterhyperpolarization amplitude **(G)** of small (<26μm) unmyelinated DRG neurons (left panel) and large (≥26 μm) myelinated DRG neurons (right panel) from CFA, EAE onset, and EAE chronic mice. **(B, C, E, F, G)** One-way ANOVA with Bonferroni's multiple comparisons test. **(D)** Kruskal-Wallis test with Dunn's multiple comparisons test. All data are represented as mean ± SEM.

Chapter 5

Persistent Colony Stimulating Factor 1 Production and Neuroinflammation in the Dorsal Root Ganglia Underlie the Differential Reversibility of Mechanical Allodynia Seen in Spared Nerve Injury and Chronic Constriction Injury

N.B. All von Frey test and animal care were done by Ms. Twinkle Joy. Mr. Benjamin Mikler assisted with GFAP and CSF1 IHC, imaging, and analysis.

5.1 Introduction

Neuropathic pain is a pain induced by a lesion or a disease to the somatosensory nervous system (Jensen et al 2011). The etiology and the pathophysiology of neuropathic pain is incredibly diverse; and it can arise from many conditions affecting the somatosensory nervous system such as peripheral nerve trauma, spinal cord injury, diabetes, HIV infection and multiple sclerosis (Alles & Smith 2018). As a result, neuropathic pain has been difficult to treat, and the prognosis of patients suffering from this debilitating condition is unpredictable. Indeed, neuropathic pain arising from similar disease states can lead to diverse outcomes. For example, a recent epidemiological study revealed that neuropathic pain caused by physical trauma led to 24.61% of patients recovering within a year, 24.71% of patients recovering within five years, and 50.67% of patients with chronic neuropathic pain symptoms beyond five years (DiBonaventura et al 2017). Despite high demand for effective novel therapeutic agents, the record of translation in pain research has been poor; a drug often works unbelievably well in animal models of neuropathic pain, yet the same drug lacks significant clinical efficacy in humans (Yezierski & Hansson 2018). It has been suggested that the poor translation may be due to the fact that most pre-clinical studies have focused on the acute state of neuropathic pain instead of examining the chronic neuropathic state (Clark 2016). The transition between acute to chronic neuropathic pain state remains ambiguous and understanding the differences between acute and chronic pain state may provide avenues for novel therapeutic agents (Voscopoulos & Lema 2010).

In order to better understand the heterogeneity of neuropathic pain phenotypes, I take advantage of the behavioral differences observed between spared nerve injury (SNI) and chronic constriction injury (CCI) models of neuropathic pain. SNI leads to permanent mechanical allodynia in contrast to CCI which produces transient mechanical hypersensitivity (Decosterd &

Woolf 2000, Mosconi & Kruger 1996). There is mounting evidence that neuroinflammation in the DRG is critical not only during the onset of neuropathic pain, but also in the maintenance of chronic neuropathic pain symptoms. Activation of satellite glial cells (SGCs) and infiltration of macrophages in the DRG play a critical role in the generation of tactile allodynia and animal models of neuropathic pain (Cobos et al 2018, Colburn et al 1999, Otoshi et al 2010, Vega-Avelaira et al 2009). Recent studies have demonstrated peripheral nerve injury causes *de novo* induction of a potent cytokine, colony stimulating factor 1 (CSF1), in the ipsilateral DRG neurons, which in turn leads to spinal microglia activation (Guan et al 2016, Okubo et al 2016). The production of CSF1 in the sensory neuron was essential for allodynic behavior in mice following a nerve injury (Guan et al 2016, Okubo et al 2016). Furthermore, the activation of SGC and IL-1β release in the DRG has been shown to be involved in the production of CSF1 following peripheral nerve injury (Lim et al 2017). Therefore, I hypothesize that the degree and the duration of neuroinflammation, mediated by IL-1β, and CSF1 production in the affected DRGs will be the underlying differences between acute and chronic tactical allodynia in animal models of neuropathic pain. Although the production of CSF1 in the DRG has been studied in various animal models of nerve injury, no studies have compared its production in the DRG between animal models in the context of persistent peripheral neuroinflammation mediated pain maintenance (Frezel et al 2016, Guan et al 2016, Krishnan et al 2018, Lim et al 2017, Okubo et al 2016, Vega-Avelaira et al 2009). In this chapter, I profile the levels of CSF1 production, *Il1b* mRNA expression, SGC activation, and macrophage expression in in the ipsilateral L4-L5 DRGs of sham, CCI, SNI animals at onset, where both CCI and SNI animals display mechanical allodynia, and chronic time points, where only SNI animals maintain tactile allodynia, to reveal potential differences in the DRGs between acute and chronic neuropathic pain states.

5.2 Methods

The methods used in this chapter are described in detail in Chapter 2. Briefly, neuron enriched cultures were generated and were treated with 100pM IL-1β (Chapter 2.2). Sham, chronic constriction injury (CCI), and spared nerve injury (SNI) were generated as described (Chapter 2.6). Behavior was tested via von Frey test (Chapter 2.6) mRNA levels in the DRG were measured via rt-qPCR (Chapter 2.7). Various markers of neuroinflammation were detected via IHC and confocal microscopy (Chapter 2.8). One-way ANOVA with Bonferroni's comparisons test and Pearson's correlation coefficient test were used where appropriate (Chapter 2.9).

5.3 Results

5.3.1 CCI animals fully recover from mechanical allodynia at 42 days post-surgery while SNI animals remain allodynic

In order to examine the potential differences in the DRGs between transient and chronic neuropathic pain, experimental time course was established by determining the following time points: 1) number of days post-surgery at which both CCI and SNI animals display mechanical allodynia (onset); 2) number of days post-surgery at which CCI animals have fully recovered from neuropathic pain, but SNI animals maintain mechanical allodynia (chronic).

Sham, CCI, and SNI animals were generated, and mechanical thresholds were measured via von Frey test over a 42-day period. A total of 83 male Sprague-Dawley rats were used for this experiment, and they were randomly assigned to either sham, CCI, or SNI surgery once the baseline withdrawal thresholds were recorded. Data from all animals, including 'non-responders' which did not develop mechanical allodynia after CCI or SNI, were collected for my study. At 7 days post-surgery, both CCI and SNI animals developed neuropathic pain as their withdrawal thresholds were significantly attenuated (6.48 ± 3.76 and 4.73 ± 2.78 g respectively) compared to

sham operated animals (14.44 ± 0.31 g) (Figure5-1). As shown previously by Decosterd and Woolf (2000), the SNI model produced a robust chronic mechanical allodynia as withdrawal threshold remained significantly attenuated (5.42 ± 3.58 g) compared to sham operated animals (13.83 ± 0.82 g) at 42 days post-surgery. In contrast, some CCI operated animals started to recover from mechanical allodynia at 28 days post-surgery, and the withdrawal threshold (8.31 ± 5.52 g) became significantly higher compared to SNI animals (4.34 ± 3.63 g) (Figure 5-1). In line with the previous observations by Mosconi and Kruger (1996), CCI animals showed peak mechanical allodynia 14 days post-surgery (3.21 ± 2.46 g) and became indistinguishable from sham animals on 35- and 42- days post-surgery as their paw withdrawal thresholds (11.31 ± 4.87 and 13.23 ± 3.49 g respectively) were no longer statistically different from the time-controlled sham animals (14.42 ± 0.58 g; P=0.09 and 13.83 ± 0.82 g; P>0.99 respectively). A few CCI animals still showed signs of neuropathic pain at 35 days post-surgery, and maximal behavioral difference between CCI and SNI was observed at 42 days post-surgery (13.83 ± 0.82 g vs 5.42 ± 3.58 g). As a result, ipsilateral L4-L5 DRG samples were extracted at 7-days and 42-days post-surgery for rt-qPCR or IHC experiments (Figure 2-3).

5.3.2. Csf1 mRNA expression is chronically elevated in the DRGs of SNI animals compared to CCI animals

First, the relationship between mechanical allodynia and CSF1 expression in the DRG was examined via measuring the relative changes in *Csf1* mRNA expression in the L4-L5 ipsilateral DRGs from sham, CCI, and SNI animals at 7 days post-surgery and 42 days post-surgery via rt-qPCR. At 7 days post-surgery, *Csf1* gene expression in the ipsilateral L4-L5 DRGs was significantly upregulated in both CCI (5.46 ± 1.81-fold increase) and SNI (5.49 ± 0.91-fold increase) animals compared to time-controlled sham animals (Figure 5-2A). However, at 42

days-post surgery, *Csf1* gene expression was no longer upregulated in L4-L5 DRGs of CCI animals (0.587 ± 0.04-fold increase) compared to time-controlled sham animals (P=0.48). In contrast, relative *Csf1* gene expression was significantly higher in L4-L5 DRGs of SNI operated animals (3.19 ± 0.50-fold increase) compared to the time-controlled CCI animals at 42 days post-surgery. However, compared to the time-controlled sham animals, it fell slightly short of achieving statistical significance (P=0.06). These results indicated that CSF1 production in the DRG may be chronically upregulated in SNI animals compared to CCI animals.

5.3.3 SNI leads to chronic upregulation of CSF1 production in the ipsilateral DRGs contrary to CCI

To examine the CSF1 protein expression, ipsilateral L4-L5 DRG sections prepared from sham, CCI and SNI animals at 7- and 42-days post-surgery were immunostained with CSF1 antibody (Figure 5-2B). At 7 days post-surgery, a significant increase in the number of CSF1 immunoreactive neurons was observed in the DRGs of CCI (23.51 ± 1.98 %) and SNI (33.94 ± 2.42 %) animals compared to sham animals (1.86 ± 0.73 %) (Figure 5-2C). Furthermore, DRG sections from SNI animals also exhibited significantly higher proportion of CSF1 expressing neurons compared to CCI animals. At 42 days post-surgery, DRG sections from SNI group maintained significantly higher percentage of CSF1 immunoreactive neurons (22.70 ± 2.17 %) compared to the time-controlled sham (0.184 ± 0.10 %). In contrast, only 4.25 ± 0.70 % of DRG neurons expressed CSF1 immunoreactivity in the sections obtained from CCI operated rats, which were virtually indistinguishable from the time-controlled sham group (P>0.9999). Furthermore, CSF1 expression in the DRG sections of CCI animals at 42 days post-surgery were also significantly reduced compared to CSF1 expression at 7 days post-surgery. Although the DRGs from SNI animals expressed significantly higher level of CSF1 expression compared to

CCI and time-controlled sham animals at 42 days post-surgery, the degree of CSF1 expression were significantly attenuated compared to 7 days post-surgery. Finally, the correlation between withdrawal thresholds and CSF1 expression in the ipsilateral L4-L5 DRGs were examined by pairing the withdrawal threshold and CSF1 expression in the DRGs from every rat used for the CSF1 IHC experiment (n=53). Pearson correlation coefficient revealed that there was a statistically significant inverse correlation between withdrawal threshold and CSF1 expression in the DRG (n=53; r= -0.7631; r^2= 0.5823; P<0.0001; data summarized in Figure 5-6). Overall, these data indicated persistent upregulation of CSF1 in the ipsilateral L4-L5 DRG is closely associated with the chronic mechanical allodynia.

5.3.4 CSF1 production in the injured DRG is only maintained in SNI but not in CCI

Since previous studies have reported CSF1 is more likely to be produced in a injured DRG neuron, CSF1 was co-immunostained with activating transcription factor 3 (ATF3) in order to examine their relationship with chronic pain behavior in CCI and SNI model of neuropathic pain (Guan et al 2016) (Figure 5-2B). First, the level of DRG neuron injury in each condition was assessed by quantifying the percentage of DRG neurons with ATF3 immunoreactivity. At 7 days post-surgery, both CCI and SNI animals showed significant signs of injury in the ipsilateral L4-L5 DRG (30.69 ± 3.18 and 52.29 ± 4.45 % respectively) compared to sham animals (2.15 ± 2.04 %) (Figure 5-2D). Furthermore, SNI produced significantly higher expression of ATF3 in the DRG compared to CCI animals 7 days post-injury. At 42 days post-surgery, both CCI and SNI animals maintained increased ATF3 expression in the ipsilateral L4-L5 DRG (19.21 ± 1.91 and 34.187 ± 3.33 %) relative to time-controlled sham animals (1.67 ± 0.39 %). SNI animals also maintained higher levels of ATF3 expression in the DRGs compared to CCI animals 42 days post-surgery. That said, at 42 days post-surgery, SNI animals showed significantly lower ATF3

expression in the DRGs compared to SNI animals during the neuropathic pain onset. CCI animals showed a trend for decreased ATF3 expression at 42 days post-surgery compared to the onset; however, this was not statistically significant (P=0.08).

Secondly, from the subpopulation of DRG neurons with ATF3 immunoreactivity, cells that co-express CSF1 were quantified. At 7 days post-injury, 53.22 ± 5.3 % of ATF3 positive DRG neurons also expressed CSF1 in CCI operated rats, and 51.81 ± 2.32 % of ATF3 positive DRG neurons expressed CSF1 in SNI operated animals (Figure 5-2E). However, at 42 days post-surgery, only 31.55 ± 3.65 % of ATF3 positive cells co-express CSF1 in CCI animals, which was significantly attenuated from CCI animals at 7 days-post surgery. In contrast, in the ipsilateral L4-L5 DRGs of SNI animals, most of injured neurons remained co-immunostained with CSF1 (51.86 ± 3.24 %), which was significantly higher compared to CCI animals at 42 days post-surgery. These results suggest that maintenance of CSF1 production in the injured DRG neurons is involved in the pathogenesis of chronic mechanical allodynia in animal models of neuropathic pain.

5.3.5 SNI leads to long term SGC activation in the ipsilateral DRGs compared to CCI

Activation of SGCs have been shown to play an important role in both onset and maintenance of pain behavior in various animal models of neuropathic pain (Li et al 2011, Lim et al 2017, Otoshi et al 2010, Silva et al 2017, Takeda et al 2008). In order to examine the difference between transient and chronic tactile allodynia observed in CCI and SNI operated animals, I profiled the SGC activation and its proximity to CSF1 positive neurons in ipsilateral L4-L5 DRG sections prepared from sham, CCI and SNI animals at 7- and 42-days post-surgery via co-immunostaining glial fibrillary acidic protein (GFAP), marker of activated SGC, and CSF1 (Figure 5-3A). Two methods were used to quantify SGC activation. First, SGC activation was

determined by quantifying the percentage of GFAP immunoreactive area in a section. Using this method, at 7 days post-surgery, both CCI and SNI animals displayed robust SGC activation (29.65 ± 1.65 and 29.07 ± 2.92 %) compared to time-controlled sham animals (5.04 ± 1.28 %) (Figure 5-3B left panel). At 42 days post-surgery, both CCI and SNI operated animals still maintained significantly higher GFAP expression (16.49 ± 1.43 and 34.60 ± 1.94 %) compared to time-controlled sham animals (5.50 ± 0.60 %); however, the total percentage of GFAP signal in CCI group was significantly lower compared to SNI group. Furthermore, at 42 days post-surgery, DRGs from the CCI group displayed significantly attenuated GFAP expression compared to 7 days post-surgery. In contrast, SNI operated animals maintained the initial level of GFAP expression in the DRGs (P=0.4531). Secondly, activation of SGC was also quantified by counting the number of 'GFAP-rings' around DRG neurons, which are indicated by arrows in Figure 5-3A. This was done to also examine the potential co-localization of activated SGCs and CSF1 positive DRG neurons. During the onset, a similar trend of SGC activation was seen as both CCI and SNI animals displayed increased 'GFAP-ring' expression (23.61 ± 0.99 and 32.60 ± 3.091 %) compared to sham animals (1.37 ± 0.55 %) (Figure 5-3B right panel). In contrast to the findings where the total percentage of GFAP immunoreactive area was determined, at 42-days post injury, SGC activation in ipsilateral L4-L5 DRGs from CCI group (11.56 ± 2.27 %) fell slightly short of achieving significance compare to time-controlled sham group (2.40 ± 0.74 %) (P=0.065). Furthermore, the CCI group at 42 days-post surgery also showed significant decrease in SGC activation compared to CCI group at onset. In contrast, SNI animals not only showed significant SGC activation (30.74 ± 3.16 %) compared to sham and CCI animals at 42 days post-surgery, but also maintained the high level of 'GFAP-ring' expression observed during the onset of neuropathic pain. Paired together with behavioral results, Pearson correlation

coefficient revealed the level of SGC activation showed significant inverse association with withdrawal thresholds in animals used in this study (n=40; r=-0.6795; r^2=0.4618; p<0.0001; Figure 5-6).

5.3.6 The degree of SGC activation correlates with the level of CSF1 production in the ipsilateral DRGs

Considering the recent observation by Lim et al 2017, which suggested SGC activation was required for CSF1 production following a nerve injury, potential spatial relationship between active SGC and CSF1 positive DRG neuron was also examined. Ipsilateral L4-L5 DRGs from CCI animals showed some co-localization at 7 days post-surgery, but this spatial association between active SGC and CSF1 positive DRG neuron was significantly attenuated at 42 days post-surgery (36.92 ± 4.78 % vs 16.88 ± 4.88 %) (Figure 5-3C). In contrast, SNI animals showed 50.00 ± 1.85 % co-localization at 7 days post-surgery, and 40.00 ± 3.40% at 42 days post-surgery, which were not significantly different (P=4484). In addition, at 42 days post-surgery SNI animals showed significantly higher level of co-localization of active SGC and CSF1 positive neuron compared to CCI animals. Furthermore, there was a strong linear relationship between the level of CSF1 expression and the degree of SGC activation in the ipsilateral L4-L5 DRGs of all the animals tested (n=40; r=0.7967; r^2=0.6347; P<0.0001). These results indicate a temporal and spatial association between SGC activation and CSF1 production in the ipsilateral DRG, which in turn contributes to tactile allodynia in nerve injured animals.

5.3.7 SNI leads to a chronic increase in macrophage expression in the ipsilateral DRGs compared to CCI

Peripheral macrophages play an important role in the pathogenesis of mechanical allodynia (Cobos et al 2018, Otoshi et al 2010, Vega-Avelaira et al 2009). In order to examine the

activated macrophage expression in ipsilateral DRGs during acute and chronic mechanical allodynia, ionized calcium binding adaptor molecule 1 (Iba1), a marker for activated macrophages, was immunostained in the ipsilateral L4-L5 DRGs of sham, CCI, and SNI animals during the onset and chronic time points (Ohsawa et al 2004) (Figure 5-4A). The degree of activated macrophage expression was determined by two methods. First, the total number of cells with Iba1 immunoreactivity was counted. During the onset of mechanical allodynia, ipsilateral L4-L5 DRGs from both CCI and SNI animals showed significantly higher number of activated macrophages (1369.88 ± 78.45 and 1692.92 ± 88.39 cells per mm^2 respectively) compared to time-controlled sham animals (786.12 ± 52.22 cells per mm^2) (Figure 5-4B left panel). In addition, DRGs from SNI animals showed slightly higher number of Iba1 immunoreactive cells at 7 days post-surgery compared to CCI animals. At 42 days post-surgery, CCI animals no longer showed significant increase of Iba1 immunoreactive cells compared to sham animals (1112.77 ± 80.25 vs 775.33 ± 65.43 cells per mm^2; P=0.10). DRGs from CCI animals also showed significantly lower number of activated macrophages compared to CCI animals during neuropathic pain onset (1112.77 ± 80.25 vs 1369.88 ± 78.45 cells per mm^2). In contrast, DRGs from SNI animals maintained higher number of activated macrophages compared to time-controlled sham animals at 42 days-post surgery (1346.38 ± 53.09 vs 775.33 ± 65.43 cells per mm^2). However, the average number of activated macrophages were significantly attenuated in DRGs of SNI animals at 42 days-post surgery compared to SNI animals during onset timepoint (1346.38 ± 53.09 vs 1692.92 ± 88.39 cells per mm^2). Secondly, the number of DRG neurons with an 'Iba1-Ring', the elongated shape around DRG neuron indicated by arrows in Figure 5-4A, were quantified in all animals at onset and chronic time point. This was done in order to examine the co-localization of activated macrophages and CSF1 positive DRG neuron.

At day 7 post-surgery, DRGs from both CCI and SNI animals showed increased number of 'Iba1-ring' (13.95 ± 1.86 and 18.33 ± 2.25 % respectively) compared to time-controlled sham animals (0.66 ± 0.22 %) (Figure 5-4B right panel). At 42 days post-surgery, CCI animals no longer showed increased 'Iba1-ring' expression in the DRG (3.90 ± 0.94 %) compared to time-controlled sham animals (0.46 ± 0.24 %; P>0.9999). As previously, CCI animals at 42 days post-surgery showed significantly less activated macrophage expression compared to CCI animals during onset (3.90 ± 0.94 % vs 13.95 ± 1.86 %). In contrast, SNI animals maintained upregulated 'Iba1-ring' expression in the DRGs (14.70 ± 1.60 %) compared to both CCI and sham animals at 42 days post-surgery. Pairing the data with animal behavior, the number of Iba1 immunoreactive cells also showed significant inverse association with withdrawal threshold (n=47; r=-0.6199; r^2=0.3843; P<0.0001; Figure 5-6).

5.3.8 Activated macrophage expression show both temporal and spatial relationship with CSF1 production in the ipsilateral DRGs

The 'Iba1-ring' showed remarkable co-localization with DRG neurons expressing CSF1 immunoreactivity. The vast majority of ipsilateral DRG neurons with 'Iba1-ring' also expressed CSF1 immunoreactivity at 7 days post-surgery for both CCI and SNI group (71.27 ± 4.41 % and 80.76 ± 1.98 % respectively) (Figure 5-4C). At 42 days post-surgery, only SNI animals maintained high CSF1/Iba1-ring co-localization as 69.73 ± 4.13 % of DRGs with 'Iba1-ring' also produced CSF1. On the other hand, CCI animals showed only 38.11 ± 4.32 % CSF1/Iba1-ring co-expression, and this was significantly lower compared CCI animals during the onset and SNI animals during the chronic time point. Pearson correlation coefficient revealed the level of 'Iba1-ring' expression correlated strongly with the level of CSF1 expression in the DRGs (n=47; r=0.9329; r^2=0.8536; P<0.0001; Figure 5-6). Taken together, the data implicated the activated

macrophage in the ipsilateral DRGs are both temporally and spatially associated with CSF1 production, which in turn is linked with chronic mechanical allodynia seen in animal models of neuropathic pain.

5.3.9 SNI leads to persistent upregulation of Il1b mRNA expression in the ipsilateral DRGs

A recent study has shown that IL-1β released by activated SGC drives the CSF1 production in the DRG neurons (Lim et al 2017). Furthermore activated macrophages are also a significant source of IL-1β in the DRG, and it can mediate tactile allodynia in animal models of neuropathic pain (Cobos et al 2018, Schuh et al 2014). Therefore, the relative *Il1b* mRNA levels were also examined in sham, CCI, and SNI animals at onset and chronic time points. At 7 days post-surgery, both CCI and SNI animals displayed significant increase in *Il1b* mRNA expression (3.10 ± 1.21 and 3.85 ± 0.51-fold change respectively) in ipsilateral L4-L5 DRGs relative to time-controlled sham animals (Figure 5-5A). At 42 days post-surgery, only SNI animals maintained significantly upregulated *Il1b* mRNA expression (4.34 ± 0.92-fold change) in the DRGs relative to time-controlled sham animals. In contrast, *Il1b* mRNA expression in DRGs of CCI animals (2.88 ± 0.06-fold increase) fell short of reaching significance compared to time-controlled sham animals (P=0.1620). These data suggest IL-1β production may still be upregulated in the ipsilateral DRGs of animals displaying chronic tactile allodynia.

5.3.10 IL-1β increases Csf1 mRNA expression in the DRG neuron enriched culture

The direct effect of IL-1β on DRG neurons was also examined by measuring relative *Csf1* mRNA levels in the DRG neuron enriched culture. The culture only received 100 pM IL-1β for 5 days and was not supplemented with any neurotrophic factors in order to observe the isolated effects of IL-1β on DRG neurons. DRG neurons treated with 100 pM IL-1β showed significant upregulation of relative *Csf1* mRNA expression (4.70 ± 0.44-fold change) compared to control,

which was consistent with the previous findings in acute mice DRG culture (Figure 5-2B) (Lim et al 2017). Furthermore, Pearson correlation coefficient suggested the relative *Il1b* mRNA expression showed significant association with the relative *Csf1* mRNA expression in each of the DRGs used in the experiment (n=25; r=0.5273; r^2=0.278; P<0.007; Figure 5-6). These results suggest increased IL-1β may account for the upregulated *Csf1* mRNA production in the DRGs of nerve injured animals.

5.4 Discussion

5.4.1 Summary of results

In this study, I discovered there are significant differences in the ipsilateral DRGs between CCI and SNI operated animals at 42 days-post injury (data trends and correlations are summarized in Figure 5-6). First, SNI, which produced robust chronic mechanical allodynia, lead to substantial production of CSF1 in the affected DRGs at both 7- and 42- days post-surgery. In contrast CCI, which recovered from tactile allodynia by 42 days post-surgery, lead to transient upregulation of CSF1 expression in the ipsilateral DRGs that was significantly diminished once the mechanical allodynia resolved. Secondly, SNI produced persistent activation of SGC, increased macrophage expression, and *Il1b* mRNA upregulation in the ipsilateral DRG in stark contrast to CCI which lead to transient increase in SGC activation, macrophage expression, and *Il1b* mRNA upregulation.

5.4.2 Implications of chronic CSF1 production for the persistent mechanical allodynia

The importance of microglia activation in the pathogenesis and maintenance of neuropathic pain in males has been extensively demonstrated (Beggs et al 2012, Chen et al 2018b, Clark et al 2007, Echeverry et al 2017, Grace et al 2016, Grace et al 2018, Guan et al 2016). While the activation of spinal microglia persists months after the initial injury in some animal models of

peripheral nerve injury, the mechanism in which maintains this proliferation and activation is not completely understood (Denk et al 2016, Yao et al 2016). Interestingly, partial sciatic nerve ligation (PSNL) and SNI lead to chronic activation of spinal microglia for more than three months along with persistent mechanical allodynia, which can be reversed via suppression of microglial activation (Echeverry et al 2017, Swartjes et al 2014). In contrast, the CCI model (Bennett & Xie 1988), which produces temporary mechanical allodynia, lead to more transient spinal microglia activation which was completely resolved by 121 days (Vacca et al 2014, Vacca et al 2016). Furthermore, Grace et al (2016) demonstrated morphine paradoxically prolongs the mechanical allodynia in CCI operated animals beyond 6 weeks through augmenting the activation of spinal microglia (Grace et al 2016). These results indicate the level and duration of spinal microglia activation bring about the difference in the transient and the chronic tactile allodynia observed in CCI and SNI respectively. In this study, SNI leads to persistent CSF1 production in the ipsilateral DRG neurons in stark contrast to CCI, which lead to short-lived CSF1 production. The temporal relationship between the CSF1 expression and the tactile allodynia was significant, which indicated the production of CSF1 in the sensory neuron underlies the difference between transient and chronic tactical allodynia observed in CCI and SNI animals. CSF1 interaction with colony stimulating factor 1 receptor (CSF1R) not only regulates the development and proliferation, but it also activates spinal microglia (Elmore et al 2014, Ginhoux et al 2010, Imai & Kohsaka 2002, Oosterhof et al 2018). Moreover, both conditional *Csf1* knockout in the DRG and intrathecal injection of CSF1R inhibitor mitigated microglia proliferation, activation, and tactile allodynia after peripheral nerve injury (Guan et al 2016, Okubo et al 2016). Therefore, the chronic upregulation of CSF1 in the ipsilateral DRGs in SNI animals demonstrated in the current study provides a potential mechanism for not only

prolonged proliferation and activation of spinal microglia, but also persistent mechanical allodynia seen in SNI operated rats in contrast to CCI animals.

That said, it must be noted although CSF1 production persisted significantly, its production in the ipsilateral DRGs at 42 days post-surgery was diminished compared to 7 days post-surgery in SNI animals. This implies CSF1 production may eventually decline back to the baseline. A recent study has shown that activated astrocytes in the spinal cord can also produce CSF1 (Tang et al 2018). Activation of astrocytes after nerve injury is often delayed; therefore, this may provide an alternate mechanism for the persistent activation and proliferation of spinal microglia at the chronic stage of neuropathic pain (Tang et al 2018). Consequently, the effects of suppressing CSF1 production in the DRG at the chronic neuropathic state on spinal microglia activation and tactical allodynia is an avenue for future investigation.

5.4.3 Implications of persistent neuroinflammation for chronic neuropathic pain

Activation of SGCs play an important role in the pathogenesis of neuropathic pain (Ohara et al 2009). Otoshi et al (2010) showed SGC activation without nerve injury leads to mechanical hypersensitivity, which recovers once the SGC activation subsides (Otoshi et al 2010). Lim et al (2017) demonstrated that activation of SGCs and the subsequent release of IL-1β is responsible for the production of CSF1 in the DRG neurons (Lim et al 2017). Consequently, blocking the SGC activation attenuated mechanical hypersensitivity and spinal microglia activation following a peripheral nerve injury (Li et al 2011, Lim et al 2017). Macrophages are another major source of IL-1β in the peripheral nervous system, and they are also essential for the pathogenesis of mechanical allodynia (Cobos et al 2018, Santa-Cecilia et al 2019, Schuh et al 2014). Inhibition of peripheral macrophages also lead to decrease in spinal microglia activation and attenuation of mechanical allodynia during the onset (Kiguchi et al 2018). The data obtained in this study add

support to these findings. There was a significant temporal relationship between the SGC activation and mechanical hypersensitivity as only animals displaying persistent pain maintained significant SGC activation. Secondly, activated macrophage expression also displayed strong temporal correlation with both mechanical allodynia and CSF1 production in this study. On top of this, there was a remarkable spatial association between activated macrophages and CSF1 production. When macrophages formed a 'ring-like' structure around the DRG neuron, vast majority of these DRG neurons produced CSF1. Finally, long term exposure to 100 pM IL-1β significantly upregulated *Csf*1 mRNA expression in the neuron enriched DRG culture suggesting the direct interaction between IL-1β and DRG neurons. Taken together with chronic upregulation of *Il1b* mRNA expression in animals with chronic tactile allodynia, persistent activation of SGCs and increased macrophage aggregation in the injured DRGs provide a potential mechanism for the maintenance of CSF1 production and the non-resolving tactile allodynia.

Activated SGCs and macrophages are the most likely source of IL-1β (Kawasaki et al 2008a, Kiguchi et al 2010, Lim et al 2017, Schuh et al 2014, Takeda et al 2008, Takeda et al 2007), and they were both strongly associated with CSF1 production and mechanical hypersensitivity in this study. However, it is likely that more complex interactions may be involved in the production of CSF1 in the injured DRG neurons. For example, despite significant activation of SGC, macrophage infiltration, and increased IL-1β levels; there was no significant production of CSF1 in the DRG neurons of EAE mice (Frezel et al 2016, Rodrigues et al 2016, Warwick et al 2014). Moreover, DRG neurons in EAE mice showed significant upregulation of ATF3; however, injured DRG neurons did not produce CSF1 (Frezel et al 2016). Although EAE mice display myelin disruption in the periphery, the EAE model does not involve significant damage the peripheral nerve in contrast to other models of neuropathic pain (Wang et al 2017). Therefore,

significant structural damage and loss of nerve innervation via Wallerian degeneration may be required for substantial production of CSF1 in the sensory neuron. Given the importance of CSF1 in the pathogenesis and persistence of neuropathic pain, examination of the precise mechanism behind CSF1 production following a nerve injury is another avenue for future investigation.

5.4.4 Implications of long-term CSF1 production for persistent peripheral neuroinflammation

The etiology of persistent peripheral neuroinflammation observed in the SNI animal in this study is uncertain. That said, a recent study has postulated that maladaptive nerve regeneration due to failed target reinnervation after a nerve injury drives the persistent tactile allodynia seen in SNI animals (Xie et al 2017). Indeed, SNI with nerve crush instead of complete transection and ligation of tibial and common peroneal nerve lead to transient tactical allodynia (Decosterd & Woolf 2000). This was accompanied by complete nerve reinnervation as indicated by disappearance of growth-associated protein 43 (GAP43), which is only upregulated while nerve is regenerating (Decosterd & Woolf 2000, Oestreicher et al 1997, Woolf et al 1990). Furthermore, the complete nerve regeneration, accompanied by resolution of microgliosis and astrogliosis, underlay the difference between transient and chronic mechanical allodynia observed between CCI (Bennett & Xie 1988) operated male and female mice (Vacca et al 2014). Given the critical importance of inflammatory mediators during nerve regeneration, persistent maladaptive regeneration due to failed reinnervation in the SNI model may indeed be responsible for the persistent neuroinflammation in the DRG (Dubovy 2011, Nadeau et al 2011, Xie et al 2017). In fact, important mediators of pain such as IL-1β, NGF, and GDNF, which are released by macrophages or SGCs following a nerve injury, are critical for peripheral nerve regeneration (Dubovy 2011, Lee et al 1998, Nadeau et al 2011, Otoshi et al 2010). Additionally, ATF3, which

is often used as a cell stress marker, is also closely associated with nerve regeneration and its expression promotes nerve growth and repair in sensory neurons (Hunt et al 2012, Seijffers et al 2007). Damaged sensory neurons often associate spatially with activated SGCs and macrophages, which can also promote regeneration (Hunt et al 2012, Krishnan et al 2018, Nascimento et al 2014, Seijffers et al 2007, Vega-Avelaira et al 2009). Therefore, CSF1 production in the injured DRG neuron may be an adaptive response for sensory neuron regeneration. Of note, I observed higher degree of ATF3 expression and co-localization with CSF1 in the DRGs of SNI group compared to the CCI group. Furthermore, there was persistent spatial association between activated macrophages and CSF1 producing neurons in the DRGs of SNI group. Macrophages express CSF1R, and their production, proliferation, and motility depend CSF1 (Krishnan et al 2018, Stanley et al 1978, Webb et al 1996). Since CSF1 can exist in both soluble and membrane bound form, CSF1 production in the injured sensory neurons and the subsequent secretion may be involved in not only the chemotaxis of macrophages, but also proliferation and activation of macrophages in the DRG (Yagiz & Rittling 2009). Indeed, recent study by Krishnan et al (2018) showed proliferation of resident macrophages in the DRG following nerve injury was CSF1R mediated (Krishnan et al 2018). Moreover, these authors also demonstrated there is a physical interaction between macrophages and SGCs, and the authors postulated they may prime one another following a nerve injury (Krishnan et al 2018). Taken together, persistent upregulation of CSF1 in the injured DRG neuron may also serve as a potential mechanism for the long-lasting peripheral neuroinflammation and the chronic pain mediated by failed target reinnervation seen in SNI animals.

5.4.5 Limitations of the study

The current study used correlations and previous peer-reviewed publications to interpret the significance differences, such as CSF1 production and peripheral neuroinflammation, observed between DRGs from CCI and SNI animals in the context of neuropathic pain maintenance. Therefore, precise mechanism for these observations remain largely uncertain, and future studies should focus on ameliorating these uncertainties.

First, significant production of CSF1 in the DRGs underlay the difference between transient and chronic tactile allodynia observed in animal models of neuropathic pain in this study. Although CSF1 was critical in the pathogenesis of neuropathic pain and blocking the actions of CSF1 has been shown to alleviate tactile allodynia following nerve injury via attenuating spinal microglia activation; this was not directly tested in animals used in the current study (Guan et al 2016, Lee et al 2018, Nho et al 2018, Okubo et al 2016). Therefore, it is unclear whether inhibition of CSF1 at chronic timepoint would mirror the previous findings and unequivocally prove CSF1 as the underlying cause of persistent mechanically allodynia in SNI animals.

Second, although there was a significant temporal and spatial association between SGCs, macrophages, and CSF1 production, cause-effect relationship was not explicitly verified by either blocking SGC activation or ablating peripheral macrophages in this study. Therefore, the causal relationship between persistent CSF1 production and neuroinflammation in the injured DRG remains ambiguous. Furthermore, *Il1b* mRNA expression was chronically upregulated in the ipsilateral DRGs of SNI animals; however, the origin of *Il1b* mRNA upregulation remains unclear. Although activated SGCs and macrophages are likely cellular sources of IL-1β (Kawasaki et al 2008a, Kiguchi et al 2010, Lim et al 2017, Schuh et al 2014, Takeda et al 2008, Takeda et al 2007), sensory neurons are also capable producer of IL-1β; thus, upregulation of

Il1b mRNA may be from the injured DRG neurons (Copray et al 2001, Li et al 2005). Regrettably, I was not able to unequivocally confirm the presence of IL-1β in these cells. Several primary antibodies against IL-1β were used; yet, none of them showed adequate specificity and reactivity to IL-1β in our samples. As a result, CSF1 production in the sensory neuron *in vivo* may be a result of other mediators. One potential candidate is NGF, which is upregulated in the ipsilateral DRG following a nerve injury (Lee et al 1998). Since both NGF and IL-1β can signal through p38-mitogen-activated protein kinase (MAPK), NGF may also be capable inducer of *Csf1* expression (Binshtok et al 2008, Ji et al 2002).

Third, in the current study general macrophage marker Iba1 was utilized. Macrophages can polarize into spectrum of phenotype ranging from pro-inflammatory M1 to anti-inflammatory M2 (Murray 2017). As a result, it was unclear whether the increased Iba1 immunoreactivity was pro- or anti-inflammatory. A future study using specific molecular markers such as chemokine ligand 13 (CXCL13) for M1 macrophages and arginase-1 (Arg1) for M2 macrophages will reveal the identity and the nature of the increased Iba1 immunoreactive cells in the DRG.

Finally, a recent revelation in the neuropathic pain field has been that there is a sex-dependent spinal microglia signaling for the pathogenesis of neuropathic pain (Sorge et al 2015). Although both male and female animals exhibit significant activation and proliferation of spinal microglia in response to peripheral nerve injury, only male animals depend on the spinal microglia for the pathogenesis of neuropathic pain (Berta et al 2016, Chen et al 2018a, Sorge et al 2015). In this study, only male rats were used, thus these results do not account for the sexual dimorphism. It is uncertain whether the differences observed in this study would also underlie the distinct pain phenotypes of CCI and SNI models in female animals. Therefore, a future study examining the

effect of ameliorating persistent CSF1 production and neuroinflammation in the primary afferents in female animals is another avenue for future investigation.

5.5 Conclusion

Although with limitations, these results suggest chronic CSF1 immunoreactivity and the persistent expression of activated SGCs (GFAP) and macrophages (Iba1) in the injured DRGs may underlie the difference between transient and chronic tactile allodynia observed in CCI and SNI models of neuropathic pain. These results add support to rapidly expanding evidence for the neuroimmune mediated maintenance of chronic neuropathic pain. Consequently, targeting the persistent CSF1 production and the peripheral neuroinflammation may be an effective potential therapeutic strategy for the treatment of chronic neuropathic pain.

Figure 5-1

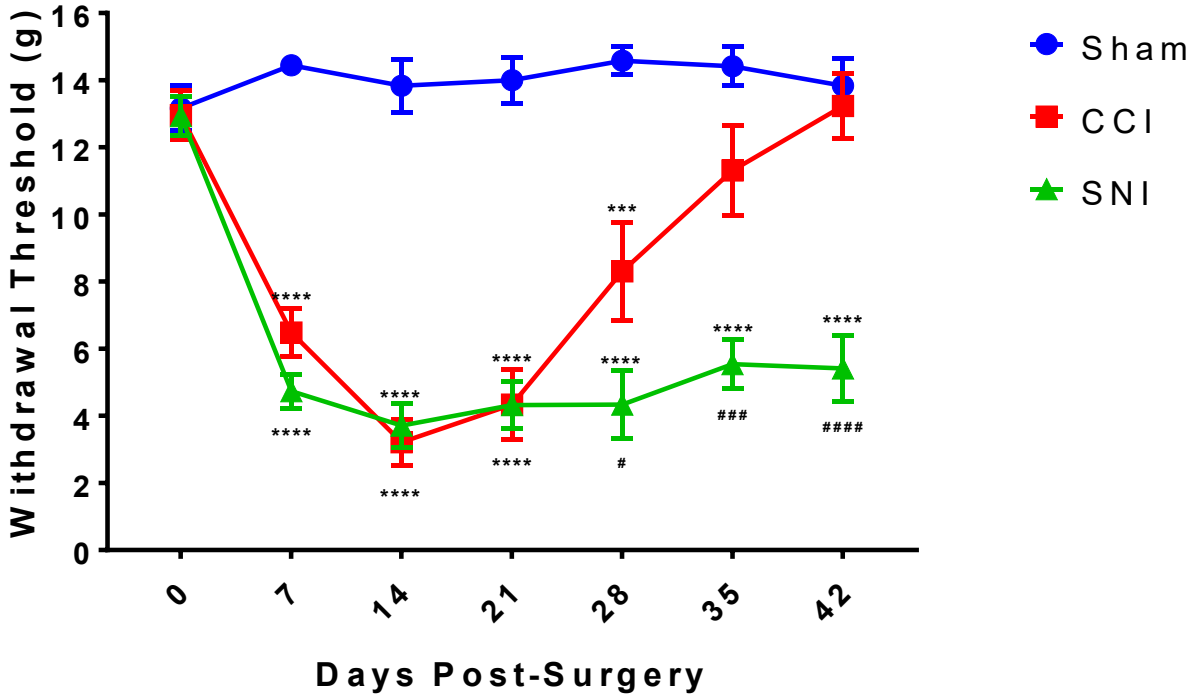

Figure 5-1. SNI produces chronic mechanical allodynia in contrast to CCI which leads to transient mechanical allodynia. Paw withdrawal thresholds were evaluated via von Frey test once per week over a 42-day period. On the day of the surgery (Day 0), rats were randomly assigned for sham (n=27), CCI (n=27), and SNI (n=29) surgery, and no difference was observed between groups. Both CCI and SNI operated animals became mechanically hypersensitive 7 days post-surgery. SNI animals maintained mechanical allodynia until 42 days post-surgery (n=13). In contrast, CCI animals (n=13) were indistinguishable from sham animals (n=12) on 35- and 42-days post-surgery (One-way ANOVA with Bonferroni's multiple comparisons test, *** P<0.001, **** P<0.0001 compared to time-controlled sham; # P<0.05, ### P<0.001, #### P<0.0001 compared to time-controlled CCI). All data points represent mean ± SEM.

Figure 5-2

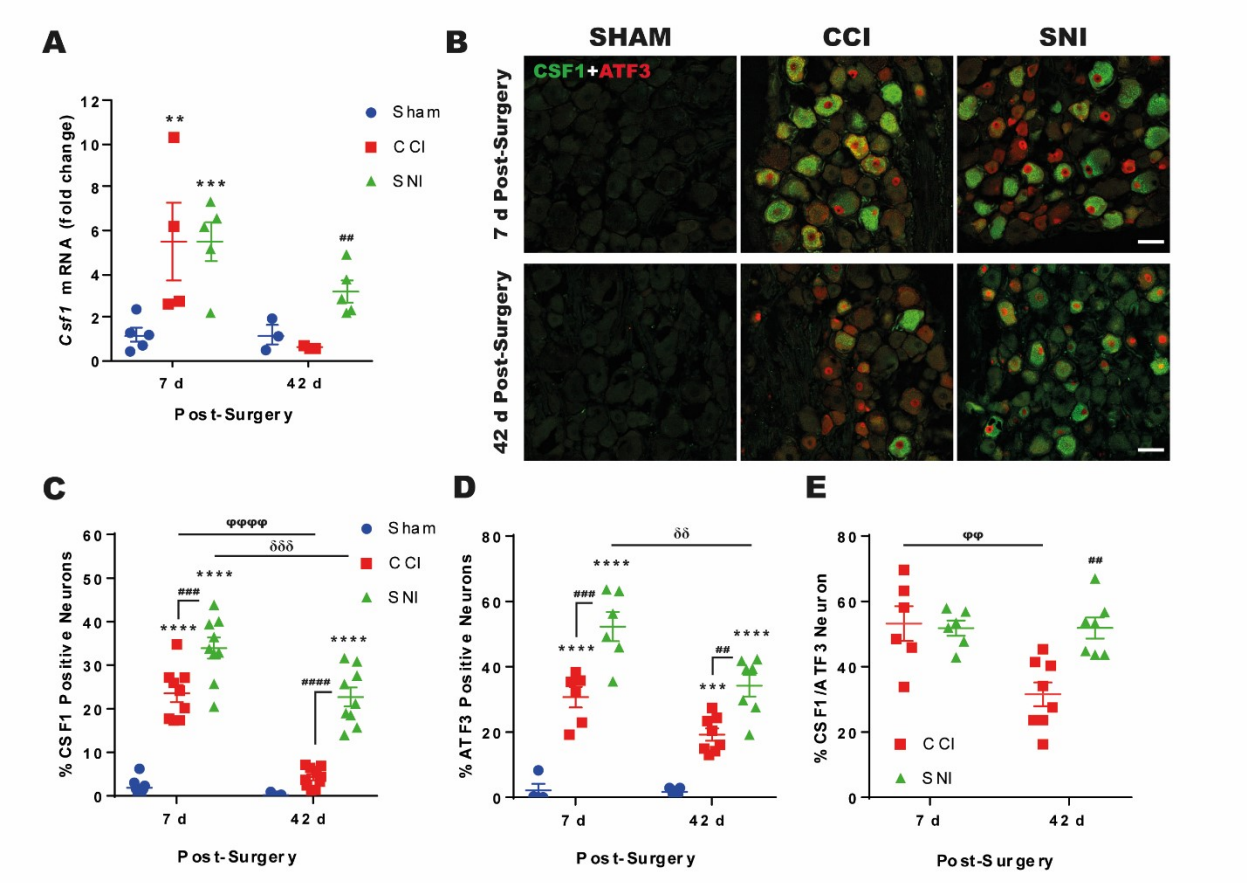
A
B
SHAM
CCI
SNI
CSF1+ATF3
7 d Post-Surgery
42 d Post-Surgery
Csf1 mRNA (fold change)
Sham
CCI
SNI
7 d
42 d
Post-Surgery
C
% CSF1 Positive Neurons
D
% ATF3 Positive Neurons
E
% CSF1/ATF3 Neuron
Post-Surgery
Post-Surgery
Post-Surgery

Figure 5-2. SNI leads to chronic upregulation of CSF1 in the ipsilateral L4-L5 DRG neurons which co-localizes with ATF3. **(A)** Fold-increase in *Csf1* mRNA levels relative to time-controlled sham were quantified in L4-L5 DRGs of CCI and SNI operated animals at 7 days post-surgery (sham, n=5; CCI, n=4; SNI, n=5) and 42 days post-surgery (sham, n=3; CCI, n=3; SNI, n=5) (One-way ANOVA with Bonferroni's multiple comparisons test, ** P<0.01, *** P<0.001 compared to appropriate time-controlled sham animals; ## P<0.01 compared to time-controlled CCI animals). **(B)** Ipsilateral L4-L5 DRG sections were prepared from sham, CCI, and SNI animals at 7- and 42- days post-surgery. DRG sections were co-immunostained with antibodies against CSF1 and ATF3 (scale bar, 50 μm). **(C)** Percentage of CSF1 expressing neurons were examined in ipsilateral L4-L5 DRG sections of sham, CCI, and SNI animals at 7 days post-surgery (sham, n=8; CCI, n=9; SNI, n=9) and 42 days post-surgery (sham, n=9; CCI, n=10; SNI, n=8). **(D)** Percentage of ATF3 expressing neurons were quantified in ipsilateral L4-L5 DRGs of sham, CCI, and SNI animals at 7 days post-surgery (sham, n=4; CCI, n=6; SNI, n=6) and 42 days post-surgery (sham, n=7; CCI, n=8, SNI, n=7). (**E)** Percentage of DRG neurons co-expressing CSF1/ATF3 were measured in ipsilateral L4-L5 DRGs of CCI and SNI animals at 7 days post-surgery (CCI, n=6; SNI, n=6) and 42 days post-surgery (CCI, n=8; SNI, n=7). **(C, D, E)** One-way ANOVA with Bonferroni's multiple comparisons test, **** P<0.0001 compared to time-controlled sham; ### P<0.001, #### P<0.0001 compared to time-controlled CCI; φφ P<0.01, φφφφ P<0.0001 compared to CCI at 7d post-surgery; δδ P<0.01, δδδ P<0.001 compared to SNI at 7d post-surgery. All data points represent mean ± SEM.

Figure 5-3

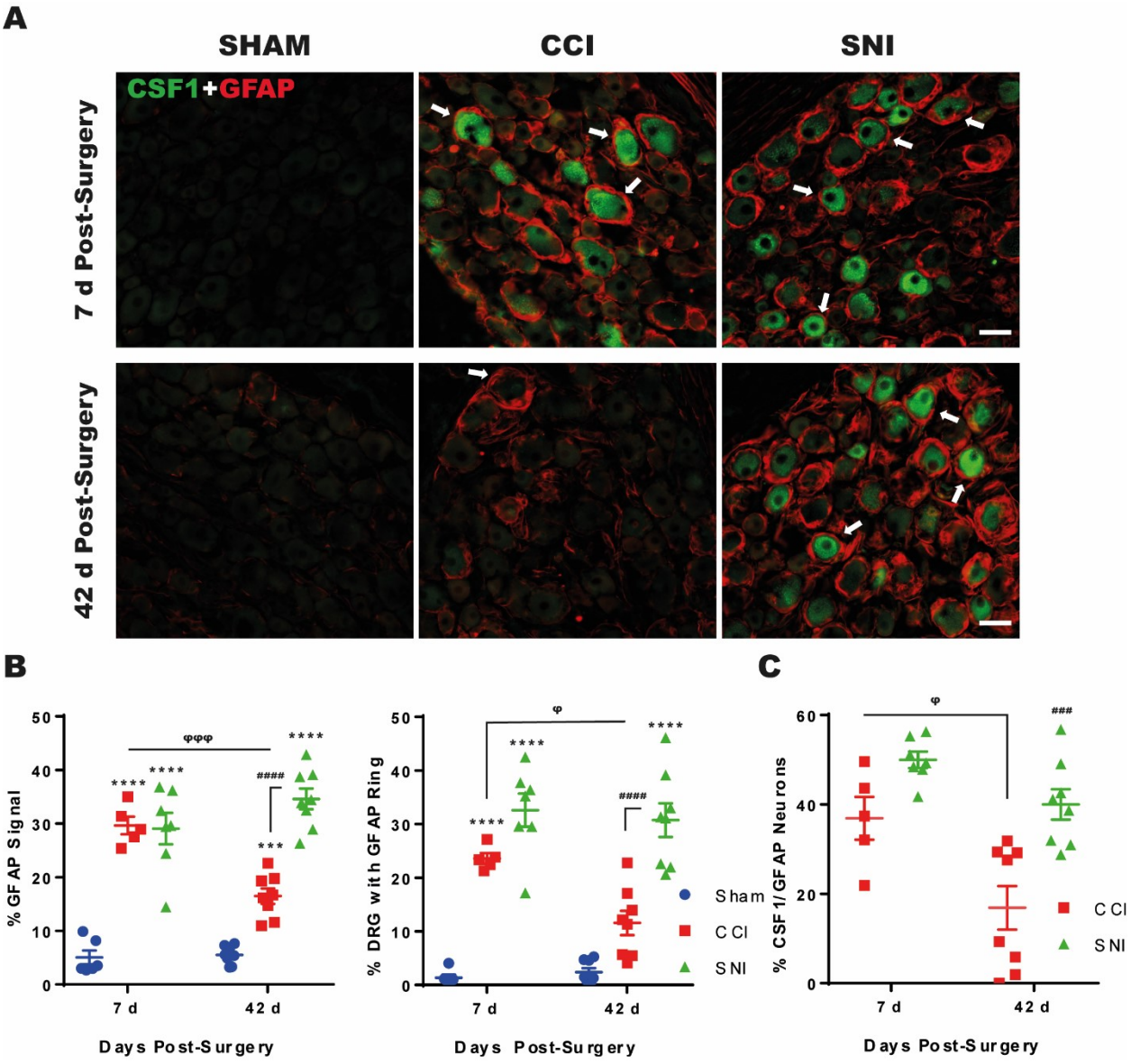
A
SHAM
CCI
SNI
CSF1+GFAP
7 d Post-Surgery
42 d Post-Surgery
B
% GFAP Signal
Days Post-Surgery
7 d
42 d
C
% DRG with GFAP Ring
% CSF1/GFAP Neurons
Sham
CCI
SNI

Figure 5-3. The level of satellite glial cell activation and its co-expression with CSF1 is associated with chronic mechanical allodynia. **(A)** Ipsilateral L4-L5 DRG sections were prepared from sham, CCI, and SNI animals at 7- and 42- days post-surgery. DRG sections were co-immunostained with antibodies against CSF1 and GFAP (scale bar, 50 μm; arrows indicate 'GFAP-ring'). **(B)** The level of satellite glial cell activation was determined by obtaining percentage of GFAP signal area in a DRG section (left panel) and quantifying the percentage of DRG neurons wrapped around the 'GFAP-ring' (right panel) in ipsilateral L4-L5 DRGs of CCI and SNI animals at 7 days post-surgery (sham, n=6; CCI, n=5; SNI, n=7) and 42 days post-surgery sham, n=8; CCI, n=8; SNI, n=8). (**C)** Percentage of DRG neurons co-expressing CSF1/GFAP-ring were measured in ipsilateral L4-L5 DRGs of CCI and SNI animals at 7 days post-surgery (CCI, n=5; SNI, n=8) and 42 days post-surgery (CCI, n=7; SNI, n=8). **(B, C)** One-way ANOVA with Bonferroni's multiple comparisons test, *** $P<0.001$, **** $P<0.0001$ compared to time-controlled sham; ### $P<0.001$, #### $P<0.0001$ compared to time-controlled CCI; φ$P<0.5$, φφ $P<0.01$, φφφ $P<0.001$ compared to CCI at 7d post-surgery. All data points represent mean ± SEM.

Figure 5-4

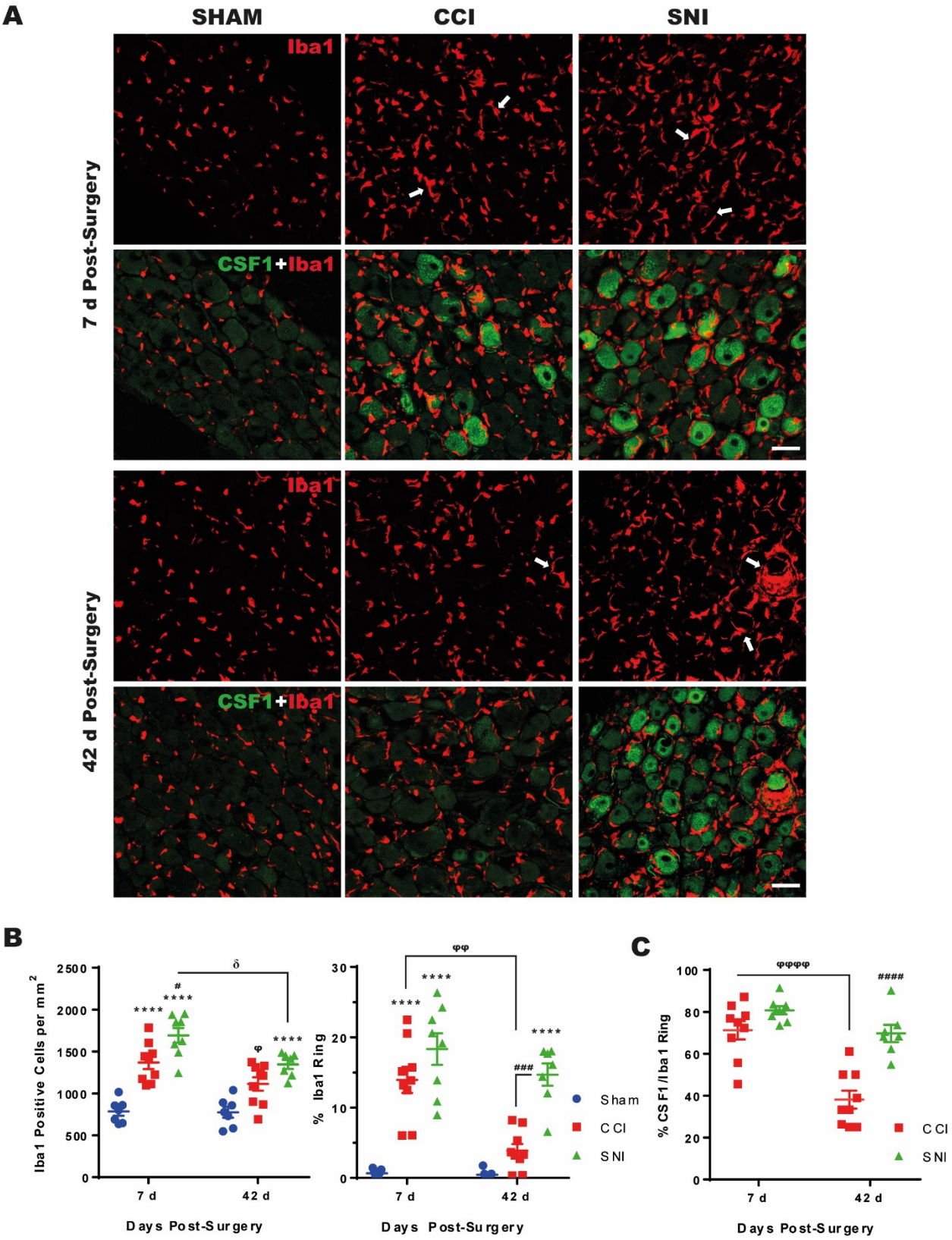
A
SHAM
CCI
SNI
Iba1
CSF1+Iba1
7 d Post-Surgery
42 d Post-Surgery
B
Iba1 Positive Cells per mm2
% Iba1 Ring
Days Post-Surgery
7 d
42 d
Sham
CCI
SNI
C
% CSF1/Iba1 Ring

Figure 5-4. Expression of activated macrophage in the ipsilateral L4-L5 DRG strongly associates with CSF1 expression and chronic mechanical hypersensitivity. **(A)** Ipsilateral L4-L5 DRG sections were prepared from sham, CCI, and SNI animals at 7- and 42- days post-surgery. DRG sections were co-immunostained with antibodies against CSF1 and Iba1 (scale bar, 50 μm; arrows indicate 'Iba1-ring'). **(B)** The amount of activated macrophages was determined by obtaining total number of Iba1 immunoreactive cells in a DRG section (left panel) and quantifying the percentage of DRG neurons wrapped around the 'Iba1-ring' (right panel) in ipsilateral L4-L5 DRGs of CCI and SNI animals at 7 days post-surgery (sham, n=7; CCI, n=9; SNI, n=8) and 42 days post-surgery sham, n=7; CCI, n=9; SNI, n=7). **(C)** Percentage of DRG neurons co-expressing CSF1/Iba1-ring were measured in ipsilateral L4-L5 DRGs of CCI and SNI animals at 7 days post-surgery (CCI, n=9; SNI, n=8) and 42 days post-surgery (CCI, n=9; SNI, n=7). **(B, C)** One-way ANOVA with Bonferroni's multiple comparisons test, **** $P<0.0001$ compared to time-controlled sham; # $P<0.05$, ### $P<0.001$, #### $P<0.0001$ compared to time-controlled CCI; φφ $P<0.01$, φφφφ $P<0.0001$ compared to CCI at 7d post-surgery; δ $P<0.05$ compared to SNI at 7d post-surgery. All data points represent mean ± SEM.

Figure 5-5

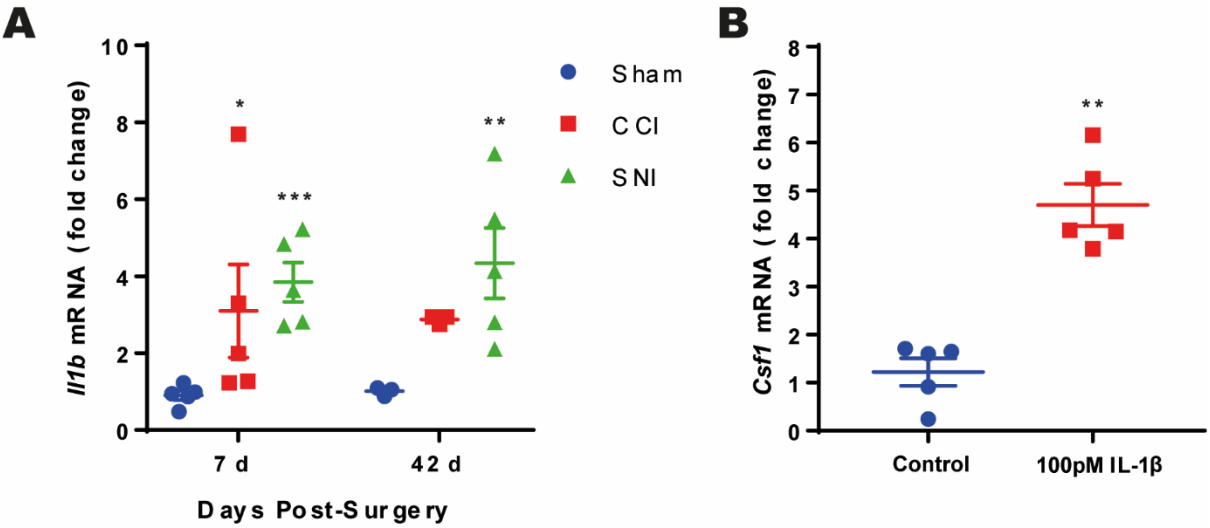

Figure 5-5. *Il1b* mRNA expression is chronically upregulated in L4-L5 DRGs of SNI animals and 100pM IL-1β treatment significantly increases *Csf1* mRNA expression in neuron enriched culture. **(A)** Fold-increase in *Il1b* mRNA levels relative to time-controlled sham were quantified in L4-L5 DRGs of CCI and SNI operated animals at 7 days post-surgery (sham, n=5; CCI, n=4; SNI, n=5) and 42 days post-surgery (sham, n=3; CCI, n=3; SNI, n=5) via rt-qPCR. (One-way ANOVA with Bonferroni's multiple comparisons test, * P<0.05, ** P<0.01, *** P<0.001 compared to appropriate time-controlled sham animals) **(B)** *Csf1* mRNA level in response to 5-day 100pM IL-1β treatment was quantified in neuron enriched DRG culture via rt-qPCR. (Unpaired two-tailed Student's t-test; ** P<0.01). All data points represent mean ± SEM.

Figure 5-6

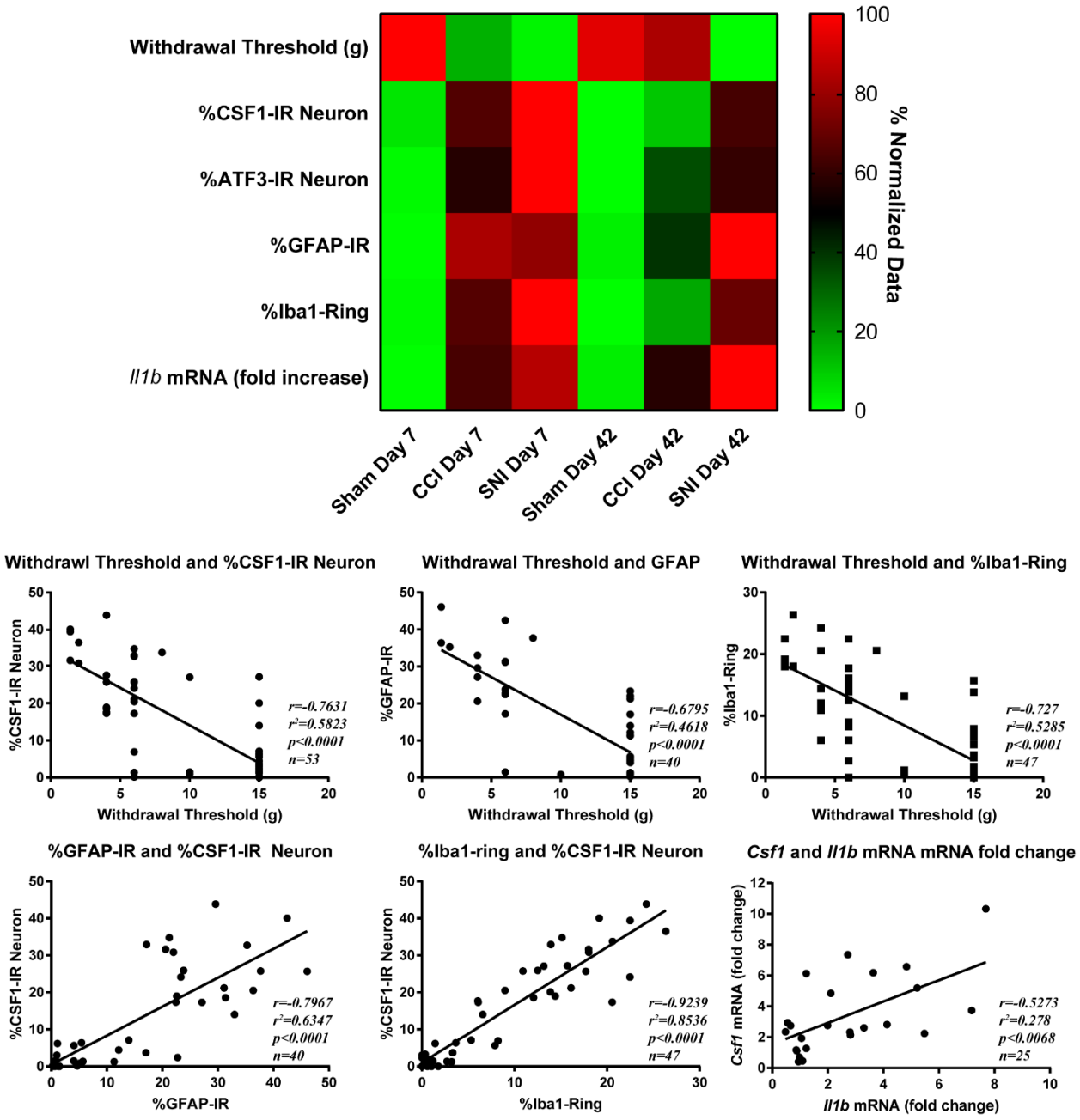

Figure 5-6. Data summary of relative levels and Pearson correlation coefficients of mechanical threshold, %CSF1-IR neuron, %ATF3-neuron, %GFAP-IR, %Iba1-ring, and *Il1b* mRNA fold change in sham, CCI, and SNI animals at onset and chronic time points.

Chapter 6

General Discussion

6.1 Summary of results

It is postulated that persistent hyperexcitability of DRG neurons and primary sensory afferents contributes indirectly to the onset (Wen et al 2007) and the maintenance of central sensitization (Pitcher & Henry 2008, Vaso et al 2014). IL-1β has been implicated to directly interact with IL-1R1 expressed in DRG neurons to not only modulate ion channel function and excitability in a cell type specific manner (Stemkowski et al 2015, Stemkowski & Smith 2012a), but also modify gene expressions to trigger a 'phenotypic switch' (Dou et al 2004, Fehrenbacher et al 2005). This thesis aims to illuminate the role of IL-1β in the persistent DRG neuron hyperexcitability and the maintenance of neuropathic pain. To do so, we examine the consequences of chronic IL-1β exposure and neuroinflammation, which occur in various animal models of neuropathic pain, on DRG neuron excitability as well as mechanical allodynia.

Through the experiments done in this thesis, we illustrate three potential IL-1β mediated mechanisms that work in parallel to promote persistent DRG neuron hyperexcitability as well as mechanical allodynia in animal models of neuropathic pain. First, we show chronic IL-1β exposure and EAE induced neuroinflammation can modulate and possibly modify ion channel function and expression to trigger enduring changes in DRG neuron excitability in a cell type specific manner. Second, we demonstrate the persistent activation of SGCs and macrophages in DRGs, which can provide chronic IL-1β secretion (Kawasaki et al 2008a, Santa-Cecilia et al 2019), contribute to chronic mechanical allodynia seen in the SNI model of neuropathic pain. This implies that DRG neurons in SNI operated animals can receive ongoing excitatory stimuli from IL-1β and other inflammatory mediators, which in turn can modulate ion channel function to promote persistent hyperexcitability. Third, we reveal cellular sources of IL-1β, such as activated SGCs and macrophages, associate both temporally and spatially with *de novo* induction

of CSF1 in the DRG neurons, which in turn causes spinal microglia activation and central sensitization. Taken together with IL-1β mediated hyperexcitability in the DRG neurons; more CSF1 as well as neurotransmitters, chemokines, and cytokines can be released in the spinal dorsal horn, which in turn can indirectly promote onset and maintenance of central sensitization.

6.2 IL-1β mediated neuroimmune interactions and its relevance to pain mechanisms

6.2.1 Can inflammation alone trigger enduring modification in DRG neuron excitability without physical nerve injury?

The data from the thesis implicate long-term IL-1β exposure can modulate as well as modify ion channel function. The modulative effects of IL-1β such as ion channel phosphorylation, i.e. increased TTX-S Na^+ channel function in small IB_4^+ DRG neurons, are expected to be transient; in contrast, modificative effects of IL-1β, such as change in gene expression, are expected to be long-lasting. For instance, nerve injury induced COX-2 expression in the DRG can last up to 18 months (Dou et al 2004, Ma et al 2010). These enduring consequences are implicated in providing sensory neurons with 'ectopic pacemaker capabilities' which cause ongoing ectopic discharges (Devor 2009). Determining which observed changes are due to modulation or modification of ion channel function may reveal important mechanisms underlying the transition between acute nociceptive pain to persistent neuropathic pain.

In contrast to our earlier study, which showed largely reversible increase in male rat medium size DRG neurons (Stemkowski et al 2015), in Chapter 3, we demonstrate chronic IL-1β treatment triggers enduring increase in AP duration in small IB_4^+ DRG neurons, which was largely mediated through decreased BK channel function. This implicates modification of gene expression either of the channels themselves or of other proteins that regulate their function. This result may be of broad interest as it has been suggested that uninjured nociceptive DRG neurons

and C-fibres become hyperexcitable following nerve injury due to inflammation, namely IL-1β mediated sensitization, and contribute to ongoing spontaneous pain seen in the majority of neuropathic pain patients (Chen et al 2011, Djouhri & Lawson 2004, Yang et al 2018). However, it is uncertain if the change in BK channel function is really mediated through change in gene expression as we have not explicitly measured transcripts of BK channel nor their subunits in response to chronic IL-1β treatment. A future study examining chronic IL-1β mediated changes in gene expression and their reversibility may provide insight to long-term consequences of chronic IL-1β exposure that occur after a peripheral nerve injury.

It is extremely unlikely that IL-1β alone is responsible for enduring changes that eventually lead to peripheral sensitization and directly to central sensitization. It is more likely that complex neuroimmune interactions mediated by a cocktail of inflammatory cytokines, chemokines, neurotrophic factors and neurotransmitters lead to persistent changes in DRG neuron excitability. In chapter 4, for the first time, we demonstrate EAE induced neuroinflammation triggers ongoing hyperexcitability in medium-large DRG neuron (female mice) excitability without peripheral nerve injury. Although we have not explicitly measured ion channel functions in this experiment, a future experiment may reveal important changes that occur within DRG neurons that may contribute to the 'phenotypic switch' and ongoing ectopic discharges. One potential candidate for further examination is the hyperpolarization-activated cyclic nucleotide-gated (HCN) channels, which activate and depolarize the membrane in response to hyperpolarization (Chaplan et al 2003). HCN channels are preferentially expressed in medium-large myelinated DRG neurons; and its activation can significantly increase DRG neuron excitability which can contribute to the pathogenesis of neuropathic pain (Noh et al 2014, Sun et al 2005, Sun et al 2017, Young et al 2014). A recent study has implicated the cyclooxygenase-1/prostaglandin E_2

(COX-1/PGE_2) pathway in regulation of HCN channel expression in the medium-large DRG neurons (Sun et al 2017). Since COX-1 expression in the DRG is significantly upregulated in response to chronic inflammation (Dou et al 2004), this may result in long term upregulation of HCN channels. Although it may be difficult to test pain behaviors in EAE mice at a chronic timepoint, it has been shown that facial sensitivity can still be tested at a chronic time point (Thorburn et al 2016). For example, Thornburn et al. showed air puffs to the whisker pad evoked more pain behaviors in EAE animals, as indicated by withdrawal of the head or forepaw swipes down the snout, compared to CFA controls at the peak of motor deficits. A future study using specific HCN channel blockers may potentially reveal channels responsible for ongoing hypersensitivity in primary sensory neurons. Alternatively, a study could further characterize EAE induced changes and reversibility in ion channel functions during the onset and chronic time point, which may reveal ion channels responsible for the maintenance of ongoing hyperexcitability.

6.2.2 Neuron-SGC-macrophage crosstalk as a source of ongoing hyperexcitability?

There is growing evidence neuroimmune interactions are critical for the pathogenesis of neuropathic pain (Grace et al 2014). Although cytokines and chemokines are putative 'neurotransmitters' of the immune system, immune cell derived inflammatory mediators, such as IL-1β and TNFα, can directly affect sensory neurons. Fascinatingly, the neurons themselves can also modulate immune cells through release of neurotransmitters and cytokines (Pinho-Ribeiro et al 2017, Sotelo 2015). Since we observe long-lasting neuroinflammation only in DRGs from SNI operated male rats, this may contribute to ongoing hyperexcitability in DRG neurons.

SGCs tightly encircle around the sensory neuron; therefore, neuron-SGC crosstalk has been implicated to play an important role in sensory neuron function (Hanani 2005). In fact, SGCs

express receptors for neurotransmitter (e.g. ATP, substance P and CGRP) as well as cytokines and neurotrophic factors (e.g. TNFα, IL-1, and NGF) (Hanani 2005). Upon nerve injury SGCs activate in a sensory neuron activity dependant manner as its activation is blocked by early blockade of primary afferent activity with TTX (Xie et al 2009). It has been shown that increased sensory neuron activity following a peripheral nerve injury leads to Ca^{2+} dependant increase in exocytosis of ATP into perineural space, which then can bind to P2X7 receptor expressed in SGCs (Zhang et al 2007). Upon activation, SGCs can secrete numerous neurotrophins (e.g. GDNF and NGF) and cytokines (e.g. IL-1β and TNFα) that can not only modulate sensory neuron excitability (Hanani 2005, Takeda et al 2008), but also induce *de novo* production of pro-nociceptive factors such as COX-2 and CSF1 (Dou et al 2004, Lim et al 2017). Consequently, these studies suggested SGC-sensory neuron crosstalk perpetuates ongoing hyperexcitability, and thus contribute indirectly to central sensitization.

In my thesis, we observe remarkable spatial association between CSF1 immunoreactive neurons and cluster of macrophages surrounding the neuron. This has been implicated to be mediated through CSF1R expressed in macrophages as CSF1 has been shown to be involved in differentiation, proliferation as well as chemotaxis of macrophages (Krishnan et al 2018, Stanley et al 1978, Webb et al 1996). Furthermore, since CSF1 producing neurons and SGCs also showed significant spatial association, macrophages and SGCs most likely co-localize as well. In fact, another study observed resident macrophages and activated SGCs co-localized following a nerve injury (Krishnan et al 2018). Therefore, macrophages are likely to participate in neuroimmune crosstalk between SGCs and macrophages. For example, following a nerve injury, *de novo* production of CSF1 can both proliferate and recruit resident macrophages (Krishnan et al 2018). Macrophages then can bind ATPs released by hyperactive sensory neuron, which in

turn leads to subsequent release of inflammatory mediators such as IL-1β and TNFα (de Torre-Minguela et al 2016). Subsequently, IL-1β and TNFα can bind to IL-1R1 and TNFα receptor type 1 (TNFαR1) expressed in both SGCs and sensory neurons (Hanani 2005), which in turn can modulate their function. For instance, TNFα can induce increased *Il1b* gene expression and is implicated to play a role in activation of NLRP3 inflammasome (Jo et al 2016). Therefore, association between sensory neurons, macrophages, and SGCs may form a positive feedback loop, which may maintain or be maintained by ongoing aberrant hyperexcitability in primary afferents and DRG neurons. One potential mechanism that may trigger and maintain these interactions may be the ongoing spontaneous activity arising from severed nerve endings that cannot reinnervate and have developed 'ectopic pacemaker capabilities' due to accumulation of TTX-S Na^+ channels (Devor 2009, Wall & Gutnick 1974a, Xie et al 2017).

This effect is somewhat observable in the current thesis as only the SNI, which cannot reinnervate transected common peroneal and tibial nerve, (Decosterd & Woolf 2000), displayed persistent increase in macrophage, activated SGC and CSF1 expression in the DRGs as opposed to the CCI, which eventually regenerates completely (Mosconi & Kruger 1996). This ongoing neuroinflammation may be particularly important for the maintenance neuropathic pain in certain type of injuries as it has been shown to sensitize uninjured DRG neurons and primary afferents (Chen et al 2011, Djouhri & Lawson 2004, Yang et al 2018). This is evident in the SNI model as tactile and nociceptive sensory information is transduced through the uninjured sural nerve, which is profoundly sensitized chronically (Decosterd & Woolf 2000). This effect may be explicitly tested by blocking nerve conduction with TTX or local anaesthetic after peripheral nerve injury as both SGC and spinal microglia activation depend on primary afferent activity (Wen et al 2007, Xie et al 2009). Since SGC activation has been suggested to be critical for

CSF1 production (Lim et al 2017), this may be a result of either preventing CSF1 release or production from primary afferents. Therefore, a future study examining the relationship between sensory neuron activity and CSF1 production as well as persistent neuroinflammation in the DRG may reveal a potential mechanism underlying the maintenance of neuropathic pain.

6.2.3 Nerve injury induced peripheral neuroinflammation: Modulation or modification?

Since cause and effect relationships between CSF1, neuroinflammation, ongoing ectopic discharges, and persistent mechanical allodynia are not explicitly tested in the current thesis, it is not unequivocally clear whether these changes modulate or modify primary afferents to promote enduring hyperexcitability and central sensitization. Approaches that directly target aberrant primary afferent and DRG neuron activity has been shown to alleviate spontaneous pain in patients with peripheral neuropathy (Haroutounian et al 2014), phantom limb pain in amputees (Vaso et al 2014) as well as mechanical allodynia in rodents (Dou et al 2004, Noh et al 2014, Weir et al 2017, Young et al 2014) long after the establishment of neuropathic pain. If persistent peripheral neuroinflammation does indeed modulate primary afferents and DRG neurons to promote persistent hyperexcitability, blocking it long after establishment of central sensitization should ameliorate neuropathic pain behaviors. On the other hand, if peripheral neuroinflammation triggers modification in primary afferents and DRG neurons, inhibition of it would not affect ongoing hyperexcitability. Since both CCI and SNI exhibit substantial expression of activated SGCs, macrophages, and CSF1 in the DRGs during the onset, we postulate continued presence of neuroinflammation is modulating primary afferent excitability to maintain mechanical allodynia. However, the duration and the concentration of IL-1β exposure can lead to different outcomes (Binshtok et al 2008, Liu et al 2006, Stemkowski et al 2015, Stemkowski & Smith 2012a). For example, Binshtok et al. demonstrated 3-minute exposure to

571 pM IL-1β caused reduced inactivation of TTX-R I_{Na} as well as profound increase in TTX-R I_{Na} amplitude in small DRG neurons. In contrast, in Chapter 3, we show 5-6 day 100 pM IL-1β treatment has no effect on TTX-R I_{Na}, but significantly increases TTX-S I_{Na} amplitude and produces leftward shift in voltage dependence of activation in small $I^{B}4$+ DRG neurons. Therefore, more profound and persistent neuroinflammation observed in SNI may modify primary afferents and DRG neurons to trigger persistent hyperexcitability. A future study examining the effects of inhibiting peripheral neuroinflammation at the chronic timepoint (beyond 42 days post-injury) may reveal important mechanisms contributing to enduring aberrant activity in the primary afferents and DRG neurons.

6.2.4 Sex differences and neuroimmune interaction

There is growing appreciation of sex differences observed in various models of neuropathic pain as well as in humans. Women are more likely to suffer from diseases associated with pain such as multiple sclerosis, osteoarthritis, and migraine (Ebers 2008, Mogil 2012). It has been suggested that distinct neuroimmune interactions underlie the sex differences in neuropathic pain (Mapplebeck et al 2017). For example, peripheral nerve injury causes profound activation of spinal microglia in both male and female rodents; however, only males depend on microglia activation for neuropathic pain behaviors (Mapplebeck et al 2018, Sorge et al 2015). It has been suggested females rely on T-cell infiltration to either PNS (Lopes et al 2017) or CNS (Sorge et al 2015) for the pathogenesis of neuropathic pain. In fact, across many species, T-cell mediated immune responses are greater in females than males (Klein & Flanagan 2016). In agreement with this, female mice are much more likely to develop neuropathic pain behavior upon EAE induction compared to male mice (Rahn et al 2014). Furthermore, EAE induction leads to substantial increase in medium-large DRG neuron excitability in female mice, as indicated by

amplified $[Ca^{2+}]_i$ increase in response to depolarization with 30 mM KCl, in stark contrast to medium-large DRG neurons in male mice, which were unaffected by EAE induction (Mifflin et al 2018). Interestingly, although inflammatory mediators produce comparable increases in excitability in dural afferents in both sexes; it is much more likely to sensitize dural afferents from female rats as it can sensitize nearly 100% of dural afferents in females in comparison to roughly 50% in males (Scheff & Gold 2011). These results suggest primary sensory afferents and DRG neurons from females may be more susceptible to neuroinflammation. Therefore, the differential reversibility in excitability between medium DRG neurons from male rats in response to chronic IL-1β and medium-large DRG neurons from female mice in response to EAE induction may have been due to sex differences. Future work could repeat the same experiments in female rats to examine the effects of long-term IL-1β exposure. Furthermore, persistent upregulation of activated SGCs, macrophages, and CSF1 production may have distinct effects in female rats as they do not depend on microglia activation for the pathogenesis of neuropathic pain (Mapplebeck et al 2018). An interesting experiment would be to block CSF1 production or CSF1R in female rats to examine the role of CSF1 in the pathogenesis and the maintenance of neuropathic pain in females. Furthermore, since primary afferents are more likely to be sensitized by neuroinflammation in females, persistent neuroinflammation in the DRG may cause more profound increase in primary afferent and DRG neuron excitability compared to males. Although there are clear differences in pain processing between males and females, it is interesting to note that treatments that target the hyperexcitable primary afferents and DRG neurons work equally well in both males and females (Haroutounian et al 2014, Vaso et al 2014). Our earlier study examining the therapeutic potential of HCN channel blocker ivabradine for the treatment of neuropathic pain demonstrated ivabradine was also equally anti-allodynic in both

males and females (Noh et al 2014). Therefore, drugs that target the peripheral neuroinflammation, which can trigger enduring changes in the primary afferents and DRG neurons, may be of substantial interest as it may provide novel therapeutic approach that could work equally well in both males and females.

6.3 Conclusion

The work from this thesis provides additional support to growing evidence that neuropathic pain is a 'neuroimmune disorder'. Peripheral neuroinflammation mediated by IL-1β as well as other inflammatory mediators can not only produce enduring hyperexcitability in the DRG neurons, but it may also trigger *de novo* induction of critical neuroimmune mediators such as CSF1. The data obtained in this thesis provide potential mechanisms that neuron-immune crosstalk may facilitate persistent hyperexcitability in the primary afferents and in the DRG, which in turn can indirectly contribute to the onset and the maintenance of central sensitization. We also postulate neuroimmune interactions mediated by IL-1β and persistent hyperexcitability in the primary afferents and DRG neurons are potential therapeutic targets that may provide sex-independent efficacy for the treatment of neuropathic pain.

References

Abdulla FA, Smith PA. 1997. Nociceptin inhibits T-type Ca2+ channel current in rat sensory neurons by a G-protein-independent mechanism. *The Journal of Neuroscience* 17: 8721-28

Abdulla FA, Smith PA. 2001a. Axotomy- and Autotomy-Induced Changes in Ca 2+ and K + Channel Currents of Rat Dorsal Root Ganglion Neurons. *Journal of Neurophysiology* 85: 644-58

Abdulla FA, Smith PA. 2001b. Axotomy and Autotomy-Induced Changes in the Excitability of Rat Dorsal Root Ganglion Neurons. *Journal of Neurophysiology* 85: 630-43

Abdulla FA, Smith PA. 2002. Changes in Na + channel currents of rat dorsal root ganglion neurons following axotomy and axotomy-induced autotomy. *J.Neurophysiol* 88 2518-29

Abraira VE, Ginty DD. 2013. The sensory neurons of touch. *Neuron* 79: 618-39

Akopian AN, Sivilotti L, Wood JN. 1996. A tetrodotoxin-resistant voltage-gated sodium channel expressed by sensory neurons. *Nature* 379: 257-62

Alcock MM. 2017. Defining pain: past, present, and future. *Pain* 158: 761-62

Alier KA, Endicott JA, Stemkowski PL, Cenac N, Cellars L, et al. 2008. Intrathecal administration of proteinase-activated receptor-2 agonists produces hyperalgesia by exciting the cell bodies of primary sensory neurons. *The Journal of pharmacology and experimental therapeutics* 324: 224-33

Alles SRA, Smith PA. 2018. Etiology and Pharmacology of Neuropathic Pain. *Pharmacological reviews* 70: 315-47

Alvarez P, Chen X, Bogen O, Green PG, Levine JD. 2012. IB4(+) nociceptors mediate persistent muscle pain induced by GDNF. *J Neurophysiol* 108: 2545-53

Amaya F, Wang H, Costigan M, Allchorne AJ, Hatcher JP, et al. 2006. The voltage-gated sodium channel Na(v)1.9 is an effector of peripheral inflammatory pain hypersensitivity. *The Journal of neuroscience : the official journal of the Society for Neuroscience* 26: 12852-60

Amir R, Michaelis M, Devor M. 1999. Membrane potential oscillations in dorsal root ganglion neurons: role in normal electrogenesis and neuropathic pain. *The Journal of neuroscience : the official journal of the Society for Neuroscience* 19: 8589-96

Auron PE, Webb AC, Rosenwasser LJ, Mucci SF, Rich A, et al. 1984. Nucleotide sequence of human monocyte interleukin 1 precursor cDNA. *Proceedings of the National Academy of Sciences of the United States of America* 81: 7907-11

Baba H, Ji RR, Kohno T, Moore KA, Ataka T, et al. 2003. Removal of GABAergic inhibition facilitates polysynaptic A fiber-mediated excitatory transmission to the superficial spinal dorsal horn. *Molecular and cellular neurosciences* 24: 818-30

Bailey AL, Ribeiro-da-Silva A. 2006. Transient loss of terminals from non-peptidergic nociceptive fibers in the substantia gelatinosa of spinal cord following chronic constriction injury of the sciatic nerve. *Neuroscience* 138: 675-90

Balasubramanyan S, Stemkowski PL, Stebbing MJ, Smith PA. 2006a. Sciatic chronic constriction injury produces cell-type-specific changes in the electrophysiological properties of rat substantia gelatinosa neurons. *J Neurophysiol* 96: 579-90

Balasubramanyan S, Stemkowski PL, Stebbing MJ, Smith PA. 2006b. Sciatic Chronic Constriction Injury Produces Cell-type Specific Changes in the Electrophysiological Properties of Rat Substantia Gelatinosa Neurons. *Journal of Neurophysiology* 96: 579-90

Bartfai T, Schultzberg M. 1993. Cytokines in neuronal cell types. *Neurochemistry international* 22: 435-44

Basbaum AI, Bautista DM, Scherrer G, Julius D. 2009. Cellular and molecular mechanisms of pain. *Cell* 139: 267-84

Beggs S, Trang T, Salter MW. 2012. P2X4R+ microglia drive neuropathic pain. *Nature neuroscience* 15: 1068-73

Begum F, Zhu W, Cortes C, MacNeil B, Namaka M. 2013. Elevation of tumor necrosis factor alpha in dorsal root ganglia and spinal cord is associated with neuroimmune modulation of pain in an animal model of multiple sclerosis. *Journal of neuroimmune pharmacology : the official journal of the Society on NeuroImmune Pharmacology* 8: 677-90

Bennett GJ, Xie YK. 1988. A peripheral mononeuropathy in rat that produces disorders of pain sensation like those seen in man. *Pain* 33: 87-107

Benson C, Paylor JW, Tenorio G, Winship I, Baker G, Kerr BJ. 2015. Voluntary wheel running delays disease onset and reduces pain hypersensitivity in early experimental autoimmune encephalomyelitis (EAE). *Experimental neurology* 271: 279-90

Berta T, Liu T, Liu YC, Xu ZZ, Ji RR. 2012. Acute morphine activates satellite glial cells and up-regulates IL-1beta in dorsal root ganglia in mice via matrix metalloprotease-9. *Molecular pain* 8: 18

Berta T, Qadri YJ, Chen G, Ji RR. 2016. Microglial Signaling in Chronic Pain with a Special Focus on Caspase 6, p38 MAP Kinase, and Sex Dependence. *Journal of dental research* 95: 1124-31

Bianchi M, Dib B, Panerai AE. 1998. Interleukin-1 and nociception in the rat. *Journal of neuroscience research* 53: 645-50

Biggs JE, Lu VB, Stebbing MJ, Balasubramanyan S, Smith PA. 2010. Is BDNF sufficient for information transfer between microglia and dorsal horn neurons during the onset of central sensitization? *Molecular pain* 6: 44

Binshtok AM, Wang H, Zimmermann K, Amaya F, Vardeh D, et al. 2008. Nociceptors Are Interleukin-1{beta} Sensors. *Journal of Neuroscience* 28: 14062-73

Boettger MK, Till S, Chen MX, Anand U, Otto WR, et al. 2002. Calcium-activated potassium channel SK1- and IK1-like immunoreactivity in injured human sensory neurones and its regulation by neurotrophic factors. *Brain : a journal of neurology* 125: 252-63

Bogen O, Dina OA, Gear RW, Levine JD. 2009. Dependence of monocyte chemoattractant protein 1 induced hyperalgesia on the isolectin B4-binding protein versican. *Neuroscience* 159: 780-86

Bogen O, Joseph EK, Chen X, Levine JD. 2008. GDNF hyperalgesia is mediated by PLCgamma, MAPK/ERK, PI3K, CDK5 and Src family kinase signaling and dependent on the IB4-binding protein versican. *Eur J Neurosci* 28: 12-19

Boroujerdi A, Kim HK, Lyu YS, Kim DS, Figueroa KW, et al. 2008. Injury discharges regulate calcium channel alpha-2-delta-1 subunit upregulation in the dorsal horn that contributes to initiation of neuropathic pain. *Pain* 139: 358-66

Bourinet E, Alloui A, Monteil A, Barrere C, Couette B, et al. 2005. Silencing of the Cav3.2 T-type calcium channel gene in sensory neurons demonstrates its major role in nociception. *The EMBO journal* 24: 315-24

Bourinet E, Altier C, Hildebrand ME, Trang T, Salter MW, Zamponi GW. 2014. Calcium-permeable ion channels in pain signaling. *Physiol Rev* 94: 81-140

Bowersox SS, Luther R. 1998. Pharmacotherapeutic potential of omega-conotoxin MVIIA (SNX-111), an N-type neuronal calcium channel blocker found in the venom of Conus magus. *Toxicon : official journal of the International Society on Toxinology* 36: 1651-8

Braz J, Solorzano C, Wang X, Basbaum AI. 2014. Transmitting pain and itch messages: a contemporary view of the spinal cord circuits that generate gate control. *Neuron* 82: 522-36

Braz JM, Basbaum AI. 2008. Genetically expressed transneuronal tracer reveals direct and indirect serotonergic descending control circuits. *The Journal of comparative neurology* 507: 1990-2003

Braz JM, Nassar MA, Wood JN, Basbaum AI. 2005. Parallel "pain" pathways arise from subpopulations of primary afferent nociceptor. *Neuron* 47: 787-93

Breese NM, George AC, Pauers LE, Stucky CL. 2005. Peripheral inflammation selectively increases TRPV1 function in IB4-positive sensory neurons from adult mouse. *Pain* 115: 37-49

Callaghan BC, Cheng HT, Stables CL, Smith AL, Feldman EL. 2012. Diabetic neuropathy: clinical manifestations and current treatments. *The Lancet. Neurology* 11: 521-34

Carson MJ, Doose JM, Melchior B, Schmid CD, Ploix CC. 2006. CNS immune privilege: hiding in plain sight. *Immunological reviews* 213: 48-65

Cavanaugh DJ, Lee H, Lo L, Shields SD, Zylka MJ, et al. 2009. Distinct subsets of unmyelinated primary sensory fibers mediate behavioral responses to noxious thermal and mechanical stimuli. *Proceedings of the National Academy of Sciences of the United States of America* 106: 9075-80

Chaplan SR, Guo HQ, Lee DH, Luo L, Liu C, et al. 2003. Neuronal hyperpolarization-activated pacemaker channels drive neuropathic pain. *The Journal of neuroscience : the official journal of the Society for Neuroscience* 23: 1169-78

Chen CJ, Kono H, Golenbock D, Reed G, Akira S, Rock KL. 2007. Identification of a key pathway required for the sterile inflammatory response triggered by dying cells. *Nature medicine* 13: 851-6

Chen G, Luo X, Qadri MY, Berta T, Ji RR. 2018a. Sex-Dependent Glial Signaling in Pathological Pain: Distinct Roles of Spinal Microglia and Astrocytes. *Neuroscience bulletin* 34: 98-108

Chen G, Zhang YQ, Qadri YJ, Serhan CN, Ji RR. 2018b. Microglia in Pain: Detrimental and Protective Roles in Pathogenesis and Resolution of Pain. *Neuron* 100: 1292-311

Chen Q, Tao J, Hei H, Li F, Wang Y, et al. 2015. Up-Regulatory Effects of Curcumin on Large Conductance Ca2+-Activated K+ Channels. *PloS one* 10: e0144800

Chen SR, Cai YQ, Pan HL. 2009a. Plasticity and emerging role of BKCa channels in nociceptive control in neuropathic pain. *J Neurochem.* 110: 352-62

Chen X, Pang RP, Shen KF, Zimmermann M, Xin WJ, et al. 2011. TNF-alpha enhances the currents of voltage gated sodium channels in uninjured dorsal root ganglion neurons following motor nerve injury. *Experimental neurology* 227: 279-86

Chen Y, Balasubramanyan S, Lai AY, Todd KG, Smith PA. 2009b. Effects of Sciatic Nerve Axotomy on Excitatory Synaptic Transmission in Rat Substantia Gelatinosa. *J.Neurophysiol* 102: 3203-15

Chen Y, Derkach VA, Smith PA. 2016. Loss of Ca(2+)-permeable AMPA receptors in synapses of tonic firing substantia gelatinosa neurons in the chronic constriction injury model of neuropathic pain. *Exp.Neurol.* 279: 168-77

Chien LY, Cheng JK, Chu D, Cheng CF, Tsaur ML. 2007. Reduced expression of A-type potassium channels in primary sensory neurons induces mechanical hypersensitivity. *The Journal of neuroscience : the official journal of the Society for Neuroscience* 27: 9855-65

Chiu IM, Barrett LB, Williams EK, Strochlic DE, Lee S, et al. 2014. Transcriptional profiling at whole population and single cell levels reveals somatosensory neuron molecular diversity. *eLife* 3

Chung JM, Kim HK, Chung K. 2004. Segmental spinal nerve ligation model of neuropathic pain. *Methods in molecular medicine* 99: 35-45

Cizkova D, Marsala J, Lukacova N, Marsala M, Jergova S, et al. 2002. Localization of N-type Ca2+ channels in the rat spinal cord following chronic constrictive nerve injury. *Experimental brain research* 147: 456-63

Clark AK, Gentry C, Bradbury EJ, McMahon SB, Malcangio M. 2007. Role of spinal microglia in rat models of peripheral nerve injury and inflammation. *Eur J Pain* 11: 223-30

Clark JD. 2016. Preclinical Pain Research: Can We Do Better? *Anesthesiology* 125: 846-49

Cobos EJ, Nickerson CA, Gao F, Chandran V, Bravo-Caparros I, et al. 2018. Mechanistic Differences in Neuropathic Pain Modalities Revealed by Correlating Behavior with Global Expression Profiling. *Cell reports* 22: 1301-12

Colburn RW, Rickman AJ, DeLeo JA. 1999. The effect of site and type of nerve injury on spinal glial activation and neuropathic pain behavior. *Experimental neurology* 157: 289-304

Colley BS, Biju KC, Visegrady A, Campbell S, Fadool DA. 2007. Neurotrophin B receptor kinase increases Kv subfamily member 1.3 (Kv1.3) ion channel half-life and surface expression. *Neuroscience* 144: 531-46

Colloca L, Ludman T, Bouhassira D, Baron R, Dickenson AH, et al. 2017. Neuropathic pain. *Nature reviews. Disease primers* 3: 17002

Compston A, Coles A. 2008. Multiple sclerosis. *Lancet* 372: 1502-17

Constantinescu CS, Farooqi N, O'Brien K, Gran B. 2011. Experimental autoimmune encephalomyelitis (EAE) as a model for multiple sclerosis (MS). *British journal of pharmacology* 164: 1079-106

Copray JC, Mantingh I, Brouwer N, Biber K, Kust BM, et al. 2001. Expression of interleukin-1 beta in rat dorsal root ganglia. *Journal of neuroimmunology* 118: 203-11

Costigan M, Scholz J, Woolf CJ. 2009. Neuropathic pain: a maladaptive response of the nervous system to damage. *Annual review of neuroscience* 32: 1-32

Coull JA, Beggs S, Boudreau D, Boivin D, Tsuda M, et al. 2005. BDNF from microglia causes the shift in neuronal anion gradient underlying neuropathic pain. *Nature* 438: 1017-21

Coull JA, Boudreau D, Bachand K, Prescott SA, Nault F, et al. 2003a. Trans-synaptic shift in anion gradient in spinal lamina I neurons as a mechanism of neuropathic pain. *Nature* 424: 938-42

Coull JA, Boudreau D, Bachand K, Prescott SA, Nault F, et al. 2003b. Trans-synaptic shift in anion gradient in spinal lamina I neurons as a mechanism of neuropathic pain. *Nature* 424: 938-42

Courteix C, Eschalier A, Lavarenne J. 1993. Streptozocin-induced diabetic rats: behavioural evidence for a model of chronic pain. *Pain* 53: 81-8

Cox JJ, Reimann F, Nicholas AK, Thornton G, Roberts E, et al. 2006. An SCN9A channelopathy causes congenital inability to experience pain. *Nature* 444: 894-8

Cummins TR, Black JA, Dib-Hajj SD, Waxman SG. 2000. Glial-derived neurotrophic factor upregulates expression of functional SNS and NaN sodium channels and their currents in axotomized dorsal root ganglion neurons. *The Journal of neuroscience : the official journal of the Society for Neuroscience* 20: 8754-61

Cummins TR, Waxman SG. 1997. Downregulation of tetrodotoxin resistant sodium currents and upregulation of rapidly repriming tetrodotoxin sensitive sodium current in small sensory neurons after nerve injury . . *The Journal of Neuroscience* 17: 3503-14

Cunha JM, Cunha FQ, Poole S, Ferreira SH. 2000. Cytokine-mediated inflammatory hyperalgesia limited by interleukin-1 receptor antagonist. *British journal of pharmacology* 130: 1418-24

Czeschik JC, Hagenacker T, Schafers M, Busselberg D. 2008. TNF-alpha differentially modulates ion channels of nociceptive neurons. *Neurosci Lett.* 434: 293-98

Dantzer R. 2018. Neuroimmune Interactions: From the Brain to the Immune System and Vice Versa. *Physiol Rev* 98: 477-504

Daou I, Beaudry H, Ase AR, Wieskopf JS, Ribeiro-da-Silva A, et al. 2016. Optogenetic Silencing of Nav1.8-Positive Afferents Alleviates Inflammatory and Neuropathic Pain. *eNeuro.* 3

Davidson S, Copits BA, Zhang J, Page G, Ghetti A, Gereau RW. 2014. Human sensory neurons: Membrane properties and sensitization by inflammatory mediators. *Pain* 155: 1861-70

de Torre-Minguela C, Barbera-Cremades M, Gomez AI, Martin-Sanchez F, Pelegrin P. 2016. Macrophage activation and polarization modify P2X7 receptor secretome influencing the inflammatory process. *Scientific reports* 6: 22586

Decosterd I, Woolf CJ. 2000. Spared nerve injury: an animal model of persistent peripheral neuropathic pain. *Pain* 87: 149-58

del Rey A, Yau HJ, Randolf A, Centeno MV, Wildmann J, et al. 2011. Chronic neuropathic pain-like behavior correlates with IL-1beta expression and disrupts cytokine interactions in the hippocampus. *Pain* 152: 2827-35

Denk F, Crow M, Didangelos A, Lopes DM, McMahon SB. 2016. Persistent Alterations in Microglial Enhancers in a Model of Chronic Pain. *Cell reports* 15: 1771-81

Devor M. 2009. Ectopic discharge in Abeta afferents as a source of neuropathic pain. *Experimental brain research* 196: 115-28

Devor M, Wall PD, Catalan N. 1992. Systemic lidocaine silences ectopic neuroma and DRG discharge without blocking nerve conduction. *Pain* 48: 261-8

Diaz A, Dickenson AH. 1997. Blockade of spinal N- and P-type, but not L-type, calcium channels inhibits the excitability of rat dorsal horn neurones produced by subcutaneous formalin inflammation. *Pain* 69: 93-100

Dib-Hajj S, Black JA, Cummins TR, Waxman SG. 2002. NaN/Nav1.9: a sodium channel with unique properties. *Trends Neurosci* 25: 253-9

DiBonaventura MD, Sadosky A, Concialdi K, Hopps M, Kudel I, et al. 2017. The prevalence of probable neuropathic pain in the US: results from a multimodal general-population health survey. *Journal of pain research* 10: 2525-38

Dinarello CA, Renfer L, Wolff SM. 1977. Human leukocytic pyrogen: purification and development of a radioimmunoassay. *Proceedings of the National Academy of Sciences of the United States of America* 74: 4624-7

Dirajlal S, Pauers LE, Stucky CL. 2003. Differential response properties of IB(4)-positive and -negative unmyelinated sensory neurons to protons and capsaicin. *J Neurophysiol* 89: 513-24

Djouhri L, Lawson SN. 2004. Abeta-fiber nociceptive primary afferent neurons: a review of incidence and properties in relation to other afferent A-fiber neurons in mammals. *Brain research. Brain research reviews* 46: 131-45

Dolphin AC. 2012. Calcium channel auxiliary alpha2delta and beta subunits: trafficking and one step beyond. *Nat Rev Neurosci* 13: 542-55

Dou W, Jiao Y, Goorha S, Raghow R, Ballou LR. 2004. Nociception and the differential expression of cyclooxygenase-1 (COX-1), the COX-1 variant retaining intron-1 (COX-1v), and COX-2 in mouse dorsal root ganglia (DRG). *Prostaglandins & other lipid mediators* 74: 29-43

Douglas WW, Ritchie JM. 1957. Nonmedullated fibres in the saphenous nerve which signal touch. *The Journal of physiology* 139: 385-99

Dowdall T, Robinson I, Meert TF. 2005. Comparison of five different rat models of peripheral nerve injury. *Pharmacology, biochemistry, and behavior* 80: 93-108

Dray A, Perkins M. 1993. Bradykinin and inflammatory pain. *Trends Neurosci* 16: 99-104

Drenth JP, Waxman SG. 2007. Mutations in sodium-channel gene SCN9A cause a spectrum of human genetic pain disorders. *The Journal of clinical investigation* 117: 3603-9

Drulovic J, Basic-Kes V, Grgic S, Vojinovic S, Dincic E, et al. 2015. The Prevalence of Pain in Adults with Multiple Sclerosis: A Multicenter Cross-Sectional Survey. *Pain Med* 16: 1597-602

Dubin AE, Patapoutian A. 2010. Nociceptors: the sensors of the pain pathway. *The Journal of clinical investigation* 120: 3760-72

Dubovy P. 2011. Wallerian degeneration and peripheral nerve conditions for both axonal regeneration and neuropathic pain induction. *Annals of anatomy = Anatomischer Anzeiger : official organ of the Anatomische Gesellschaft* 193: 267-75

Duffy SS, Perera CJ, Makker PG, Lees JG, Carrive P, Moalem-Taylor G. 2016. Peripheral and Central Neuroinflammatory Changes and Pain Behaviors in an Animal Model of Multiple Sclerosis. *Frontiers in immunology* 7: 369

Ebbinghaus M, Natura G, Segond von Banchet G, Hensellek S, Bottcher M, et al. 2017. Interleukin-17A is involved in mechanical hyperalgesia but not in the severity of murine antigen-induced arthritis. *Scientific reports* 7: 10334

Ebbinghaus M, Uhlig B, Richter F, von Banchet GS, Gajda M, et al. 2012. The role of interleukin-1beta in arthritic pain: main involvement in thermal, but not mechanical, hyperalgesia in rat antigen-induced arthritis. *Arthritis and rheumatism* 64: 3897-907

Ebers GC. 2008. Environmental factors and multiple sclerosis. *The Lancet. Neurology* 7: 268-77

Echeverry S, Shi XQ, Yang M, Huang H, Wu Y, et al. 2017. Spinal microglia are required for long-term maintenance of neuropathic pain. *Pain* 158: 1792-801

Elmore MR, Najafi AR, Koike MA, Dagher NN, Spangenberg EE, et al. 2014. Colony-stimulating factor 1 receptor signaling is necessary for microglia viability, unmasking a microglia progenitor cell in the adult brain. *Neuron* 82: 380-97

Emery EC, Young GT, Berrocoso EM, Chen L, McNaughton PA. 2011. HCN2 ion channels play a central role in inflammatory and neuropathic pain. *Science* 333: 1462-6

Everill B, Kocsis JD. 1999. Reduction in potassium currents in identified cutaneous afferent dorsal root ganglion neurons after axotomy. *J Neurophysiol* 82: 700-8

Faber CG, Lauria G, Merkies IS, Cheng X, Han C, et al. 2012a. Gain-of-function Nav1.8 mutations in painful neuropathy. *Proceedings of the National Academy of Sciences of the United States of America* 109: 19444-9

Faber CG, Lauria G, Merkies IS, Cheng X, Han C, et al. 2012b. Gain-of-function Nav1.8 mutations in painful neuropathy. *Proc.Natl.Acad.Sci.U.S.A* 109: 19444-49

Fang X, Djouhri L, McMullan S, Berry C, Waxman SG, et al. 2006. Intense isolectin-B4 binding in rat dorsal root ganglion neurons distinguishes C-fiber nociceptors with broad action potentials and high Nav1.9 expression. *The Journal of neuroscience : the official journal of the Society for Neuroscience* 26: 7281-92

Fehrenbacher JC, Burkey TH, Nicol GD, Vasko MR. 2005. Tumor necrosis factor alpha and interleukin-1beta stimulate the expression of cyclooxygenase II but do not alter prostaglandin E2 receptor mRNA levels in cultured dorsal root ganglia cells. *Pain* 113: 113-22

Ferrari LF, Bogen O, Levine JD. 2010. Nociceptor subpopulations involved in hyperalgesic priming. *Neuroscience* 165: 896-901

Ferreira SH, Lorenzetti BB, Bristow AF, Poole S. 1988. Interleukin-1 beta as a potent hyperalgesic agent antagonized by a tripeptide analogue. *Nature* 334: 698-700

Finnerup NB, Attal N, Haroutounian S, McNicol E, Baron R, et al. 2015. Pharmacotherapy for neuropathic pain in adults: a systematic review and meta-analysis. *The Lancet. Neurology* 14: 162-73

Fjell J, Cummins TR, Dib-Hajj SD, Fried K, Black JA, Waxman SG. 1999. Differential role of GDNF and NGF in the maintenance of two TTX- resistant sodium channels in adult DRG neurons. *Brain Research.Molecular Brain Research* 67: 267-82

Foley PL, Vesterinen HM, Laird BJ, Sena ES, Colvin LA, et al. 2013. Prevalence and natural history of pain in adults with multiple sclerosis: systematic review and meta-analysis. *Pain* 154: 632-42

Frezel N, Sohet F, Daneman R, Basbaum AI, Braz JM. 2016. Peripheral and central neuronal ATF3 precedes CD4+ T-cell infiltration in EAE. *Experimental neurology* 283: 224-34

Fukuoka H, Kawatani M, Hisamitsu T, Takeshige C. 1994. Cutaneous hyperalgesia induced by peripheral injection of interleukin-1 beta in the rat. *Brain research* 657: 133-40

Garlanda C, Dinarello CA, Mantovani A. 2013. The interleukin-1 family: back to the future. *Immunity* 39: 1003-18

Gaskin DJ, Richard P. 2012. The economic costs of pain in the United States. *The journal of pain : official journal of the American Pain Society* 13: 715-24

Ginhoux F, Greter M, Leboeuf M, Nandi S, See P, et al. 2010. Fate mapping analysis reveals that adult microglia derive from primitive macrophages. *Science* 330: 841-5

Gold MS. 1999. Tetrodotoxin-resistant Na+ currents and inflammatory hyperalgesia. *Proc.Natl.Acad.Sci.U.S.A* 96: 7645-49

Gold MS, Shuster MJ, Levine JD. 1996. Characterization of six voltage-gated K+ currents in adult rat sensory neurons. *J.Neurophysiol* 75: 2629-46

Golden JP, Hoshi M, Nassar MA, Enomoto H, Wood JN, et al. 2010. RET signaling is required for survival and normal function of nonpeptidergic nociceptors. *The Journal of neuroscience : the official journal of the Society for Neuroscience* 30: 3983-94

Gould HJ, 3rd, Diamond I. 2016. Ranolazine: A potential treatment for refractory neuropathic pain. *Journal of the neurological sciences* 369: 310-11

Gould HJ, 3rd, Garrett C, Donahue RR, Paul D, Diamond I, Taylor BK. 2009. Ranolazine attenuates behavioral signs of neuropathic pain. *Behavioural pharmacology* 20: 755-8

Grace PM, Hutchinson MR, Maier SF, Watkins LR. 2014. Pathological pain and the neuroimmune interface. *Nat Rev Immunol.* 14: 217-31

Grace PM, Strand KA, Galer EL, Urban DJ, Wang X, et al. 2016. Morphine paradoxically prolongs neuropathic pain in rats by amplifying spinal NLRP3 inflammasome activation. *Proceedings of the National Academy of Sciences of the United States of America* 113: E3441-50

Grace PM, Wang X, Strand KA, Baratta MV, Zhang Y, et al. 2018. DREADDed microglia in pain: Implications for spinal inflammatory signaling in male rats. *Experimental neurology* 304: 125-31

Guan Z, Kuhn JA, Wang X, Colquitt B, Solorzano C, et al. 2016. Injured sensory neuron-derived CSF1 induces microglial proliferation and DAP12-dependent pain. *Nature neuroscience* 19: 94-101

Gushchina S, Pryce G, Yip PK, Wu D, Pallier P, et al. 2018. Increased expression of colony-stimulating factor-1 in mouse spinal cord with experimental autoimmune

encephalomyelitis correlates with microglial activation and neuronal loss. *Glia* 66: 2108-25

Gustafson-Vickers SL, Lu VB, Lai AY, Todd KG, Ballanyi K, Smith PA. 2008. Long-term actions of interleukin-1beta on delay and tonic firing neurons in rat superficial dorsal horn and their relevance to central sensitization. *Molecular pain* 4: 63

Hadden JW, Hadden EM, Middleton E, Jr. 1970. Lymphocyte blast transformation. I. Demonstration of adrenergic receptors in human peripheral lymphocytes. *Cellular immunology* 1: 583-95

Han HC, Lee DH, Chung JM. 2000. Characteristics of ectopic discharges in a rat neuropathic pain model. *Pain* 84: 253-61

Hanani M. 2005. Satellite glial cells in sensory ganglia: from form to function. *Brain research. Brain research reviews* 48: 457-76

Hanani M. 2013. Satellite Glial Cells and Chronic Pain In *Encyclopedia of Pain*, ed. GF Gebhart, RF Schmidt, pp. 3436-43. Berlin, Heidelberg: Springer Berlin Heidelberg

Haroutounian S, Nikolajsen L, Bendtsen TF, Finnerup NB, Kristensen AD, et al. 2014. Primary afferent input critical for maintaining spontaneous pain in peripheral neuropathy. *Pain* 155: 1272-9

Harper AA, Lawson SN. 1985. Conduction velocity is related to morphological cell type in rat dorsal root ganglion neurones. *The Journal of physiology* 359: 31-46

Hashizume H, DeLeo JA, Colburn RW, Weinstein JN. 2000. Spinal glial activation and cytokine expression after lumbar root injury in the rat. *Spine* 25: 1206-17

Hendrich J, Alvarez P, Chen X, Levine JD. 2012. GDNF induces mechanical hyperalgesia in muscle by reducing I(BK) in isolectin B4-positive nociceptors. *Neuroscience* 219: 204-13

Hildebrand ME, Xu J, Dedek A, Li Y, Sengar AS, et al. 2016. Potentiation of Synaptic GluN2B NMDAR Currents by Fyn Kinase Is Gated through BDNF-Mediated Disinhibition in Spinal Pain Processing. *Cell reports* 17: 2753-65

Hu X, Huang F, Wang ZJ. 2018. CaMKIIalpha Mediates the Effect of IL-17 To Promote Ongoing Spontaneous and Evoked Pain in Multiple Sclerosis. *The Journal of neuroscience : the official journal of the Society for Neuroscience* 38: 232-44

Huang G, Xiao P, Hung YS, Iannetti GD, Zhang ZG, Hu L. 2013. A novel approach to predict subjective pain perception from single-trial laser-evoked potentials. *NeuroImage* 81: 283-93

Huang Y, Zang Y, Zhou L, Gui W, Liu X, Zhong Y. 2014. The role of TNF-alpha/NF-kappa B pathway on the up-regulation of voltage-gated sodium channel Nav1.7 in DRG neurons of rats with diabetic neuropathy. *Neurochemistry international* 75: 112-9

Hudmon A, Choi JS, Tyrrell L, Black JA, Rush AM, et al. 2008. Phosphorylation of sodium channel Na(v)1.8 by p38 mitogen-activated protein kinase increases current density in dorsal root ganglion neurons. *The Journal of neuroscience : the official journal of the Society for Neuroscience* 28: 3190-201

Hunt D, Raivich G, Anderson PN. 2012. Activating transcription factor 3 and the nervous system. *Frontiers in molecular neuroscience* 5: 7

Iadarola JM, Caudle RM. 1997. Good pain, bad pain. *Science* 278: 239-40

Iannitti T, Kerr BJ, Taylor BK. 2014. Mechanisms and pharmacology of neuropathic pain in multiple sclerosis. *Current topics in behavioral neurosciences* 20: 75-97

Igwe OJ, Murray JN, Moolwaney AS. 2001. Interleukin 1-induced cyclooxygenase and nitric oxide synthase gene expression in the rat dorsal root ganglia is modulated by antioxidants. *Neuroscience* 105: 971-85

Imai Y, Kohsaka S. 2002. Intracellular signaling in M-CSF-induced microglia activation: role of Iba1. *Glia* 40: 164-74

Jagodic MM, Pathirathna S, Nelson MT, Mancuso S, Joksovic PM, et al. 2007. Cell-specific alterations of T-type calcium current in painful diabetic neuropathy enhance excitability of sensory neurons. *The Journal of neuroscience : the official journal of the Society for Neuroscience* 27: 3305-16

Jarvis MF, Honore P, Shieh CC, Chapman M, Joshi S, et al. 2007. A-803467, a potent and selective Nav1.8 sodium channel blocker, attenuates neuropathic and inflammatory pain in the rat. *Proc.Natl.Acad.Sci.U.S.A* 104: 8520-25

Jensen TS, Baron R, Haanpaa M, Kalso E, Loeser JD, et al. 2011. A new definition of neuropathic pain. *Pain* 152: 2204-5

Ji RR, Samad TA, Jin SX, Schmoll R, Woolf CJ. 2002. p38 MAPK activation by NGF in primary sensory neurons after inflammation increases TRPV1 levels and maintains heat hyperalgesia. *Neuron* 36: 57-68

Ji RR, Xu ZZ, Wang X, Lo EH. 2009. Matrix metalloprotease regulation of neuropathic pain. *Trends in pharmacological sciences* 30: 336-40

Jin X, Gereau RWt. 2006. Acute p38-mediated modulation of tetrodotoxin-resistant sodium channels in mouse sensory neurons by tumor necrosis factor-alpha. *The Journal of neuroscience : the official journal of the Society for Neuroscience* 26: 246-55

Jo EK, Kim JK, Shin DM, Sasakawa C. 2016. Molecular mechanisms regulating NLRP3 inflammasome activation. *Cellular & molecular immunology* 13: 148-59

Joseph EK, Levine JD. 2010. Hyperalgesic priming is restricted to isolectin B4-positive nociceptors. *Neuroscience* 169: 431-35

Kajander KC, Bennett GJ. 1992. Onset of a painful peripheral neuropathy in rat: a partial and differential deafferentation and spontaneous discharge in A beta and A delta primary afferent neurons. *J Neurophysiol* 68: 734-44

Kalyvas A, David S. 2004. Cytosolic phospholipase A2 plays a key role in the pathogenesis of multiple sclerosis-like disease. *Neuron* 41: 323-35

Katz B, Miledi R. 1967. Ionic requirements of synaptic transmitter release. *Nature* 215: 651

Kawasaki Y, Xu ZZ, Wang X, Park JY, Zhuang ZY, et al. 2008a. Distinct roles of matrix metalloproteases in the early- and late-phase development of neuropathic pain. *Nature medicine* 14: 331-6

Kawasaki Y, Zhang L, Cheng JK, Ji RR. 2008b. Cytokine mechanisms of central sensitization: distinct and overlapping role of interleukin-1beta, interleukin-6, and tumor necrosis factor-alpha in regulating synaptic and neuronal activity in the superficial spinal cord. *The Journal of neuroscience : the official journal of the Society for Neuroscience* 28: 5189-94

Kerr BJ, Bradbury EJ, Bennett DL, Trivedi PM, Dassan P, et al. 1999. Brain-derived neurotrophic factor modulates nociceptive sensory inputs and NMDA-evoked responses in the rat spinal cord. *The Journal of neuroscience : the official journal of the Society for Neuroscience* 19: 5138-48

Khan N, Smith MT. 2014. Multiple sclerosis-induced neuropathic pain: pharmacological management and pathophysiological insights from rodent EAE models. *Inflammopharmacology* 22: 1-22

Kiguchi N, Kobayashi D, Saika F, Matsuzaki S, Kishioka S. 2017. Pharmacological Regulation of Neuropathic Pain Driven by Inflammatory Macrophages. *International journal of molecular sciences* 18

Kiguchi N, Kobayashi D, Saika F, Matsuzaki S, Kishioka S. 2018. Inhibition of peripheral macrophages by nicotinic acetylcholine receptor agonists suppresses spinal microglial activation and neuropathic pain in mice with peripheral nerve injury. *Journal of neuroinflammation* 15: 96

Kiguchi N, Maeda T, Kobayashi Y, Fukazawa Y, Kishioka S. 2010. Macrophage inflammatory protein-1alpha mediates the development of neuropathic pain following peripheral nerve injury through interleukin-1beta up-regulation. *Pain* 149: 305-15

Kim KJ, Yoon YW, Chung JM. 1997. Comparison of three rodent neuropathic pain models. *Experimental brain research* 113: 200-6

Kim SH, Chung JM. 1992. An experimental model for peripheral neuropathy produced by segmental spinal nerve ligation in the rat. *Pain* 50: 355-63

Kim YI, Na HS, Kim SH, Han HC, Yoon YW, et al. 1998. Cell type-specific changes of the membrane properties of peripherally-axotomized dorsal root ganglion neurons in a rat model of neuropathic pain. *Neuroscience* 86: 301-9

Kirschner DA, Ganser AL. 1980. Compact myelin exists in the absence of basic protein in the shiverer mutant mouse. *Nature* 283: 207-10

Klein SL, Flanagan KL. 2016. Sex differences in immune responses. *Nature reviews. Immunology* 16: 626-38

Komiyama Y, Nakae S, Matsuki T, Nambu A, Ishigame H, et al. 2006. IL-17 plays an important role in the development of experimental autoimmune encephalomyelitis. *J Immunol* 177: 566-73

Koplovitch P, Devor M. 2018. Dilute lidocaine suppresses ectopic neuropathic discharge in dorsal root ganglia without blocking axonal propagation: a new approach to selective pain control. *Pain* 159: 1244-56

Krishnan A, Bhavanam S, Zochodne D. 2018. An Intimate Role for Adult Dorsal Root Ganglia Resident Cycling Cells in the Generation of Local Macrophages and Satellite Glial Cells. *Journal of neuropathology and experimental neurology* 77: 929-41

La JH, Feng B, Kaji K, Schwartz ES, Gebhart GF. 2016. Roles of isolectin B4-binding afferents in colorectal mechanical nociception. *Pain* 157: 348-54

Laedermann CJ, Abriel H, Decosterd I. 2015. Post-translational modifications of voltage-gated sodium channels in chronic pain syndromes. *Front Pharmacol* 6: 263

Lai J, Gold MS, Kim CS, Biana D, Ossipov MH, et al. 2002. Inhibition of neuropathic pain by decreased expression of the tetrodotoxin-resistant sodium channel, NaV1.8. *Pain* 95: 143-52

Lee S, Shi XQ, Fan A, West B, Zhang J. 2018. Targeting macrophage and microglia activation with colony stimulating factor 1 receptor inhibitor is an effective strategy to treat injury-triggered neuropathic pain. *Molecular pain* 14: 1744806918764979

Lee SE, Shen H, Taglialatela G, Chung JM, Chung K. 1998. Expression of nerve growth factor in the dorsal root ganglion after peripheral nerve injury. *Brain research* 796: 99-106

Leo M, Argalski S, Schafers M, Hagenacker T. 2015. Modulation of Voltage-Gated Sodium Channels by Activation of Tumor Necrosis Factor Receptor-1 and Receptor-2 in Small DRG Neurons of Rats. *Mediators.Inflamm.* 2015: 124942

Lewin GR, Moshourab R. 2004. Mechanosensation and pain. *Journal of neurobiology* 61: 30-44

Li CL, Li KC, Wu D, Chen Y, Luo H, et al. 2016. Somatosensory neuron types identified by high-coverage single-cell RNA-sequencing and functional heterogeneity. *Cell research* 26: 83-102

Li JY, Xie W, Strong JA, Guo QL, Zhang JM. 2011. Mechanical hypersensitivity, sympathetic sprouting, and glial activation are attenuated by local injection of corticosteroid near the lumbar ganglion in a rat model of neuropathic pain. *Regional anesthesia and pain medicine* 36: 56-62

Li L, Zhou XF. 2001. Pericellular Griffonia simplicifolia I isolectin B4-binding ring structures in the dorsal root ganglia following peripheral nerve injury in rats. *J Comp Neurol.* 439: 259-74

Li M, Shi J, Tang JR, Chen D, Ai B, et al. 2005. Effects of complete Freund's adjuvant on immunohistochemical distribution of IL-1beta and IL-1R I in neurons and glia cells of dorsal root ganglion. *Acta pharmacologica Sinica* 26: 192-8

Li Y, Ji A, Weihe E, Schafer MK. 2004. Cell-specific expression and lipopolysaccharide-induced regulation of tumor necrosis factor alpha (TNFalpha) and TNF receptors in rat dorsal root ganglion. *The Journal of neuroscience : the official journal of the Society for Neuroscience* 24: 9623-31

Liljencrantz J, Olausson H. 2014. Tactile C fibers and their contributions to pleasant sensations and to tactile allodynia. *Frontiers in behavioral neuroscience* 8: 37

Lim H, Lee H, Noh K, Lee SJ. 2017. IKK/NF-kappaB-dependent satellite glia activation induces spinal cord microglia activation and neuropathic pain after nerve injury. *Pain* 158: 1666-77

Lippoldt EK, Ongun S, Kusaka GK, McKemy DD. 2016. Inflammatory and neuropathic cold allodynia are selectively mediated by the neurotrophic factor receptor GFRalpha3. *Proceedings of the National Academy of Sciences of the United States of America* 113: 4506-11

Liu CN, Wall PD, Ben-Dor E, Michaelis M, Amir R, Devor M. 2000a. Tactile allodynia in the absence of C-fiber activation: altered firing properties of DRG neurons following spinal nerve injury. *Pain* 85: 503-21

Liu FY, Sun YN, Wang FT, Li Q, Su L, et al. 2012. Activation of satellite glial cells in lumbar dorsal root ganglia contributes to neuropathic pain after spinal nerve ligation. *Brain research* 1427: 65-77

Liu L, Yang TM, Liedtke W, Simon SA. 2006. Chronic IL-1beta Signaling Potentiates Voltage-Dependent Sodium Currents in Trigeminal Nociceptive Neurons. *Journal of Neurophysiology* 95: 1478-90

Liu T, Jiang CY, Fujita T, Luo SW, Kumamoto E. 2013. Enhancement by interleukin-1beta of AMPA and NMDA receptor-mediated currents in adult rat spinal superficial dorsal horn neurons. *Molecular pain* 9: 16

Liu T, van Rooijen N, Tracey DJ. 2000b. Depletion of macrophages reduces axonal degeneration and hyperalgesia following nerve injury. *Pain* 86: 25-32

Llinas R, Sugimori M, Simon SM. 1982. Transmission by presynaptic spike-like depolarization in the squid giant synapse. *Proceedings of the National Academy of Sciences of the United States of America* 79: 2415-9

Lopes DM, Malek N, Edye M, Jager SB, McMurray S, et al. 2017. Sex differences in peripheral not central immune responses to pain-inducing injury. *Scientific reports* 7: 16460

Lu J, Kurejova M, Wirotanseng LN, Linker RA, Kuner R, Tappe-Theodor A. 2012. Pain in experimental autoimmune encephalitis: a comparative study between different mouse models. *Journal of neuroinflammation* 9: 233

Lu KT, Wang YW, Wo YY, Yang YL. 2005. Extracellular signal-regulated kinase-mediated IL-1-induced cortical neuron damage during traumatic brain injury. *Neurosci Lett.* 386: 40-45

Lu Y, Perl ER. 2007. Selective action of noradrenaline and serotonin on neurones of the spinal superficial dorsal horn in the rat. *The Journal of physiology* 582: 127-36

Luo ZD, Calcutt NA, Higuera ES, Valder CR, Song YH, et al. 2002. Injury type-specific calcium channel alpha 2 delta-1 subunit up-regulation in rat neuropathic pain models correlates with antiallodynic effects of gabapentin. *The Journal of pharmacology and experimental therapeutics* 303: 1199-205

Ma C, Greenquist KW, Lamotte RH. 2006. Inflammatory mediators enhance the excitability of chronically compressed dorsal root ganglion neurons. *J Neurophysiol* 95: 2098-107

Ma C, Shu Y, Zheng Z, Chen Y, Yao H, et al. 2003. Similar electrophysiological changes in axotomized and neighboring intact dorsal root ganglion neurons. *J Neurophysiol* 89: 1588-602

Ma W, Chabot JG, Vercauteren F, Quirion R. 2010. Injured nerve-derived COX2/PGE2 contributes to the maintenance of neuropathic pain in aged rats. *Neurobiology of aging* 31: 1227-37

MacGillivray MK, Cruz TF, McCulloch CA. 2000. The recruitment of the interleukin-1 (IL-1) receptor-associated kinase (IRAK) into focal adhesion complexes is required for IL-1beta -induced ERK activation. *J Biol.Chem.* 275: 23509-15

Mandolesi G, Gentile A, Musella A, Fresegna D, De Vito F, et al. 2015. Synaptopathy connects inflammation and neurodegeneration in multiple sclerosis. *Nature reviews. Neurology* 11: 711-24

Mapplebeck JC, Beggs S, Salter MW. 2017. Molecules in pain and sex: a developing story. *Molecular brain* 10: 9

Mapplebeck JCS, Dalgarno R, Tu Y, Moriarty O, Beggs S, et al. 2018. Microglial P2X4R-evoked pain hypersensitivity is sexually dimorphic in rats. *Pain* 159: 1752-63

Matsuyoshi H, Masuda N, Chancellor MB, Erickson VL, Hirao Y, et al. 2006. Expression of hyperpolarization-activated cyclic nucleotide-gated cation channels in rat dorsal root ganglion neurons innervating urinary bladder. *Brain research* 1119: 115-23

Matzner O, Devor M. 1994. Hyperexcitability at sites of nerve injury depends on voltage-sensitive Na+ channels. *J Neurophysiol* 72: 349-59

McGivern JG. 2007. Ziconotide: a review of its pharmacology and use in the treatment of pain. *Neuropsychiatric disease and treatment* 3: 69-85

Melanson M, Miao P, Eisenstat D, Gong Y, Gu X, et al. 2009. Experimental autoimmune encephalomyelitis-induced upregulation of tumor necrosis factor-alpha in the dorsal root ganglia. *Mult Scler* 15: 1135-45

Mifflin KA, Yousuf MS, Thorburn KC, Huang J, Perez-Munoz ME, et al. 2018. Voluntary wheel running reveals sex-specific nociceptive factors in murine experimental autoimmune encephalomyelitis. *Pain*

Miller LG, Galpern WR, Dunlap K, Dinarello CA, Turner TJ. 1991. Interleukin-1 augments gamma-aminobutyric acidA receptor function in brain. *Molecular pharmacology* 39: 105-8

Mogil JS. 2012. Sex differences in pain and pain inhibition: multiple explanations of a controversial phenomenon. *Nat Rev Neurosci* 13: 859-66

Molliver DC, Radeke MJ, Feinstein SC, Snider WD. 1995. Presence or absence of TrkA protein distinguishes subsets of small sensory neurons with unique cytochemical characteristics and dorsal horn projections. *J Comp Neurol.* 361: 404-16

Molliver DC, Wright DE, Leitner ML, Parsadanian AS, Doster K, et al. 1997. IB4-binding DRG neurons switch from NGF to GDNF dependence in early postnatal life. *Neuron* 19: 849-61

Moore A, Derry S, Eccleston C, Kalso E. 2013. Expect analgesic failure; pursue analgesic success. *BMJ* 346: f2690

Mosconi T, Kruger L. 1996. Fixed-diameter polyethylene cuffs applied to the rat sciatic nerve induce a painful neuropathy: ultrastructural morphometric analysis of axonal alterations. *Pain* 64: 37-57

Moulin DE, Clark AJ, Gilron I, Ware MA, Watson CP, et al. 2007. Pharmacological management of chronic neuropathic pain - consensus statement and guidelines from the Canadian Pain Society. *Pain research & management : the journal of the Canadian Pain Society = journal de la societe canadienne pour le traitement de la douleur* 12: 13-21

Murray PJ. 2017. Macrophage Polarization. *Annual review of physiology* 79: 541-66

Na HS, Ko KH, Back SK, Sung B, Yoo DJ, Hong SK. 2000. Role of signals from the dorsal root ganglion in neuropathic pain in a rat model. *Neurosci Lett* 288: 147-50

Nadeau S, Filali M, Zhang J, Kerr BJ, Rivest S, et al. 2011. Functional recovery after peripheral nerve injury is dependent on the pro-inflammatory cytokines IL-1beta and TNF: implications for neuropathic pain. *The Journal of Neuroscience* 31: 12533-42

Nagy JI, Hunt SP. 1982. Fluoride-resistant acid phosphatase-containing neurones in dorsal root ganglia are separate from those containing substance P or somatostatin. *Neuroscience* 7: 89-97

Nascimento DS, Castro-Lopes JM, Moreira Neto FL. 2014. Satellite glial cells surrounding primary afferent neurons are activated and proliferate during monoarthritis in rats: is there a role for ATF3? *PloS one* 9: e108152

Nho B, Lee J, Ko KR, Lee SJ, Kim S. 2018. Effective control of neuropathic pain by transient expression of hepatocyte growth factor in a mouse chronic constriction injury model. *FASEB journal : official publication of the Federation of American Societies for Experimental Biology* 32: 5119-31

Noh S, Kumar N, Bukhanova N, Chen Y, Stemkowsi PL, Smith PA. 2014. The heart-rate-reducing agent, ivabradine, reduces mechanical allodynia in a rodent model of neuropathic pain. *Eur J Pain* 18: 1139-47

Nowak L, Bregestovski P, Ascher P, Herbet A, Prochiantz A. 1984. Magnesium gates glutamate-activated channels in mouse central neurones. *Nature* 307: 462-5

Nurmikko TJ, Gupta S, Maclver K. 2010. Multiple sclerosis-related central pain disorders. *Current pain and headache reports* 14: 189-95

Nystrom B, Hagbarth KE. 1981. Microelectrode recordings from transected nerves in amputees with phantom limb pain. *Neurosci Lett* 27: 211-6

O'Connor AB, Schwid SR, Herrmann DN, Markman JD, Dworkin RH. 2008. Pain associated with multiple sclerosis: systematic review and proposed classification. *Pain* 137: 96-111

Obata K, Noguchi K. 2006. BDNF in sensory neurons and chronic pain. *Neuroscience research* 55: 1-10

Obata K, Yamanaka H, Fukuoka T, Yi D, Tokunaga A, et al. 2003. Contribution of injured and uninjured dorsal root ganglion neurons to pain behavior and the changes in gene expression following chronic constriction injury of the sciatic nerve in rats. *Pain* 101: 65-77

Obreja O, Rathee PK, Lips KS, Distler C, Kress M. 2002. IL-1 beta potentiates heat-activated currents in rat sensory neurons: involvement of IL-1RI, tyrosine kinase, and protein kinase C. *FASEB journal : official publication of the Federation of American Societies for Experimental Biology* 16: 1497-503

Ocana M, Cendan CM, Cobos EJ, Entrena JM, Baeyens JM. 2004. Potassium channels and pain: present realities and future opportunities. *European journal of pharmacology* 500: 203-19

Oestreicher AB, De Graan PN, Gispen WH, Verhaagen J, Schrama LH. 1997. B-50, the growth associated protein-43: modulation of cell morphology and communication in the nervous system. *Progress in neurobiology* 53: 627-86

Ohara PT, Vit JP, Bhargava A, Romero M, Sundberg C, et al. 2009. Gliopathic pain: when satellite glial cells go bad. *The Neuroscientist : a review journal bringing neurobiology, neurology and psychiatry* 15: 450-63

Ohsawa K, Imai Y, Sasaki Y, Kohsaka S. 2004. Microglia/macrophage-specific protein Iba1 binds to fimbrin and enhances its actin-bundling activity. *Journal of neurochemistry* 88: 844-56

Okubo M, Yamanaka H, Kobayashi K, Dai Y, Kanda H, et al. 2016. Macrophage-Colony Stimulating Factor Derived from Injured Primary Afferent Induces Proliferation of Spinal Microglia and Neuropathic Pain in Rats. *PloS one* 11: e0153375

Olechowski CJ, Truong JJ, Kerr BJ. 2009. Neuropathic pain behaviours in a chronic-relapsing model of experimental autoimmune encephalomyelitis (EAE). *Pain* 141: 156-64

Oosterhof N, Kuil LE, van der Linde HC, Burm SM, Berdowski W, et al. 2018. Colony-Stimulating Factor 1 Receptor (CSF1R) Regulates Microglia Density and Distribution, but Not Microglia Differentiation In Vivo. *Cell reports* 24: 1203-17 e6

Otoshi K, Kikuchi S, Konno S, Sekiguchi M. 2010. The reactions of glial cells and endoneurial macrophages in the dorsal root ganglion and their contribution to pain-related behavior after application of nucleus pulposus onto the nerve root in rats. *Spine* 35: 264-71

Ozaktay AC, Cavanaugh JM, Asik I, DeLeo JA, Weinstein JN. 2002. Dorsal root sensitivity to interleukin-1 beta, interleukin-6 and tumor necrosis factor in rats. *European spine journal : official publication of the European Spine Society, the European Spinal Deformity Society, and the European Section of the Cervical Spine Research Society* 11: 467-75

Patzig J, Jahn O, Tenzer S, Wichert SP, de Monasterio-Schrader P, et al. 2011. Quantitative and integrative proteome analysis of peripheral nerve myelin identifies novel myelin proteins and candidate neuropathy loci. *The Journal of neuroscience : the official journal of the Society for Neuroscience* 31: 16369-86

Peirs C, Seal RP. 2016. Neural circuits for pain: Recent advances and current views. *Science* 354: 578-84

Pender MP. 1986. Ascending impairment of nociception in rats with experimental allergic encephalomyelitis. *Journal of the neurological sciences* 75: 317-28

Perez-Garcia MJ, Cena V, de Pablo Y, Llovera M, Comella JX, Soler RM. 2004. Glial cell line-derived neurotrophic factor increases intracellular calcium concentration. Role of calcium/calmodulin in the activation of the phosphatidylinositol 3-kinase pathway. *The Journal of biological chemistry* 279: 6132-42

Pertin M, Gosselin RD, Decosterd I. 2012. The spared nerve injury model of neuropathic pain. *Methods Mol Biol* 851: 205-12

Pinho-Ribeiro FA, Verri WA, Jr., Chiu IM. 2017. Nociceptor Sensory Neuron-Immune Interactions in Pain and Inflammation. *Trends in immunology* 38: 5-19

Pitcher GM, Henry JL. 2008. Governing role of primary afferent drive in increased excitation of spinal nociceptive neurons in a model of sciatic neuropathy. *Exp.Neurol.* 214: 219-28

Plata-Salaman CR, Ffrench-Mullen JM. 1992. Interleukin-1 beta depresses calcium currents in CA1 hippocampal neurons at pathophysiological concentrations. *Brain research bulletin* 29: 221-3

Postea O, Biel M. 2011. Exploring HCN channels as novel drug targets. *Nature reviews. Drug discovery* 10: 903-14

Preibisch S, Saalfeld S, Tomancak P. 2009. Globally optimal stitching of tiled 3D microscopic image acquisitions. *Bioinformatics* 25: 1463-5

Priest BT, Murphy BA, Lindia JA, Diaz C, Abbadie C, et al. 2005. Contribution of the tetrodotoxin-resistant voltage-gated sodium channel NaV1.9 to sensory transmission and nociceptive behavior. *Proceedings of the National Academy of Sciences of the United States of America* 102: 9382-7

Rahn EJ, Iannitti T, Donahue RR, Taylor BK. 2014. Sex differences in a mouse model of multiple sclerosis: neuropathic pain behavior in females but not males and protection from neurological deficits during proestrus. *Biology of sex differences* 5: 4

Rasband MN, Park EW, Vanderah TW, Lai J, Porreca F, Trimmer JS. 2001. Distinct potassium channels on pain-sensing neurons. *Proceedings of the National Academy of Sciences of the United States of America* 98: 13373-8

Reichling DB, Levine JD. 2009. Critical role of nociceptor plasticity in chronic pain. *Trends Neurosci* 32: 611-18

Ren K, Torres R. 2009. Role of interleukin-1beta during pain and inflammation. *Brain Res Rev* 60: 57-64

Renganathan M, Cummins TR, Waxman SG. 2001. Contribution of Na(v)1.8 sodium channels to action potential electrogenesis in DRG neurons. *J Neurophysiol* 86: 629-40

Rexed B. 1952. The cytoarchitectonic organization of the spinal cord in the cat. *The Journal of comparative neurology* 96: 414-95

Richter F, Natura G, Ebbinghaus M, von Banchet GS, Hensellek S, et al. 2012. Interleukin-17 sensitizes joint nociceptors to mechanical stimuli and contributes to arthritic pain through neuronal interleukin-17 receptors in rodents. *Arthritis and rheumatism* 64: 4125-34

Robinson DR, McNaughton PA, Evans ML, Hicks GA. 2004. Characterization of the primary spinal afferent innervation of the mouse colon using retrograde labelling. *Neurogastroenterol.Motil.* 16: 113-24

Rodrigues DH, Leles BP, Costa VV, Miranda AS, Cisalpino D, et al. 2016. IL-1beta Is Involved with the Generation of Pain in Experimental Autoimmune Encephalomyelitis. *Molecular neurobiology* 53: 6540-47

Ruscheweyh R, Forsthuber L, Schoffnegger D, Sandkuhler J. 2007. Modification of classical neurochemical markers in identified primary afferent neurons with Abeta-, Adelta-, and C-fibers after chronic constriction injury in mice. *The Journal of comparative neurology* 502: 325-36

Salomons TV, Iannetti GD, Liang M, Wood JN. 2016. The "Pain Matrix" in Pain-Free Individuals. *JAMA neurology* 73: 755-6

Samad TA, Moore KA, Sapirstein A, Billet S, Allchorne A, et al. 2001a. Interleukin-1beta-mediated induction of Cox-2 in the CNS contributes to inflammatory pain hypersensitivity. *Nature* 410: 471-75

Samad TA, Moore KA, Sapirstein A, Billet S, Allchorne A, et al. 2001b. Interleukin-1beta-mediated induction of Cox-2 in the CNS contributes to inflammatory pain hypersensitivity. *Nature* 410: 471-5

Santa-Cecilia FV, Ferreira DW, Guimaraes RM, Cecilio NT, Fonseca MM, et al. 2019. The NOD2 signaling in peripheral macrophages contributes to neuropathic pain development. *Pain* 160: 102-16

Sarantopoulos CD, McCallum JB, Rigaud M, Fuchs A, Kwok WM, Hogan QH. 2007. Opposing effects of spinal nerve ligation on calcium-activated potassium currents in axotomized and adjacent mammalian primary afferent neurons. *Brain research* 1132: 84-99

Schafers M, Brinkhoff J, Neukirchen S, Marziniak M, Sommer C. 2001. Combined epineurial therapy with neutralizing antibodies to tumor necrosis factor-alpha and interleukin-1 receptor has an additive effect in reducing neuropathic pain in mice. *Neurosci Lett* 310: 113-6

Schafers M, Lee DH, Brors D, Yaksh TL, Sorkin LS. 2003. Increased sensitivity of injured and adjacent uninjured rat primary sensory neurons to exogenous tumor necrosis factor-alpha after spinal nerve ligation. *The Journal of neuroscience : the official journal of the Society for Neuroscience* 23: 3028-38

Scheff NN, Gold MS. 2011. Sex differences in the inflammatory mediator-induced sensitization of dural afferents. *J Neurophysiol* 106: 1662-8

Schettini G, Meucci O, Florio T, Scala G, Landolfi E, Grimaldi M. 1988. Effect of interleukin 1 beta on transducing mechanisms in 235-1 clonal pituitary cells. Part II: Modulation of calcium fluxes. *Biochemical and biophysical research communications* 155: 1097-104

Scholz J, Woolf CJ. 2007a. The neuropathic pain triad: neurons, immune cells and glia. *Nature neuroscience* 10: 1361-8

Scholz J, Woolf CJ. 2007b. The neuropathic pain triad: neurons, immune cells and glia. *Nature neuroscience* 10: 1361-68

Schuh CD, Pierre S, Weigert A, Weichand B, Altenrath K, et al. 2014. Prostacyclin mediates neuropathic pain through interleukin 1beta-expressing resident macrophages. *Pain* 155: 545-55

Segond von Banchet G, Boettger MK, Konig C, Iwakura Y, Brauer R, Schaible HG. 2013. Neuronal IL-17 receptor upregulates TRPV4 but not TRPV1 receptors in DRG neurons and mediates mechanical but not thermal hyperalgesia. *Molecular and cellular neurosciences* 52: 152-60

Seijffers R, Mills CD, Woolf CJ. 2007. ATF3 increases the intrinsic growth state of DRG neurons to enhance peripheral nerve regeneration. *The Journal of neuroscience : the official journal of the Society for Neuroscience* 27: 7911-20

Seltzer Z, Dubner R, Shir Y. 1990. A novel behavioral model of neuropathic pain disorders produced in rats by partial sciatic nerve injury. *Pain* 43: 205-18

Shen KF, Zhu HQ, Wei XH, Wang J, Li YY, et al. 2013. Interleukin-10 down-regulates voltage gated sodium channels in rat dorsal root ganglion neurons. *Exp.Neurol.* 247: 466-75

Shubayev VI, Myers RR. 2001. Axonal transport of TNF-alpha in painful neuropathy: distribution of ligand tracer and TNF receptors. *Journal of neuroimmunology* 114: 48-56

Sikandar S, Minett MS, Millet Q, Santana-Varela S, Lau J, et al. 2018. Brain-derived neurotrophic factor derived from sensory neurons plays a critical role in chronic pain. *Brain : a journal of neurology* 141: 1028-39

Silva JR, Lopes AH, Talbot J, Cecilio NT, Rossato MF, et al. 2017. Neuroimmune-Glia Interactions in the Sensory Ganglia Account for the Development of Acute Herpetic Neuralgia. *The Journal of neuroscience : the official journal of the Society for Neuroscience* 37: 6408-22

Silverman JD, Kruger L. 1990. Selective neuronal glycoconjugate expression in sensory and autonomic ganglia: relation of lectin reactivity to peptide and enzyme markers. *Journal of neurocytology* 19: 789-801

Sivilotti L, Woolf CJ. 1994. The contribution of GABAA and glycine receptors to central sensitization: disinhibition and touch-evoked allodynia in the spinal cord. *J Neurophysiol* 72: 169-79

Sommer C, Petrausch S, Lindenlaub T, Toyka KV. 1999. Neutralizing antibodies to interleukin 1-receptor reduce pain associated behavior in mice with experimental neuropathy. *Neurosci Lett.* 270: 25-28

Sorge RE, Mapplebeck JC, Rosen S, Beggs S, Taves S, et al. 2015. Different immune cells mediate mechanical pain hypersensitivity in male and female mice. *Nature neuroscience* 18: 1081-3

Sotelo J. 2015. The nervous and the immune systems: conspicuous physiological analogies. *Journal of comparative physiology. A, Neuroethology, sensory, neural, and behavioral physiology* 201: 185-94

Stanley ER, Chen DM, Lin HS. 1978. Induction of macrophage production and proliferation by a purified colony stimulating factor. *Nature* 274: 168-70

Stemkowski PL. 2011. *The effect of long-term interleukin-1 beta exposure on sensory neuron electrical membrane properties implications for neuropathic pain*. PhD thesis. University of Alberta. 324 pp.

Stemkowski PL, Garcia-Caballero A, Gadotti VM, M'Dahoma S, Chen L, et al. 2017. Identification of interleukin-1 beta as a key mediator in the upregulation of Cav3.2-USP5 interactions in the pain pathway. *Molecular pain* 13: 1744806917724698

Stemkowski PL, Noh MC, Chen Y, Smith PA. 2015. Increased excitability of medium-sized dorsal root ganglion neurons by prolonged interleukin-1beta exposure is K(+) channel dependent and reversible. *The Journal of physiology* 593: 3739-55

Stemkowski PL, Smith PA. 2012a. Long-term IL-1beta exposure causes subpopulation-dependent alterations in rat dorsal root ganglion neuron excitability. *Journal of Neurophysiology* 107: 1586-97

Stemkowski PL, Smith PA. 2012b. Sensory neurons, ion channels, inflammation and the onset of neuropathic pain. *Can.J.Neurol.Sci.* 39: 416-35

Storch MK, Stefferl A, Brehm U, Weissert R, Wallstrom E, et al. 1998. Autoimmunity to myelin oligodendrocyte glycoprotein in rats mimics the spectrum of multiple sclerosis pathology. *Brain Pathol* 8: 681-94

Stucky CL, Lewin GR. 1999. Isolectin B(4)-positive and -negative nociceptors are functionally distinct. *The Journal of neuroscience : the official journal of the Society for Neuroscience* 19: 6497-505

Study RE, Kral MG. 1996. Spontaneous action potential activity in isolated dorsal root ganglion neurons from rats with a painful neuropathy. *Pain* 65: 235-42

Sukhotinsky I, Ben-Dor E, Raber P, Devor M. 2004. Key role of the dorsal root ganglion in neuropathic tactile hypersensibility. *Eur J Pain* 8: 135-43

Sun Q, Xing GG, Tu HY, Han JS, Wan Y. 2005. Inhibition of hyperpolarization-activated current by ZD7288 suppresses ectopic discharges of injured dorsal root ganglion neurons in a rat model of neuropathic pain. *Brain research* 1032: 63-9

Sun W, Yang F, Wang Y, Fu H, Yang Y, et al. 2017. Contribution of large-sized primary sensory neuronal sensitization to mechanical allodynia by upregulation of hyperpolarization-activated cyclic nucleotide gated channels via cyclooxygenase 1 cascade. *Neuropharmacology* 113: 217-30

Suter MR, Berta T, Gao YJ, Decosterd I, Ji RR. 2009. Large A-fiber activity is required for microglial proliferation and p38 MAPK activation in the spinal cord: different effects of resiniferatoxin and bupivacaine on spinal microglial changes after spared nerve injury. *Molecular pain* 5: 53

Swartjes M, van Velzen M, Niesters M, Aarts L, Brines M, et al. 2014. ARA 290, a peptide derived from the tertiary structure of erythropoietin, produces long-term relief of neuropathic pain coupled with suppression of the spinal microglia response. *Molecular pain* 10: 13

Szkudelski T. 2001. The mechanism of alloxan and streptozotocin action in B cells of the rat pancreas. *Physiological research* 50: 537-46

Takeda M, Takahashi M, Matsumoto S. 2008. Contribution of activated interleukin receptors in trigeminal ganglion neurons to hyperalgesia via satellite glial interleukin-1beta paracrine mechanism. *Brain, behavior, and immunity* 22: 1016-23

Takeda M, Takahashi M, Matsumoto S. 2009. Contribution of the activation of satellite glia in sensory ganglia to pathological pain. *Neuroscience and biobehavioral reviews* 33: 784-92

Takeda M, Tanimoto T, Kadoi J, Nasu M, Takahashi M, et al. 2007. Enhanced excitability of nociceptive trigeminal ganglion neurons by satellite glial cytokine following peripheral inflammation. *Pain* 129: 155-66

Tamura R, Nemoto T, Maruta T, Onizuka S, Yanagita T, et al. 2014. Up-regulation of NaV1.7 sodium channels expression by tumor necrosis factor-alpha in cultured bovine adrenal chromaffin cells and rat dorsal root ganglion neurons. *Anesth.Analg.* 118: 318-24

Tang Y, Liu L, Xu D, Zhang W, Zhang Y, et al. 2018. Interaction between astrocytic colony stimulating factor and its receptor on microglia mediates central sensitization and behavioral hypersensitivity in chronic post ischemic pain model. *Brain, behavior, and immunity* 68: 248-60

Taylor AM, Osikowicz M, Ribeiro-da-Silva A. 2012. Consequences of the ablation of nonpeptidergic afferents in an animal model of trigeminal neuropathic pain. *Pain* 153: 1311-19

Thompson AJ, Baranzini SE, Geurts J, Hemmer B, Ciccarelli O. 2018. Multiple sclerosis. *Lancet* 391: 1622-36

Thorburn KC, Paylor JW, Webber CA, Winship IR, Kerr BJ. 2016. Facial hypersensitivity and trigeminal pathology in mice with experimental autoimmune encephalomyelitis. *Pain* 157: 627-42

Todd AJ. 2010. Neuronal circuitry for pain processing in the dorsal horn. *Nat Rev Neurosci* 11: 823-36

Todd AJ. 2013. Nociceptive Circuitry in the Spinal Cord In *Encyclopedia of Pain*, ed. GF Gebhart, RF Schmidt, pp. 2179-85. Berlin, Heidelberg: Springer Berlin Heidelberg

Trang T, Beggs S, Wan X, Salter MW. 2009. P2X4-receptor-mediated synthesis and release of brain-derived neurotrophic factor in microglia is dependent on calcium and p38-mitogen-activated protein kinase activation. *The Journal of neuroscience : the official journal of the Society for Neuroscience* 29: 3518-28

Tsantoulas C, McMahon SB. 2014. Opening paths to novel analgesics: the role of potassium channels in chronic pain. *Trends Neurosci* 37: 146-58

Tsuda M, Shigemoto-Mogami Y, Koizumi S, Mizokoshi A, Kohsaka S, et al. 2003. P2X4 receptors induced in spinal microglia gate tactile allodynia after nerve injury. *Nature* 424: 778-83

Ulmann L, Hatcher JP, Hughes JP, Chaumont S, Green PJ, et al. 2008. Up-regulation of P2X4 receptors in spinal microglia after peripheral nerve injury mediates BDNF release and neuropathic pain. *The Journal of neuroscience : the official journal of the Society for Neuroscience* 28: 11263-8

Usoskin D, Furlan A, Islam S, Abdo H, Lonnerberg P, et al. 2015. Unbiased classification of sensory neuron types by large-scale single-cell RNA sequencing. *Nature neuroscience* 18: 145-53

Uzawa A, Mori M, Taniguchi J, Kuwabara S. 2014. Modulation of the kallikrein/kinin system by the angiotensin-converting enzyme inhibitor alleviates experimental autoimmune encephalomyelitis. *Clinical and experimental immunology* 178: 245-52

Vacca V, Marinelli S, Pieroni L, Urbani A, Luvisetto S, Pavone F. 2014. Higher pain perception and lack of recovery from neuropathic pain in females: a behavioural, immunohistochemical, and proteomic investigation on sex-related differences in mice. *Pain* 155: 388-402

Vacca V, Marinelli S, Pieroni L, Urbani A, Luvisetto S, Pavone F. 2016. 17beta-estradiol counteracts neuropathic pain: a behavioural, immunohistochemical, and proteomic investigation on sex-related differences in mice. *Scientific reports* 6: 18980

van Hecke O, Austin SK, Khan RA, Smith BH, Torrance N. 2014. Neuropathic pain in the general population: a systematic review of epidemiological studies. *Pain* 155: 654-62

Vaso A, Adahan HM, Gjika A, Zahaj S, Zhurda T, et al. 2014. Peripheral nervous system origin of phantom limb pain. *Pain* 155: 1384-91

Vega-Avelaira D, Geranton SM, Fitzgerald M. 2009. Differential regulation of immune responses and macrophage/neuron interactions in the dorsal root ganglion in young and adult rats following nerve injury. *Molecular pain* 5: 70

Vilceanu D, Honore P, Hogan QH, Stucky CL. 2010. Spinal nerve ligation in mouse upregulates TRPV1 heat function in injured IB4-positive nociceptors. *The journal of pain : official journal of the American Pain Society* 11: 588-99

Viviani B, Bartesaghi S, Gardoni F, Vezzani A, Behrens MM, et al. 2003. Interleukin-1beta enhances NMDA receptor-mediated intracellular calcium increase through activation of the Src family of kinases. *The Journal of neuroscience : the official journal of the Society for Neuroscience* 23: 8692-700

Voscopoulos C, Lema M. 2010. When does acute pain become chronic? *British journal of anaesthesia* 105 Suppl 1: i69-85

Wager TD, Atlas LY, Lindquist MA, Roy M, Woo CW, Kross E. 2013. An fMRI-based neurologic signature of physical pain. *The New England journal of medicine* 368: 1388-97

Wall PD, Devor M. 1983a. Sensory afferent impulses originate from dorsal root ganglia as well as from the periphery in normal and nerve injured rats. *Pain* 17: 321-39

Wall PD, Devor M. 1983b. Sensory afferent impulses result from dorsal root ganglia as well as from the periphery in normal and nerve-injured rats. *Pain* 17: 321-39

Wall PD, Devor M, Inbal R, Scadding JW, Schonfeld D, et al. 1979a. Autotomy following peripheral nerve lesions: experimental anaesthesia dolorosa. *Pain* 7: 103-11

Wall PD, Gutnick M. 1974a. Ongoing activity in peripheral nerves: the physiology and pharmacology of impulses originating from a neuroma. *Experimental neurology* 43: 580-93

Wall PD, Gutnick M. 1974b. Properties of afferent nerve impulses originating from a neuroma. *Nature* 248: 740-3

Wall PD, Scadding JW, Tomkiewicz MM. 1979b. The production and prevention of experimental anesthesia dolorosa. *Pain* 6: 175-82

Wang IC, Chung CY, Liao F, Chen CC, Lee CH. 2017. Peripheral sensory neuron injury contributes to neuropathic pain in experimental autoimmune encephalomyelitis. *Scientific reports* 7: 42304

Wang J, Chen G, Lu B, Wu CP. 2003. GDNF acutely potentiates Ca2+ channels and excitatory synaptic transmission in midbrain dopaminergic neurons. *Neuro-Signals* 12: 78-88

Warwick RA, Ledgerwood CJ, Brenner T, Hanani M. 2014. Satellite glial cells in dorsal root ganglia are activated in experimental autoimmune encephalomyelitis. *Neurosci Lett* 569: 59-62

Watkins LR, Maier SF. 2002. Beyond Neurons: Evidence That Immune and Glial Cells Contribute to Pathological Pain States. *Physiological Reviews* 82: 981-1011

Waxman SG, Zamponi GW. 2014. Regulating excitability of peripheral afferents: emerging ion channel targets. *Nature neuroscience* 17: 153-63

Webb SE, Pollard JW, Jones GE. 1996. Direct observation and quantification of macrophage chemoattraction to the growth factor CSF-1. *Journal of cell science* 109 (Pt 4): 793-803

Weir GA, Middleton SJ, Clark AJ, Daniel T, Khovanov N, et al. 2017. Using an engineered glutamate-gated chloride channel to silence sensory neurons and treat neuropathic pain at the source. *Brain : a journal of neurology* 140: 2570-85

Wen YR, Suter MR, Kawasaki Y, Huang J, Pertin M, et al. 2007. Nerve conduction blockade in the sciatic nerve prevents but does not reverse the activation of p38 mitogen-activated protein kinase in spinal microglia in the rat spared nerve injury model. *Anesthesiology* 107: 312-21

West SJ, Bannister K, Dickenson AH, Bennett DL. 2015. Circuitry and plasticity of the dorsal horn--toward a better understanding of neuropathic pain. *Neuroscience* 300: 254-75

Westenbroek RE, Hell JW, Warner C, Dubel SJ, Snutch TP, Catterall WA. 1992. Biochemical properties and subcellular distribution of an N-type calcium channel alpha 1 subunit. *Neuron* 9: 1099-115

White FA, Sun J, Waters SM, Ma C, Ren D, et al. 2005. Excitatory monocyte chemoattractant protein-1 signaling is up-regulated in sensory neurons after chronic compression of the dorsal root ganglion. *Proceedings of the National Academy of Sciences of the United States of America* 102: 14092-7

Wolf G, Gabay E, Tal M, Yirmiya R, Shavit Y. 2006. Genetic impairment of interleukin-1 signaling attenuates neuropathic pain, autotomy, and spontaneous ectopic neuronal activity, following nerve injury in mice. *Pain* 120: 315-24

Woolf CJ. 1983a. Evidence for a central component of post-injury pain hypersensitivity. *Nature* 306: 686-88

Woolf CJ. 1983b. Evidence for a central component of post-injury pain hypersensitivity. *Nature* 306: 686-8

Woolf CJ. 2011. Central sensitization: implications for the diagnosis and treatment of pain. *Pain* 152: S2-15

Woolf CJ, Reynolds ML, Molander C, O'Brien C, Lindsay RM, Benowitz LI. 1990. The growth-associated protein GAP-43 appears in dorsal root ganglion cells and in the dorsal horn of the rat spinal cord following peripheral nerve injury. *Neuroscience* 34: 465-78

Woolf CJ, Thompson SW. 1991. The induction and maintenance of central sensitization is dependent on N-methyl-D-aspartic acid receptor activation; implications for the treatment of post-injury pain hypersensitivity states. *Pain* 44: 293-9

Wu G, Ringkamp M, Murinson BB, Pogatzki EM, Hartke TV, et al. 2002. Degeneration of myelinated efferent fibers induces spontaneous activity in uninjured C-fiber afferents. *The Journal of neuroscience : the official journal of the Society for Neuroscience* 22: 7746-53

Xie MX, Yang J, Pang RP, Zeng WA, Ouyang HD, et al. 2018. Bulleyaconitine A attenuates hyperexcitability of dorsal root ganglion neurons induced by spared nerve injury: The role of preferably blocking Nav1.7 and Nav1.3 channels. *Molecular pain* 14: 1744806918778491

Xie W, Strong JA, Zhang JM. 2009. Early blockade of injured primary sensory afferents reduces glial cell activation in two rat neuropathic pain models. *Neuroscience* 160: 847-57

Xie W, Strong JA, Zhang JM. 2017. Active Nerve Regeneration with Failed Target Reinnervation Drives Persistent Neuropathic Pain. *eNeuro* 4

Xu ZZ, Kim YH, Bang S, Zhang Y, Berta T, et al. 2015. Inhibition of mechanical allodynia in neuropathic pain by TLR5-mediated A-fiber blockade. *Nature medicine* 21: 1326-31

Yagiz K, Rittling SR. 2009. Both cell-surface and secreted CSF-1 expressed by tumor cells metastatic to bone can contribute to osteoclast activation. *Experimental cell research* 315: 2442-52

Yaksh TL. 1989. Behavioral and autonomic correlates of the tactile evoked allodynia produced by spinal glycine inhibition: effects of modulatory receptor systems and excitatory amino acid antagonists. *Pain* 37: 111-23

Yang J, Xie MX, Hu L, Wang XF, Mai JZ, et al. 2018. Upregulation of N-type calcium channels in the soma of uninjured dorsal root ganglion neurons contributes to neuropathic pain by increasing neuronal excitability following peripheral nerve injury. *Brain, behavior, and immunity* 71: 52-65

Yao H, Donnelly DF, Ma C, LaMotte RH. 2003. Upregulation of the hyperpolarization-activated cation current after chronic compression of the dorsal root ganglion. *The Journal of neuroscience : the official journal of the Society for Neuroscience* 23: 2069-74

Yao Y, Echeverry S, Shi XQ, Yang M, Yang QZ, et al. 2016. Dynamics of spinal microglia repopulation following an acute depletion. *Scientific reports* 6: 22839

Yasaka T, Tiong SY, Hughes DI, Riddell JS, Todd AJ. 2010. Populations of inhibitory and excitatory interneurons in lamina II of the adult rat spinal dorsal horn revealed by a combined electrophysiological and anatomical approach. *Pain* 151: 475-88

Yekkirala AS, Roberson DP, Bean BP, Woolf CJ. 2017. Breaking barriers to novel analgesic drug development. *Nature reviews. Drug discovery* 16: 545-64

Yezierski RP, Hansson P. 2018. Inflammatory and Neuropathic Pain From Bench to Bedside: What Went Wrong? *The journal of pain : official journal of the American Pain Society* 19: 571-88

Young GT, Emery EC, Mooney ER, Tsantoulas C, McNaughton PA. 2014. Inflammatory and neuropathic pain are rapidly suppressed by peripheral block of hyperpolarisation-activated cyclic nucleotide-gated ion channels. *Pain* 155: 1708-19

Yousuf MS, Samtleben S, Noh MC, Thorburn KC, Catuneanu A, et al. *World Congress on Pain, Boston, 2018*: 2111. IASP

Yu L, Yang F, Luo H, Liu FY, Han JS, et al. 2008. The role of TRPV1 in different subtypes of dorsal root ganglion neurons in rat chronic inflammatory nociception induced by complete Freund's adjuvant. *Molecular pain* 4: 61

Yunoki T, Takimoto K, Kita K, Funahashi Y, Takahashi R, et al. 2014. Differential contribution of Kv4-containing channels to A-type, voltage-gated potassium currents in somatic and visceral dorsal root ganglion neurons. *Journal of Neurophysiology* 112: 2492-504

Zelenka M, Schafers M, Sommer C. 2005. Intraneural injection of interleukin-1beta and tumor necrosis factor-alpha into rat sciatic nerve at physiological doses induces signs of neuropathic pain. *Pain* 116: 257-63

Zhang RX, Li A, Liu B, Wang L, Ren K, et al. 2008. IL-1ra alleviates inflammatory hyperalgesia through preventing phosphorylation of NMDA receptor NR-1 subunit in rats. *Pain* 135: 232-9

Zhang X, Chen Y, Wang C, Huang LY. 2007. Neuronal somatic ATP release triggers neuron-satellite glial cell communication in dorsal root ganglia. *Proceedings of the National Academy of Sciences of the United States of America* 104: 9864-9

Zhang XL, Mok LP, Lee KY, Charbonnet M, Gold MS. 2012. Inflammation-induced changes in BK(Ca) currents in cutaneous dorsal root ganglion neurons from the adult rat. *Molecular pain* 8: 37

Zhao X, Tang Z, Zhang H, Atianjoh FE, Zhao JY, et al. 2013. A long noncoding RNA contributes to neuropathic pain by silencing Kcna2 in primary afferent neurons. *Nature neuroscience* 16: 1024-31

Zhu W, Frost EE, Begum F, Vora P, Au K, et al. 2012. The role of dorsal root ganglia activation and brain-derived neurotrophic factor in multiple sclerosis. *Journal of cellular and molecular medicine* 16: 1856-65

Zimmermann K, Leffler A, Babes A, Cendan CM, Carr RW, et al. 2007. Sensory neuron sodium channel Nav1.8 is essential for pain at low temperatures. *Nature* 447: 855-8

Zotterman Y. 1939. Touch, pain and tickling: an electro-physiological investigation on cutaneous sensory nerves. *The Journal of physiology* 95: 1-28

Zwick M, Davis BM, Woodbury CJ, Burkett JN, Koerber HR, et al. 2002. Glial cell line-derived neurotrophic factor is a survival factor for isolectin B4-positive, but not vanilloid receptor 1-positive, neurons in the mouse. *The Journal of neuroscience : the official journal of the Society for Neuroscience* 22: 4057-65